

REPORT
161

GEOCHRONOLOGY OF THE RUDALL PROVINCE, WESTERN AUSTRALIA: IMPLICATIONS FOR THE AMALGAMATION OF THE WEST AND NORTH AUSTRALIAN CRATONS

by DW MAIDMENT





Government of **Western Australia**
Department of **Mines and Petroleum**

REPORT 161

GEOCHRONOLOGY OF THE RUDALL PROVINCE, WESTERN AUSTRALIA: IMPLICATIONS FOR THE AMALGAMATION OF THE WEST AND NORTH AUSTRALIAN CRATONS

by
DW Maidment

Perth 2017



**Geological Survey of
Western Australia**

MINISTER FOR MINES AND PETROLEUM
Hon Bill Johnston MLA

ACTING DIRECTOR GENERAL, DEPARTMENT OF MINES AND PETROLEUM
Tim Griffin

EXECUTIVE DIRECTOR, GEOLOGICAL SURVEY OF WESTERN AUSTRALIA
Rick Rogerson

REFERENCE

The recommended reference for this publication is:

Maidment, DW 2017, Geochronology of the Rudall Province, Western Australia: implications for the amalgamation of the West and North Australian Cratons: Geological Survey of Western Australia, Report 161, 95p.

National Library of Australia Cataloguing-in-Publication entry

Creator: Maidment, D. W. (David W.), author.
Title: Geochronology of the Rudall Province, Western Australia: implications for the amalgamation of the West and North Australian Cratons / David W Maidment.
ISBN: 9781741687019 (ebook)
Subjects: Geology, Stratigraphic--Proterozoic. Geology--Western Australia--Rudall Province. Cratons--Australia
Other Authors/Contributors: Geological Survey of Western Australia, issuing body.
Dewey Number: 551.8109941
ISSN 0508-4741



U–Pb measurements were conducted using the SHRIMP II ion microprobes at the John de Laeter Centre of Isotope Research at Curtin University in Perth, Australia.

Grid references in this publication refer to the Geocentric Datum of Australia 1994 (GDA94). Locations mentioned in the text are referenced using Map Grid Australia (MGA) coordinates, Zone 51. All locations are quoted to at least the nearest 100 m.

Disclaimer

This product was produced using information from various sources. The Department of Mines and Petroleum (DMP) and the State cannot guarantee the accuracy, currency or completeness of the information. DMP and the State accept no responsibility and disclaim all liability for any loss, damage or costs incurred as a result of any use of or reliance whether wholly or in part upon the information provided in this publication or incorporated into it by reference.

Copy editor: K Coyle
Cartography: J Peng and A Symonds
Desktop publishing: RL Hitchings

Published 2017 by Geological Survey of Western Australia

This Report is published in digital format (PDF) and is available online at <www.dmp.wa.gov.au/GSWApublications>.

Further details of geological publications and maps produced by the Geological Survey of Western Australia are available from:

Information Centre
Department of Mines and Petroleum
100 Plain Street | EAST PERTH WESTERN AUSTRALIA 6004
Telephone: +61 8 9222 3459 Facsimile: +61 8 9222 3444
www.dmp.wa.gov.au/GSWApublications

Cover photograph: Folded felsic dyke in granitic gneiss of the Kalkan Supersuite, Talbot Terrane, east of Rudall Crossing

Contents

Abstract	1
Introduction	1
Geological overview of the Rudall Province.....	2
Talbot Terrane	2
Connaughton Terrane	6
Tabletop Terrane.....	7
Neoproterozoic and Paleozoic sedimentary cover	8
Deformation and metamorphism	10
D ₁ event	12
D ₂ event (Yapungku Orogeny)	12
D ₃ event	13
D ₄ event (Miles Orogeny)	13
D ₅ event	16
D ₆ event (Paterson Orogeny).....	16
Late-stage dolerite dykes	17
U–Pb zircon geochronology.....	17
Analytical methods	17
GA 2005670100 – quartz–feldspar–muscovite schist, Talbot Terrane	17
GA 2005670080 – granitic gneiss, Talbot Terrane.....	21
GA 2005670129-02 – quartz–feldspar–muscovite schist, Larry Formation, Talbot Terrane.....	22
GA 2005670110 – quartzite, Fingoon Quartzite, Talbot Terrane.....	24
‘Aplite’ (microgranite) dykes, Talbot Terrane.....	25
GA 2005670072 – micromonzogranite dyke, Talbot Terrane.....	25
GA 2005670092 – micromonzogranite dyke, Talbot Terrane.....	27
GA 2005670165 – quartzite, Connaughton Terrane	31
GA 2005670162 – granitic gneiss, Connaughton Terrane	32
GA 2006670087 – quartzite, Tabletop Terrane	38
GA 2005670178 – leucogranite, Tabletop Terrane	40
GA 2005670186 – monzogranite, Tabletop Terrane	42
GA 2005670188 – monzogranite, Tabletop Terrane	42
GA 2005670187 – quartzofeldspathic schist, Tabletop Terrane	45
GA 2006670110 – amphibolite, Tabletop Terrane	45
GA 2006670119 – leucogranite, Tabletop Terrane	49
Whole-rock geochemistry	51
Analytical methods	52
Rudall Province granite geochemistry	52
Tabletop Terrane amphibolite geochemistry	56
Sm–Nd isotopes	57
Analytical methods	57
Results	58
Discussion	59
Age and provenance of the metasedimentary successions.....	59
Talbot Terrane	59
Connaughton Terrane	63
Tabletop Terrane.....	63
Timing of the Yapungku Orogeny	64
Constraints from overprinting relationships.....	64
Direct dating of metamorphism	67
Geodynamic setting of the Krackatinny Supersuite.....	68
Geodynamic setting of the Kalkan Supersuite and Camel Suite	69
Reassessing the geodynamic evolution of the Rudall Province.....	69
Geodynamic context from other parts of Proterozoic Australia.....	70
1800–1760 Ma regional geodynamic setting.....	70
1680 Ma regional geodynamic setting	74
1590–1550 Ma regional geodynamic setting	75
1330–1285 Ma regional geodynamic setting.....	79
Paleomagnetic constraints on craton assembly	82
Nature of the Anketell Regional Gravity Ridge.....	83
Geodynamic evolution of the Rudall Province — plausible alternatives.....	84
Scenario 1: ‘early’ amalgamation	84
Scenario 2: ‘late’ amalgamation.....	84
Implications for mineral systems	85
Conclusions	86
Acknowledgements	87
References	88

Appendices

1. Summary of SHRIMP analytical sessions
2. U–Pb geochronology data tables
3. Whole-rock geochemical data

Note: Appendices 1–3 are available as a downloadable zip file on eBookshop

Figures

1.	Location of the Rudall Province	2
2.	Simplified interpreted basement geology of the Rudall Province	3
3.	Generalized outcrop geology of the Rudall Province	4
4.	Outcrop photos of structurally lower units in the Talbot Terrane	5
5.	Generalized lithostratigraphy of the Talbot Terrane	6
6.	Outcrop photos of structurally higher units in the Talbot Terrane	7
7.	Outcrop photos of granitic gneiss in the Talbot Terrane and units in the Connaughton Terrane	8
8.	Outcrop photos of units in the Tabletop Terrane	9
9.	Outcrop photos of granitic rocks of the Krackatinny Supersuite in the Tabletop Terrane	10
10.	Outcrop photos and photomicrograph of D_1/D_2 structures in the Talbot and Connaughton Terranes	11
11.	Outcrop photos of M_2 kyanite and F_4 folds in the Talbot Terrane	14
12.	Photomicrograph and outcrop photos of D_4 and D_5 structures in the Talbot Terrane and Yeneena Basin	15
13.	Locations of U–Pb geochronology samples	18
14.	Outcrop photos and photomicrographs of quartz–feldspar–muscovite schist and granitic gneiss, Talbot Terrane	19
15.	Images of zircons from quartz–feldspar–muscovite schist, Talbot Terrane	20
16.	U–Pb analytical data for zircons from quartz–feldspar–muscovite schist, Talbot Terrane	21
17.	Images of zircons from granitic gneiss, Talbot Terrane	22
18.	U–Pb analytical data for zircons from granitic gneiss, Talbot Terrane	23
19.	Outcrop photos and photomicrographs of quartz–feldspar–muscovite schist, Larry Formation, Talbot Terrane	23
20.	Images of zircons from quartz–feldspar–muscovite schist, Larry Formation, Talbot Terrane	24
21.	U–Pb analytical data for zircons from quartz–feldspar–muscovite schist, Larry Formation, Talbot Terrane	25
22.	Outcrop photo and photomicrograph of quartzite, Fingoon Quartzite, Talbot Terrane	26
23.	Images of zircons from quartzite, Fingoon Quartzite, Talbot Terrane	27
24.	U–Pb analytical data for zircons from quartzite, Fingoon Quartzite, Talbot Terrane	28
25.	Probability density diagram of detrital zircon dates from quartzite, Fingoon Quartzite, Talbot Terrane	28
26.	Outcrop photos and photomicrograph of felsic dykes, Talbot Terrane	29
27.	CL image of zircons from a felsic dyke in ultramafic rock, Talbot Terrane	29
28.	U–Pb analytical data for zircons from a felsic dyke in ultramafic rock, Talbot Terrane	30
29.	Outcrop photos and photomicrograph of a felsic dyke in granitic gneiss, Talbot Terrane	30
30.	CL image of zircons from a felsic dyke in granitic gneiss, Talbot Terrane	32
31.	U–Pb analytical data for zircons from a felsic dyke in granitic gneiss, Talbot Terrane	32
32.	Outcrop photos and photomicrographs of quartzite and granitic gneiss, Connaughton Terrane	33
33.	Images of zircons from quartzite, Connaughton Terrane	34
34.	U–Pb analytical data for zircons from quartzite, Connaughton Terrane	35
35.	Probability density diagram of detrital zircon dates from quartzite, Connaughton Terrane	35
36.	Images of zircons from granitic gneiss, Connaughton Terrane	36
37.	U–Pb analytical data for zircons from granitic gneiss, Connaughton Terrane	36
38.	Outcrop photos and photomicrographs of quartzite and leucogranite, Tabletop Terrane	37
39.	Images of zircons from quartzite, Tabletop Terrane	39
40.	U–Pb analytical data for zircons from quartzite, Tabletop Terrane	39
41.	Probability density diagram of detrital zircon dates from quartzite, Tabletop Terrane	40
42.	Images of zircons from leucogranite, Tabletop Terrane	41
43.	U–Pb analytical data for zircons from leucogranite, Tabletop Terrane	42
44.	Outcrop photos and photomicrographs of monzogranite, Tabletop Terrane	43
45.	Images of zircons from foliated monzogranite, Tabletop Terrane	44
46.	U–Pb analytical data for zircons from foliated monzogranite, Tabletop Terrane	44
47.	Images of zircons from weakly foliated monzogranite, Tabletop Terrane	46
48.	U–Pb analytical data for zircons from weakly foliated monzogranite, Tabletop Terrane	46
49.	Outcrop photos and photomicrographs of quartzofeldspathic schist, amphibolite and leucogranite, Tabletop Terrane	47
50.	Images of zircons from quartzofeldspathic schist, Tabletop Terrane	48
51.	U–Pb analytical data for zircons from quartzofeldspathic schist, Tabletop Terrane	48
52.	Images of zircons from amphibolite, Tabletop Terrane	50
53.	U–Pb analytical data for zircons from amphibolite, Tabletop Terrane	50
54.	Images of zircons from leucogranite, southeastern Tabletop Terrane	51
55.	U–Pb analytical data for zircons from leucogranite, southeastern Tabletop Terrane	52

56.	Locations of samples analysed for whole-rock geochemistry	53
57.	Plot of major elements vs SiO ₂ for granitic rocks of the Rudall Province	55
58.	Mantle-normalized trace element diagrams for granitic rocks of the Rudall Province	56
59.	Distribution of the geochemical groups of the 1589–1549 Ma Krackatinny Supersuite and the 1310–1286 Ma Camel Suite	57
60.	N-MORB-normalized trace element plot for amphibolite from the Tabletop Terrane	58
61.	εNd evolution diagram for granitic rocks of the Rudall Province	60
62.	Time–space diagram for the terranes of the Rudall Province	62
63.	Outcrop photos showing the structural setting of felsic dykes southeast of Rudall Crossing, Talbot Terrane	66
64.	Outcrop photos of monzogranite sample site of Nelson (1996b)	68
65.	Time–space diagram of 1800–1200 Ma tectono-thermal events in western and central Australia	71
66.	Tectonism from 1800–1760 Ma in western and central Australia	72
67.	Tectonism at c. 1680 Ma in western and central Australia	75
68.	Tectonism from 1590–1550 Ma in western and central Australia	77
69.	Tectonism from 1330–1285 Ma in western and central Australia	79
70.	Bouguer gravity image of the Paterson and Petermann Orogens, showing the Anketell Gravity Ridge	83

Tables

1.	Summary of tectono-thermal events in the Rudall Province	12
2.	Sm–Nd isotope data for igneous rocks from the Rudall Province	59
3.	Summary of SHRIMP U–Pb zircon dating for the Rudall Province	61
4.	Summary of 1800–1760 Ma tectono-thermal events in western and central Australia	73
5.	Summary of c. 1680 Ma tectono-thermal events in western and central Australia	76
6.	Summary of 1590–1550 Ma tectono-thermal events in western and central Australia	78
7.	Summary of 1330–1285 Ma tectono-thermal events in western and central Australia	80

Geochronology of the Rudall Province, Western Australia: implications for the amalgamation of the West and North Australian Cratons

by

DW Maidment

Abstract

U–Pb zircon dating of igneous and metasedimentary rocks from the Rudall Province reveals aspects of an extended, multiphase history that has implications for models of the assembly of Proterozoic Australia. Quartzite units in the Tabletop and Connaughton Terranes that yield maximum depositional ages of c. 2833 Ma and 2284 Ma are interpreted to represent Neoproterozoic to early Paleoproterozoic units sourced from the adjacent Pilbara region. The Fingoon Quartzite in the Talbot Terrane was deposited after c. 1794 Ma and might comprise part of a cover sequence sourced from granitic rocks of the 1804–1762 Ma Kalkan Supersuite.

Granitic rocks of the Krackatinny Supersuite in the Tabletop Terrane yield ages of 1589–1549 Ma and include high Sr/Y sodic rocks with adakitic characteristics, low Sr/Y sodic rocks and high-K granitic rocks with A-type affinities. This magmatism could have occurred in a continental magmatic arc or alternatively an intraplate rift developed in previously thickened crust. Sm–Nd isotope compositions suggest a relatively evolved source for these rocks, possibly involving an Archean mafic underplate. Metamorphosed mafic rocks in the Tabletop Terrane intruded by the Krackatinny Supersuite have geochemical characteristics more clearly indicative of an arc setting but their age remains poorly constrained. Less voluminous potassic leucogranites dated at 1310–1286 Ma comprise the newly defined Camel Suite.

Moderate- to high-P metamorphism and deformation during the Yapungku Orogeny has previously been interpreted to reflect collision of the West and North Australian Cratons at 1800–1765 Ma, synchronous with the emplacement of the Kalkan Supersuite. Re-examination of felsic dykes previously used to constrain the minimum age of the Yapungku Orogeny, however, suggests that these dykes and the granitic rocks of the Kalkan Supersuite only provide a maximum age constraint for this deformation. This opens up the possibility that the Yapungku Orogeny occurred later than previously thought, potentially coinciding with one of two metamorphic events dated at c. 1680 and 1330 Ma in the Connaughton and Talbot Terranes. Two ‘end-member’ scenarios are considered plausible. The first incorporates amalgamation of the West Australian with the North Australian Craton, or an intervening crustal block, close to the currently accepted age of c. 1765 Ma. The second scenario involves final amalgamation as late as c. 1300 Ma, with magmatism in the Tabletop Terrane reflecting Mesoproterozoic convergence. Although further work is required to develop a more robust event framework for the Rudall Province, the possibility that the Yapungku Orogeny occurred later than previously thought should be considered in reconstructions of Proterozoic Australia.

KEYWORDS: cratons, geochemistry, geochronology, granitic rock, isotopes, metamorphism, orogeny, tectonics

Introduction

The Rudall Province, comprising part of the Paterson Orogen of north-central Western Australia, preserves a complex record of Paleo- to Neoproterozoic sedimentation, magmatism and deformation near the northeastern margin of the West Australian Craton (Fig. 1). The geological evolution of the Rudall Province forms a key constraint for geodynamic models describing the Proterozoic assembly of Australia because it forms an isolated inlier that appears to record the effects of plate margin tectonism between the West and North Australian Cratons (Smithies and Bagas, 1997; Bagas, 2004; Betts and Giles, 2006; Betts et al., 2016). Almost all recent

models incorporate collision of the West Australian Craton with the North Australian Craton during the Yapungku Orogeny, which is considered to have affected the Rudall Province between c. 1800 and 1765 Ma (Smithies and Bagas, 1997; Li, 2000; Betts et al., 2002; Bagas, 2004; Betts and Giles, 2006; Betts et al., 2008; Cawood and Korsch, 2008; Payne et al., 2009; Huston et al., 2012; Johnson, 2013; Betts et al., 2016). Maximum pressure attained during the Yapungku Orogeny was up to ~12 kbar, unusually high for Paleoproterozoic tectonism in Australia, and has been interpreted to be a result of crustal thickening during continental collision (Smithies and Bagas, 1997).

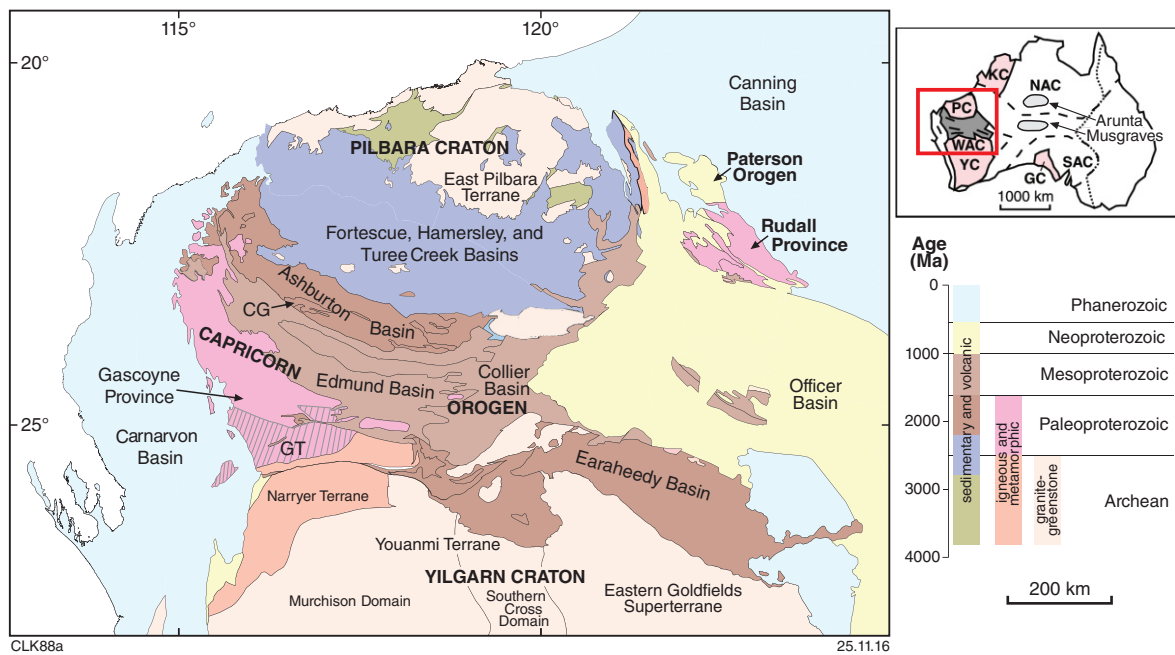


Figure 1. Location of the Rudall Province relative to other Paleoproterozoic domains of Western Australia (modified after Kirkland et al., 2013a). CG: Capricorn Group; GC: Gawler Craton; GT: Glenburgh Terrane; KC: Kimberley Craton; NAC: North Australian Craton; PC: Pilbara Craton; SAC: South Australian Craton; YC: Yilgarn Craton; WAC: West Australian Craton

Despite its key position, the Rudall Province remains relatively understudied, due in part to its remote location and difficulty of access. There are relatively few geochronological constraints on the timing of sedimentation, deformation and metamorphism, and key events such as the Yapungku Orogeny have not been directly dated but are constrained by interpretations of overprinting relationships between intrusive rocks and structural fabrics at a few key localities. In this study, SHRIMP U–Pb zircon geochronology, geochemistry and Sm–Nd isotope data for igneous and sedimentary units of the Rudall Province are presented to provide further constraints on Paleoproterozoic–Mesoproterozoic tectonism. The results reveal additional complexity in the evolution of the province and raise the possibility that the amalgamation of the West and North Australian Cratons might have occurred later than currently thought.

Geological overview of the Rudall Province

The Rudall Province forms a northwesterly trending belt of deformed and metamorphosed Paleoproterozoic–Mesoproterozoic sedimentary and igneous rocks which crop out about 100 km to the east of the Pilbara Craton, forming part of the Paterson Orogen (Fig. 1). The province forms an inlier within Neoproterozoic to Paleozoic sedimentary rocks of the Yeneena, Officer and Canning Basins and is overlain by Permian fluvio-glacial sedimentary rocks and unconsolidated recent sediments, including widespread dune fields.

The Rudall Province has been subdivided into the Talbot, Connaughton and Tabletop Terranes (Fig. 2; Bagas and Smithies, 1998b). Bagas (2004) suggested that the differences in geological history between different parts of the Rudall Province indicate that the province might contain exotic terranes, noting similarities between the Connaughton Terrane and the Arunta Orogen of the North Australian Craton. Kirkland et al. (2013b), however, showed that the Lu–Hf isotope characteristics and U–Pb ages of zircon from the Rudall Province have an affinity with the West Australian Craton and considered all the terranes to represent semi-autochthonous blocks, implying that the boundary between the West and North Australian Cratons is further to the northeast. The Rudall Province is relatively well exposed in the northwest as low hills and undulating areas of subcrop but is generally less well exposed towards the southeast and east, where surficial cover is more extensive (Fig. 3).

Talbot Terrane

The Talbot Terrane in the northwestern part of the province consists of siliciclastic and chemical metasedimentary rocks, voluminous granitic gneiss and minor ultramafic and mafic rocks that have been metamorphosed under amphibolite facies peak metamorphic conditions (Clarke, 1991; Hickman and Bagas, 1998, 1999). The complexity of deformation makes it difficult to determine original contact relationships between units but a distinctive compositionally layered granitic gneiss and associated metasedimentary rocks in the western part of the Talbot Terrane (Fig. 4a–c) contains an early layer-parallel

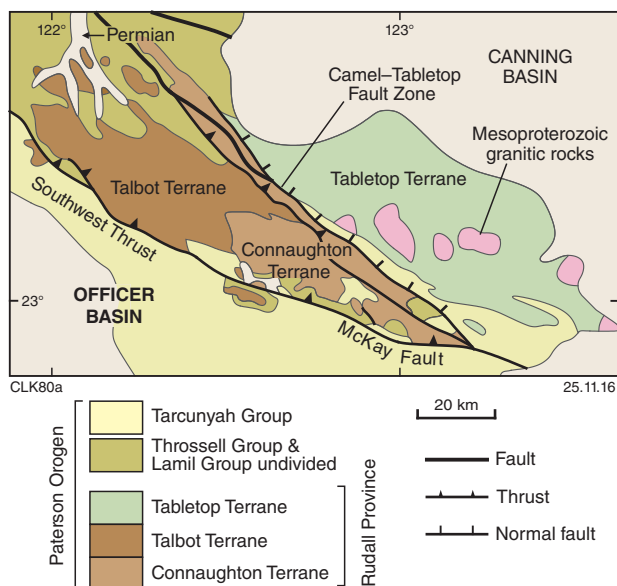


Figure 2. Simplified interpreted basement geology of the Rudall Province, showing the main lithotectonic zones and surrounding basins (modified after Smithies and Bagas [1997] and Hickman and Bagas [1999])

foliation not recognized in other granitic rocks and has been suggested to be the oldest exposed unit (Hickman and Bagas, 1999). The layered gneiss is dominated by deformed granite and monzogranite and contains abundant large xenoliths of amphibolite, serpentinite and metasedimentary rock (Hickman and Bagas, 1998). A U–Pb zircon date of 2015 ± 26 Ma has been obtained for one sample (Nelson, 1995a), and two age components of 1972 ± 4 and 1802 ± 14 Ma were obtained from another sample (Nelson, 1995i). All three dates have been interpreted as felsic igneous components of the unit (Hickman and Bagas, 1998) but it is also possible that zircon inheritance could influence some of these dates.

Siliciclastic, quartzofeldspathic and minor chemical metasedimentary rocks form recognizable lithostratigraphic units that crop out across much of the Talbot Terrane (Hickman and Bagas, 1996, 1998; Bagas et al., 2000). These metasedimentary rocks have been subdivided into the Larry Formation, Fingoon Quartzite, Yandagoo Formation, Butler Creek Formation and Poynton Formation (Fig. 5; Hickman and Bagas, 1998, 1999). The succession has been disrupted by shearing, faulting and the intrusion of voluminous granitic bodies but gradational contacts have been described in places between the four lowermost units, which has been used to suggest that they might locally retain their original stratigraphic relationships (Hickman and Bagas, 1998, 1999). The Larry Formation is considered to represent the stratigraphically oldest unit, with locally preserved cross-bedding and graded bedding in the upper part of the unit suggesting younging towards the structurally overlying Fingoon Quartzite (Hickman and Bagas, 1999).

The Larry Formation predominantly consists of quartz–feldspar–mica paragneiss (Fig. 4d,e), which grades to muscovitic quartzite of the Fingoon Quartzite (Fig. 4f) and then into pelitic to psammitic metasedimentary rocks of the Yandagoo Formation, which includes banded iron-formation, chert and iron-rich graphitic units (Fig. 6a,b). The Butler Creek Formation (Fig. 6c) comprises a succession of generally psammitic metasedimentary rocks, including quartz–feldspar(–biotite) gneiss, quartz–muscovite–feldspar schist, muscovite-bearing quartzite, quartz–biotite schist and rare banded iron-formation. Muscovite-bearing quartzite, quartz–feldspar–muscovite schist and biotite–plagioclase–quartz schist of the Poynton Creek Formation (Fig. 6d) have an uncertain relationship with other units due to younger deformation and have been tentatively placed at the top of the succession (Hickman and Bagas, 1998).

The Talbot Terrane contains voluminous sheet-like bodies of granitic gneiss comprising the Kalkan Supersuite (Budd et al., 2001) which have been dated between c. 1801 and 1762 Ma (Fig. 7a,b; Hickman and Bagas, 1999; Bagas, 2004; Kirkland et al., 2013a). In most areas the contacts between granitic gneiss and metasedimentary rocks are sheared or poorly exposed but apparent intrusive contacts are preserved in some areas. The dominant granitic gneiss type consists of K-feldspar–quartz–plagioclase–biotite gneiss with coarse-grained K-feldspar augen up to several centimetres long, although more equigranular variants are also present.

Lenses and pods of ultramafic rock are present within the metasedimentary succession and the granitic gneiss. These outcrops define folded, sheared and boudinaged layers of serpentinitized dunite and pyroxenite that form a discontinuous zone up to several hundred metres wide over a strike length of about 50 km (Carr, 1989; Hickman and Bagas, 1998). Carr (1989) suggested that these rocks have a komatiitic affinity, based on whole-rock and chromite geochemistry, and suggested they comprise remnants of a differentiated intrusive body, which is consistent with the observation of Hickman and Bagas (1998) that the ultramafic unit transgresses stratigraphic boundaries in the eastern part of the zone. The ultramafic bodies are foliated and are in places constrained within shear zones considered to have been active during the Yapungku Orogeny (Carr, 1989; Hickman and Bagas, 1999). Hickman and Bagas (1999) interpreted these relationships to indicate that the ultramafic rocks were emplaced during the Yapungku Orogeny, although a pre-Yapungku Orogeny timing is also possible. Carr (1989) suggested that the ultramafic rocks might represent part of an ophiolite complex but noted significant differences from typical ophiolite successions, including their interpreted komatiitic character and the lack of associated mafic rocks (e.g. layered gabbro, sheeted dykes or basalt). Carr (1989) suggested that these differences might have been due to differences in the character of oceanic magmatism in the Paleoproterozoic, combined with a younger separation of mantle and crustal components, but these differences could also be interpreted to indicate that the ultramafic rocks are not in fact part of an ophiolite complex but instead represent a deformed intrusion.

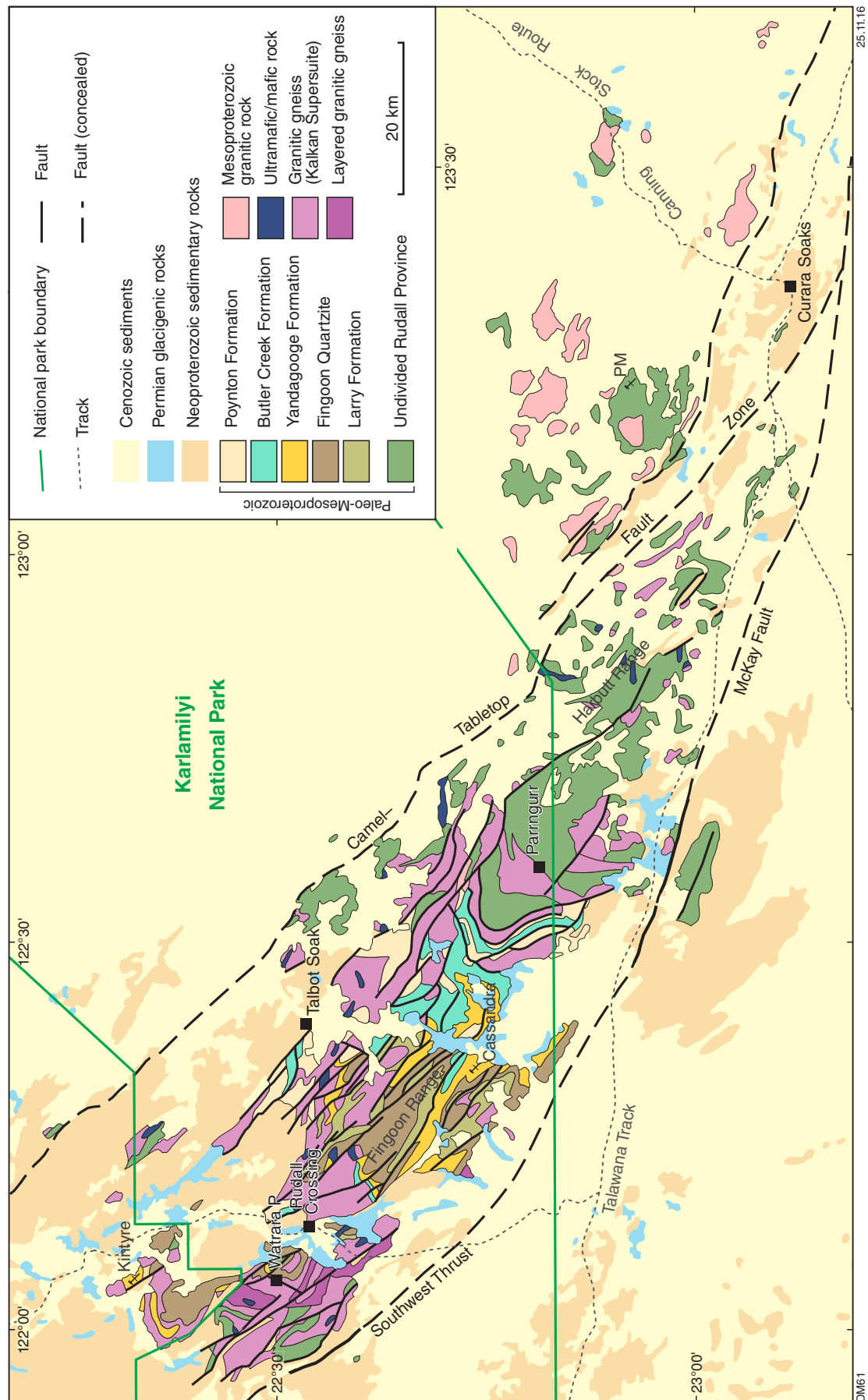


Figure 3. Generalized outcrop geology of the Rudall Province, modified from Geoscience Australia 1:1 000 000 national surface geology map



Figure 4. Outcrop photos of structurally lower units in the Talbot Terrane: a) layered granitic orthogneiss (MGA 408104E 7502260N); b) layered orthogneiss with amphibolite xenoliths (MGA 407125E 7499730N); c) interlayered muscovite-rich and quartzofeldspathic schist from the northwestern Talbot Terrane (MGA 401169E 7507480N); d) layered feldspar-rich psammitic gneiss of the Larry Formation (MGA 427657E 7490640N); e) folding of a more siliceous layer within the Larry Formation (MGA 427657E 7490640N); f) tight folding within the Fingoon Quartzite (MGA 421780E 7502670N)

The only metasedimentary unit dated prior to the present study is the Fingoon Quartzite, which yielded an essentially unimodal zircon age component with a weighted mean date of 1790 ± 10 Ma (Nelson, 1995e), recalculated as 1791 ± 10 Ma by Kirkland et al. (2013a). This maximum depositional age overlaps with the dates for the older granitic components of the Kalkan Supersuite, and has been used to infer that the Fingoon Quartzite and associated metasedimentary rocks were deposited at about the same time as the felsic magmatism (Bagas et al., 2004). The Fingoon Quartzite, however, lacks granitic intrusions, and it remains a possibility that the Fingoon Quartzite was deposited after the magmatism (Hickman and Bagas, 1999), although these authors favoured synmagmatic deposition based on gradational contacts observed in places between the Fingoon Quartzite and units interpreted to have been intruded by the Kalkan Supersuite.

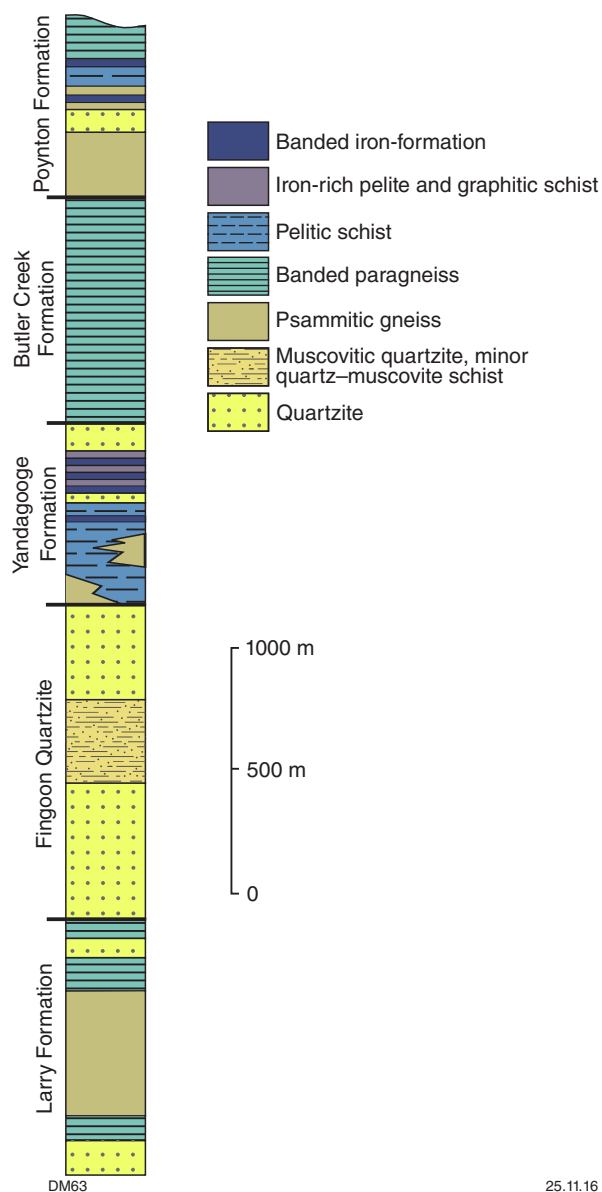


Figure 5. Generalized lithostratigraphy of the Talbot Terrane (after Hickman and Bagas, 1999)

A biotite monzogranite in the Talbot Terrane yielded a date of 1453 ± 10 Ma (Nelson, 1996b), which has been taken as evidence of a Mesoproterozoic magmatic event post-dating high-grade metamorphism (Bagas, 2004). The monzogranite has a considerably more juvenile zircon Lu–Hf isotope signature than any other granitic rocks from the Rudall Province and a mantle-like oxygen isotope signature (Kirkland et al., 2013b). However, as discussed below, there is some uncertainty as to whether this sample was taken from an in situ outcrop or a boulder derived from Permian glaciogenic sedimentary rocks.

Connaughton Terrane

The supracrustal rocks of the Connaughton Terrane are characterized by a significantly higher proportion of mafic rocks than those of the Talbot Terrane (Bagas and Smithies, 1998b). The boundary between the Talbot and Connaughton Terranes is not clearly defined but has been taken at the sheared contact between a package of metasedimentary schist, amphibolite, quartzite and chert, and a layer-parallel body of granitic gneiss to the northwest assigned to the Talbot Terrane (Bagas and Smithies, 1998b). This boundary is considered to represent an originally southeasterly dipping thrust fault which was subsequently folded by a regional west-northwesterly trending anticlinal structure (Bagas and Smithies, 1998b). A narrow fault-bound northwesterly trending belt of metasedimentary and meta-igneous rocks extending along the northeastern margin of the Talbot Terrane is also considered to be part of the Connaughton Terrane (Fig. 2).

Amphibolite and mafic granulite of the Connaughton Terrane is interlayered with metamorphosed siliciclastic and chemical sedimentary rocks, including quartzite, pelitic schist, chert, banded iron-formation, graphitic and sulfidic schist and calc-silicate rock. The mafic rocks (Fig. 7c,d) have a tholeiitic composition and have been interpreted as metavolcanic units (Bagas and Smithies, 1998b). The complexly folded and deformed succession has not been divided into formalized stratigraphic units, and the relationship between these rocks and the metasedimentary units of the Talbot Terrane is unclear. Smithies and Bagas (1998) suggested that the character of the siliciclastic and chemical sedimentary rocks of the Connaughton Terrane is consistent with a shallow-water restricted continental basin or a deeper water outer continental shelf environment.

As with the Talbot Terrane, deformed and metamorphosed granitic rocks form a significant component of the Connaughton Terrane (Bagas and Smithies, 1998b). Two of these have yielded dates of 1769 ± 7 Ma (Nelson, 1995m) and 1777 ± 7 Ma (Nelson, 1996d) and most granitic rocks within the zone are considered to be part of the Kalkan Supersuite. A volumetrically minor phase of magmatism is indicated by a 1291 ± 10 Ma date for a pegmatite dyke (Nelson, 1995b) and by an unpublished 1286 ± 6 Ma date for a monzogranite near the boundary between the Connaughton and Tabletop Terranes (referred to in Bagas, 2004). A medium-grained quartz–microcline–muscovite–garnet–biotite gneiss yielded zircon age components at 1873–1764, 1672 ± 70

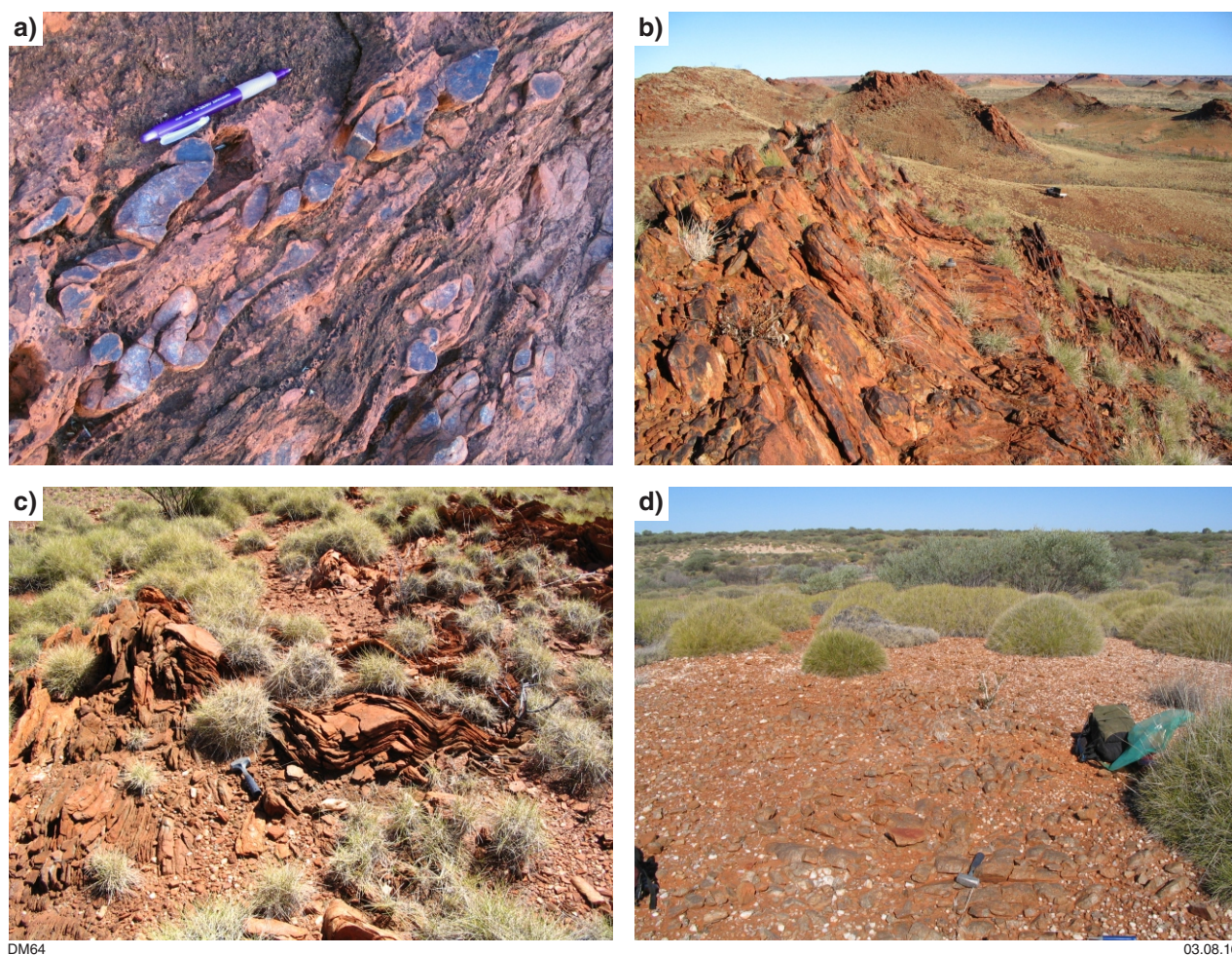


Figure 6. Outcrop photos of structurally higher units in the Talbot Terrane: a) tightly folded chert bed in pelitic schist of the Yandagooge Formation (MGA 404455E 7530765N); b) outcrop of folded Yandagooge Formation in Tracy Hills, about 1.5 km north of the Kintyre U prospect (MGA 404952E 7531160N); c) quartz-feldspar-mica schist of the Butler Creek Formation, deformed by F4 folds near the northwestern end of the Fingoon Range (MGA 417130E 7500740N); d) poorly exposed quartzite in the Poynton Formation near Talbot Soak (MGA 437285E 7507580N)

and 1222 ± 63 Ma (Nelson, 1996c). The c. 1672 Ma component was considered to represent zircon inheritance and the c. 1222 Ma date obtained from two analyses of a zircon rim was interpreted to represent a magmatic age (Nelson, 1996c), but Kirkland (2013a) noted that other interpretations are possible, particularly as it was unclear whether this rock had a sedimentary or igneous protolith.

Tabletop Terrane

The Tabletop Terrane forms a poorly exposed domain in the northeastern part of the province, separated from the Talbot and Connaughton Terranes by the regional-scale, northwesterly trending Camel-Tabletop Fault Zone (Fig. 3; Bagas and Smithies, 1998b). Many of the outcropping rocks in the Tabletop Terrane consist of weakly metamorphosed granitic rocks preserving igneous textures and generally show evidence of significant strain only near discrete faults and shear zones (Figs 8a-f, 9a-d). These felsic intrusive rocks consist of fine- to medium-grained, equigranular to porphyritic biotite \pm

hornblende tonalite, monzogranite and leucogranite, with calc-alkaline, I-type compositions (Smithies and Bagas, 1998; Bagas, 1999). Trends in geochemical data suggest that the tonalites and leucogranites are not directly related (Smithies and Bagas, 1998; Bagas, 1999) but there are very few geochronological data to constrain the timing of magmatic events, with a 1310 ± 4 Ma date obtained for a leucogranite (Nelson, 1996e) and a 1476 ± 10 Ma date for a granodiorite (Thevissen, 1991). These granitic rocks have been assigned to the Krackatinny Supersuite (Budd et al., 2001), which has been used as a grouping for all the felsic intrusive rocks in the Tabletop Terrane, although dating indicates that they do not represent a single magmatic episode. Smithies and Bagas (1998) noted that some tonalites from the Tabletop Terrane are Sr-undepleted and Y-depleted, in contrast with many Australian Proterozoic granitic rocks, which are commonly Sr-depleted and Y-undepleted. These authors noted that the geochemical characteristics of the tonalites showed similarities with Late Cretaceous to Cainozoic subduction-related granites and Archean granites, and favoured an arc setting for these rocks.

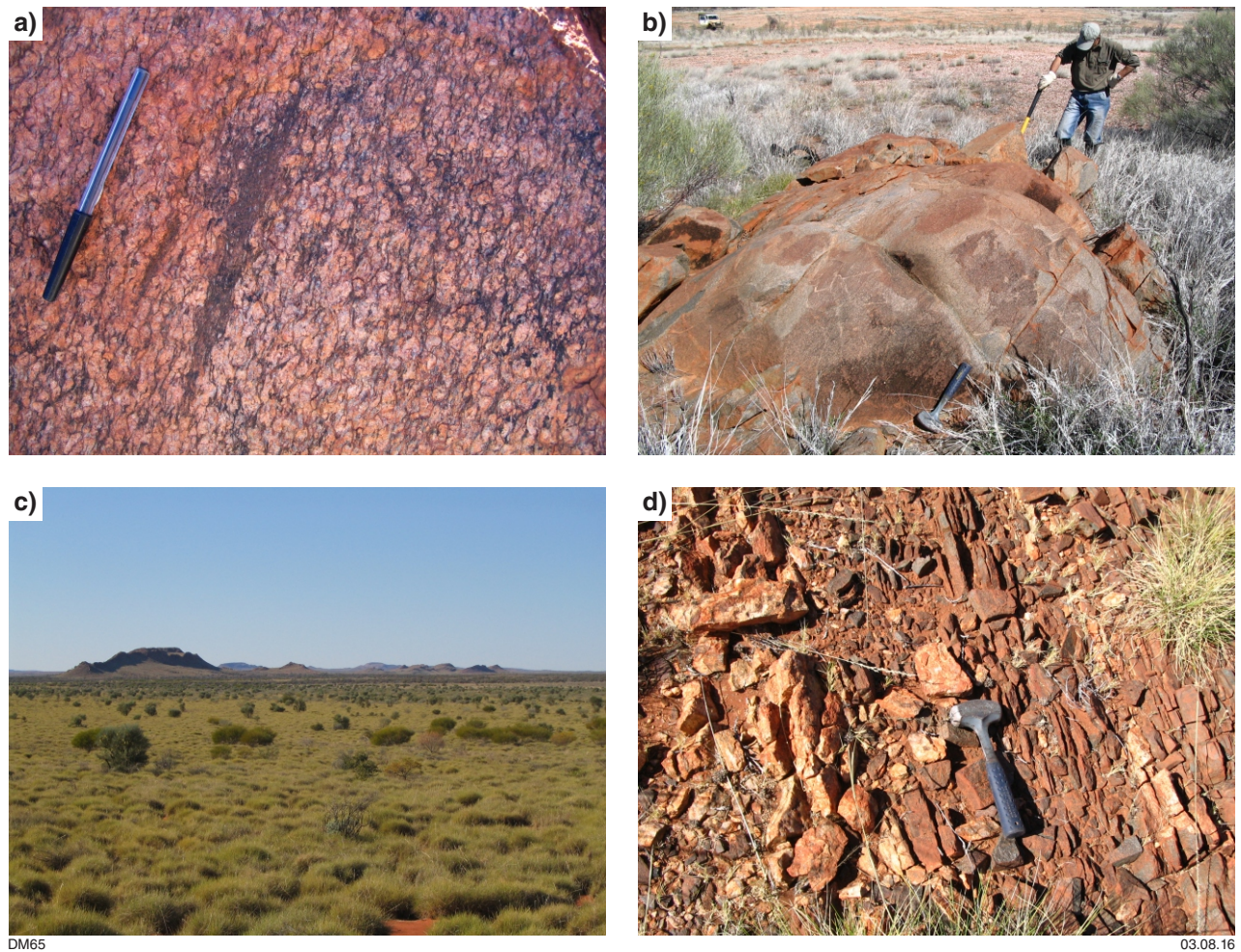


Figure 7. Outcrop photos of granitic gneiss in the Talbot Terrane and units in the Connaughton Terrane: a) K-feldspar augen granitic gneiss of the Kalkan Supersuite with metasedimentary xenolith and pervasive S_2 foliation, Split Rock area, 4 km east of Rudall Crossing in the Talbot Terrane (MGA 415805E 7507200N); b) seriate-textured granitic gneiss of the Kalkan Supersuite, Talbot Terrane (MGA 424644E 7501260N); c) ridge-forming quartzite among generally poorly exposed lithologies in the Harbutt Range area, Connaughton Terrane; d) typical low exposure of foliated amphibolite, intruded by pegmatite dyke, 4 km south of the Harbutt Range (MGA 484024E 7461230N)

There are very few exposures of supracrustal rocks in the Tabletop Terrane but, where exposed, these comprise quartzite, calc-silicate rock and banded iron-formation. There has been no dating to constrain the age of the supracrustal succession, with only a c. 1476 Ma minimum age provided by the oldest dated granitic rock (Thevisen, 1991). Actinolite-rich and lesser actinolite–hornblende–amphibolite (Fig. 8c) is widespread in the Tabletop Terrane but is generally poorly exposed. These mafic rocks are typically relatively weathered but preserve primary igneous textures in places. Small ultramafic intrusive bodies have also been identified. The generally greenschist facies to lower amphibolite metamorphic grade of the mafic rocks distinguishes this zone from the Talbot and Connaughton Terranes, which are characterized by amphibolite to granulite facies peak metamorphic assemblages (Bagas, 1999, 2004). The Camel–Tabletop Fault Zone (Figs 2, 3) has previously been suggested to be a collisional boundary separating the Tabletop Terrane from the Connaughton and Talbot Terranes (Bagas and Lubieniecki, 2001), but Kirkland et al. (2013b) noted

that Lu–Hf isotope compositions of zircon from c. 1310 Ma leucogranite indicate sources similar to those present in the rest of the Rudall Province and suggested all the terranes of the Rudall Province are essentially autochthonous, with affinities to the West Australian Craton.

Neoproterozoic and Paleozoic sedimentary cover

The Paleoproterozoic to Mesoproterozoic rocks of the Rudall Province are unconformably overlain by sedimentary rocks of the Neoproterozoic Yeneena and Officer Basins (Fig. 10a). The Tarcunyah Group of the Officer Basin forms fault-bound outliers in the southern Rudall Province, but mostly occurs to the southwest of the Southwest Thrust – McKay Fault (Grey et al., 2005). The Throssell Range Group, Isdell Formation and Lamil Group crop out to the northeast of the Southwest Thrust – McKay Fault and together comprise the Yeneena Basin,

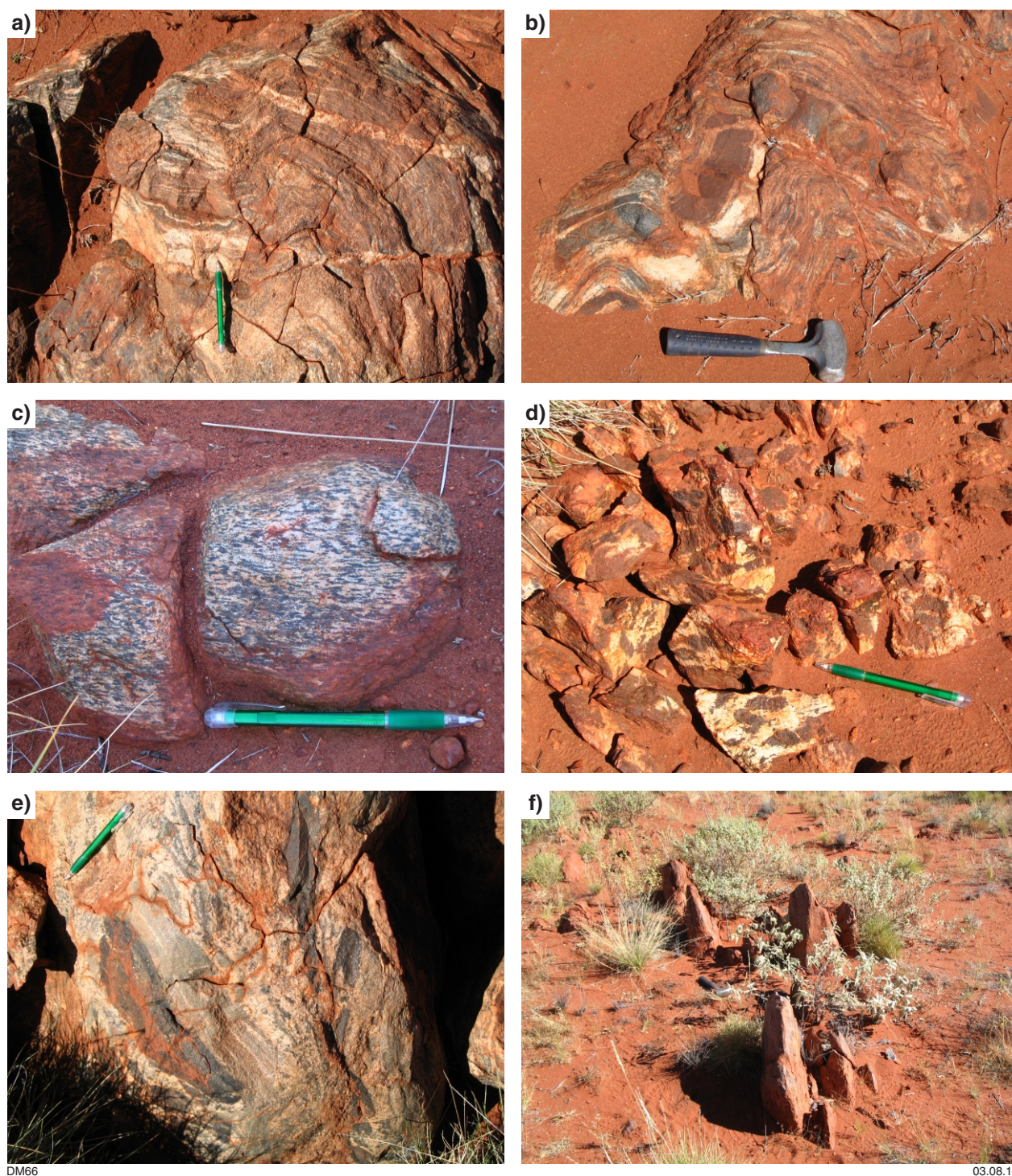


Figure 8. Outcrop photos of units in the Tabletop Terrane: a) thin leucogranite dykes crosscutting foliated and folded quartz, biotite and plagioclase-rich unit (MGA 515087E 7463820N); b) interlayered mafic and felsic rocks with strong layer-parallel foliation, deformed by younger folding (MGA 515087E 7463820N); c) foliated leucocratic actinolite-bearing amphibolite about 4 km west of PM prospect (MGA 518447E 7464820N); d) leucogranite veining within ultramafic rock about 8 km west-southwest of PM prospect (MGA 515234E 7463810N); e) foliated metasedimentary and meta-igneous xenoliths in leucogranite about 4 km west of PM prospect (MGA 518306E 7464420N); f) low outcrops of leucogranite near the Camel–Tabletop Fault Zone in the northwestern Tabletop Terrane (MGA 484807E 7480490N), dated at 1310 ± 4 Ma (Nelson, 1996)

an apparent correlative of lower parts of the Centralian Superbasin (Grey et al., 2005; Bagas and Nelson, 2005). The age of the Yeneena Basin sedimentation is constrained by maximum depositional ages of 950–850 Ma derived from detrital zircons, minimum dates of 835–816 Ma derived from mafic intrusive rocks, and an unpublished Pb–Pb carbonate date of 858 ± 29 Ma for the Isdell Formation, interpreted as the timing of diagenesis (Reed, 1996; Bagas and Nelson, 2005; Maidment et al., 2008; Whitaker et al., 2010).

Late Paleozoic to Mesozoic sedimentary rocks of the Canning Basin onlap the Rudall Province and Yeneena Basin in the northeastern part of the region (Roach et al., 2010), while Permian fluvioglacial sedimentary rocks of the Paterson Formation are preserved within paleovalley networks incised into the basement rocks within the Rudall Province. Unconsolidated sediments, including linear dune fields, form a thin veneer over much of the region.

Deformation and metamorphism

Structural frameworks have been developed for the Rudall Province during regional mapping programs carried out by the GSWA (Chin et al., 1980; Clarke, 1991; Smithies and Bagas, 1997; Bagas and Smithies, 1998b; Hickman and Bagas, 1999; Bagas et al., 2000; Bagas, 2004). These are similar in many aspects, recognizing a major high-grade deformational event (the Yapungku Orogeny), which affected the Paleoproterozoic basement rocks, and younger Neoproterozoic orogenic events (the Miles and Paterson Orogenies), which affected both the Paleoproterozoic basement and the Neoproterozoic sedimentary rocks of the Yeneena Basin (Table 1). In detail, there are differences between the interpretations, mainly regarding the number of pre-Neoproterozoic events, with the framework presented in Hickman and Bagas (1999) and Bagas (2004) representing the most recent and widely accepted synthesis. This scheme has largely been developed in the Talbot and Connaughton

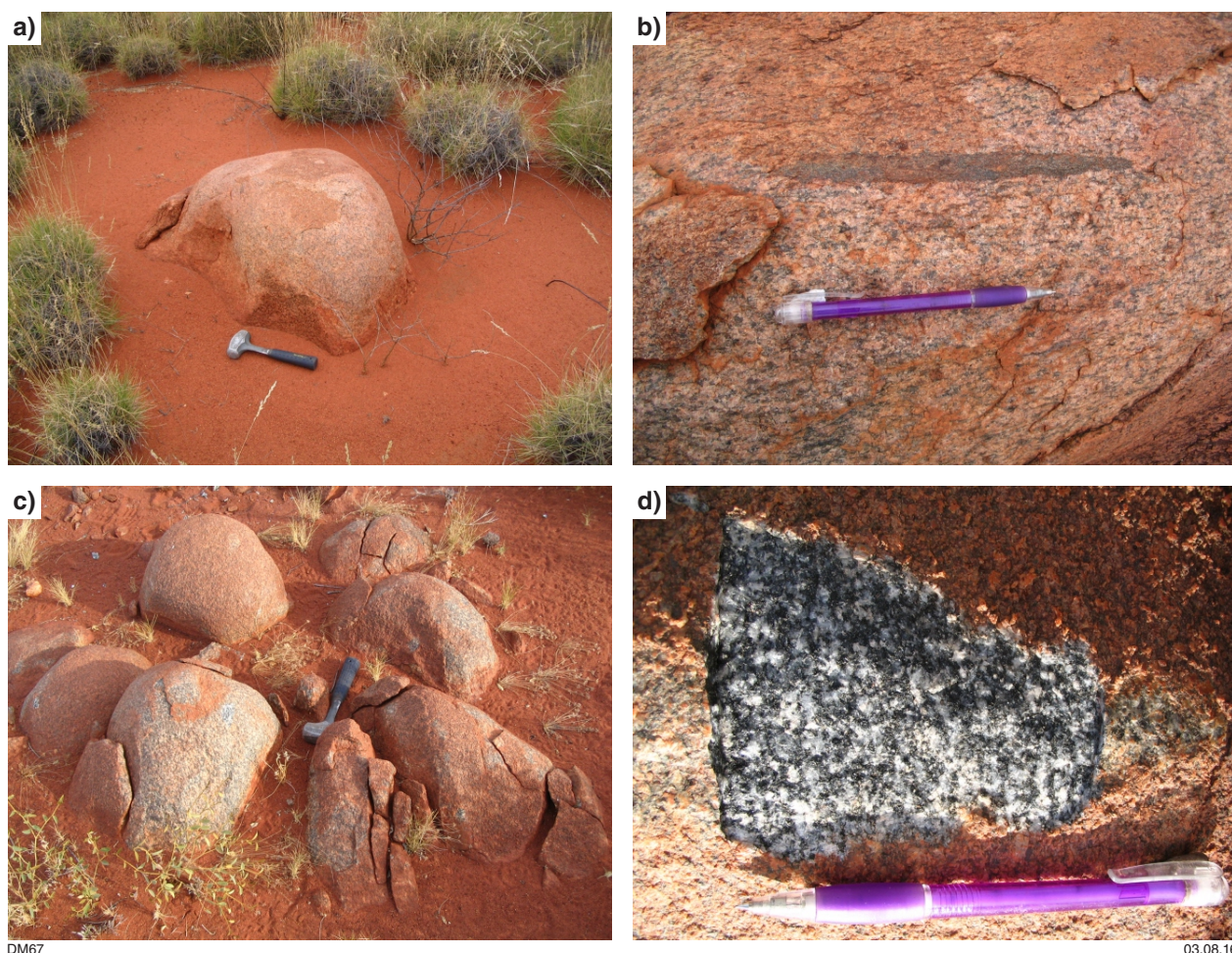


Figure 9. Outcrop photos of granitic rocks of the Krackatinny Supersuite in the Tabletop Terrane: a) typical tor-like exposure of granitic rocks in the northeastern Tabletop Terrane (MGA 531511E 7476210N); b) weakly to moderately foliated quartz-plagioclase-K-feldspar-biotite monzogranite containing well-foliated metasedimentary xenolith (MGA 531511E 7476210N); c) and d) quartz-biotite-K-feldspar-muscovite-plagioclase monzogranite, containing a variably developed foliation (MGA 515579E 7474860N)

Terranes where there is relatively good exposure and commonalities in their geological history. The structural evolution of the Tabletop Terrane is less well constrained due to poor outcrop but there is evidence that there may be differences in the nature and timing of some events. These differences include the presence of widespread magmatism of the Krakatanny Supersuite in the Tabletop Terrane, which is not known in the Connaughton and Talbot Terranes, and the generally low metamorphic grade of exposed rocks in the Tabletop Terrane, which contrasts with amphibolite to granulite facies rocks that dominate the other parts of the Rudall Province. The absolute timing of the deformational and metamorphic events remains relatively poorly constrained, limited by a paucity of geochronological data for the region.

Several regional-scale faults subdivide the region into distinct geological domains. The northwesterly to west-northwesterly trending Southwest Thrust – McKay Fault effectively forms the southwestern margin of the Rudall Province, although small basement inliers do occur

immediately to the southwest of this structure (Fig. 2). It is not known when this structure was initiated, but it was active as a southwesterly directed thrust fault during Neoproterozoic deformation (Hickman and Bagas, 1999; Bagas, 2004). The Southwest Thrust – McKay Fault merges with the north-northwesterly trending Vines Fault to the northwest, which strikes subparallel to the eastern margin of the Pilbara Craton. The northwesterly trending Camel–Tabletop Fault Zone forms another major structure within the Rudall Province, separating the Tabletop Terrane from the Talbot and Connaughton Terranes to the southwest (Fig. 2). The fault zone can be traced for at least 100 km, and likely extends considerably further beneath Neoproterozoic and younger cover, based on geophysical images. In addition to probable thrust or transpressional movement during the Miles and Paterson Orogenies, the Camel–Tabletop Fault Zone was also active in an extensional sense during Neoproterozoic basin development, localizing a narrow graben that is infilled by sedimentary rocks of the Tarcunyah Group (Bagas and Smithies, 1998b).

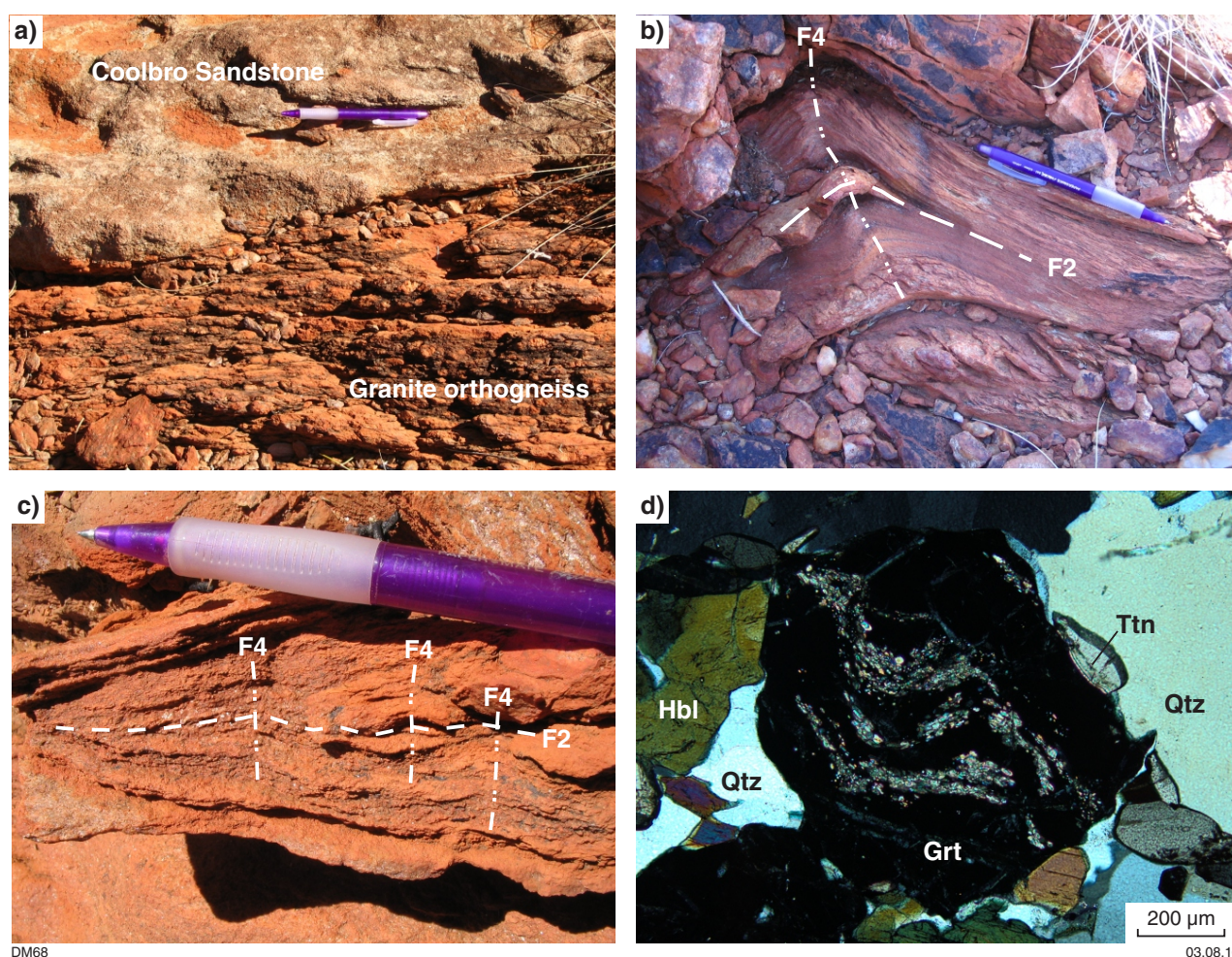


Figure 10. Outcrop photos and photomicrograph of D₁/D₂ structures in the Talbot and Connaughton Terranes: a) unconformable contact between underlying granitic gneiss of the 1800–1765 Ma Kalkan Supersuite and feldspathic arenite of the Neoproterozoic Coolbro Sandstone of the Yeneena Basin in the northwest Talbot Terrane (MGA 393587E 7510290N); b) and c) interpreted recumbent F₂ folds overprinted by upright, northwesterly trending F₄ folds and crenulations, Tracy Hills area, northwestern Talbot Terrane (MGA 404640E 7531370N); d) garnet-bearing amphibolite from Connaughton Terrane, about 9 km south of Parnngurr Community (MGA 457310E 7467800N). Peak metamorphic D₂/M₂ conditions of 700–750 °C and 10–12 kbar have been obtained from rocks in this area (Smithies and Bagas, 1997). Sigmoidal inclusion trails in garnet might represent an S₁ foliation

Table 1. Summary of tectono-thermal events in the Rudall Province, after Hickman and Bagas (1999) and Bagas (2004)

<i>Event</i>	<i>Name</i>	<i>Inferred age</i>	<i>Structure</i>	<i>Metamorphism</i>
D ₁	Yapungku Orogeny (early)	≥1802 ± 14 Ma	Layer-parallel schistosity (S ₁)	Low-pressure, mid-amphibolite facies (M ₁)
D ₂	Yapungku Orogeny (main)	1800–1765 Ma	Tight to isoclinal folds, WNW- to N-trending and overturned towards SSW (F ₂); NE-dipping schistosity (S ₂) with L ₂ stretching lineation in S ₂ typically parallel to F ₂ fold axes	Moderate- to high-pressure (to ~12 kbar), high-temperature, amphibolite–granulite facies (M ₂)
D ₃	Miles Orogeny (early)	Neoproterozoic*	Localized faulting along unconformity between Rudall Province and Yeneena Basin; localized recumbent folding in lower Yeneena Basin (F ₃)	None identified
D ₄	Miles Orogeny (main)	810–650 Ma?	Upright, tight to isoclinal NW-trending folds (F ₄) with steeply NE-dipping axial plane cleavage (S ₄); down-dip stretching lineations (L ₄) in S ₄ and associated anastomosing fault system	Lower greenschist facies (M ₄)
D ₅	–	650–550 Ma?	NE-trending open folds with SE-dipping axial planes (F ₅) and strike-slip faults	None identified
D ₆	Paterson Orogeny	c. 550 Ma?	N- to NW-trending dextral faults and ENE-striking sinistral faults; cleavage axial to conjugate kink bands; dextral reactivation of D ₄ faults	None identified

NOTE: * Alternatively, Clarke (1991) interpreted a high-grade D₃ event which pre-dated deposition of the Neoproterozoic Yeneena Basin

D₁ event

The earliest deformation (D₁) recognized in the Rudall Province occurs in the western part of the Talbot Terrane, where it consists of a poorly preserved, layer-parallel foliation that is in places folded by F₂ folds and overprinted by the S₂ foliation (Clarke, 1991; Hickman and Bagas, 1999; Bagas et al., 2000; Bagas, 2004). The foliation is defined by oriented micas in metasedimentary schists and by feldspar, quartz and mica in deformed orthogneiss (Hickman and Clarke, 1994). The S₁ foliation is associated with mineral assemblages including staurolite and andalusite that developed under low-pressure amphibolite facies conditions (Clarke, 1991; Smithies and Bagas, 1997). Inclusion trails of epidote, titanite and amphibole within M₂ garnet porphyroblasts in amphibolite, interpreted as possible relict S₁ (Smithies and Bagas, 1997), are the only potential evidence of this event reported from the Connaughton Terrane.

The D₁ event has not been directly dated but is considered to pre-date, or be synchronous with, the early stages of intrusion of the 1804–1762 Ma Kalkan Supersuite (Hickman and Bagas, 1999; Bagas, 2004). A granitic gneiss with a post-S₁ leucocratic component yielded a date of 1802 ± 14 Ma (Nelson, 1995i), which was considered by Bagas (2004) to provide a minimum age for D₁ deformation. Bagas (2004) suggested that D₁ might only marginally pre-date c. 1802 Ma if the D₁ event was the cause of magmatism and considered the D₁/M₁ event to represent an early phase of the Yapungku Orogeny (Hickman and Bagas, 1999; Bagas, 2004).

D₂ event (Yapungku Orogeny)

The D₂/M₂ event formed widespread northwesterly to north-northwesterly trending, tight to isoclinal folds (Fig. 10b,c) associated with the development of a pervasive regional S₂ schistosity and mineral lineation, L₂

(Clarke, 1991; Hickman and Clarke, 1994; Hickman and Bagas, 1999). The S₂ foliation is defined by aligned mica and quartz and is typically subparallel to the S₁ foliation, with the exception of F₂ fold hinges (Clarke, 1991). Hickman and Bagas (1999) backstripped the effects of Neoproterozoic folding to determine that the orientation of fold axes before this deformation was west-northwest, with folds overturned towards the south-southwest. This is consistent with the interpretation that the L₂ lineation reflects a northeasterly–southwesterly transport direction (Clarke, 1991). The S₂ foliation pervasively overprints most units within the Talbot and Connaughton Terranes, including granitic gneisses of the Kalkan Supersuite.

Thermobarometry of amphibolite and mafic granulite from the Connaughton Terrane indicates that the D₂/M₂ event attained peak conditions of ~800 °C and 12 kbar, indicating burial to depths of ~40 km, with a steeply decompressive retrograde path (Smithies and Bagas, 1997). Peak metamorphic conditions are less well constrained in the Talbot Terrane (Fig. 11a) but appear to have occurred at lower pressures and temperatures (Smithies and Bagas, 1997). A broadly west-northwesterly trending sillimanite–kyanite isograd has been defined that crosscuts the boundary between the Talbot and Connaughton Terranes, implying that the two zones were adjacent before peak metamorphism (Smithies and Bagas, 1997).

The D₂/M₂ event has been termed the Yapungku Orogeny (Smithies and Bagas, 1997; Bagas and Smithies, 1998b), who suggested that the high-pressure conditions reflected crustal thickening associated with a collision of the Rudall Province with an unknown continental block to the northeast. Subsequent interpretations have developed this interpretation to suggest that the colliding block was the North Australian Craton (Tyler, 2000; Betts and Giles, 2006; Cawood and Korsch, 2008; Huston et al., 2012; Johnson, 2013; Betts et al., 2016). The Yapungku Orogeny has not been directly dated but is generally considered to be

broadly coeval with the emplacement of the 1804–1762 Ma Kalkan Supersuite (Bagas and Smithies, 1998b; Hickman and Bagas, 1999; Bagas, 2004). The granitic gneisses of the Kalkan Supersuite contain a high-grade foliation assigned to S_2 , with the youngest date obtained from a K-feldspar augen granitic gneiss being 1765 ± 15 Ma (Nelson, 1995k), recalculated by Kirkland et al. (2013a) to 1762 ± 13 Ma. The currently accepted minimum age for the Yapungku Orogeny has been derived from dating of a felsic dyke considered to post-date the S_2 foliation, which yielded a date of 1778 ± 16 Ma (Nelson, 1995j), recalculated to 1773 ± 15 Ma by Kirkland et al. (2013a). Hickman and Bagas (1999) noted that the c. 1870 Ma and 1612 Ma spread of individual ages of zircons from this felsic dyke might in part be due to contamination from enclosing granitic gneiss but suggested that individual zircon analyses between c. 1765 and 1703 Ma reflect the emplacement age of the dyke and considered the D_2 event to be c. 1760 Ma. In a later evaluation of this sample, Bagas (2004) considered the weighted mean date of 1778 ± 16 Ma reflects the intrusion age of the felsic dyke, and suggested that the dyke could have been emplaced as late as the younger limit of uncertainty (1762 Ma), thus providing a younger age limit for the Yapungku Orogeny of c. 1765 Ma. The constraints provided by this felsic dyke are discussed in more detail below, and it is also possible to interpret that the felsic dykes and granitic rocks provide only a maximum age for deformation, rather than a minimum age (Maidment, 2014).

D₃ event

Deformation assigned to a D_3 event has been recognized by different authors but there are significant differences between the nature, timing and number of deformational events interpreted to have occurred in the period between the D_2 (Yapungku) and D_4 (Miles) Orogenies. Clarke (1991) recognized a D_3 event that pre-dated deposition of the Neoproterozoic Yeneena Basin. This event was considered to be characterized by upright to inclined, open to tight, northwesterly trending folds accompanied by an amphibolite facies S_3 axial plane foliation that crenulates S_2 that are unconformably overlain by basal conglomerate of the Yeneena Basin. This folding was considered to be responsible for fold interference patterns in the northwestern part of the Talbot Terrane.

In contrast, Hickman and Clarke (1994), Hickman and Bagas (1998, 1999) and Bagas (2004) considered that the third phase of deformation affected the Yeneena Basin and that all pre-Neoproterozoic folding was part of the Yapungku Orogeny. A major syncline and mesoscopic isoclinal folding affecting the northwestern Talbot Terrane and overlying sedimentary succession was interpreted as an F_3 synform overprinted by F_4 folding by Hickman and Clarke (1994), who considered the F_3 folds to have originally been recumbent and east–west or northeasterly trending. Hickman and Bagas (1998, 1999) noted that the contact between the Yeneena Basin and the underlying basement rocks in the northern part of the Talbot Terrane was faulted and quartz veined in places, and that this tectonized contact is offset by younger faulting assigned to

the D_4 event. This deformation was also assigned to their D_3 event. Bagas and Smithies (1998b) and Bagas (2004) considered this event to be an early stage of the Miles Orogeny, based on similarities in stress fields.

D₄ event (Miles Orogeny)

The Miles Orogeny is considered to be responsible for widespread, upright east-southeasterly to southeasterly trending folding of both Paleoproterozoic basement rocks and the Neoproterozoic cover succession (Fig. 11b–f; Clarke, 1991; Hickman and Clarke, 1994; Hickman and Bagas, 1999; Bagas, 2004). This event was termed the Paterson Orogeny in earlier mapping of the region (Clarke, 1991; Hickman and Clarke, 1994), but was renamed the Miles Orogeny in later studies (Hickman and Bagas, 1998; Bagas and Smithies, 1998b; Bagas, 2004), with the term Paterson Orogeny reassigned to a younger event. The Miles Orogeny reached lower greenschist facies metamorphic conditions and caused widespread retrograde metamorphism and alteration of the Rudall Province rocks, particularly along major structures. Crenulation of S_2 by F_4 folding is common in micaceous units (Fig. 12a).

D_4 deformation in the Yeneena Basin immediately to the north of the Rudall Province comprises upright to overturned, tight to isoclinal northwesterly trending folds with gentle plunges (Fig. 12b; Clarke, 1991; Hickman and Clarke, 1994; Hickman and Bagas, 1999; Bagas, 2004). The limbs of these folds are often sheared out along faults, which form a complex anastomosing network with displacements of up to 3 km or more on some structures (Hickman and Bagas, 1998). Farther to the north, folding is generally less intense and is open to tight in style (Hewson, 1996; Bagas, 2000). The Southwest Thrust – McKay Fault along the southwestern margin of the Rudall Province was active at this time and accommodated at least 4 km of movement during southwesterly directed thrusting (Hickman and Bagas, 1998, 1999). In the northwestern part of the Rudall Province, basement rocks have locally been thrust southwestwards over basal units of the Yeneena Basin along moderately northeasterly dipping thrust faults during this deformation (Fig. 12c,d). The Neoproterozoic sedimentary succession of the northwestern Officer Basin exposed to the southwest of the Southwest Thrust – McKay Fault is not deformed as strongly as similarly aged rocks of the Yeneena Basin to the northeast.

In the metamorphosed basement rocks of the Rudall Province, northwesterly striking, upright to inclined folding has been assigned to the same fold generation as similarly oriented folding in the Neoproterozoic cover succession. In contrast with the folding in the Yeneena Basin, fold axes in the basement rocks typically plunge more steeply to the northwest and southeast, which is considered to be the result of prior deformation (Hickman and Bagas, 1999). The trends of these folds are generally similar to those that formed during the Yapungku Orogeny but the lower metamorphic grade of S_4 foliations and the folding of the high-grade S_2 foliation in F_4 fold hinges distinguish the D_4 structures.

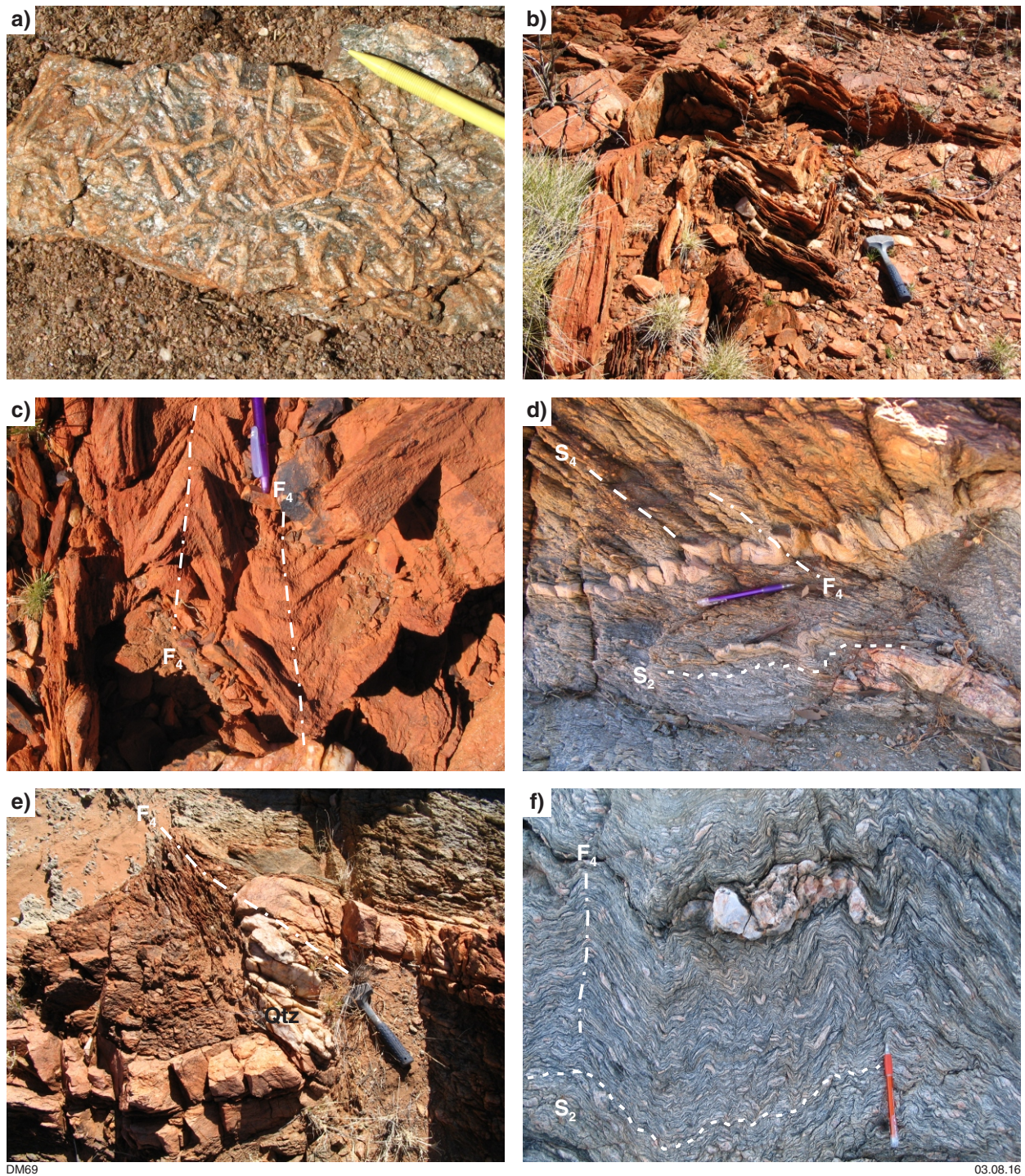


Figure 11. Outcrop photos of M₂ kyanite and F₄ folds in the Talbot Terrane: a) kyanite (M₂) developed within a thin metapelitic unit in the upper Fingoon Quartzite near Watrara Pool in the northwestern Talbot Terrane (MGA 405025E 7511250N); b) upright F₄ folds with steeply northwesterly plunging fold axes in the Butler Creek Formation near the northwestern end of the Fingoon Range (MGA 417130E 7500740N); c) upright, west-northwesterly trending F₄ folds with associated axial plane foliation that crenulates the layer-parallel S₂ foliation, Yandagoo Formation, Tracy Hills, northwestern Talbot Terrane (MGA 404640E 7531370N); d), e) and f) F₄/S₄ overprinting high-grade S₂ foliation in granitic gneiss of the 1800–1765 Ma Kalkan Supersuite, 2 km east of Rudall Crossing (MGA 414093E 7507160N). Narrow felsic dykes within the granitic gneiss also contain the S₂ foliation and are deformed by F₄ folds. In places, the relatively competent felsic dykes are fractured by attenuation on the limbs of F₄ folds and infilled by massive quartz (e)

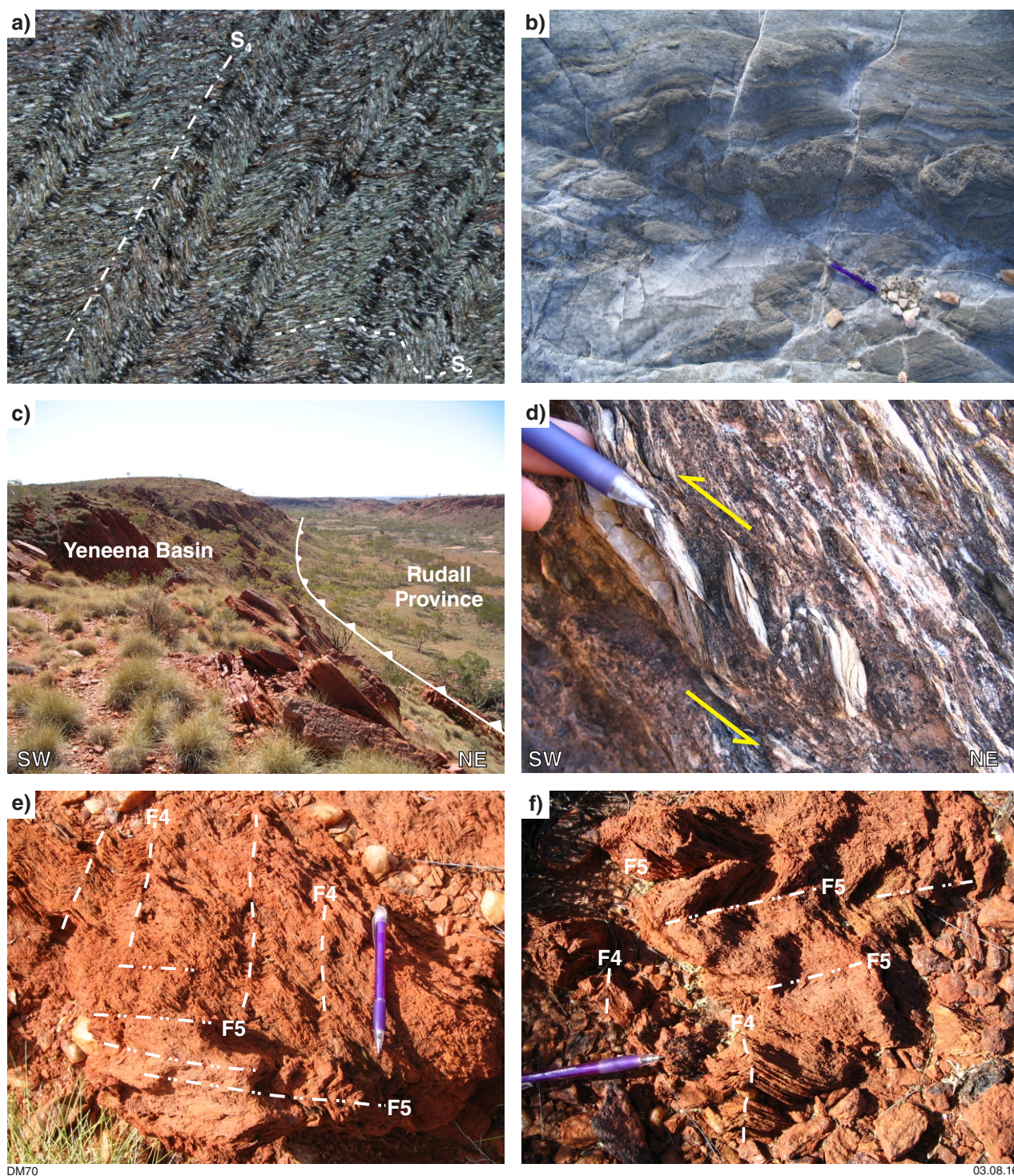


Figure 12. Photomicrograph and outcrop photos of D₄ and D₅ structures in the Talbot Terrane and Yeneena Basin: a) S₄ crenulation of S₂ foliation in pelitic schist of the Yandagoo Formation, Tracy Hills (MGA 404216E 7530825N); b) F₄ (Miles Orogeny) folding of feldspar-rich Coolbro Sandstone 2 km northeast of Rudall Crossing (MGA 413530E 7508150N); c) view to northwest along northeast-dipping D₄ fault that thrust Rudall Province basement above Neoproterozoic sedimentary rocks of the Yeneena Basin in the northwestern Talbot Terrane (MGA 404051E 7516550N); d) detail of thrust fault in Rudall Province basement, showing top-to-southwest shear sense indicators (MGA 404127E 7516670N); e) and f) interference between west-northwesterly trending F₄ folds and north-northeasterly trending folds interpreted as F₅ in metapelitic schist of the Yandagoo Formation near the Cassandra prospect (MGA 432109E 7485720N)

It has been difficult to establish a precise age for the Miles Orogeny, hampered in part by uncertainty regarding the depositional age of the Yeneena Basin succession, which provides a maximum age for the deformation. Bagas (2004) considered that the Miles Orogeny occurred between c. 1070 and 678 Ma, based on maximum depositional ages of c. 1070 Ma from the Lamil Group and an unpublished 678 ± 12 Ma U–Pb titanite date for a monzogranite of the O’Callaghans Supersuite, a series of granitic intrusions in the northern Paterson Orogen which crosscut D_4 structures in places. Based on these constraints, Bagas (2004) suggested a 750–720 Ma age for the Miles Orogeny, consistent with an unpublished 717 ± 5 Ma $^{40}\text{Ar}/^{39}\text{Ar}$ phlogopite date for mineralization at the Maroochydore copper deposit in the Yeneena Basin (Reed, 1996), and potentially coeval with the Areyonga Movement in the Amadeus Basin ~700 km to the east-southeast (Wells et al., 1970).

More recent geochronological data have provided further constraints on the age of the Miles Orogeny. Maximum depositional ages of 950–850 Ma for units in the Yeneena Basin (Bagas and Nelson, 2005; Maidment et al., 2008), a c. 858 Ma interpreted age of diagenesis for the Isdell Formation (Whitaker et al., 2010) and dates of 835–816 Ma for deformed mafic intrusive rocks (Reed, 1996; Huston et al., 2010) confirm that the Miles Orogeny took place at or after c. 815 Ma. Huston et al. (2010) suggested that the Miles Orogeny caused inversion of the Yeneena Basin shortly after its deposition — possibly c. 810 Ma — and was a driver for fluid flow that resulted in the formation of both sediment-hosted copper deposits in the Yeneena Basin and unconformity-related uranium mineralization in the Rudall Province. This is consistent with Pb–Pb and Sm–Nd dates of 811 ± 39 and 791 ± 42 Ma, respectively, for mineralization at the Nifty copper deposit (Cross et al., 2011) and possibly also by 841 ± 10 Ma and $837 \pm 35/-31$ Ma dates for pitchblende mineralization in interpreted D_4 structures at the Kintyre uranium deposit (Huston et al., 2010; Cross et al., 2011).

An alternative interpretation is that the Miles Orogeny took place closer to c. 650 Ma, as part of the same event that generated granitic rocks of the O’Callaghans Supersuite, which yield U–Pb zircon and titanite dates between c. 678 and 607 Ma but mostly 645–625 Ma (Dunphy and McNaughton, 1998; Bagas, 2004; Maidment et al., 2010).

$^{40}\text{Ar}/^{39}\text{Ar}$ dates of 671–646 Ma for muscovite in the northern Rudall Province and overlying Yeneena Basin (Durocher et al., 2003) reflect a thermal event of similar age but were obtained from an area distant from any granitic intrusions and might thus reflect the effects of deformation and crustal thickening rather than contact metamorphism. This timing is consistent with a 652 ± 7 Ma U–Pb monazite date for a concordant reef at the Telfer Au–Cu deposit (Maidment et al., 2010), considered to have formed in an anticlinal structure that developed during the Miles Orogeny. More regionally, similarly aged intraplate tectonism has also been identified in the western Musgrave Province of central Australia, with dates of 628 ± 4 and 631 ± 12 Ma for metamorphic zircon (Kirkland et al., 2014a; Kirkland et al., 2014b),

623 ± 5 Ma for metamorphic muscovite (Kirkland et al., 2013c) and 625 ± 11 Ma for pegmatite (Kirkland et al., 2011b). This is similar to the timing of the Rinkabeena Movement in the Ngalia and Georgina Basins of central Australia (Wells and Moss, 1983), which generated horst-like structures in an interpreted dextral shearing regime (Edgoose, 2013).

D₅ event

Localized, northeasterly trending open folds with southeasterly dipping axial planes that re-fold D_4 structures have been described in the northwestern Officer Basin and parts of the Rudall Province (Fig. 12e,f; Bagas, 2004). In the Officer Basin, this deformation has been termed the Blake Movement, which developed during northwesterly directed compression against the southeastern margin of the Pilbara Craton (Williams, 1992, 1994). The timing and driver of this deformation is unclear, with suggestions that it reflects relaxation following the Miles Orogeny (Hickman and Clarke, 1994; Hickman and Bagas, 1999), or deformation associated with the younger (D_6) Paterson Orogeny (Bagas and Smithies, 1998b; Bagas, 2004). The D_5 event does not appear to be a major event in the Rudall Province and has no associated metamorphic overprint.

D₆ event (Paterson Orogeny)

The last deformational event documented in the Rudall Province is the Paterson Orogeny. This event has been associated with subvertical north- to northwesterly striking dextral faults, east-northeasterly striking sinistral faults and east to east-southeasterly trending open folds (Hickman and Clarke, 1994; Hickman and Bagas, 1998; Bagas, 2004). Bagas (2004) placed these structures within a south-southwesterly directed shortening regime, which reactivated northwesterly trending D_4 structures in a dextral transpressional sense. The amount of shortening and deformation is difficult to quantify but, if significant movements did occur during this period, most movement is likely to have been partitioned into the Southwest Thrust – McKay Fault and the Camel–Tabletop Fault Zone (e.g. Bagas, 2004), since displacements on other structures appear to be relatively minor.

The timing of the Paterson Orogeny is also imprecisely constrained. Deformation assigned to the Paterson Orogeny affected the Boondawari Formation of the northwestern Officer Basin (Bagas, 2004), which has an inferred age of 635–580 Ma. Other dates which might reflect isotope resetting or cooling associated with the Paterson Orogeny in the Talbot Terrane include a K-feldspar $^{40}\text{Ar}/^{39}\text{Ar}$ date of 554 ± 7 Ma (Durocher et al., 2003) and a 595 ± 27 Ma Rb–Sr date obtained from granitic gneiss (Chin and de Laeter, 1981). It is evident that the number, character and timing of Neoproterozoic deformational events remain open questions. The Neoproterozoic structural evolution of the Paterson Orogen has particular significance given that the two major periods of mineralization in the region took place at 840–810 Ma and 655–605 Ma (Huston et al., 2010).

Late-stage dolerite dykes

Numerous weakly deformed dolerite dykes occur over a wide area of the Paterson Orogen, intruding both the Rudall Province and Neoproterozoic rocks of the Yeneena and Officer Basins. These dykes form prominent linear magnetic highs on aeromagnetic images, with a typically north–south to north-northwesterly trend. These dykes have not been dated but crosscut structures associated with the Miles and Paterson Orogenies and pre-date deposition of Carboniferous–Permian sedimentary rocks of the Canning Basin. One possibility is that they form part of the c. 510 Ma Kalkarindji Supersuite, which forms a large igneous province dated at 508 ± 5 Ma in the northwestern Officer Basin (Macdonald et al., 2005).

U–Pb zircon geochronology

Thirteen samples of metasedimentary and igneous rocks were collected from the Talbot, Connaughton and Tabletop Terranes to provide better constraints on the main episodes of sedimentation, magmatism and metamorphism in the Rudall Province. Samples of quartzite and quartzofeldspathic schist were sampled from the Talbot Terrane to build on the single metasedimentary sample previously dated from the area (Nelson, 1995e), and quartzite samples from the Connaughton and Tabletop Terranes represent the first definitively metasedimentary samples to be dated from these terranes. Several samples of granitic rock were collected from the poorly exposed Tabletop Terrane to better understand the magmatic history in this area, which contains high Sr/Y tonalitic intrusions possibly emplaced in an arc setting (Smithies and Bagas, 1998).

Analytical methods

Samples were crushed and milled at the Mineral Separation Laboratory at Geoscience Australia. Mineral density separation was undertaken using a Wilfley table with multiple iterations employed to reduce the sample to ~1–2% of its post-milling weight. Highly magnetic minerals were removed by hand magnet before magnetic separation using a Frantz isodynamic separator. Handpicking of zircons from igneous samples focused on unfractured grains from the fraction with the weakest paramagnetism. For metasedimentary samples, a random selection of zircon grains was separated from the least paramagnetic fraction, with the aim of sampling a representative spread of the detrital source regions, while minimizing the proportion of metamict grains. Zircon grains were mounted with zircon standards QGNG and SL13 in epoxy resin disks and polished to expose grain interiors. Mounts were documented before analysis by reflected and transmitted light photomicroscopy and cathodoluminescence (CL) imaging on a Hitachi S-2250N scanning electron microscope.

U–Pb analyses were undertaken using the SHRIMP ion microprobes at the John de Laeter Centre of Curtin University in Perth. Analytical procedures adopted follow those of Compston et al. (1984), Claoué-Long

et al. (1995) and Nelson (1997). Data were reduced using SQUID 2.50.09.06.12 (revision of Ludwig, 2009) and Isoplot 3.71.09.06.01 (revision of Ludwig, 2003) add-ins for Microsoft Excel 2003, with decay constants recommended by Steiger and Jäger (1977). Corrections for common Pb used measured ^{204}Pb and compositions of crustal common Pb modelled by Stacey and Kramers (1975). Calibration of Pb/U ratios assumed a $^{206}\text{Pb}/^{238}\text{U}$ age of 1842 Ma for zircon standard QGNG (Black et al., 2003) and the $^{207}\text{Pb}/^{206}\text{Pb}$ measurement of this standard was used to monitor the accuracy of measured $^{207}\text{Pb}/^{206}\text{Pb}$ in grains of unknown age. For each analytical session, the weighted mean $^{207}\text{Pb}/^{206}\text{Pb}$ age for QGNG (denoted $^{207}\text{Pb}/^{206}\text{Pb}_{\text{QGNG}}$) is calculated (Appendix 1). These values were within analytical uncertainty of the c. 1851 Ma $^{207}\text{Pb}/^{206}\text{Pb}$ age established for this standard and no adjustments for instrumental mass fractionation were required.

Discordance of 204-corrected dates is calculated as $100 \times [1 - (^{206}\text{Pb}/^{238}\text{U} \text{ date}) / (^{207}\text{Pb}/^{206}\text{Pb} \text{ date})]$. Analyses <10% discordant were used for assessment of detrital zircon ages and for calculating weighted mean ages, the uncertainties of which are quoted at the 95% confidence level. Individual analyses are quoted at the 1σ level.

GA 2005670100 – quartz–feldspar–muscovite schist, Talbot Terrane

Quartz–K-feldspar–muscovite schist was sampled from the northwestern Talbot Terrane (Fig. 13; MGA 401083E 7507460N) in an area where unassigned metasedimentary schist occurs adjacent to layered granitic orthogneiss. Hickman and Bagas (1999) suggested that these metasedimentary rocks might pre-date the layered orthogneiss and thus comprise some of the oldest rocks in the Talbot Terrane.

The sample (Fig. 14a,b) contains a high-grade, layer-parallel foliation defined by medium- to coarse-grained muscovite, which is folded about mesoscale tight, upright, northwesterly trending F_4 folds. The schist forms part of a compositionally layered unit defined by differing abundances of quartz, muscovite and feldspar (Fig. 4c). In thin section, the schist consists of thin interlayered domains of granoblastic medium-grained quartz, microcline and lesser plagioclase, bound by laminae of layer-parallel muscovite, which comprises up to 15% of the rock (Fig. 14c).

Zircons from the schist are slightly elongate irregular subhedral grains and fragments up to 250 μm long, with some of the larger fragments from grains that were originally >250 μm long (Fig. 15a). Some grains have relatively pristine crystal faces, whereas others have faces that are less sharply defined, with complex surface irregularities and pitting. The zircons are generally red–brown, with larger grains opaque to translucent in transmitted light, possibly reflecting radiation damage. In CL images, the grains have a uniformly dark appearance, with a few having thin, discontinuous rims of bright zircon a few micrometres thick (Fig. 15b). Zoning patterns are difficult to distinguish but where visible

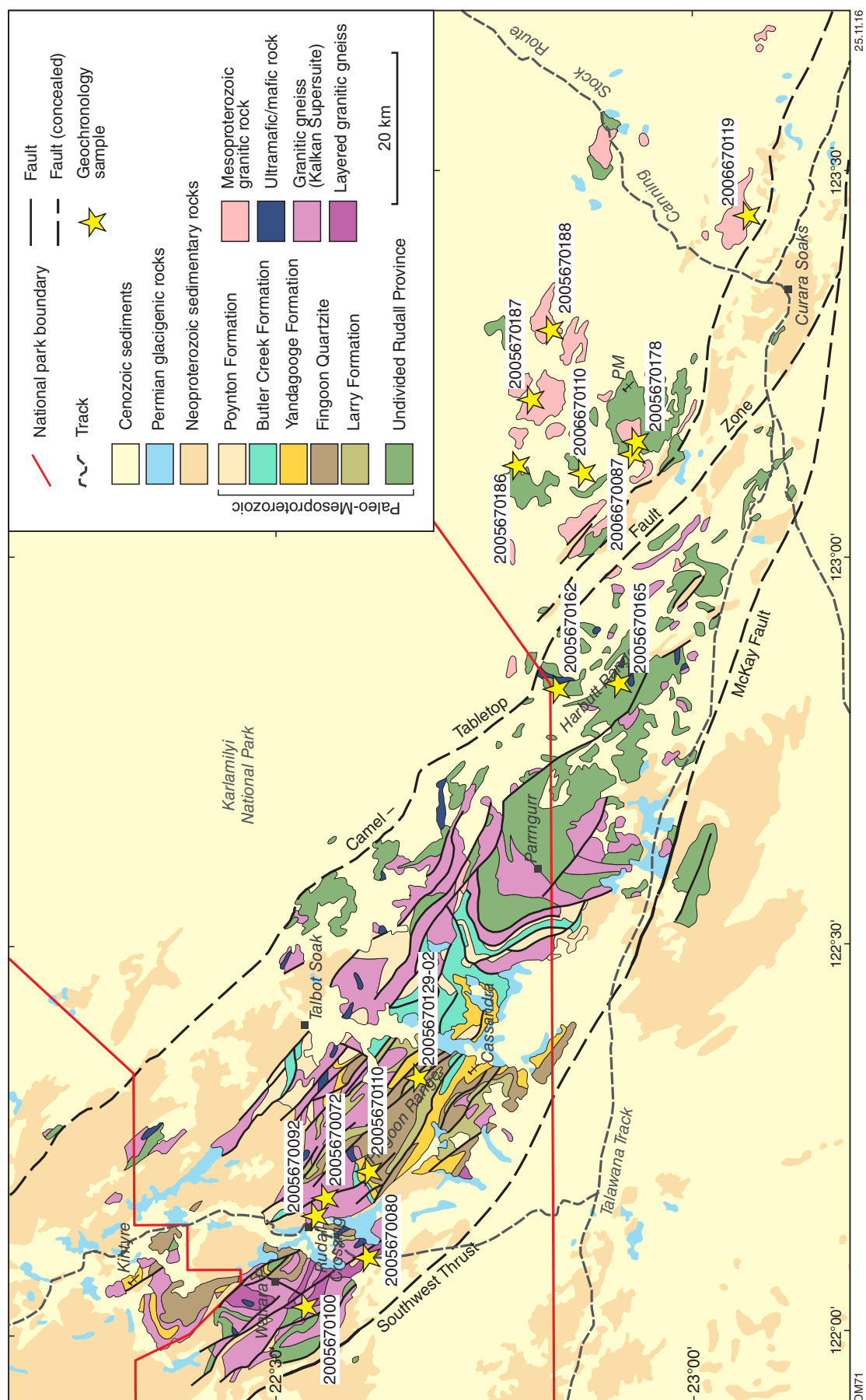


Figure 13. Locations of U–Pb geochronology samples on simplified outcrop geology map of the Rudall Province, modified from Geoscience Australia 1:1 000 000 outcrop geology map

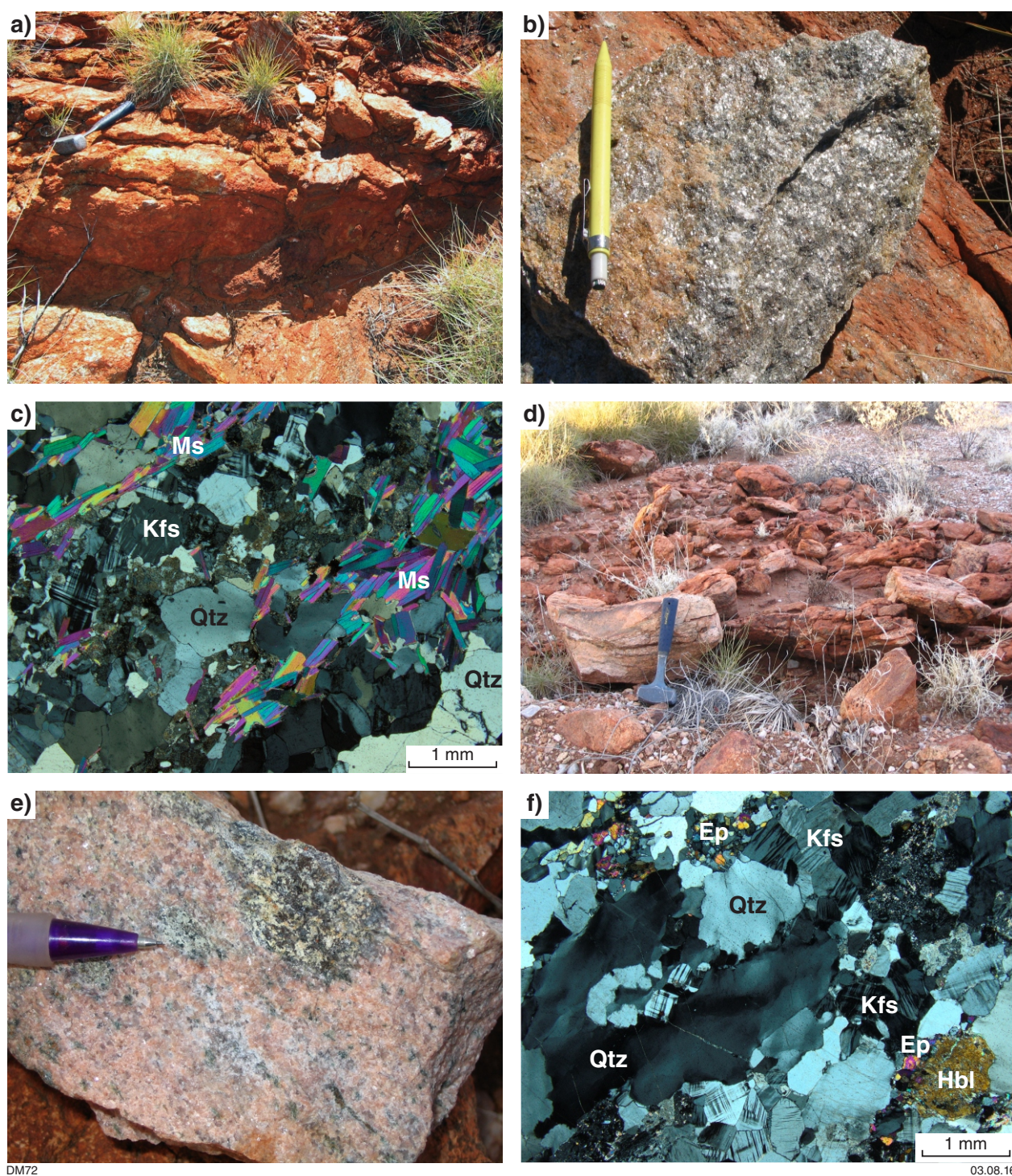


Figure 14. Outcrop photos and photomicrograph of quartz-feldspar-muscovite schist and granitic gneiss, Talbot Terrane: a) quartz-feldspar-muscovite schist sample site (GA 2005670100); b) hand specimen of quartz-feldspar-muscovite schist; c) thin-section image of quartz-feldspar-muscovite schist, showing muscovite folia separating quartzofeldspathic domains in cross-polarized light (XPL); d) outcrop photo of layered orthogneiss sample site (GA 2005670080), Talbot Terrane; e) hand specimen of layered orthogneiss, showing biotite-rich aggregate (xenolith?) in monzogranite; f) thin section image of layered orthogneiss (XPL)

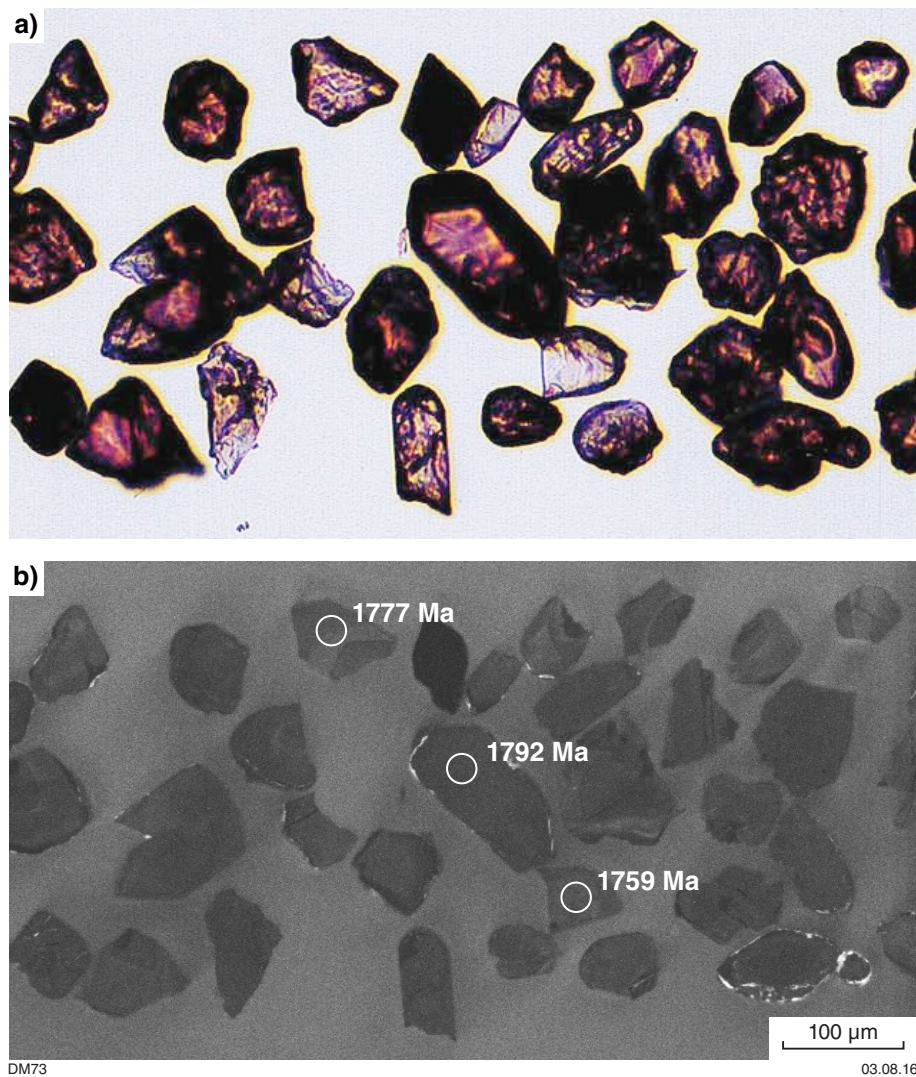


Figure 15. Images of zircons from quartz-feldspar-muscovite schist, Talbot Terrane (GA 2005670100): a) transmitted light; and b) CL image, showing relatively uniform intensity and zoning patterns, with analysis sites

consist of broad concentric zones or oscillatory zoning. Some of the more opaque grains have irregular patches of slightly darker zircon that are also less reflective in optical imaging. These were avoided in analysis as zones of potential radiation damage. No cores of significantly different CL intensity are apparent.

All of the 29 analyses are concordant to near-concordant, with moderate to high U contents (441–1777 ppm), Th/U of 0.09 – 0.32 and $^{207}\text{Pb}^*/^{206}\text{Pb}^*$ dates of 1792–1773 Ma (Fig. 16; Table A2-1). This group has a weighted mean date of 1780 ± 2 Ma (MSWD = 1.05). A single analysis of a near-concordant grain with the highest U content of 4153 ppm (5.1) has a significantly younger date of c. 1759 Ma and is interpreted to have undergone a small amount of ancient radiogenic Pb loss.

The muscovite-rich character and compositional layering of the schist are consistent with a metasedimentary

origin for this unit but the uniform character and age of the zircons raises the question as to whether the sampled layer might instead represent a highly deformed igneous rock. It is difficult to discriminate confidently between these alternatives but the muscovite-rich character is perhaps more consistent with a metasedimentary protolith given the commonly biotite-rich, muscovite-poor and porphyritic character of granitic gneisses in the Rudall Province, although a few muscovite-bearing units have been interpreted as orthogneisses (Hickman and Bagas, 1998). The irregular surfaces of some zircons and the possible rounding of crystal terminations might also be evidence of limited sedimentary transport and abrasion, but metamorphic processes might also have modified these grains. The 1780 ± 2 Ma date for this rock is thus tentatively interpreted as a maximum depositional age for a metasedimentary protolith to the schist, which might have

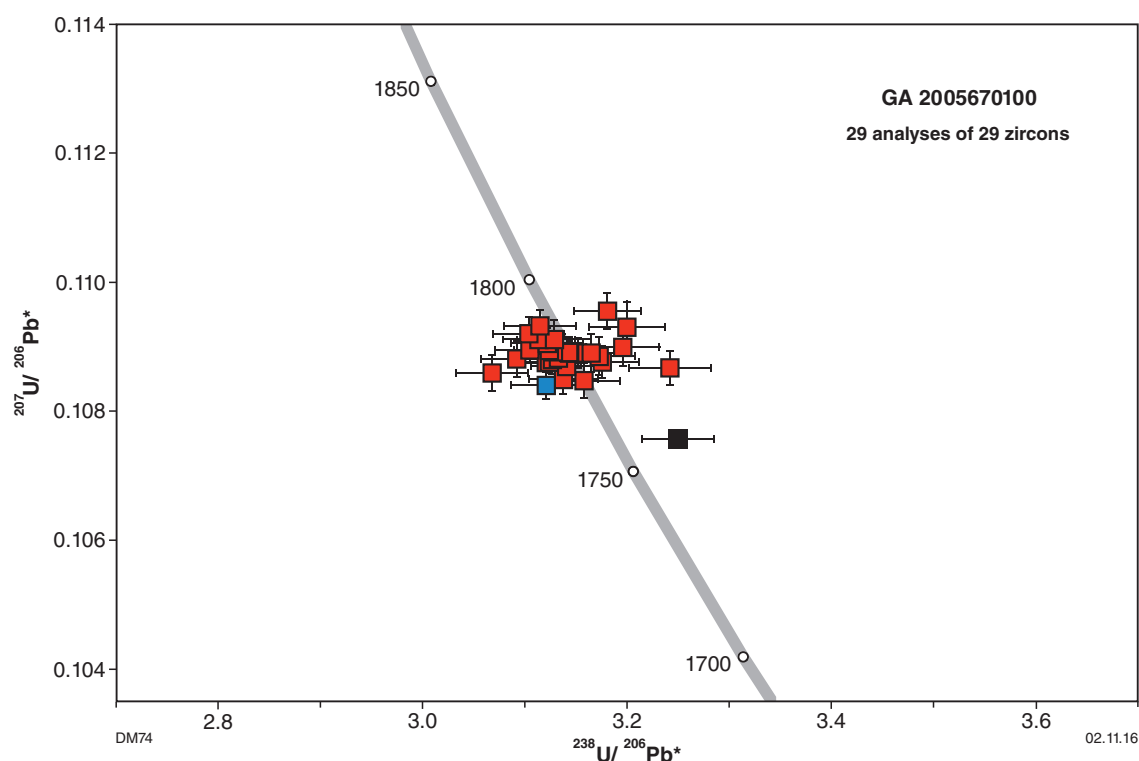


Figure 16. U–Pb analytical data for zircons from quartz–feldspar–muscovite schist, Talbot Terrane (GA 2005670100)

been an immature feldspar-rich sandstone or siltstone. A volcanic or volcanoclastic origin is also a possibility, although the lack of acicular zircons and the muscovite-rich character of the schist are more consistent with a metasedimentary unit derived from a granitic source. Given the deformed and metamorphosed nature of this unit, however, a magmatic age remains a possible interpretation and further dating of the metasedimentary succession is required to provide more confidence in the interpretation of this date.

GA 2005670080 – granitic gneiss, Talbot Terrane

A unit of compositionally layered granitic gneiss was sampled from the southwestern part of the Talbot Terrane (Fig. 13; MGA 407035E 7499300N), where it comprises poorly exposed quartz–feldspar–biotite gneiss with sporadic xenoliths of amphibolite, ultramafic rock and metasedimentary rock (Hickman and Bagas, 1998). The gneiss contains centimetre-scale layering defined by variable proportions of feldspar and biotite and thin lenses of biotite aggregates up to 3 cm across. The sampled rock consists of an equigranular, relatively homogeneous, medium-grained granitic gneiss containing no obvious xenoliths (Fig. 14d,e). In thin section, the sample consists of granoblastic quartz and K-feldspar aggregates that define a high-grade foliation, with subsidiary plagioclase and minor hornblende (Fig. 14f). Minor retrograde alteration is evident, with some sericitic alteration of K-feldspar and epidote associated with mafic minerals.

Zircons from the granitic gneiss consist of red–brown, euhedral to subhedral, equant to elongate prismatic grains up to 200 µm long (Fig. 17a). In CL images, most grains have dark, oscillatory zoned cores with a thin, bright structureless rim typically a few micrometres thick but up to 25 µm thick on a few grains (Fig. 17b). A relatively small proportion of the dark oscillatory zoned cores also contain cores of moderate intensity, oscillatory zoned zircon.

Thirty-eight analyses were obtained from 33 zircons. Thirty-two analyses were obtained from zircon cores (Fig. 18). Two of these (7.1 and 18.1) are >10% discordant and are not considered further. Twenty-three analyses of dark CL cores yielded $^{207}\text{Pb}^*/^{206}\text{Pb}^*$ dates of 1818–1757 Ma (Table A2-2). Nineteen analyses indicate moderate to high U contents (376–1020 ppm), Th/U of 0.14 – 0.59, and a weighted mean $^{207}\text{Pb}^*/^{206}\text{Pb}^*$ date of 1804 ± 3 Ma (MSWD = 1.5). This date is interpreted to be the age of crystallization of the igneous protolith and slightly extends the older age limit of the Kalkan Supersuite. Four analyses of dark CL cores with near-concordant dates of 1785–1757 Ma have on average higher U contents than the main group (686–1148 ppm) and are interpreted to have lost a small amount of radiogenic Pb during younger metamorphism. Seven analyses of moderate CL intensity cores within dark CL zircon have moderate U contents (216–799 ppm), Th/U of 0.08 – 0.66 and $^{207}\text{Pb}^*/^{206}\text{Pb}^*$ dates of 2453–1845 Ma. These are interpreted to be xenocrysts incorporated within the granitic protolith.

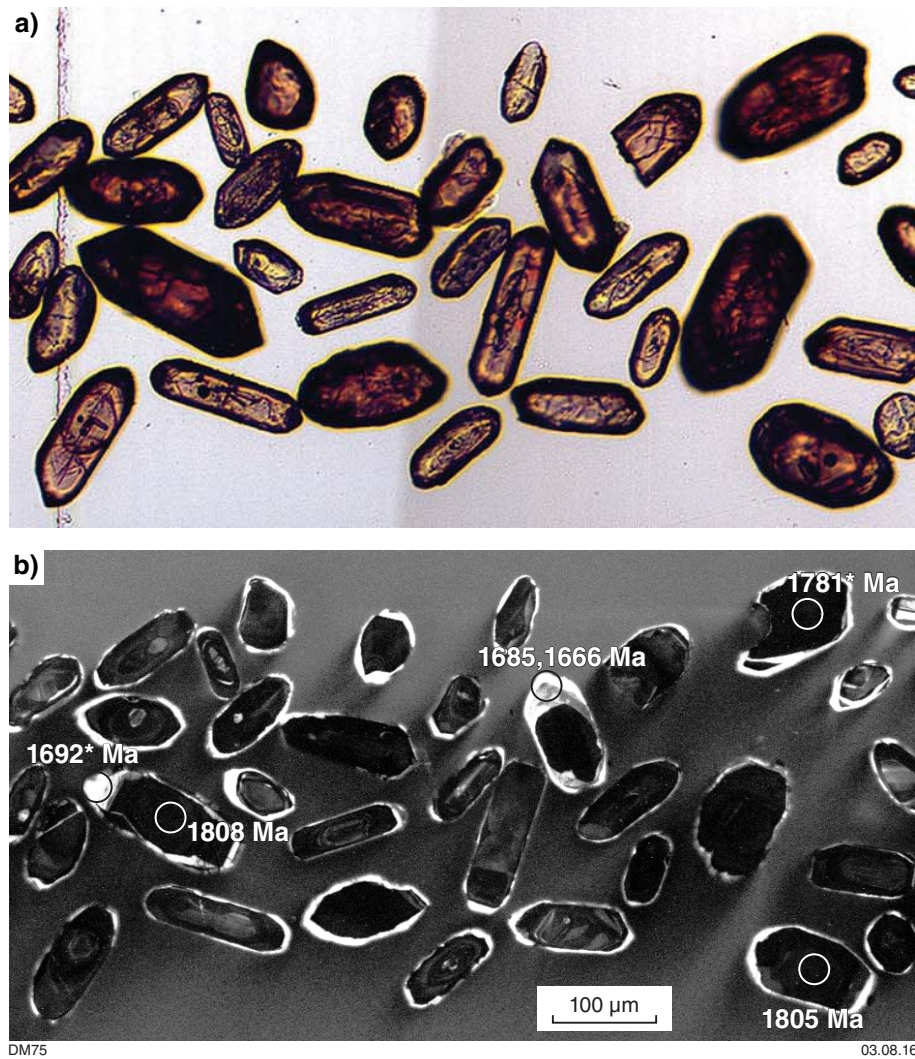


Figure 17. Images of zircons from granitic gneiss, Talbot Terrane (GA 2005670080): a) transmitted light; b) CL image, showing dark magmatic cores and bright recrystallized rims; * indicates analysis >10% discordant

Six analyses were obtained from bright CL rims, with two (4.2 and 6.3) repeat analyses of prior analysis sites. These rim analyses indicate low U contents (33–157 ppm) and low Th/U ratios (0.01 – 0.52). Two analyses (5.1 and 8.1) are >10% discordant and have a high proportion of common Pb, yielding unreliable and imprecise dates that are not considered further. The remaining four analyses define a statistically coherent group with $^{207}\text{Pb}^*/^{206}\text{Pb}^*$ dates ranging between c. 1687 Ma and 1662 Ma and yield a weighted mean date of 1679 ± 25 Ma (MSWD = 0.21). This date is interpreted to reflect the timing of a high-grade metamorphic event.

GA 2005670129-02 – quartz–feldspar–muscovite schist, Larry Formation, Talbot Terrane

The Larry Formation was sampled from Larry Creek in the southeastern Fingoon Range (Fig. 13; MGA 431181E

7493130N). In this area, the Larry Formation consists of quartz–feldspar–mica schist and gneiss with centimetre-to decimetre-scale layering (Fig. 19a,b), which has been interpreted as a feldspar-rich metasedimentary package (Hickman and Bagas, 1998). The unit contains a pervasive layer-parallel high-grade foliation, interpreted as S_2 , which has been deformed by tight, northwesterly plunging, moderately northeasterly inclined to recumbent folds, possibly F_4 . The unit is intruded by small quartz–K-feldspar pegmatite bodies that are subparallel to layering but do not contain the layer-parallel foliation and are tightly folded by the northwesterly trending folds. Metasedimentary rocks of the Larry Formation rocks are generally highly weathered, with dissected plateaus in the area indicating proximity to a Tertiary weathering surface (Hickman and Bagas, 1998). This has resulted in the pervasive weathering of feldspars and micas to sericite and clays, although primary textures are typically preserved.

In thin section, the sampled layer consists of granoblastic quartz aggregates in a clay-rich, quartz-poor groundmass

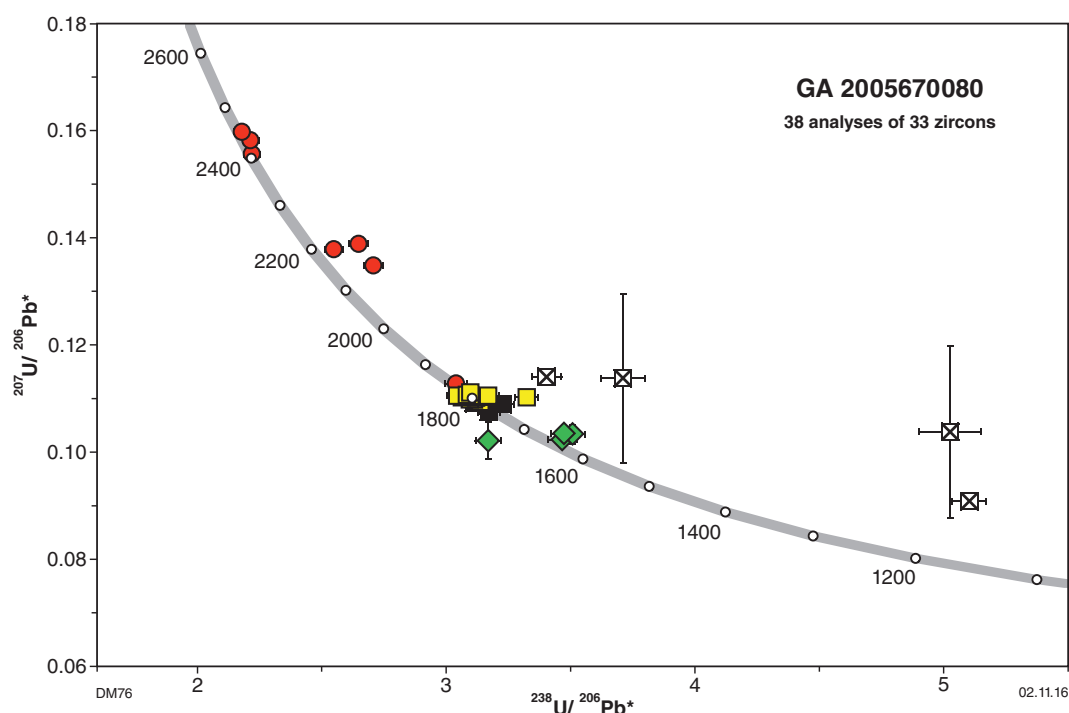


Figure 18. U–Pb analytical data for zircons from layered orthogneiss, Talbot Terrane (GA 2005670080)

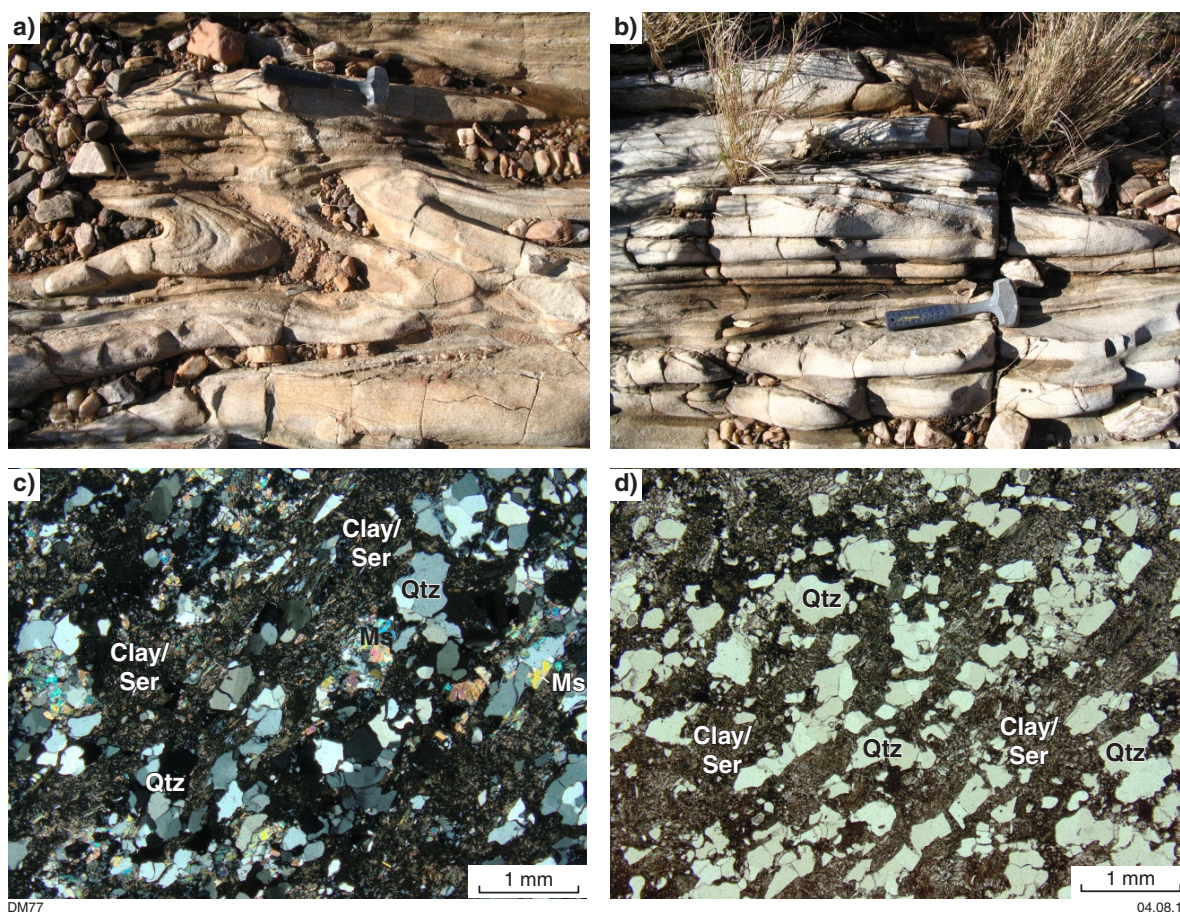


Figure 19. Outcrop photos and photomicrographs of quartz–feldspar–muscovite schist, Larry Formation, Talbot Terrane: a) and b) layered quartz–feldspar–muscovite rock, interpreted as a metasedimentary rock; c) thin-section image of Larry Formation sample (GA 2005670129-2), showing quartz and muscovite in a clay- and sericite-rich weathered matrix after feldspar and mica (XPL); d) plane-polarized (PPL) thin section image of Larry Formation sample, showing quartz- and (originally) feldspar-rich layers

(Fig. 19c,d). Relict muscovite within some clay pseudomorphs suggests that muscovite may have been the dominant mica. Subordinate equigranular and structureless clay-rich grains may have been derived from weathering of feldspar. Numerous thin laminae of granoblastic quartz aggregates generally <1 mm thick within the clay-rich groundmass contain fine- to medium-grained muscovite that has been armoured from weathering. The pre-weathering lithology is considered to have been a quartz–muscovite–feldspar ± biotite schist.

Zircons from the sample are equant, colourless to light brown, subhedral to irregular and typically 100–250 µm long (Fig. 20a). The surfaces of most grains are irregular, though primary magmatic faces are evident on some grains. In CL images, the grains have similar moderate intensities and oscillatory zoning (Fig. 20b). Many of the zircons have very thin, irregular bright rims up to 10 µm thick, which in some grains forms embayments into oscillatory zoned zircon.

Eighteen analyses (Fig. 21) indicate U contents of 125–380 ppm, Th/U of 0.94 – 1.42 and $^{207}\text{Pb}^*/^{206}\text{Pb}^*$ dates of 1771–1741 Ma (Table A2-3), with a weighted mean date of 1760 ± 5 Ma (MSWD = 0.83). This date is tentatively interpreted as the age of a local granitic source that dominated the provenance of the sedimentary protolith and is thus interpreted as a maximum depositional age for the Larry Formation. The interpretation of a detrital origin is consistent with the compositional layering in the sampled unit, the

muscovite-rich compositions and the lack of phenocrysts, although these features are not sufficient to demonstrate a sedimentary origin. The irregular surfaces on many zircon grains could be a result of abrasion during sedimentary transport but modification by in situ metamorphic processes is also possible. Given these uncertainties, it is also possible to interpret the 1760 ± 5 Ma date as the timing of magmatic crystallization of a deformed igneous protolith that intruded the unit, in which case this date would provide a minimum rather than maximum age for the Larry Formation.

GA 2005670110 – quartzite, Fingoon Quartzite, Talbot Terrane

The Fingoon Quartzite was sampled from the Fingoon Range in the central Talbot Terrane (Fig. 13; MGA 418265E 7500080N). At this location (Fig. 22a), muscovite-bearing quartzite consists of thickly layered units folded by upright northwesterly trending, open to close folds overprinted by a north-northwesterly striking fracture cleavage which forms a foliation in more muscovite-rich layers. In thin section, the quartzite consists of a mosaic of medium-grained quartz with narrow zones of fine-grained recrystallized quartz along grain boundaries (Fig. 22b). Muscovite is fine-grained, comprising about 5–10% of the rock, and has a weak preferred orientation.

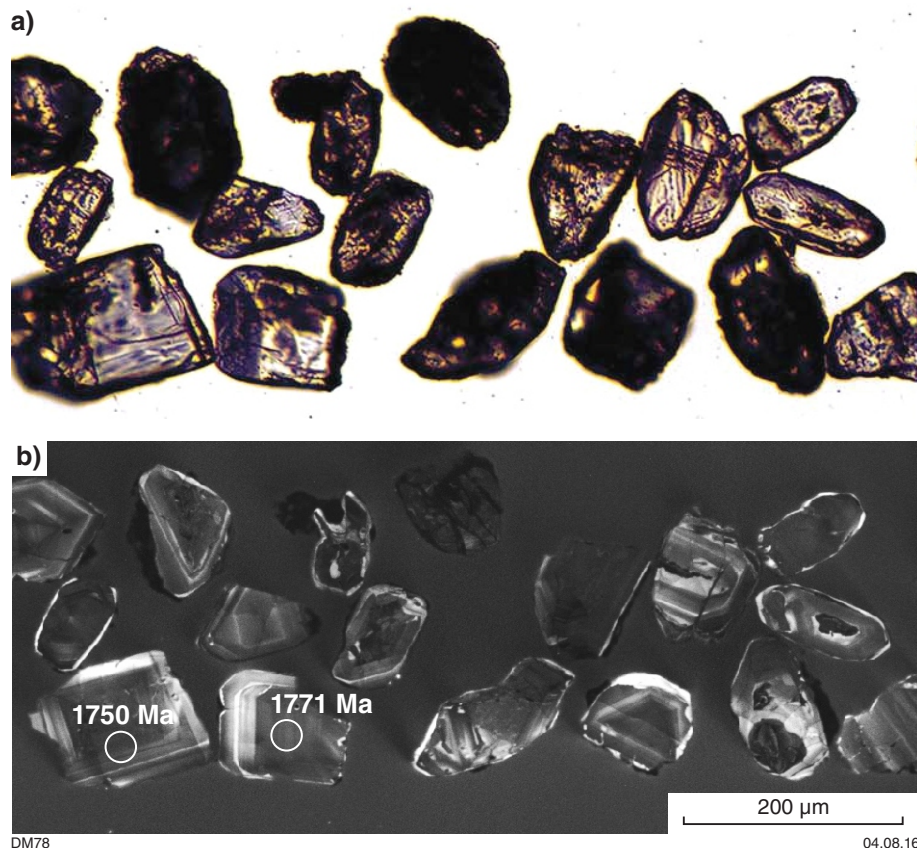


Figure 20. Images of zircons from quartz–feldspar–muscovite schist, Larry Formation, Talbot Terrane (GA 2005670129-02): a) transmitted light, showing modified euhedral forms; b) CL image showing the relatively uniform character of zircons

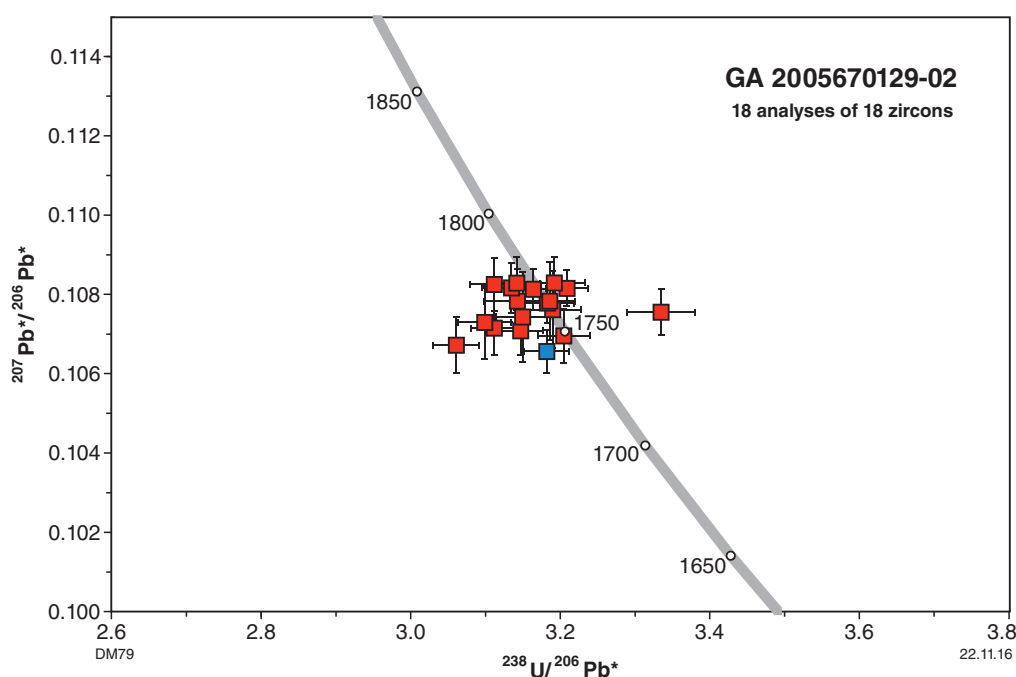


Figure 21. U–Pb analytical data for zircons from quartz–feldspar–muscovite schist, Larry Formation, Talbot Terrane (GA 2005670129-02)

Zircons from the quartzite are typically relatively equant, irregular to subhedral and <100 µm long (Fig. 23a). In CL images, most grains show oscillatory zoning and have a range of brightness (Fig. 23b). Many grains have very thin, dark rims of unzoned zircon.

Eighty-two analyses were obtained from 81 zircon cores, with the dark rims too thin to be analysed (Fig. 24; Table A2-4). Four analyses (36.1, 36.2, 38.1 and 41.1) indicate high common Pb ($f_{204} > 1\%$) and two (39.1 and 50.1) are >10% discordant. These analyses are unreliable and are not considered further. The remaining analyses form an essentially unimodal distribution, dominated by dates of 1826–1753 Ma, with a few ranging as old as c. 2571 Ma (Fig. 25). The youngest 57 analyses indicate U contents of 46–596 ppm, Th/U values of 0.21 – 2.03 and have $^{207}\text{Pb}^*/^{206}\text{Pb}^*$ dates of 1809–1753 Ma, which comprise a group with a weighted mean $^{207}\text{Pb}^*/^{206}\text{Pb}^*$ date of 1794 ± 3 Ma (MSWD = 1.3). This is interpreted as a maximum age for deposition of the sedimentary protolith.

Eighteen of the remaining 19 analyses have U contents of 67–532 ppm, Th/U values of 0.10 – 1.74 and $^{207}\text{Pb}^*/^{206}\text{Pb}^*$ dates of 2571–1811 Ma, and are considered to represent older provenance components. The remaining analysis (37.1; U = 828 ppm, Th/U = 0.06) has a $^{207}\text{Pb}^*/^{206}\text{Pb}^*$ date of 1742 ± 9 Ma (1σ) but has an elevated common Pb content ($f_{204} > 0.37\%$) and is 6% discordant. This high-U grain might have been affected by minor Pb loss and is not considered a reliable constraint on the depositional age of the protolith.

‘Aplite’ (microgranite) dykes, Talbot Terrane

Numerous fine-grained felsic veins and dykes are exposed over a wide area to the southeast of the Rudall River crossing (Hickman and Bagas, 1998). These generally discontinuous dykes range in width from a few centimetres to about 2 m and have a variety of orientations as a consequence of younger deformation. The felsic dykes mostly occur within a broad area of K-feldspar augen granitic gneiss of the Kalkan Supersuite but also intrude a small body of ultramafic rock enclosed within the granitic gneiss. A dyke from this area yielding a date of 1778 ± 16 Ma was considered by Nelson (1995j) and Hickman and Bagas (1999) to post-date the S_2 foliation and thus provide a minimum age for the Yapungku Orogeny. Because this date represents one of the key lines of evidence to support an 1800–1765 Ma age for the Yapungku Orogeny, further examination of this area was carried out to assess the structural setting of the felsic dykes and two samples were taken in an attempt to provide a more precise age.

GA 2005670072 – micromonzogranite dyke, Talbot Terrane

The sample dated by Nelson (1995j) was taken from a felsic dyke within an isolated 150 × 60 m body of ultramafic rock enclosed within granitic gneiss.

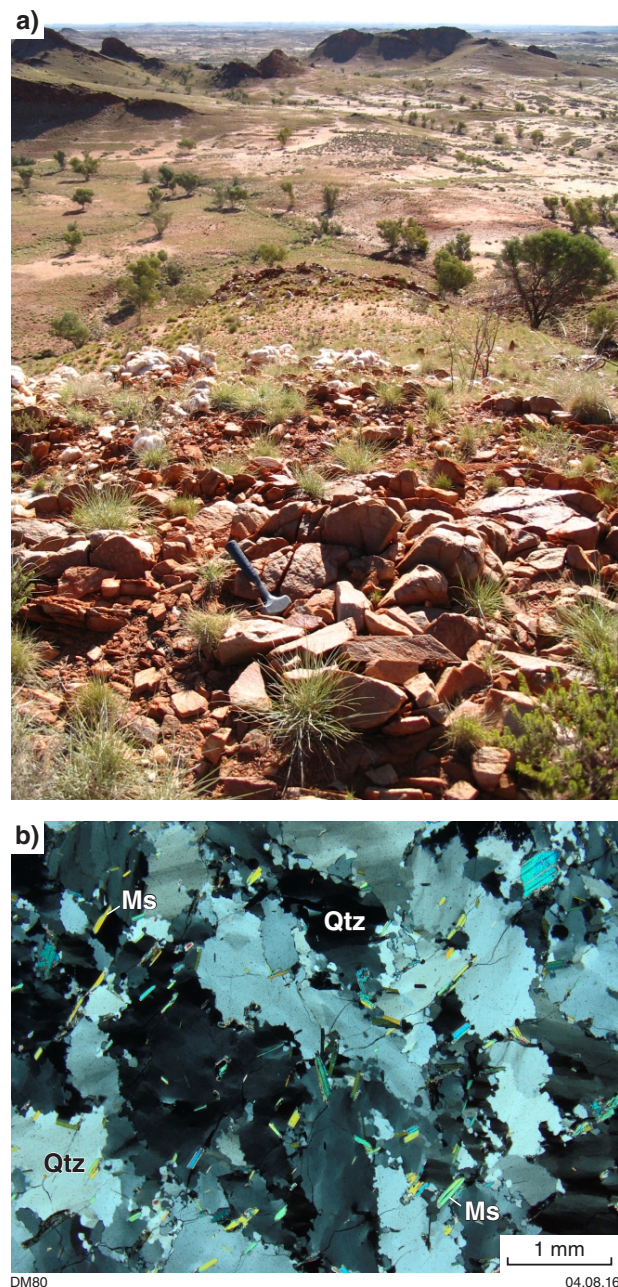


Figure 22. Outcrop photos and photomicrograph of quartzite, Fingoon Quartzite, Talbot Terrane: a) sample site (GA 2005670110) from the Fingoon Range, view to northwest up-sequence towards Yandagoo Formation; b) thin section image of Fingoon Quartzite sample, with oriented muscovite defining a foliation

The sample site information of Nelson (1995j) is not sufficiently precise to be certain about which dyke was sampled but one significantly more continuous and thicker dyke (Fig. 26a; MGA 415052E, 7504980N) was the only one observed with evidence of previous sampling and is considered likely to be the same one sampled by Nelson (1995j). All other minor dykes and veins observed within the ultramafic body have a similar appearance and structural setting, and the sampled dyke is representative of those in the area, although it cannot be conclusively demonstrated that the sampled dyke is the one previously dated.

The sampled dyke is up to 2 m wide and crops out over a strike length of about 40 m. The western end of the dyke is steeply dipping and strikes approximately east–west, while the eastern end strikes northeasterly. This is possibly a result of folding of the dyke, which appears to have affected a nearby smaller dyke (Fig. 26b). The ultramafic host rock contains a variably developed foliation, which dips steeply to moderately towards the north-northeast where observed, and is composed of a recrystallized assemblage dominated by medium-grained actinolite/tremolite. The contact of the dyke with its host rock is typically not well exposed but in the northern part of the dyke the margin of an irregular embayment is locally subparallel to the foliation in the ultramafic host rock and contains a foliation subparallel to that in the host rock (Fig. 26c). In the thickest part of the dyke, there is no distinct foliation evident in the weathered surface but broken fragments more clearly show a foliation defined by quartz–feldspar aggregates and rare oriented biotite and muscovite. This foliation is more apparent in other felsic dykes in the area, particularly in thinner dykes, which in places contain a foliation parallel to that in the host ultramafic rock. Some of these dykes contain two foliations, consisting of an earlier pervasive foliation defined by quartz–feldspar aggregates and oriented micas, overprinted by a northwesterly trending, steeply dipping cleavage. At one locality, the earlier foliation is folded by a steeply plunging, northwesterly trending fold, possibly an F_4 structure (Fig. 26b). The age of the main foliation in the felsic dykes is not certain, being generally less well developed in the fine-grained, equigranular felsic dykes but is consistent with the foliation assigned to S_2 by previous workers in the surrounding granitic gneiss.

In thin section, the dyke sample consists of a granoblastic assemblage of fine- to medium-grained microcline, quartz and plagioclase with trace amounts of biotite, muscovite, epidote and opaque minerals (Fig. 26d). No zircon was noted in the thin section examined. A weakly defined foliation is defined by quartz and feldspar aggregates and oriented mica. A thin section of the previously dated sample of Nelson (1995j) was examined for comparison. This sample has a similar mineralogy and texture to that sampled in this study, with a slightly better developed foliation, consistent with both samples having been taken from the same dyke or dyke suite.

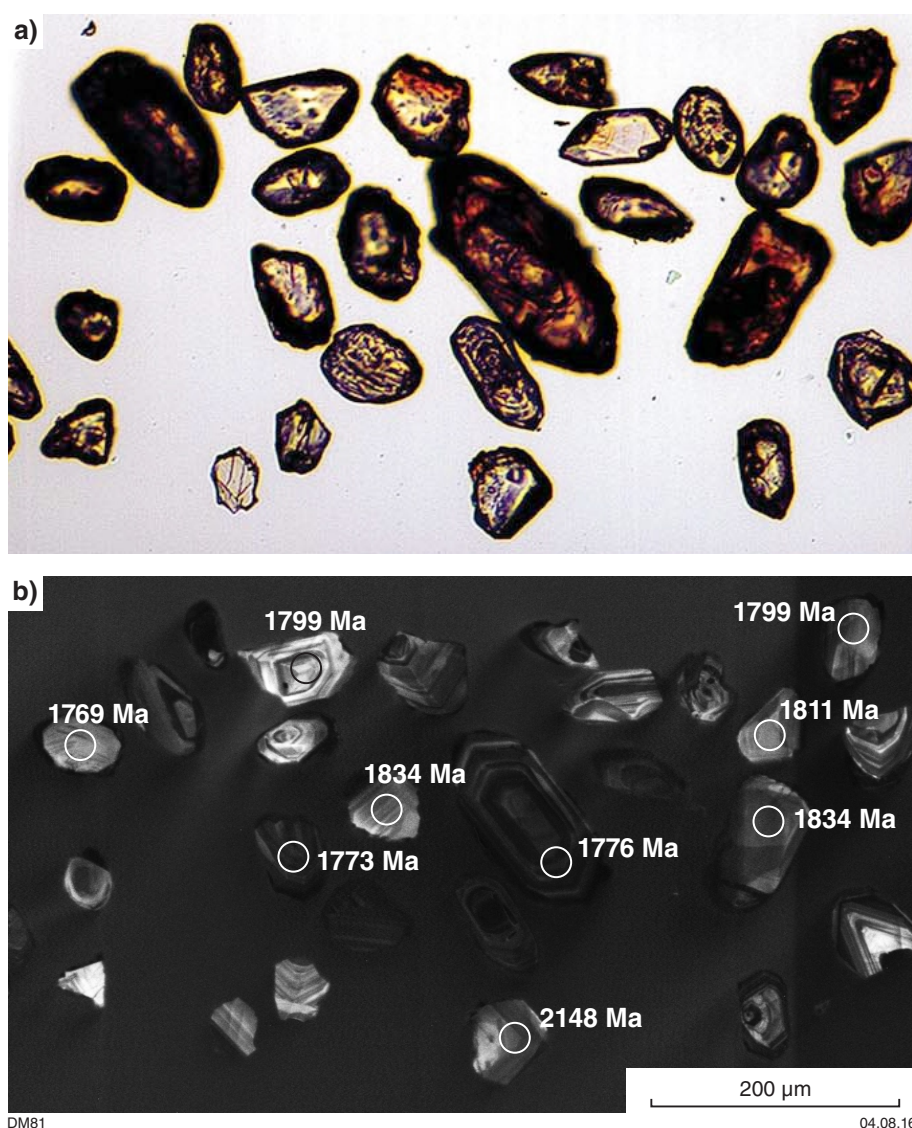


Figure 23. Images of zircons from quartzite, Fingoon Quartzite, Talbot Terrane (GA 2005670110):
a) transmitted light; b) CL image

Only six zircons were recovered from 8.5 kg of crushed rock. The grains are euhedral, 60–180 µm long and fractured in places. In CL images, they have moderate to dark intensities, are oscillatory or sector-zoned and have thin, dark rims (Fig. 27). Two analyses were completed on zircon rims and one of a zircon core (Fig. 28; Table A2-5). The zircon core has a low U content (93 ppm), Th/U of 1.52 and yields a concordant $^{207}\text{Pb}^*/^{206}\text{Pb}^*$ date of 1775 ± 17 Ma (1σ), indistinguishable from a previous date of 1773 ± 15 Ma for the dyke sampled from this area (Nelson, 1995j; recalculated by Kirkland et al., 2013a). Two analyses of zircon rims have high U (2240 and 3012 ppm), high Th/U (3.44 and 2.89), are highly discordant (73% and 51%), and do not yield meaningful dates.

The paucity of zircon recovered from a relatively large amount of sample material suggests that there might be few magmatic zircons in the dyke, with the very few zircons that were obtained possibly being xenocrysts.

This is consistent with the lack of zircons observed in thin section, and the very low Zr content of the sample (45 ppm). The c. 1775 Ma date from the oscillatory zoned core is thus interpreted as an imprecise maximum age for the intrusion of the dyke.

GA 2005670092 – micromonzogranite dyke, Talbot Terrane

A relatively thick felsic dyke up to 2 metres wide occurs about 1.7 km southeast of Rudall Crossing (Fig. 13; MGA 413085E 7505780N). The dyke forms a steeply dipping, north-northwesterly trending body within an extensive area of granitic gneiss (Fig. 29a). The host rock is strongly foliated adjacent to the contact, with a steeply dipping, northwesterly trending foliation interpreted as S_4 that is slightly oblique to the dyke margin (Fig. 29b).

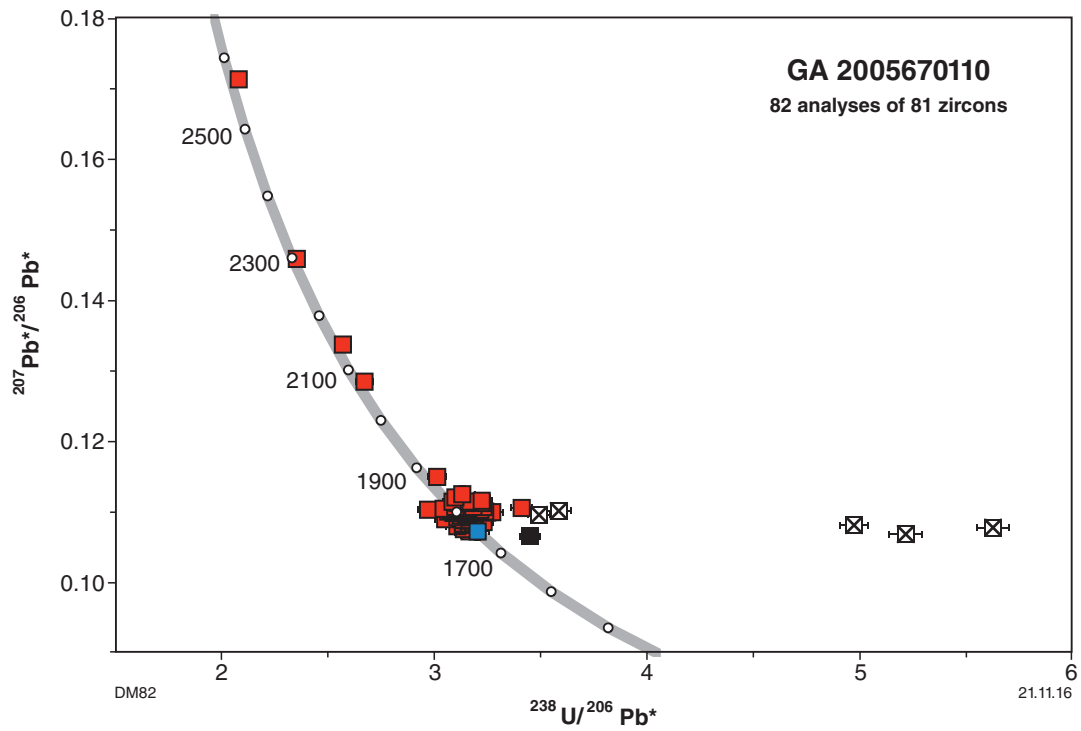


Figure 24. U–Pb analytical data for zircons from quartzite, Fingoon Quartzite, Talbot Terrane (GA 2005670110)

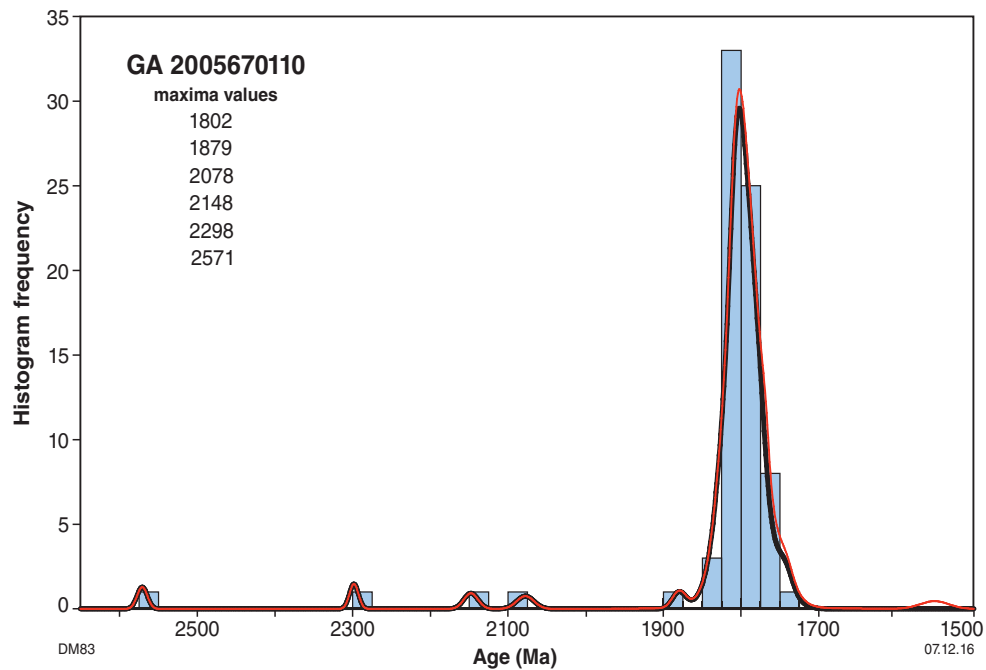


Figure 25. Probability density diagram of detrital zircon dates from quartzite, Fingoon Quartzite, Talbot Terrane. Black line: data <10% discordant; red line: all data

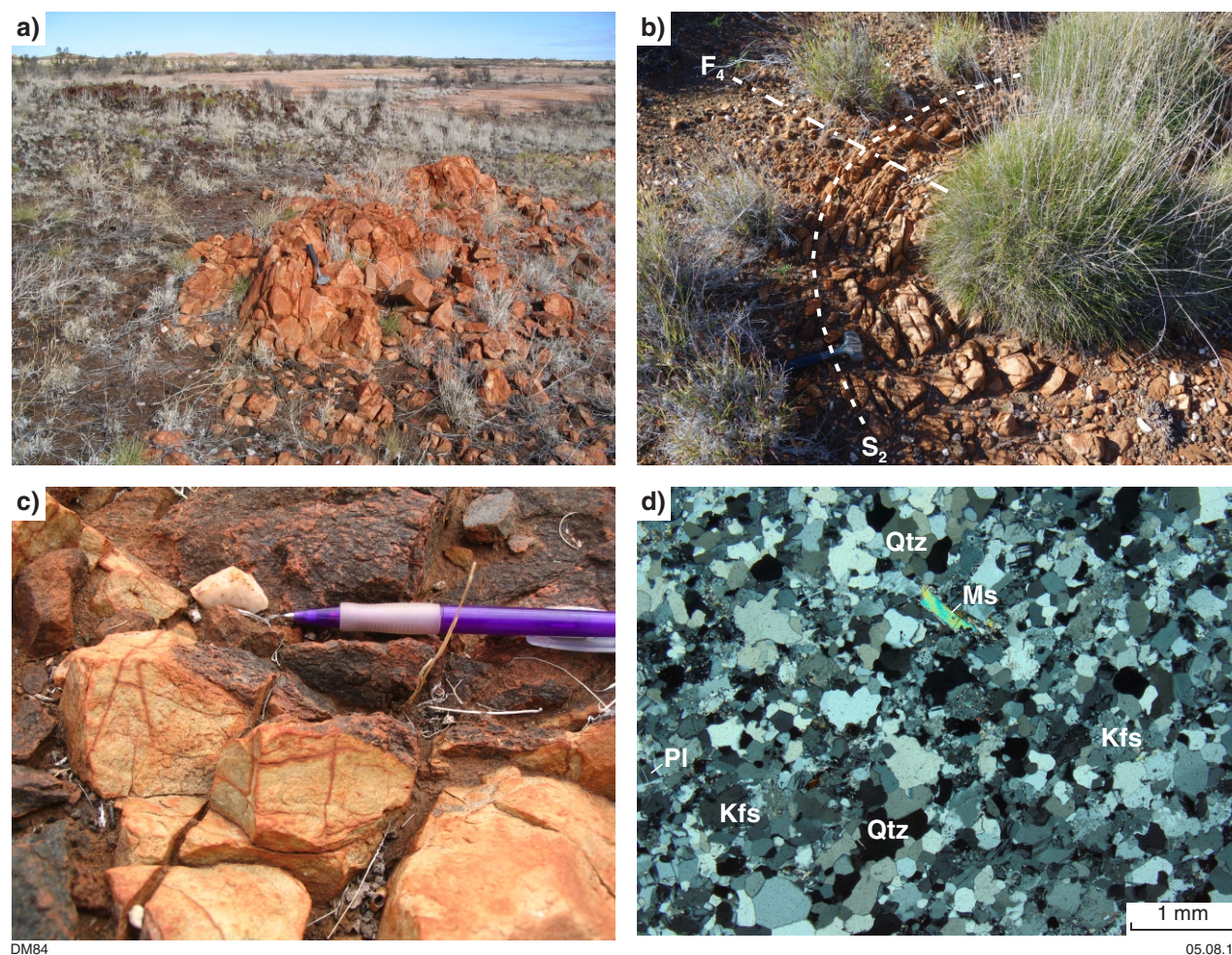


Figure 26. Outcrop photos and photomicrograph of felsic dykes ~1.7 km southeast of Rudall Crossing, Talbot Terrane: a) felsic dyke within ultramafic rock sampled for geochronology (GA 2005670072); b) felsic dyke in ultramafic rock, near GA 2005670072, containing high-grade foliation folded by (F_4 ?) fold (MGA 415130E 7504930N); c) irregular contact of sampled dyke, showing foliation in dyke subparallel to foliation in host ultramafic rock; d) thin section image of felsic dyke sample, showing granoblastic recrystallized texture

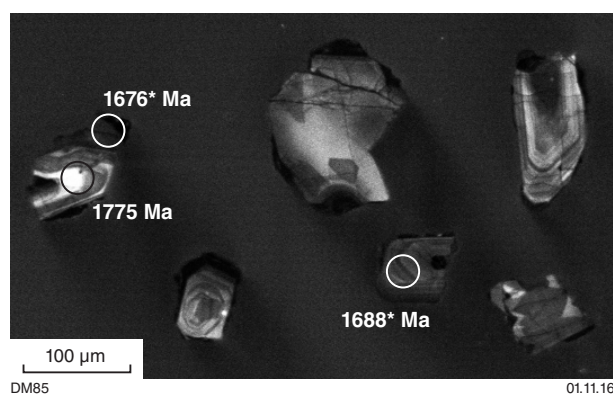


Figure 27. CL image of zircons from a felsic dyke in ultramafic rock, Talbot Terrane (GA 2005670072); * indicates analysis >10% discordant

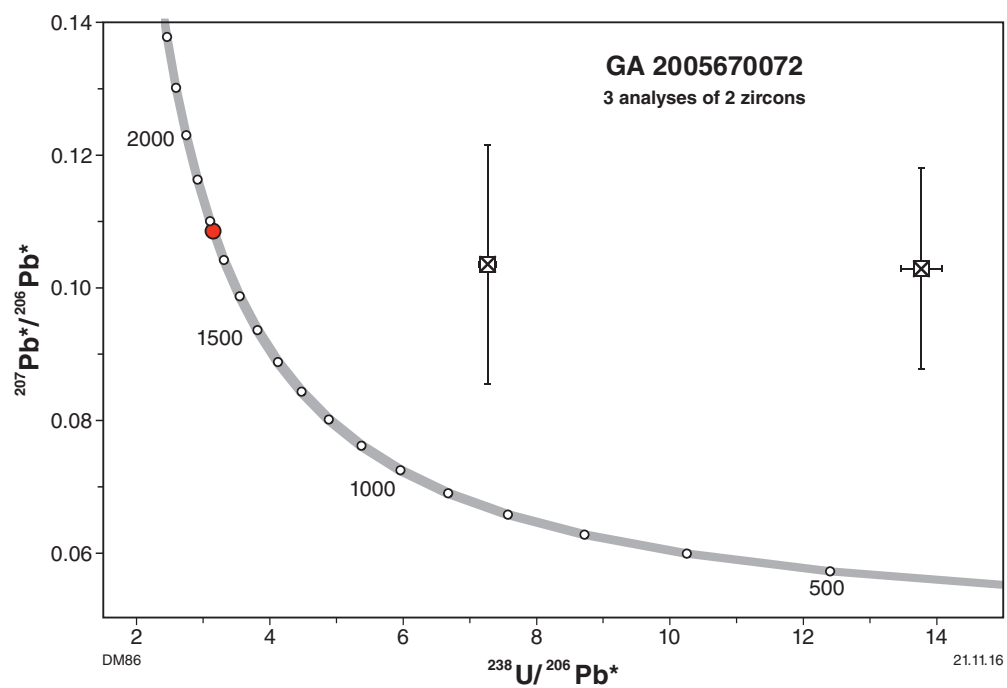
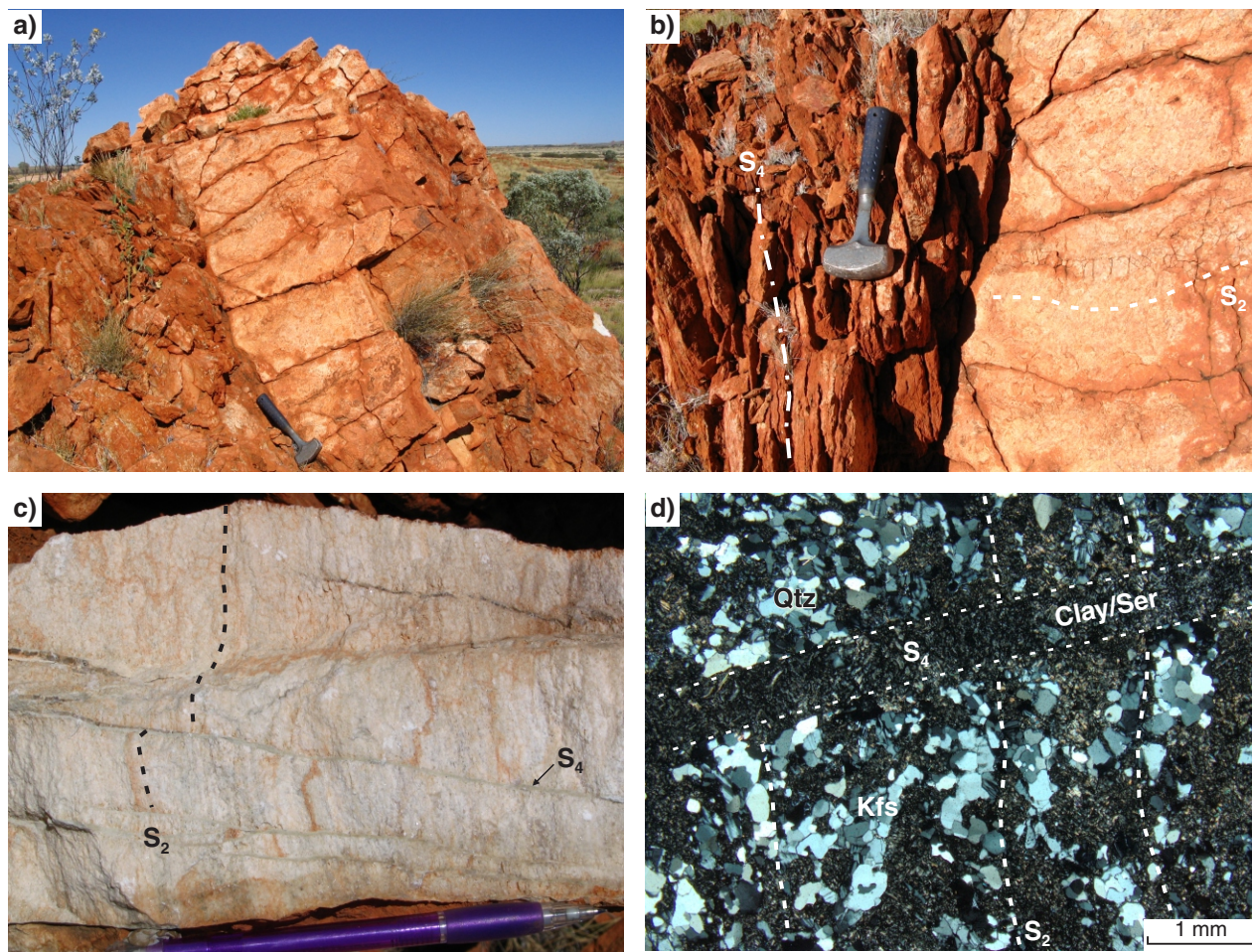


Figure 28. U-Pb analytical data for zircons from a felsic dyke in ultramafic rock, Talbot Terrane (GA 2005670072)



DM87

05.08.16

Although outcrop is not continuous in the area, the dyke does not appear to extend more than a few metres along strike, and might form a boudin within the more highly strained granitic gneiss. The felsic dyke consists of a generally granoblastic, equigranular assemblage of quartz, microcline and plagioclase with minor biotite, and on weathered surfaces superficially appears to lack the strong foliation that is present in the host rock (Fig. 29b). However, broken surfaces reveal a pervasive moderately north-northeasterly dipping foliation defined by flattened aggregates of quartz, feldspar and biotite, which is overprinted by a spaced cleavage defined by fine-grained chlorite and sericite that is subparallel to the foliation in the host rock adjacent to the margin of the dyke (Fig. 29c). The early, higher grade foliation is possibly the regional S_2 foliation, which has a range of orientations in the area due to younger folding. The lower-grade, north-northwesterly striking foliation is consistent with the regional S_4 foliation, which is more consistently northeasterly to north-northeasterly trending, formed under greenschist facies conditions during the Miles Orogeny. The lower intensity of the S_4 foliation in the dyke might be due to differences in competency with the more biotite-rich host rock, with deformation taken up along discrete slickensides on the margin of the dyke and fractures within it. The rock has undergone pervasive greenschist facies retrograde alteration and weathering, with replacement of feldspar and mica by sericite, chlorite, clay and epidote (Fig. 29d).

Only six zircons were recovered from 5.1 kg of crushed rock. The zircons range from 70 to 120 μm long and have irregular to euhedral shapes. In CL images the grains show a wide range of intensities and are oscillatory or irregularly zoned (Fig. 30). Seven analyses of five grains were completed (Fig. 31; Table A2-6). Two analyses of grain 1 yielded indistinguishable and unexpectedly young $^{206}\text{Pb}/^{238}\text{U}$ dates with a mean of 302 ± 6 Ma; MSWD = 0.07. Analysis 3.1 is of a high-U grain (1065 ppm) and is >10% reversely discordant, with high common Pb and an imprecise $^{207}\text{Pb}/^{206}\text{Pb}$ date of 1679 ± 98 Ma (1σ) and is not considered reliable. The remaining four analyses yield near-concordant $^{207}\text{Pb}/^{206}\text{Pb}$ dates of 1170–1039 Ma but do not form a statistically coherent group.

None of the dates obtained are considered to define the magmatic age of the felsic dyke, with the very low number of recovered grains suggesting that little or no magmatic zircon formed during crystallization. This is consistent with the very low Zr content of this sample (41 ppm).

Figure 29. (left) Outcrop photos and photomicrograph of a felsic dyke in granitic gneiss, sampled for dating, Talbot Terrane: a) and b) outcrop photos of a felsic dyke within granitic gneiss of the Kalkan Supersuite (GA 2005670092). The granitic host rock contains a steeply dipping cleavage interpreted as S_4 that is not as evident within the dyke in weathered faces. The dyke contains a more moderately dipping, high-grade foliation that controls later fracturing; c) broken surface of dyke, showing pervasive foliation interpreted as S_2 overprinted by a spaced cleavage that is subparallel to the more intensely developed foliation in the host rock interpreted as S_4 ; d) thin section image of felsic dyke, showing earlier, higher grade foliation overprinted by younger cleavage (XPL)

A second, larger, sample from another part of the dyke (GA 2006670002) with 56 ppm Zr returned only four zircons from 17.4 kg of rock, which were not mounted for analysis, as this result appears to confirm there are few or no magmatic zircons. Although it is possible that the Mesoproterozoic and Paleozoic zircons in this sample represent xenocrysts, the extremely low number of zircons recovered means that very small amounts of contamination (from the field or during processing) cannot be ruled out as a possible source of these grains. Given this uncertainty, no significance is attached to any of the dates obtained from this sample, but this negative result does have implications for the interpretation of the felsic dyke date of Nelson (1995j), as discussed later in this report.

GA 2005670165 – quartzite, Connaughton Terrane

Quartzite was sampled from a prominent strike ridge in the central part of the Connaughton Terrane (Figs 13, 32a; MGA 483024E 7465554N). The quartzite forms part of a folded and possibly structurally repeated succession comprising quartzite, amphibolite, metachert, banded iron-formation, granitic gneiss and ultramafic rock. A poorly defined layering is visible despite extensive recrystallization. In thin section, the quartzite consists almost entirely of quartz, with trace amounts of muscovite and zircon (Fig. 32b). The quartz consists of an interlocking mosaic of elongate, medium-grained domains with prominent undulose extinction that are separated from each other by narrow zones of fine-grained, recrystallized granoblastic quartz.

Zircons from the quartzite range from multifaceted prismatic grains to more equant rounded grains, typically 100–150 μm long (Fig. 33a,c). In CL images, most grains consist of a core of oscillatory zoned zircon mantled by a variably developed, unzoned dark rim up to 50 μm thick that modifies the rounded cores into faceted prisms (Fig. 33b,c).

Eighty-two analyses were obtained from zircon cores (Fig. 34; Table A2-7). One analysis (28.1) is >10% discordant and one analysis (76.1) indicates relatively high common Pb. These two analyses are considered unreliable and are excluded from further evaluation. The remaining 80 analyses have $^{207}\text{Pb}/^{206}\text{Pb}$ dates of 3142–2282 Ma, with maxima at c. 2875, 2685, 2660, 2510, 2480 and 2315 Ma (Fig. 35). The two youngest core analyses yield a weighted mean $^{207}\text{Pb}/^{206}\text{Pb}$ date of 2284 ± 10 Ma (MSWD = 0.24), which is taken as a maximum depositional age for the protolith.

Thirteen analyses of zircon rims were completed, three of which were duplicate analyses of a previous analysis site. Post-analysis examination showed three analyses (53.1, 57.1 and 57.1A) slightly overlapped zircon cores and these are not considered further. The remaining analyses have high U contents (673–2012 ppm) and low Th/U (0.03–0.12), with $^{207}\text{Pb}/^{206}\text{Pb}$ dates of 1339–1300 Ma. Eight of these 10 analyses have a weighted mean $^{207}\text{Pb}/^{206}\text{Pb}$ date of 1334 ± 4 Ma (MSWD = 1.3).

Two analyses (51.2 and 56.1) have slightly younger dates but form statistical outliers and are interpreted to have undergone a small degree of Pb loss. The 1334 ± 4 Ma date is thus interpreted as the age of high-grade metamorphism.

GA 2005670162 – granitic gneiss, Connaughton Terrane

Megacrystic granitic gneiss was sampled from the Connaughton Terrane ~10 km north of the Harbutt Range and ~4 km southwest of the Camel–Tabletop Fault Zone (Fig. 13; MGA 482971E 7474620N). The sampled unit crops out discontinuously over a strike length of about 6 km and is broadly conformable with a succession of banded iron-formation, amphibolite, muscovite–biotite schist and ultramafic rock. The gneiss consists of abundant

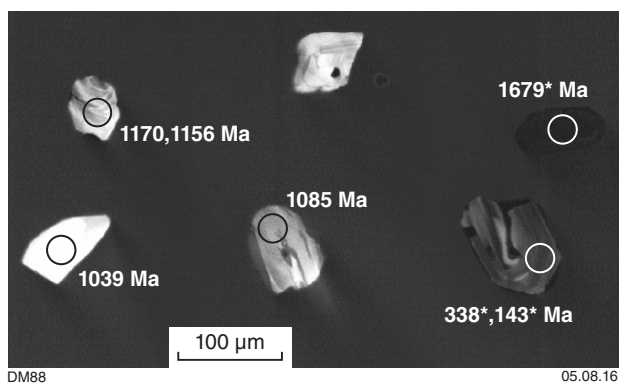


Figure 30. CL image of zircons from a felsic dyke in granitic gneiss, Talbot Terrane (GA 2005670092); * indicates analysis >10% discordant

K-feldspar megacrysts to 2 cm in a medium-grained matrix of quartz, K-feldspar and biotite with minor plagioclase, and has a layer-parallel foliation defined by biotite and quartz–feldspar aggregates (Fig. 32c). Minor garnet has been described from this unit (Bagas and Smithies, 1998b) but was not observed in the dated sample. Minor epidote forms discrete grains replacing biotite, and feldspar is commonly sericitized (Fig. 32d).

Zircons from the gneiss consist of generally elongate (aspect ratios 2–4), subhedral to euhedral grains up to 250 µm long (Fig. 36a), which in CL images consist of oscillatory zoned cores with a range of brightness (Fig. 36b). Some cores contain domains of moderate intensity to dark zircon, which in places has zoning that is discordant with brighter, oscillatory zoned zircon. Zircon cores are mantled in some grains by a thin rim of moderate intensity, generally <10 µm thick.

Thirty-three analyses were obtained from 32 grains (Fig. 37; Table A2-8), including four analyses of darker CL, texturally discordant domains within cores (3.1, 26.1, 28.1 and 32.1) and one analysis of a thin rim (15.1). The darker domains in cores have U contents of 184–420 ppm and Th/U values of 0.26 – 0.65, within the ranges obtained from other analyses of zircon cores, which have U contents of 35–601 ppm and Th/U values of 0.08 – 3.04. The dates from the darker domains also coincide with age components from other cores, with no systematic clustering, and are subsequently treated as part of the magmatic and xenocryst components of this sample.

The $^{207}\text{Pb}^*/^{206}\text{Pb}^*$ dates obtained from zircon cores form a complex spectrum between c. 1891 and 1669 Ma, with a dominant mode at c. 1780 Ma, and subsidiary modes at c. 1805, 1740 and 1690 Ma. One analysis (32.1) is highly discordant and is not considered further.

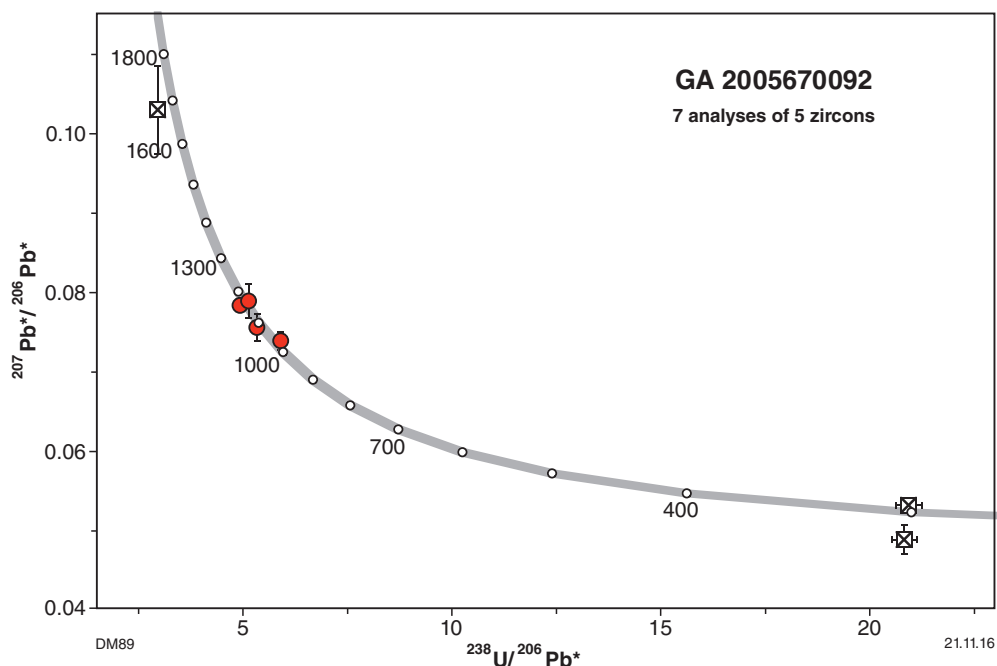


Figure 31. U–Pb analytical data for zircons from a felsic dyke in granitic gneiss, Talbot Terrane (GA 2005670092)

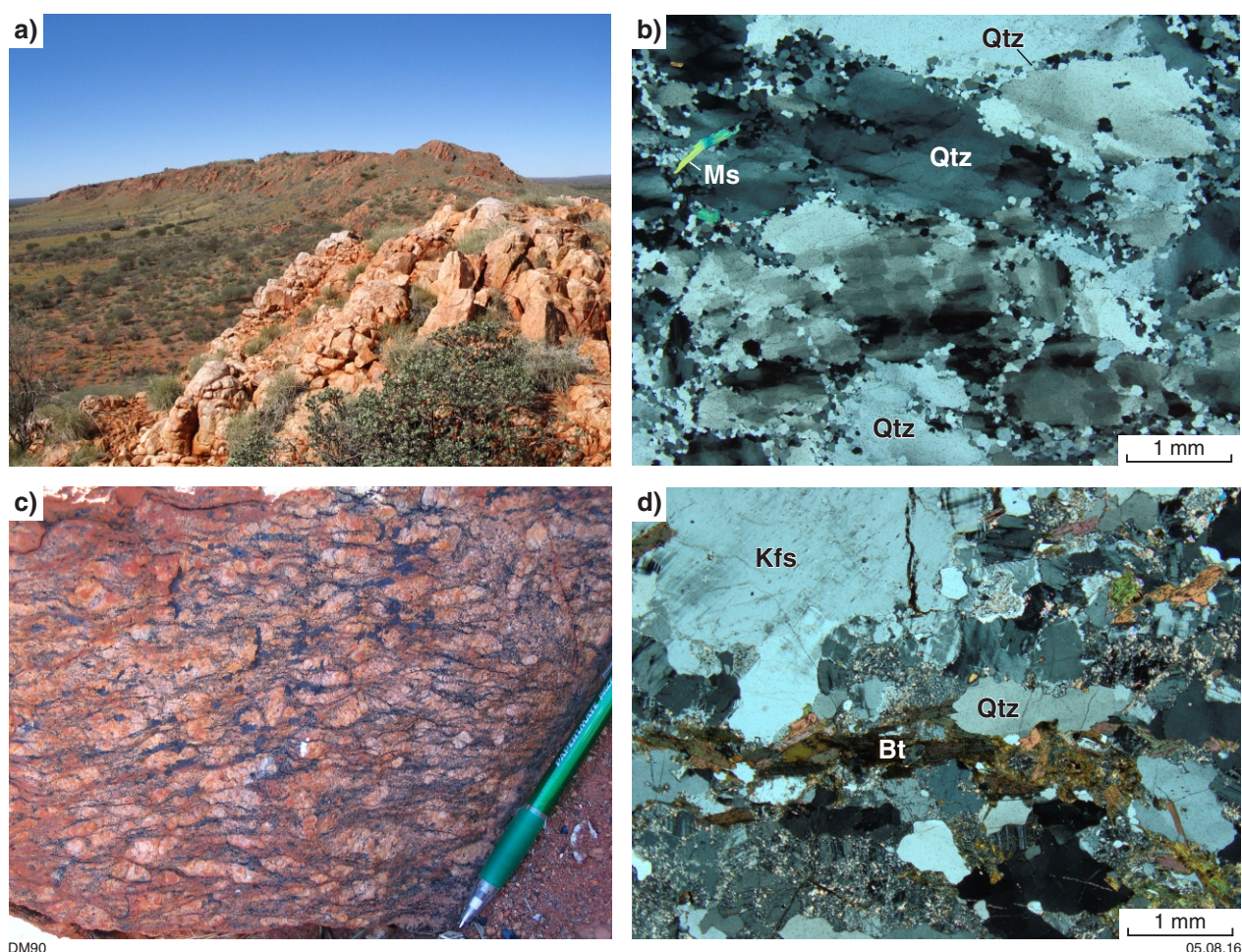


Figure 32. Outcrop photos and photomicrographs of quartzite and granitic gneiss, Connaughton Terrane: a) ridge-forming quartzite unit in the Connaughton Terrane, sampled for geochronology (GA 2005670165); b) thin section image of sampled quartzite, showing quartz-dominant composition and fine-grained domains of recrystallization along the boundaries of larger grains; c) outcrop photo of K-feldspar augen granitic gneiss from the Connaughton Terrane, north of the Harbutt Range (GA 20056700162); d) thin section image of sampled K-feldspar augen gneiss (XPL)

Two analyses (23.1 and 25.1) with dates of c. 1891 and 1841 Ma are significantly older than the main age components and are interpreted as the age of xenocrystic cores. Three cores with dates of c. 1809, 1805 and 1804 Ma (2.1, 8.1 and 10.1) yield a weighted mean date of 1806 ± 10 Ma (MSWD = 0.07), slightly older than the dominant c. 1780 Ma age component, and are also interpreted to represent xenocrysts. Seventeen analyses with $^{207}\text{Pb}^*/^{206}\text{Pb}^*$ dates of 1792–1767 Ma have U contents of 64–574 ppm, Th/U values of 0.17 – 1.57 and yield a weighted mean $^{207}\text{Pb}^*/^{206}\text{Pb}^*$ date of 1781 ± 4 Ma (MSWD = 0.67). This is interpreted to reflect the magmatic age of the rock, based on the generally uncomplicated oscillatory zoning in these grains, their relatively uniform compositions and the dominance of this age component. This date is best regarded as a minimum age, to allow for the possibility of unresolved minor ancient loss of radiogenic Pb, which is evident in other analyses with younger apparent ages.

Of the remaining 10 analyses, five (5.1, 7.1, 14.1, 21.1 and 24.1) form a distinctive group with high Th/U

(2.00 – 3.04), low U (29–70 ppm) and $^{207}\text{Pb}^*/^{206}\text{Pb}^*$ dates of 1757–1723 Ma, yielding a weighted mean date of 1739 ± 20 Ma (MSWD = 0.38). The Th/U values of these grains are unusually high for magmatic zircon (Kirkland et al., 2015b) and are distinct from those of the main age component. One possibility is that these zircons formed as part of the main magmatic population and were more susceptible to Pb loss or isotopic disturbance during metamorphism. If these dates were affected by recrystallization, it is possible there was a discrete metamorphic event at c. 1739 Ma, but it is also possible that they represent a coincidental clustering of isotopically disturbed dates, with their relatively large uncertainties due to low U contents making it difficult to resolve isotope variability. Another possibility, although considered less likely, is that the high Th/U zircons represent a younger phase of magmatic zircon growth and reflect the age of the granitic precursor. Analysis 26.1 has a $^{207}\text{Pb}^*/^{206}\text{Pb}^*$ date that is within uncertainty of the high Th/U group at c. 1737 Ma but with higher U (195 ppm) and lower Th/U (0.33).

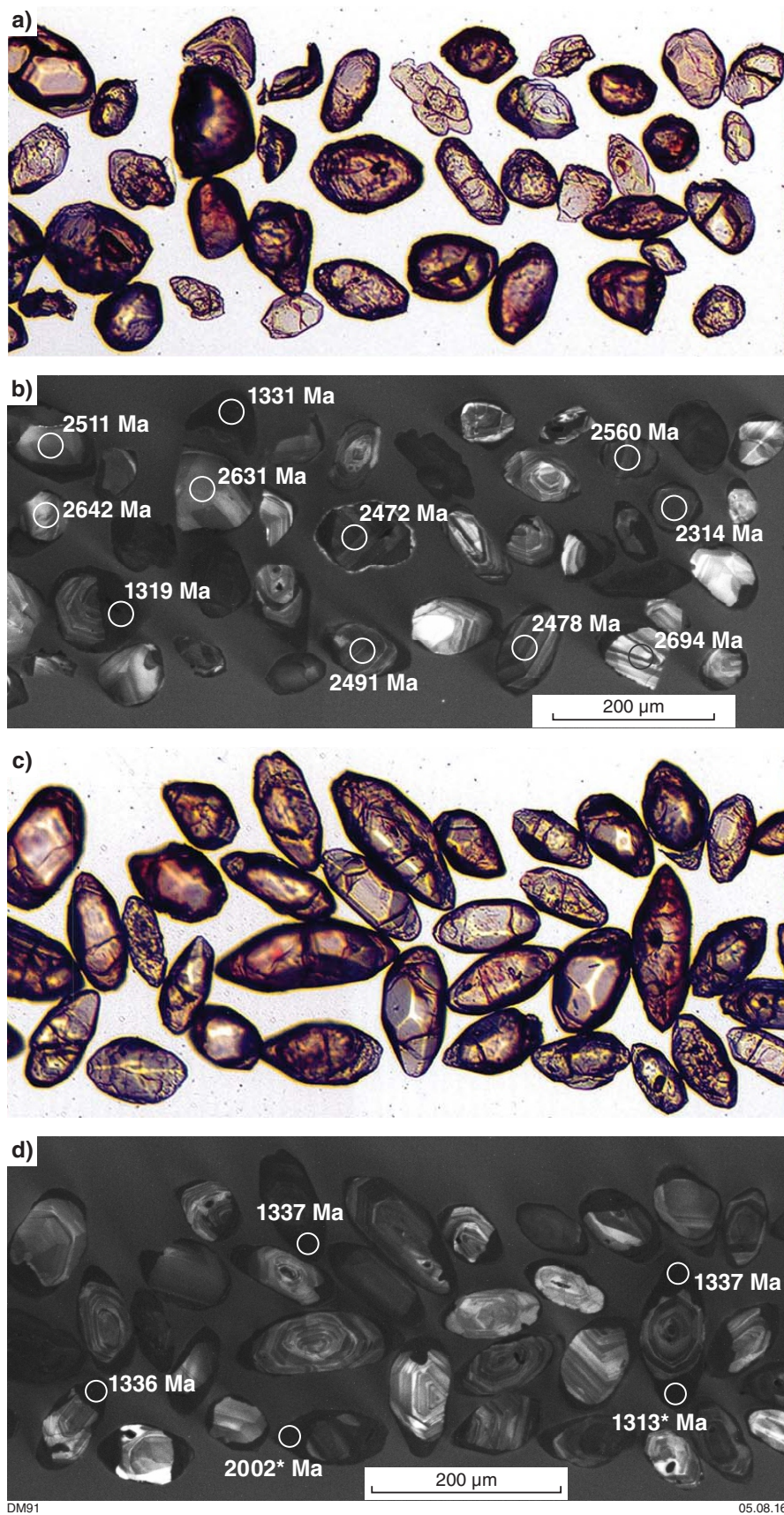


Figure 33. Images of zircons from quartzite, Connaughton Terrane (GA 2005670165): a) and b) transmitted light and CL image of randomly selected grains; c) and d) transmitted light and CL image of prismatic grains used to target metamorphic zircon overgrowths (dark rims); * indicates analysis >10% discordant

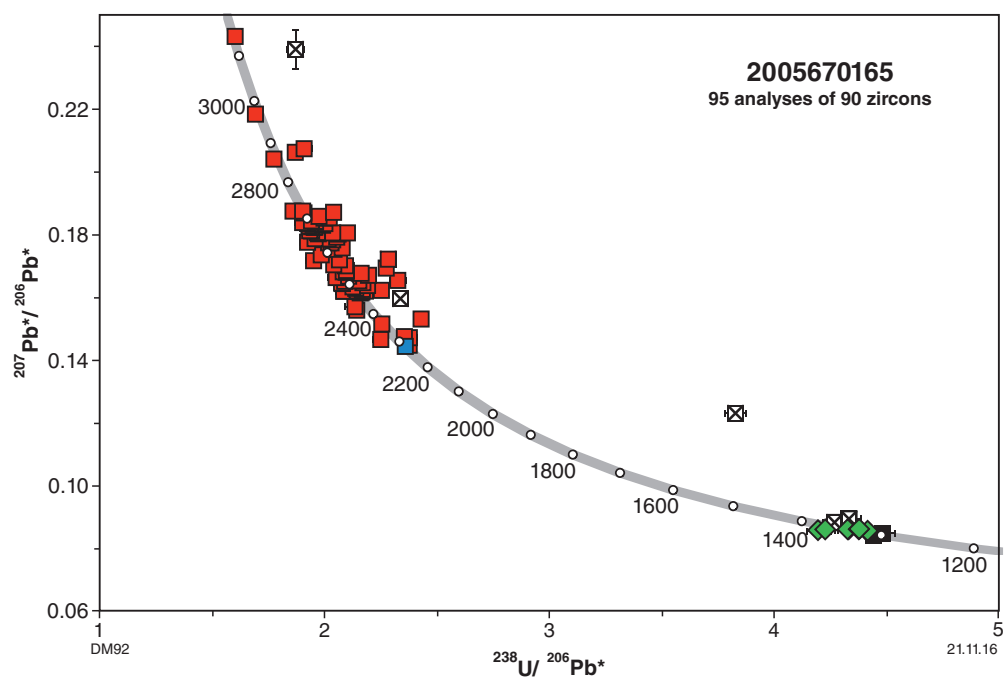


Figure 34. U–Pb analytical data for zircons from quartzite, Connaughton Terrane (GA 2005670165)

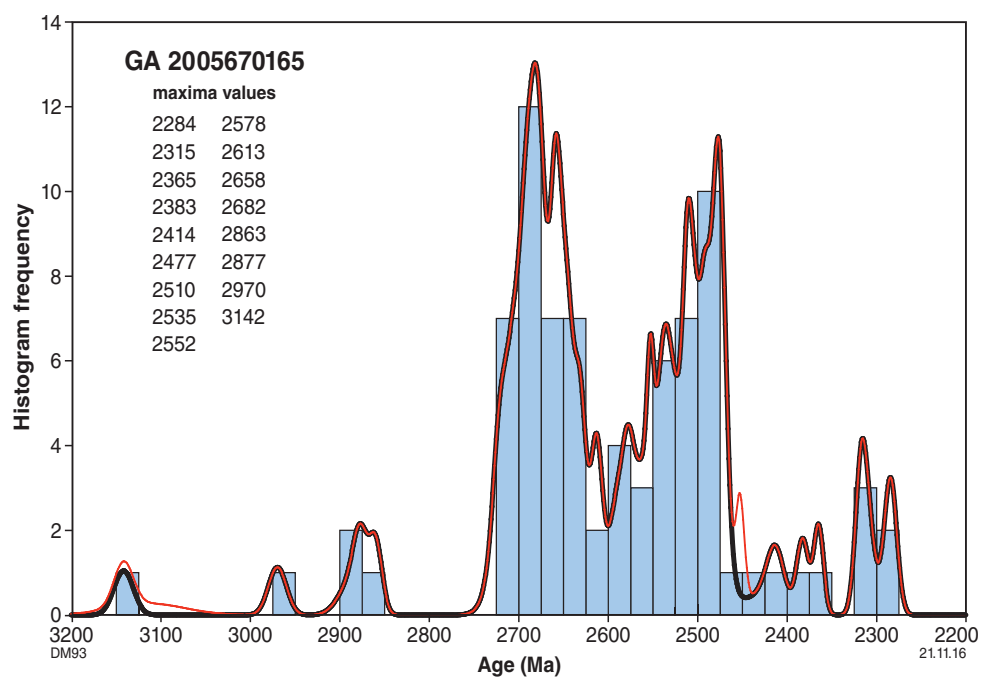


Figure 35. Probability density diagram of detrital zircon dates from quartzite, Connaughton Terrane. Black line: data <10% discordant; red line: all data

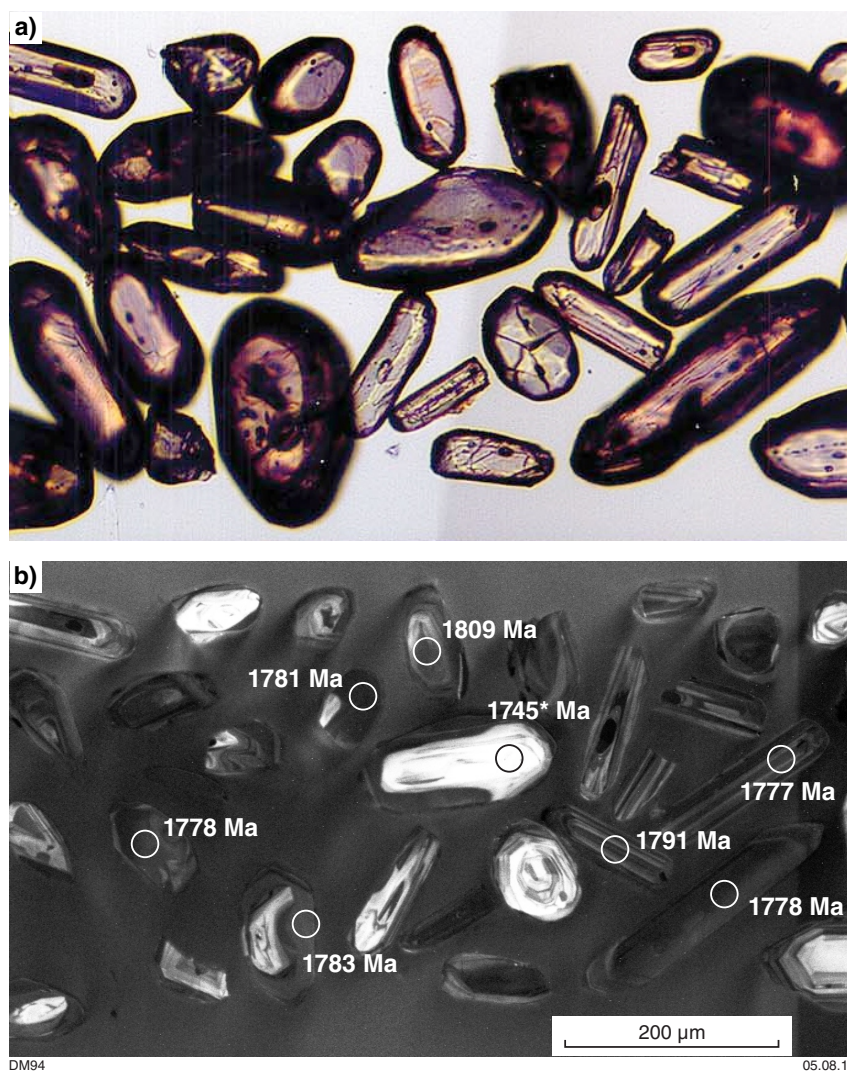


Figure 36. Images of zircons from granitic gneiss, Connaughton Terrane (GA 2005670162): a) transmitted light; b) CL image

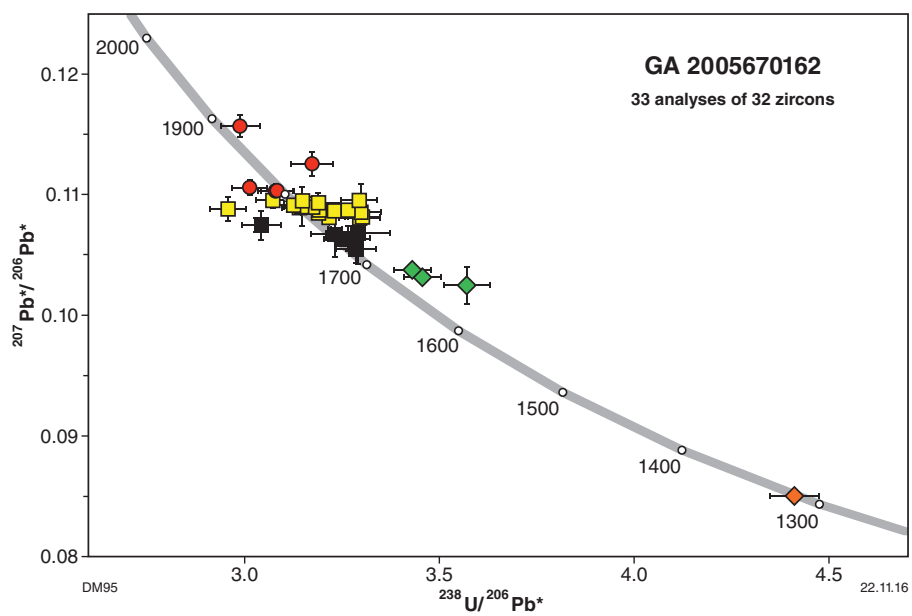


Figure 37. U-Pb analytical data for zircons from granitic gneiss, Connaughton Terrane (GA 2005670162)

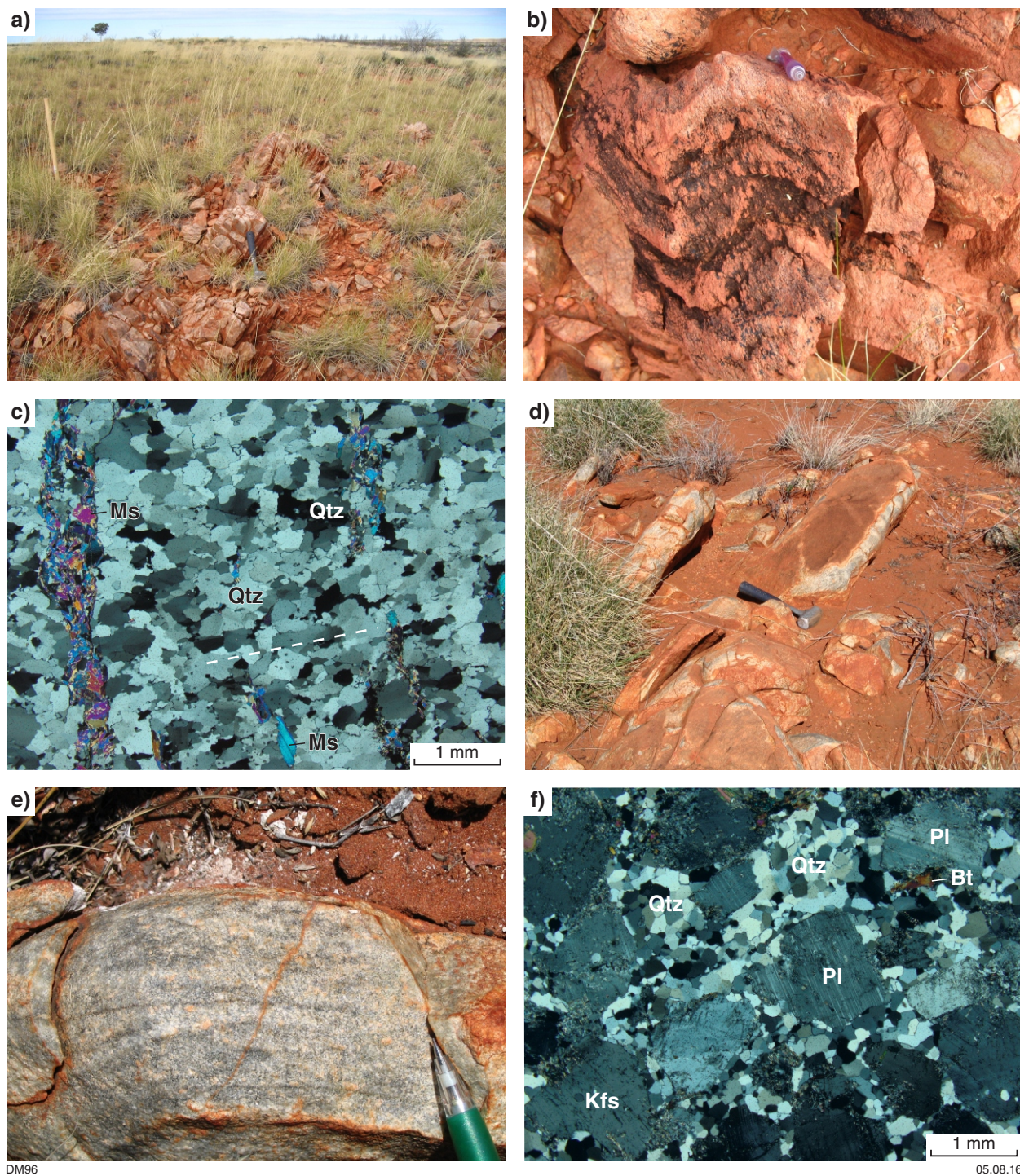


Figure 38. Outcrop photos and photomicrographs of quartzite and leucogranite, Tabletop Terrane: a) quartzite sample site (GA 2006670087); b) folded quartzite with associated axial plane cleavage; c) thin-section image of quartzite, with flattening of quartz grains defining a weak earlier foliation overprinted by a foliation defined by muscovite; d) leucogranite sample site of (GA 2005670178); e) hand specimen of leucogranite sample GA 2005670178; f) thin section image of leucogranite sample GA 2005670178, showing interstitial recrystallized quartz between magmatic feldspar grains (XPL)

This analysis was from a zone of darker CL zircon that forms an irregular embayment within a brighter core, and more clearly reflects recrystallization, supporting the suggestion that the dates from the high Th/U zircons reflect isotopic disturbance. This analysis can be combined with those of the high Th/U group, yielding a weighted mean $^{207}\text{Pb}^*/^{206}\text{Pb}^*$ date of 1738 ± 13 Ma (MSWD = 0.31) but again it is unclear if this group has geological significance.

Three near-concordant analyses of cores (12.1, 16.1 and 19.1) have significantly younger $^{207}\text{Pb}^*/^{206}\text{Pb}^*$ dates of c. 1693, 1681 and 1669 Ma, with U contents of 424, 601 and 55 ppm and Th/U of 0.13, 0.87 and 1.44, respectively, yielding a weighted mean $^{207}\text{Pb}^*/^{206}\text{Pb}^*$ date of 1688 ± 8 Ma (MSWD = 1.04). A second analysis of one of these grains (16.2) yielded a date of c. 1768 Ma, forming part of the main age component, and suggesting that these younger dates might reflect isotopic disturbance during metamorphism. The relatively tight group of ages at c. 1688 Ma suggests metamorphism might have taken place at this time but alternatively could represent a coincidental clustering of disturbed isotope compositions affected by a younger event.

One analysis of a moderate intensity rim (15.1) has a moderate U content of 298 ppm Th/U of 0.30 and a concordant $^{207}\text{Pb}^*/^{206}\text{Pb}^*$ date of 1315 ± 11 (1 σ). Although only represented by a single analysis (because none of the other thin rims were able to be analysed), this is interpreted as the age of a high-grade metamorphic event. It is possible that metamorphism at this time was responsible for all the isotopic disturbance noted above, forming a discordia line, but a lack of apparent ages between c. 1688 and 1315 Ma makes it difficult to discriminate between a single metamorphic overprint of a ≥ 1781 Ma granitic rock and minor recent loss of radiogenic Pb from zircons in a rock affected by events at both c. 1688 and 1315 Ma.

It is perhaps significant that broadly similar age components were obtained by Nelson (1996c) from a garnet-bearing quartzofeldspathic gneiss sampled from drillcore about 3 km to the east-southeast. Seven analyses of zircon cores yielded dates of 1873–1764 Ma, three analyses of rims and cores yielded a weighted mean date of 1672 ± 70 Ma, and two analyses of rims yielded a weighted mean date of 1222 ± 63 Ma. Nelson (1996c) interpreted the 1672 Ma and older ages to be inherited components within a paragneiss and the c. 1222 Ma date to represent an episode of igneous zircon growth. It is possible, however, that the c. 1672 and 1222 Ma dates instead reflect metamorphic events affecting an igneous rock emplaced between c. 1873 and 1764 Ma. Although the dates obtained from this sample are imprecise, the broad similarities between the age components in the two samples are at least consistent with two discrete events.

GA 2006670087 – quartzite, Tabletop Terrane

A quartzite unit was sampled adjacent to the western margin of a large leucogranite intrusion in Tabletop

Terrane (Figs 13, 38a,b; MGA 513542E 7465160N). The quartzite unit strikes north–south and has a weak layering defined by partings on bedding planes. The quartzite contains a moderately east-dipping layer-parallel foliation which is overprinted by a steeply north-dipping spaced cleavage. Farther to the south, the unit is affected by steeply south-southwesterly plunging mesoscopic folds, which are overprinted by a moderately south-dipping spaced cleavage. Banded iron-formation has been mapped immediately to the west of the quartzite (Bagas, 1999) but only secondary iron oxides in quartzite were observed in this study.

In thin section, the quartzite comprises >95% quartz, which forms a fine- to medium-grained recrystallized mosaic with sutured ('bulged') grain boundaries (Fig. 38c). Discontinuous folia of muscovite define the layer-parallel foliation. Rare isolated grains up to 1 mm in size are composed of a recrystallized aggregate of very fine-grained muscovite and chlorite. Trace zircon, biotite and fine-grained opaque minerals are also present. A foliation defined by partial flattening of quartz grains overprints the layer-parallel foliation at a high angle and is interpreted as the east–west trending spaced cleavage seen in outcrop.

Zircons from the quartzite are equant to elongate, typically prismatic and faceted, and up to 200 μm long (Fig. 39a). In CL images, most grains consist of a rounded core of oscillatory zoned zircon mantled by two phases of zircon formation that give the grains their prismatic shape (Fig. 39b). The first overgrowth phase is structureless and dark in CL images, ranging from a few micrometres to 30 μm thick. The second phase consists of structureless to weakly concentrically zoned, moderate intensity zircon that mantles the dark zircon overgrowths, typically forming smooth, irregular embayments in the darker zircon. The moderate CL intensity zircon rims are generally <10 μm thick, with a few up to 30 μm thick. A smaller proportion of grains have a thin, late-stage rim of structureless bright CL zircon generally several micrometres thick. It is not immediately apparent from the textural relationships whether this is related to the formation of the moderate CL zircon overgrowth or represents a separate younger episode of zircon growth. The ubiquitous presence of the multiple stages of zircon growth and the euhedral, prismatic form of the grains suggests that the zircon rims formed in situ, after deposition of the sedimentary protolith.

Eighty-one analyses of zircon cores (Fig. 40; Table A2-9) indicate a wide range of U contents (17–783 ppm) and Th/U (0.02 – 2.14). Four analyses are >10% discordant, with the remaining 77 having $^{207}\text{Pb}^*/^{206}\text{Pb}^*$ dates of 3579–2830 Ma. The resulting spectrum of dates has no dominant age component but has maxima at c. 3550, 3265, 3230 and 3000 Ma (Fig. 41). The two youngest core analyses have $^{207}\text{Pb}^*/^{206}\text{Pb}^*$ dates of 2838 ± 4 Ma and 2830 ± 3 Ma (1 σ) and a weighted mean date of 2833 ± 5 Ma (2 σ MSWD = 3.1), which is taken as a maximum depositional age for the protolith.

Three analyses of the dark CL rims mantling zircon cores indicate high U contents (627–783 ppm) and low Th/U (0.04 – 0.07). One of these (62.1) is discordant and excluded from further consideration but its c. 2392 Ma

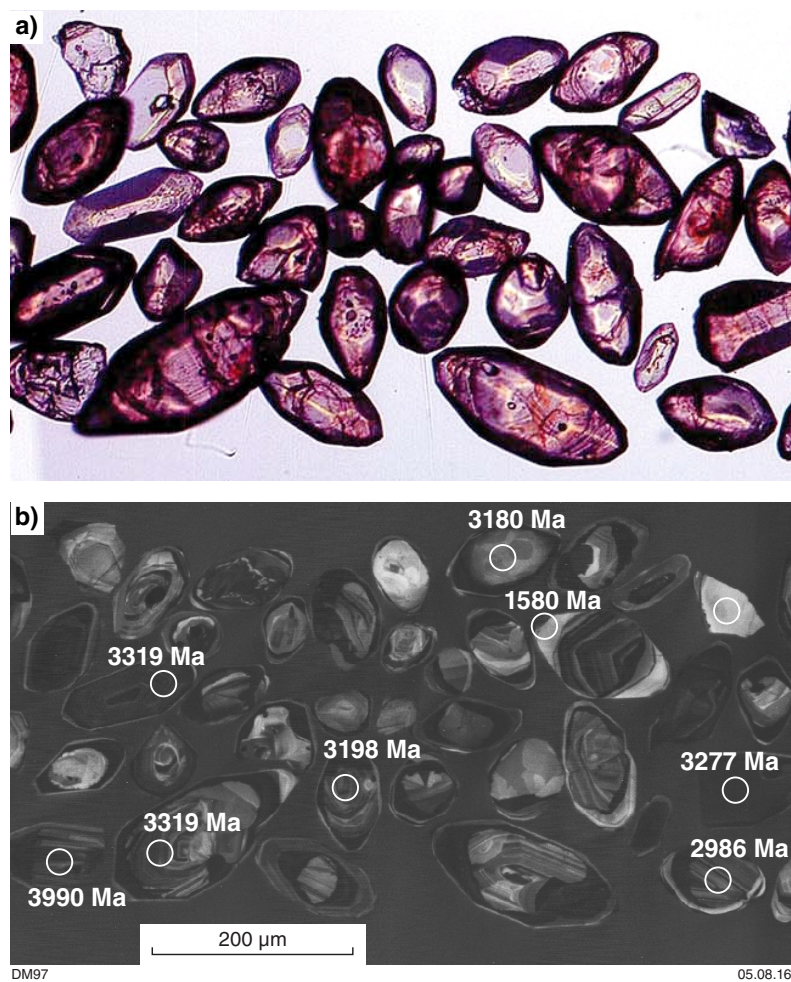


Figure 39. Images of zircons from quartzite, Tabletop Terrane (GA 2006670087): a) transmitted light, showing prismatic forms resulting from metamorphic zircon growth; b) CL image, showing pattern of inner darker rims and moderate to bright rims mantling detrital cores

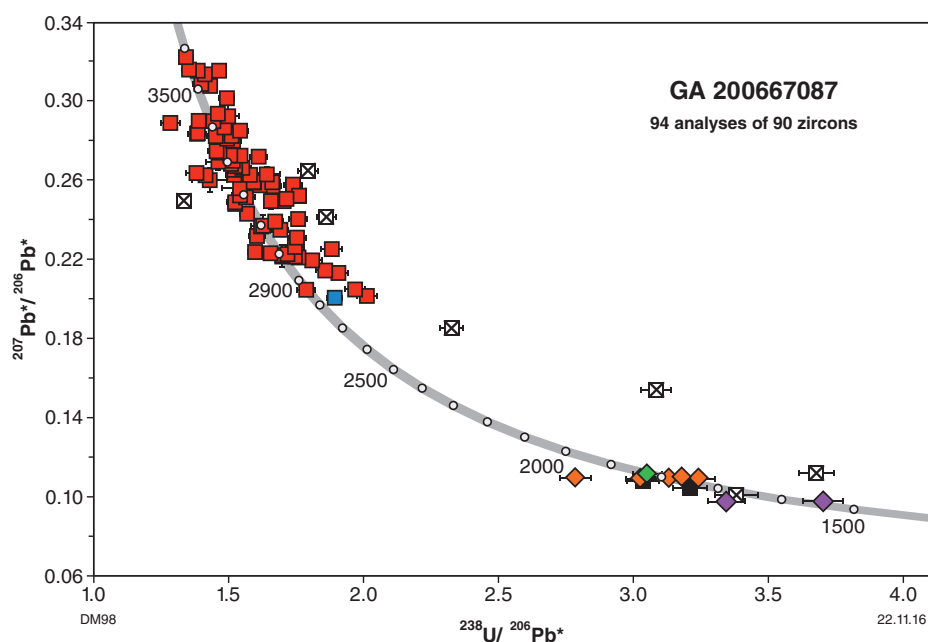


Figure 40. U-Pb analytical data for zircons from quartzite, Tabletop Terrane (GA 2006670087)

(minimum) $^{207}\text{Pb}^*/^{206}\text{Pb}^*$ date is significantly older than the other two analyses (58.1 and 60.2), which have $^{207}\text{Pb}^*/^{206}\text{Pb}^*$ dates of c. 1831 Ma and 1820 Ma respectively, although analysis 58.1 is also >10% discordant and does not provide a reliable date.

Eight analyses of the moderate CL intensity rims were attempted, with one site analysed twice (7.1 and 7.1A). One analysis (61.1) slightly overlapped a bright CL rim and is discounted from further consideration. The moderate intensity rims have U contents of 77–556 ppm, Th/U of 0.13 – 0.30 and $^{207}\text{Pb}^*/^{206}\text{Pb}^*$ dates of 1794–1705 Ma. The two youngest dates (7.1A and 65.1) are slightly younger than the main group of five analyses, which comprise a group with a weighted mean $^{207}\text{Pb}^*/^{206}\text{Pb}^*$ date of 1790 ± 7 Ma (MSWD = 0.55). This date is interpreted to reflect the timing of high-grade metamorphism, with the two younger analyses interpreted to be affected by minor Pb loss.

The geological significance of the dark CL zones is difficult to assess. One possibility is that this generation of zircon formation reflects metamorphism at c. 1820 Ma. Another possibility is that it is related to c. 1790 Ma metamorphism, and represents incomplete isotopic resetting or Pb loss affecting the outer parts of zircon cores rimmed by moderate CL overgrowths.

Only one late-stage, bright CL rim was sufficiently thick to be analysed. Two analyses were carried out in the same site (57.1 and 57.1A), with measured U contents of 128 and 84 ppm, and Th/U of 0.16 and 0.20. The two analyses yield $^{207}\text{Pb}^*/^{206}\text{Pb}^*$ dates of 1579 ± 24 and 1580 ± 24 Ma (1σ), and have a weighted mean date of 1580 ± 34 Ma (MSWD = 0.001). Although analysed at only a single

site, this date is taken to be indicative of the timing of a relatively high-temperature metamorphic event. The date is indistinguishable from a 1589 ± 6 Ma age obtained from the leucogranite that is in contact with the quartzite immediately to the east (GA 2005670178, see below), and the c. 1580 Ma age is interpreted to reflect contact metamorphism associated with this intrusion.

GA 2005670178 – leucogranite, Tabletop Terrane

Leucogranite crops out sporadically in the south-central part of the outcropping Tabletop Terrane over an approximately 4×4 km area (Fig. 13; MGA 515201E 7463830N). A broad zone several kilometres wide surrounding the leucogranite is composed of a complex mix of amphibolite, quartzite, quartz–muscovite schist and ultramafic rock intruded by numerous leucogranite dykes, and might represent a roof zone above the buried extension of the outcropping leucogranite body (Bagas, 1999). The contact between the leucogranite and its host rocks is generally poorly exposed but contact zones were observed in the eastern and southwestern margins where xenoliths of metasedimentary and ultramafic rock occur within the leucogranite (Fig. 8e). Small bodies of pyroxenite close to the contact (e.g. near the Copper Hills PM prospect; MGA 523063E 7464620N) contain thin leucogranite veins, which are associated with narrow zones of contact metamorphism and alteration of the pyroxenite to an actinolite \pm hornblende-bearing assemblage. In some places, complex hybridized zones occur along the contacts of leucogranite and pyroxenite, resulting in mixed rocks comprising actinolite, quartz, K-feldspar and plagioclase.

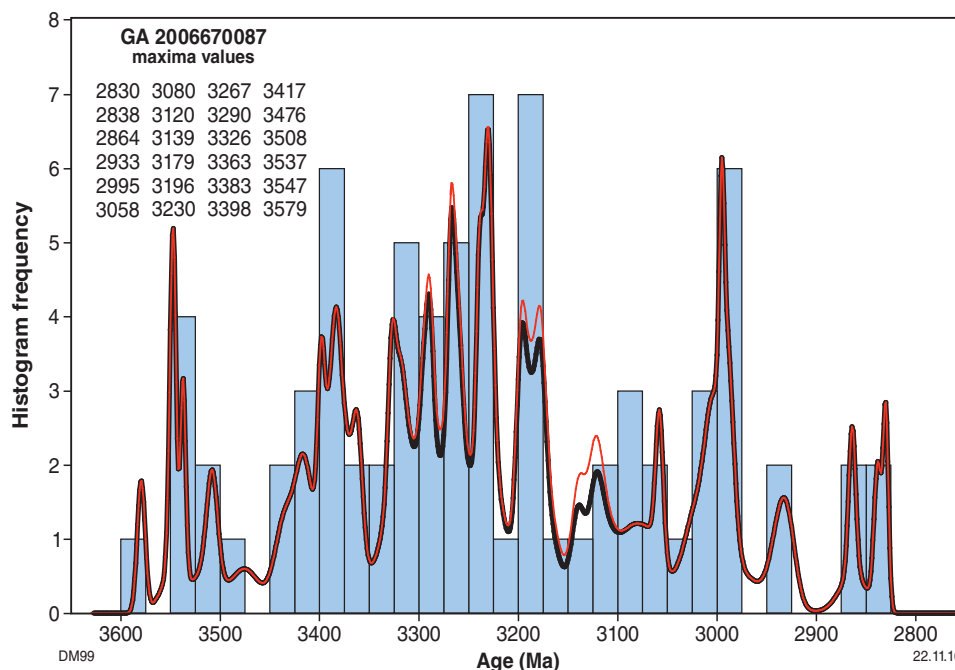


Figure 41. Probability density diagrams of detrital zircon dates for the Tabletop Terrane quartzite. Black line: data <10% discordant; red line: all data

At one locality near the contact of the main leucogranite body (MGA 515087E 7463820N), thin leucogranite veins crosscut a complexly interlayered and foliated unit composed of mafic, felsic and possible metasedimentary components, indicating that tectonism affected the host rocks before emplacement of the leucogranite (Fig. 8a). Numerous late-stage, northerly trending dolerite dykes intrude the leucogranite, forming a dyke swarm focused on the intrusion.

The dated leucogranite sample contains a weak foliation defined by a steeply east-dipping quartz and feldspar-rich layering and minor biotite folia (Fig. 38d,e). In thin section, the leucogranite consists of equigranular, medium-grained plagioclase and K-feldspar crystals with interstitial domains of finer grained recrystallized granoblastic quartz (Fig. 38f). Fine- to medium-grained biotite forms a foliation that anastomoses around feldspar-rich domains. Biotite is commonly associated with late epidote and the

feldspars are commonly sericitized. Minor hornblende and accessory zircon and apatite are present.

Zircons from the leucogranite consist of euhedral to subhedral grains up to 200 μm long, with aspect ratios of 2–3 (Fig. 42a). In CL images, the grains have a relatively uniform appearance and are dominated by oscillatory zoned zircon, with some containing cores of oscillatory zoned zircon of different intensity (Fig. 42b).

Thirty-two analyses were carried out, with one grain analysed twice in two separate locations (Fig. 43; Table A2-10). Twenty-four of the analyses form a group with low to moderate U contents (45–199 ppm), high Th/U (0.81 – 3.32) and $^{207}\text{Pb}^*/^{206}\text{Pb}^*$ dates of 1616–1553 Ma, yielding a weighted mean date of 1589 ± 5 Ma (MSWD = 0.84), which is interpreted as a magmatic age. The remaining eight analyses have dates of 2465–1694 Ma and are interpreted to represent xenocrystic zircons.

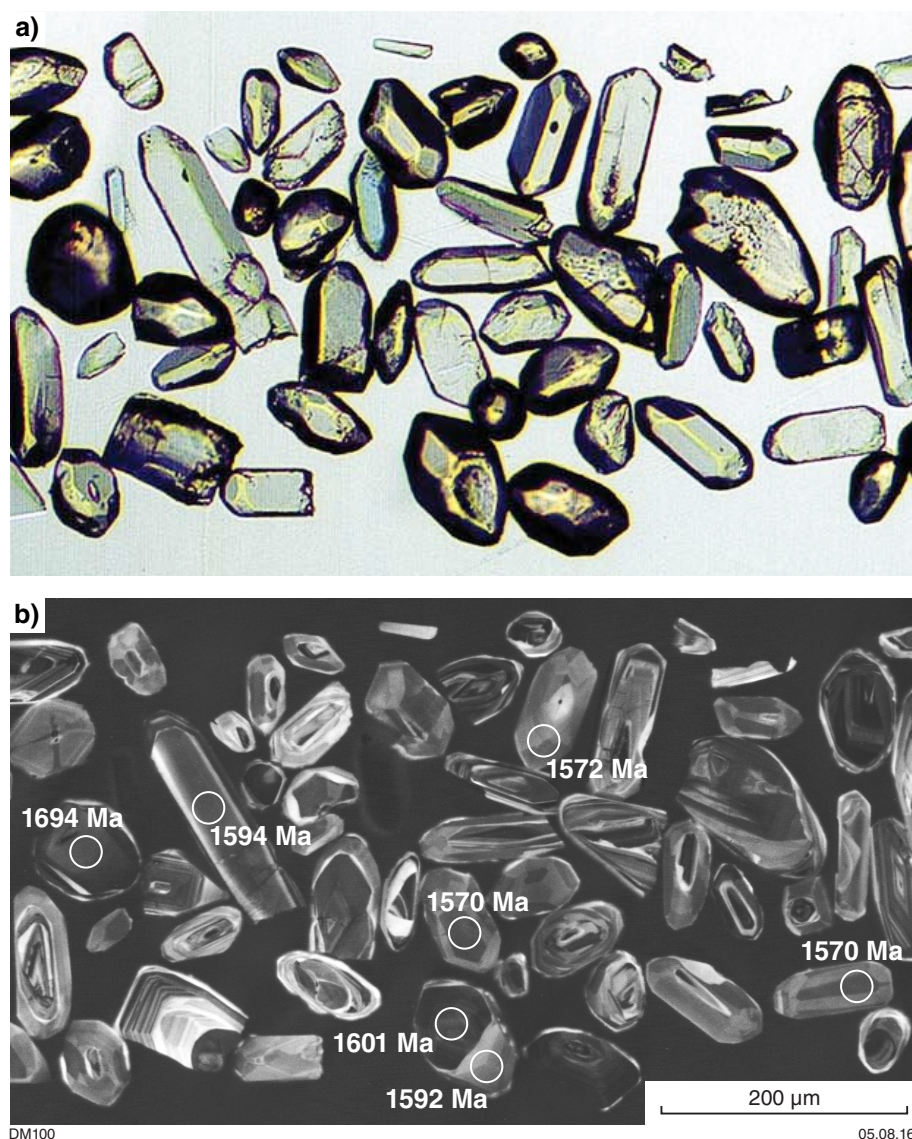


Figure 42. Images of zircons from leucogranite, Tabletop Terrane (GA 2005670178): a) transmitted light; b) CL image

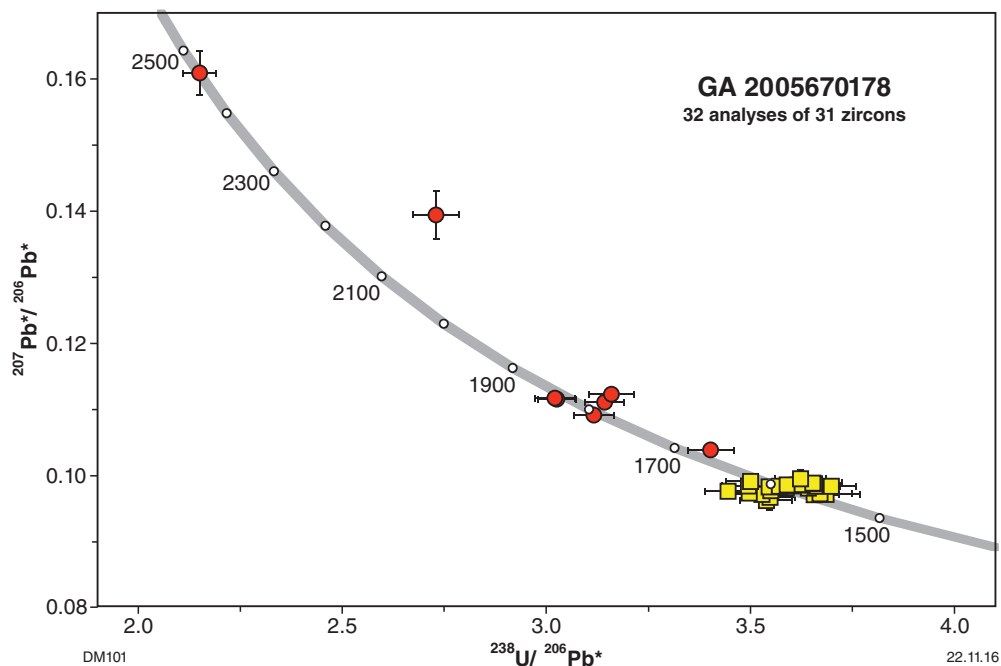


Figure 43. U–Pb analytical data for zircons from leucogranite, Tabletop Terrane (GA 2005670178)

GA 2005670186 – monzogranite, Tabletop Terrane

Small, isolated outcrops of relatively unweathered monzogranite occur in the northeastern margin of the exposed Tabletop Terrane, within a broader area of scattered amphibolite exposures. A small monzogranite outcrop was sampled to test the age of the Krackatinny Supersuite in this area (Fig. 13; MGA 511785E 7479760N). The sampled rock consists of quartz, plagioclase, K-feldspar and biotite with K-feldspar phenocrysts to 1 cm, overprinted by a relatively strongly developed, steeply dipping foliation (Fig. 44a). Irregular, biotite-poor leucogranite veins 1–4 cm thick intrude the monzogranite and crosscut the foliation (Fig. 44b). Some veins are broadly conformable with the foliation but lack the foliation and contain small xenoliths of foliated monzogranite, while others more clearly crosscut the foliation and earlier leucogranite veins. In thin section, oriented biotite associated with recrystallized, medium-grained zones of quartz and K-feldspar defines the dominant foliation, which wraps around domains of coarse-grained K-feldspar, quartz and biotite (Fig. 44c). Minor hornblende is present, with accessory zircon and titanite, and epidote replaces biotite in places.

Zircons from the granite consist of uniform, euhedral crystals typically 50–100 μm long (Fig. 45a). In CL images, the crystals consist of dark to moderate intensity oscillatory zoned zircon, with a few having bright rims a few micrometres thick that were not able to be analysed (Fig. 45b). In some crystals, the oscillatory zoned zircon has zones of differing intensity, although these zones are conformable and appear to form part of the same crystallization event.

Twenty-nine analyses were obtained, with two grains analysed twice in different sites to determine if there was any difference between zones of differing brightness (Fig. 46; Table A2-11). The darkest grains in CL images were generally avoided to reduce the possibility of analysing zircon with radiation damage but three dark grains were analysed to determine if there was any difference in age. All analyses form a concordant to near-concordant group, with U contents of 235–1998 ppm, relatively uniform Th/U (0.39 – 0.80) and $^{207}\text{Pb}^*/^{206}\text{Pb}^*$ dates of 1597–1563 Ma. Twenty-seven analyses yield a weighted mean $^{207}\text{Pb}^*/^{206}\text{Pb}^*$ date of 1577 ± 2 Ma (MSWD = 0.75). The remaining two analyses have marginally younger dates of c. 1566 Ma and 1563 Ma. One of these analyses (1.2) has the highest U content (1843 ppm) and does not form a statistically coherent pairing with a second analysis from the centre of the same grain (1.1). The other (27.1) also has high U (1198 ppm) and has the highest measured proportion of common Pb. These two analyses might have been affected by minor ancient loss of radiogenic Pb, and the 1577 ± 2 Ma date for the main group is interpreted as the crystallization age of the monzogranite.

GA 2005670188 – monzogranite, Tabletop Terrane

An 8×3.5 km area of partially exposed monzogranite in the northeastern part of the Tabletop Terrane forms the most northeasterly outcrop of the Krackatinny Supersuite sampled in this study (Figs 13, 44d). Variably foliated, actinolite- and hornblende-bearing amphibolite — including a plagioclase-rich variety preserving igneous textures — crops out to the southeast of the monzogranite.

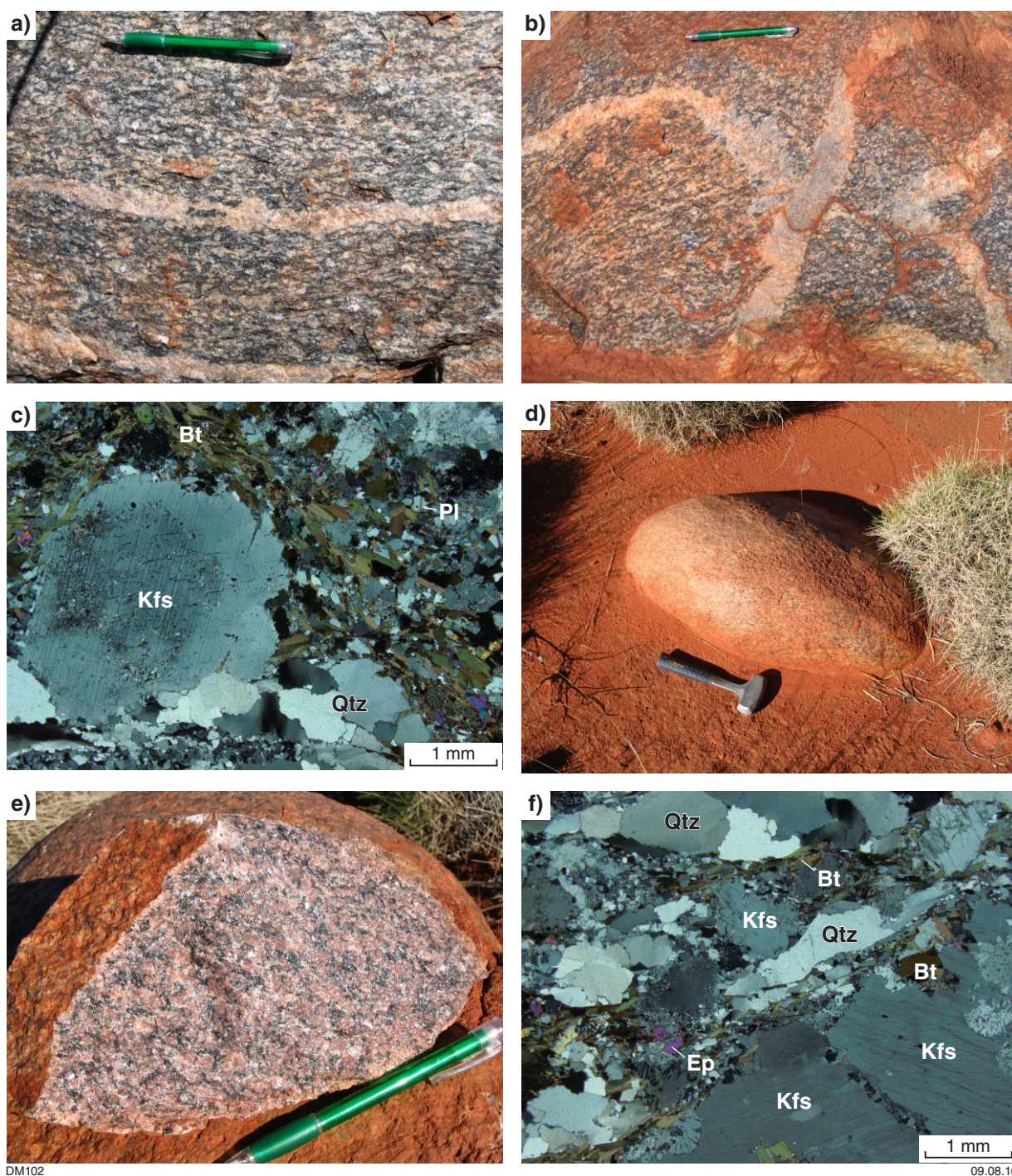


Figure 44. Outcrop photos and photomicrographs of monzogranite, Tabletop Terrane: a) foliated monzogranite (GA 2005670186), showing leucogranite vein subparallel to foliation and apparent xenolith; b) foliated monzogranite (GA 2005670186), showing leucogranite dykes crosscutting foliated monzogranite; c) thin-section image of monzogranite sample GA 2005670186 (XPL); d) typical exposure of monzogranite outcrop, northeastern part of Tabletop Terrane (GA 2005670188); e) hand specimen of monzogranite sample GA 2005670188, showing weakly foliated, pink K-feldspar-rich composition; f) thin-section image of monzogranite sample GA 2005670188 (XPL)

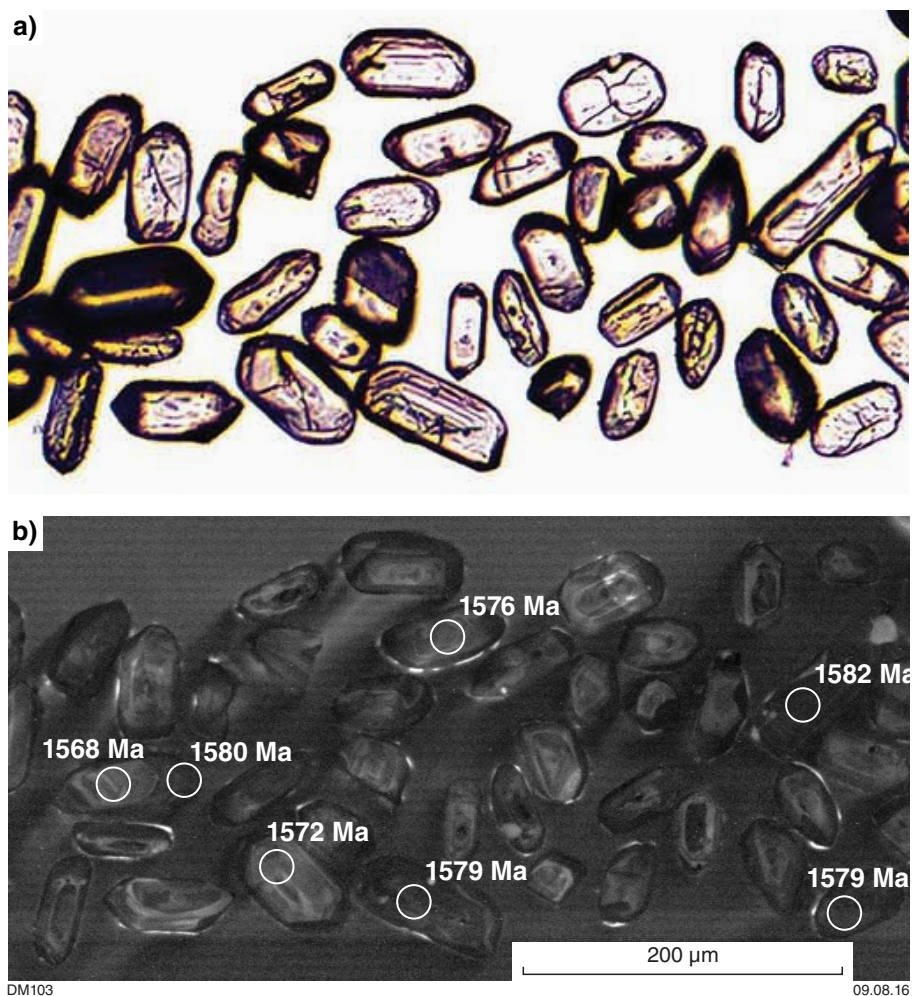


Figure 45. Images of zircons from foliated monzogranite, Tabletop Terrane (GA 2005670186): a) transmitted light; b) CL image

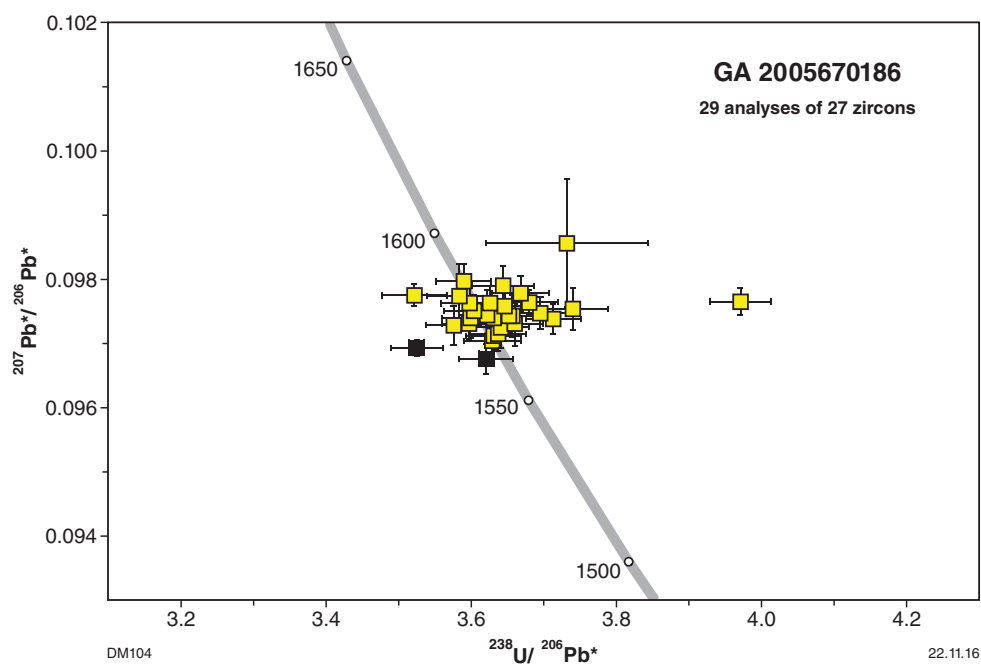


Figure 46. U-Pb analytical data for zircons from foliated monzogranite, Tabletop Terrane (GA 2005670186)

This amphibolite appears to pre-date the monzogranite body, since the monzogranite contains small xenoliths of actinolite–plagioclase partially altered to biotite along xenolith margins. Larger outcrops of actinolite-bearing amphibolite cropping out within the area of monzogranite might represent larger xenoliths. A variably developed, steeply dipping, northwesterly trending foliation in the monzogranite is possibly related to a high-strain zone evident in aeromagnetic imagery, which may be a splay off a larger west-northwesterly trending structure that occurs to the north of the granite.

A sample was taken from a relatively unweathered top of medium- to coarse-grained monzonite comprising pinkish K-feldspar, quartz, plagioclase and biotite with a seriate to slightly porphyritic texture (Fig. 44e; MGA 531426E 7476170N). In thin section, the biotite folia and domains of recrystallized granoblastic to sutured quartz define a weak foliation that wraps more feldspathic domains (Fig. 44f). Fine-grained polygonal quartz occurs along narrow zones of recrystallization along the contacts between larger quartz grains. Biotite comprises up to 5% of the rock and is altered to epidote in places. Minor hornblende and accessory zircon and titanite are present.

Zircons from the granite comprise uniform purple–red, euhedral to subhedral crystals and fragments up to 250 μm long, some with a metamict appearance (Fig. 47a). In CL images, the zircon shows oscillatory zoning (Fig. 47b), with a few grains having thin rims of structureless bright zircon up to several micrometres thick.

Thirty-one analyses were obtained from 30 zircons (Fig. 48; Table A2-12). Two analyses (10.1 and 16.1) have high common Pb ($f_{204} > 1\%$) and are not considered further. Of the remaining 29 analyses, 28 have moderate to high U contents (196–1157 ppm), Th/U of 0.45 – 1.41 and a weighted mean $^{207}\text{Pb}^*/^{206}\text{Pb}^*$ date of 1554 ± 2 Ma (MSWD = 1.3), interpreted as the magmatic age of the monzogranite. A single analysis of high-U (1595 ppm) zircon (19.1) has a slightly younger, near-concordant $^{207}\text{Pb}^*/^{206}\text{Pb}^*$ date of c. 1528 Ma and is interpreted to have undergone a small amount of ancient radiogenic Pb loss.

GA 2005670187 – quartzofeldspathic schist, Tabletop Terrane

Poorly exposed quartzofeldspathic schist occurs in several areas of the northern part of the exposed Tabletop Terrane, and has been mapped as a distinct lithological unit (Bagas, 1999). In some areas, the schist occurs in higher strain zones parallel to the Camel–Tabletop Fault Zone and may represent more highly deformed versions of late-stage granitic rocks, but it is also possible that units represent older volcanic or volcanoclastic units (Smithies and Bagas, 1998). An irregularly shaped area of quartzofeldspathic schist up to 5×3.5 km in extent in the northeastern part of the Tabletop Terrane was sampled to provide a constraint on the timing and origin of these rocks (Fig. 13).

The sample was collected from a broad area of low scattered outcrops of relatively homogeneous, fine-grained quartzofeldspathic schist with a pervasive steeply dipping, approximately northerly trending foliation (Fig. 49a; MGA 520659E 7478320N). The contacts with surrounding rocks are not exposed but outcrops of leucogranite and tonalite occur to the east of the quartzofeldspathic schist and are also in faulted contact with the western margin of the schist. In thin section, the quartzofeldspathic schist consists of a foliated assemblage of fine-grained quartz, K-feldspar and plagioclase, with minor biotite and accessory muscovite, zircon, apatite and opaque minerals (Fig. 49b). Fine- to medium-grained, flattened domains of quartz and feldspar occur within the fine-grained groundmass and are wrapped by the foliation. Feldspar is commonly altered to sericite and minor epidote replaces biotite.

Zircons from the schist are dominated by relatively uniform, euhedral to subhedral crystals generally < 150 μm long but ranging up to 250 μm long (Fig. 50a). In CL images, the zircon is generally of moderate intensity with oscillatory zoning (Fig. 50b).

Twenty-nine of 30 analyses (Fig. 51; Table A2-13), comprise a group with moderate U (142–543 ppm), Th/U of 0.54 – 1.13 and $^{207}\text{Pb}^*/^{206}\text{Pb}^*$ dates of 1562–1533 Ma, yielding a weighted mean date of 1549 ± 3 Ma (MSWD = 1.2). One analysis (29.1) with lower U (67 ppm) and higher Th/U (1.55) has a $^{207}\text{Pb}^*/^{206}\text{Pb}^*$ date of c. 1518 Ma and is excluded from the calculation as potentially having been affected by minor ancient loss of radiogenic Pb.

The date obtained from the quartzofeldspathic schist is similar to a 1554 ± 2 Ma date obtained from monzogranite 11 km to the east-southeast (GA 2005670188), which has been assigned to the same map unit as granitic rocks immediately east of the quartzofeldspathic schist (Bagas and Smithies, 1998). The schist is interpreted as a highly strained and recrystallized granitic rock and thus the 1549 ± 3 Ma date is interpreted to represent the age of magmatic crystallization. A lack of compositional layering, relict volcanic textures or acicular zircons suggests the alternative interpretation of a volcanic protolith for this sample is unlikely. The strong foliation in the sampled area is subparallel to a north-northwesterly to northerly striking fault along the western margin of the quartzofeldspathic schist, and the structural reworking of the granitic rocks appears to be related to movement on this structure.

GA 2006670110 – amphibolite, Tabletop Terrane

Amphibolite was sampled in the central northwestern part of the Tabletop Terrane (Fig. 13; MGA 510849E 7471200N) with the aim of constraining the emplacement age of the widespread low- to medium-grade metamorphosed mafic rocks in the area. Most of these mafic rocks are very poorly exposed, forming low areas

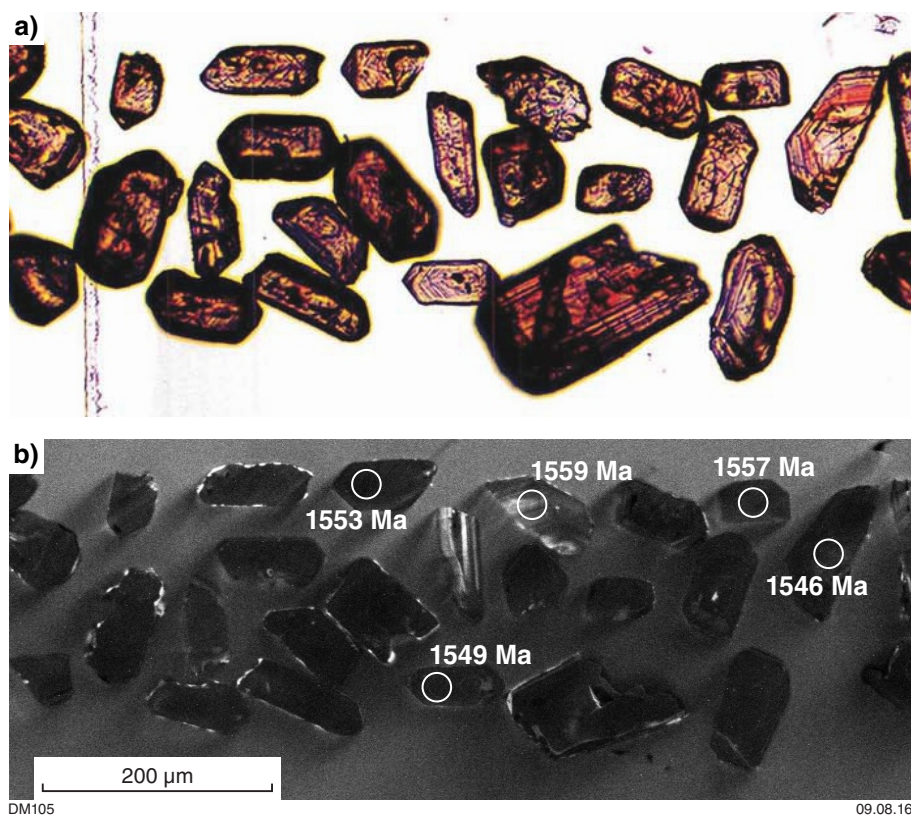


Figure 47. Images of zircons from weakly foliated monzogranite, Tabletop Terrane (GA 2005670188): a) transmitted light; b) CL image

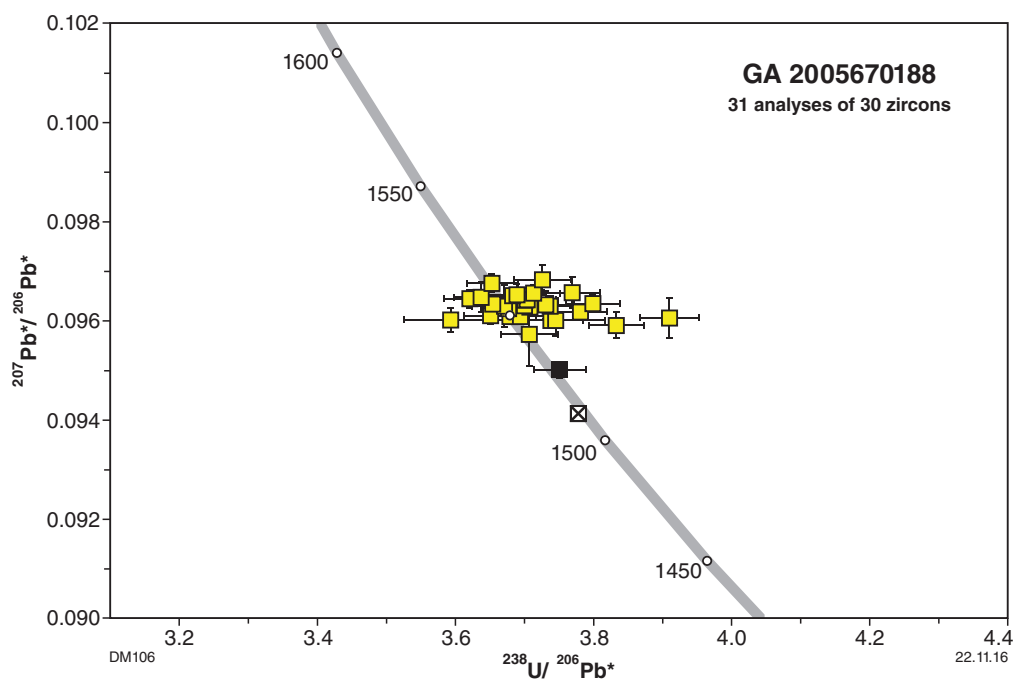


Figure 48. U-Pb analytical data for zircons from weakly foliated monzogranite, Tabletop Terrane (GA 2005670188)

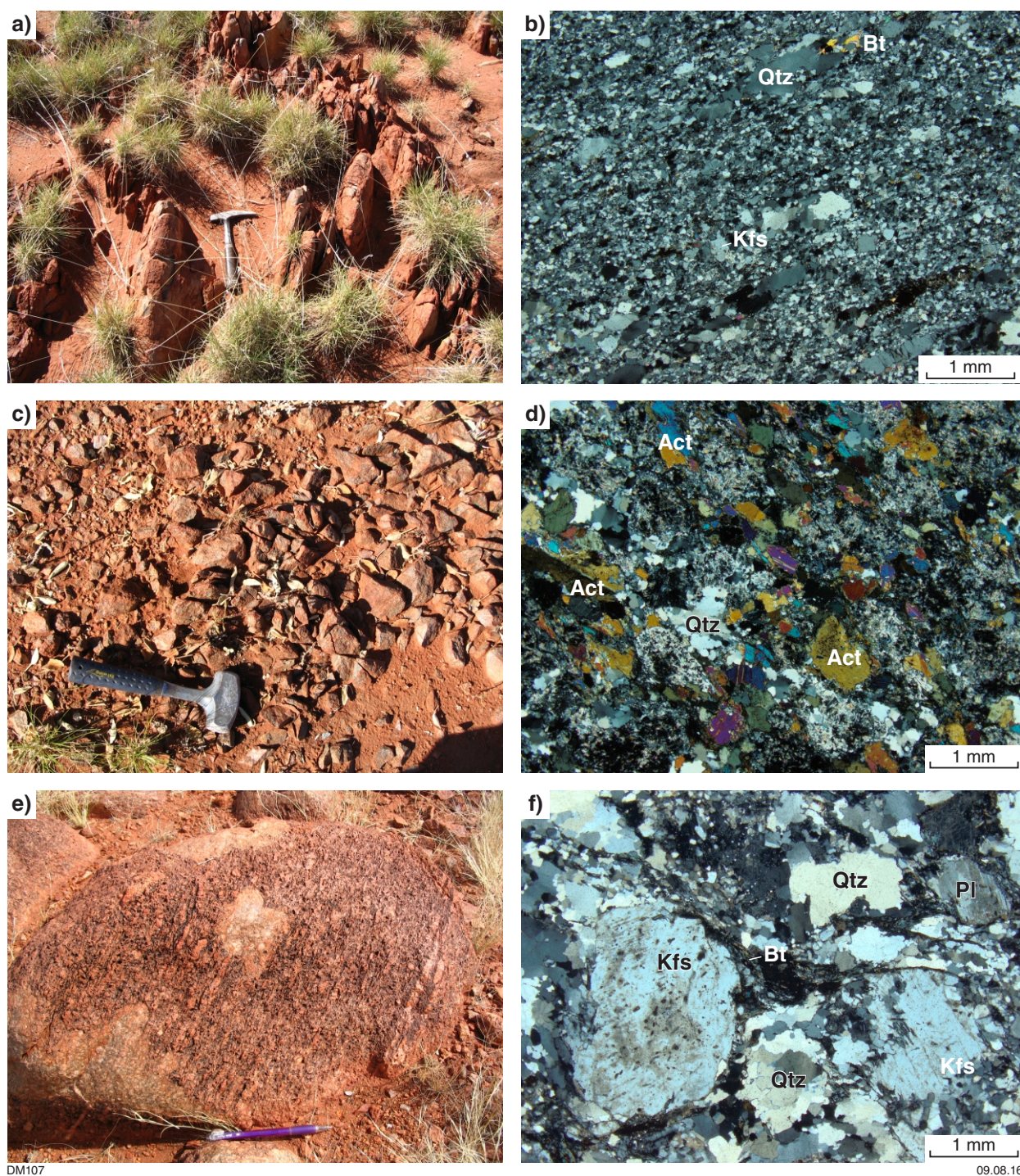


Figure 49. Outcrop photos and photomicrographs of quartzofeldspathic schist, amphibolite and leucogranite, Tabletop Terrane: a) typical exposure of felsic schist (GA 2005670187); b) thin-section of quartzofeldspathic schist sample GA 2005670187 (XPL); c) typical low outcrop of amphibolite in the Tabletop Terrane (GA 2006670110); d) thin-section of amphibolite sample GA 2006670110, showing actinolite- and hornblende-bearing assemblage, with irregular, thin (<1 mm thick) quartz-rich zone (XPL) — feldspar is typically weathered to sericite; e) foliated leucogranite outcrop from the southeastern Tabletop Terrane (GA 2006670119); f) thin-section image of leucogranite sample GA 2006670119 (XPL), showing biotite foliation wrapping K-feldspar grain

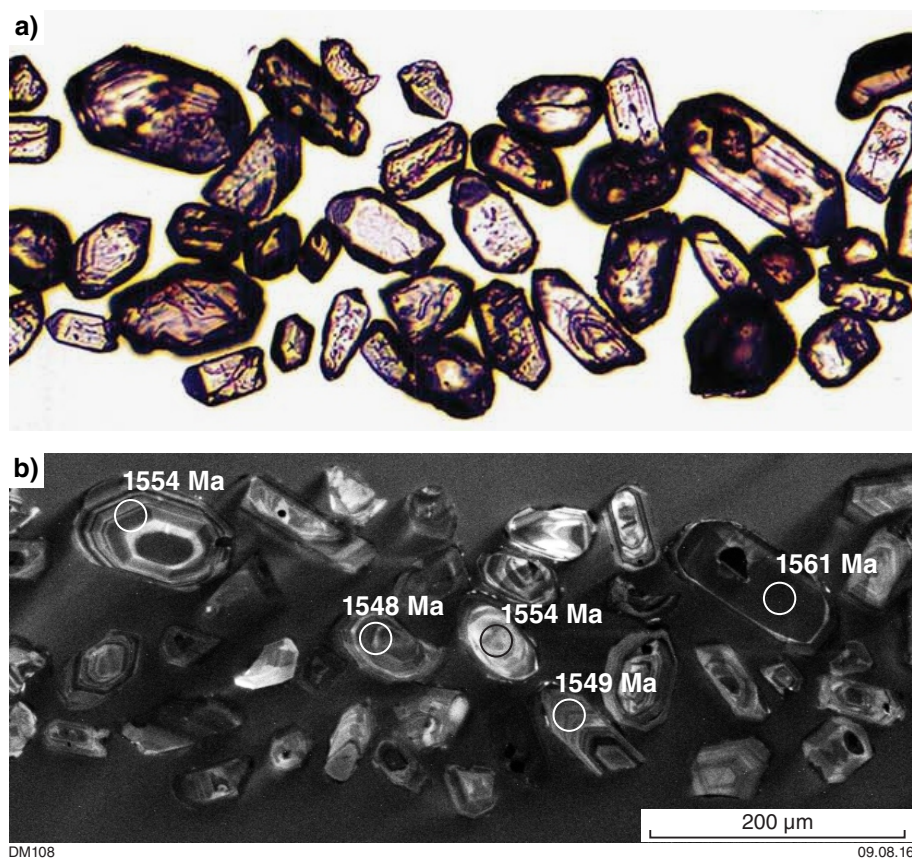


Figure 50. Images of zircons from quartzofeldspathic schist, Tabletop Terrane (GA 2005670187): a) transmitted light; b) CL image

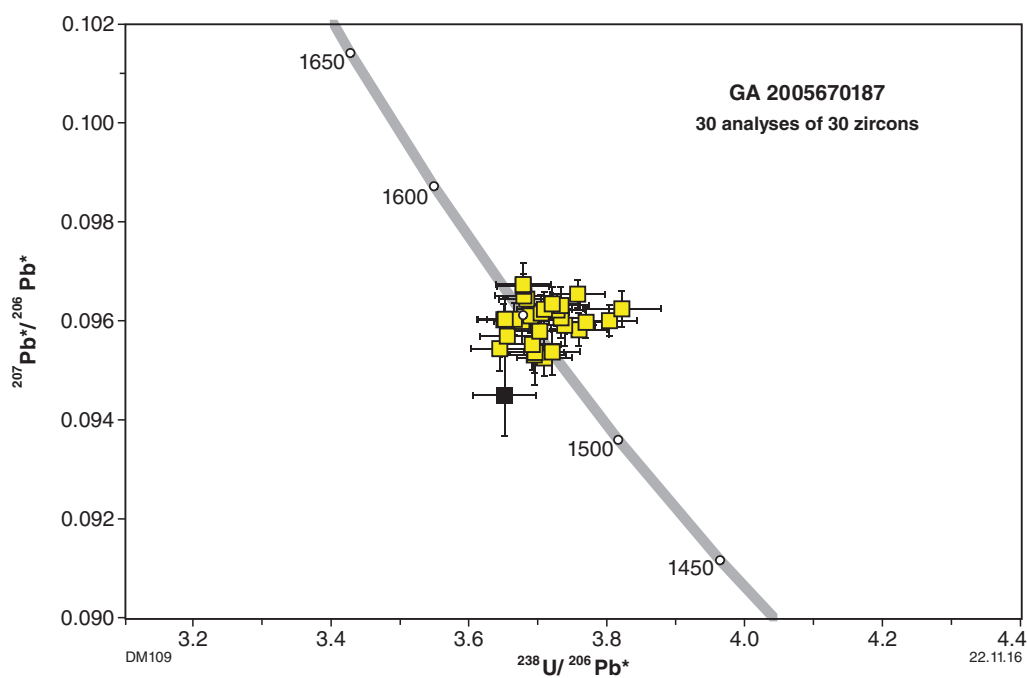


Figure 51. U-Pb analytical data for zircons from quartzofeldspathic schist, Tabletop Terrane (GA 2005670187)

of weathered subcrop marginal to areas of more resistant granitic rocks. In the area sampled, amphibolite ranges from medium-grained actinolite- or hornblende-bearing units to coarse-grained plagioclase-rich leucocratic variants interpreted to be derived from leucogabbro and anorthosite (Bagas, 1999). Locally, primary igneous textures defined by plagioclase laths are preserved, despite partial recrystallization under greenschist to lower amphibolite facies conditions, as indicated by the presence of actinolite and hornblende. The sampled unit consists of a relatively leucocratic, poorly exposed amphibolite containing a weakly developed, steeply dipping west-northwesterly trending foliation (Fig. 49c). Minor exposures of leucogranite also occur in the area of the sampled amphibolite but contacts are not exposed. A larger body of leucogranite several metres wide crops out about 250 m to the east, where narrow veins of leucogranite intrude the amphibolite. Late-stage northerly trending dolerite dykes also intrude the amphibolite about 1.5 km to the northeast.

In thin section, the amphibolite consists of medium-grained assemblage of actinolite and minor hornblende with saussuritized plagioclase and lesser quartz (Fig. 49d). Small irregular domains up to a few millimetres thick are quartz-rich, with quartz grains forming small isolated aggregates and thin laminae within the foliated amphibolite. In some areas near the quartz-rich domains, clusters of very small inclusions with pleochroic halos within amphibole might be zircons, although their small size makes identification uncertain.

Zircons from the amphibolite consist of euhedral to subhedral, prismatic grains up to 200 μm long (Fig. 52a). In CL images, the zircons comprise a relatively homogeneous group with oscillatory and sector zoning (Fig. 52b). Although many grains are entirely composed of zircon with uniform intensity and zoning, some consist of a rounded core of relatively dark oscillatory or sector-zoned zircon mantled by oscillatory or sector-zoned zircon of slightly higher CL intensity that in places truncates the zoning in the core.

Twenty-three analyses were obtained, with four grains analysed twice in separate sites to assess core and rim relationships (Fig. 53; Table A2-14). Despite the differences evident in CL images, there was no resolvable difference in their dates. All the analyses are concordant to near-concordant, with low to moderate U contents (47–456 ppm), Th/U of 0.29 – 0.70 and $^{207}\text{Pb}^*/^{206}\text{Pb}^*$ dates of 1599–1549 Ma, with a weighted mean $^{207}\text{Pb}^*/^{206}\text{Pb}^*$ date of 1571 ± 4 Ma (MSWD = 1.07). Although the CL images reveal textural complexity in some zircons, any potential differences in the timing of zircon growth are within the limits of analytical uncertainty, and the 1571 ± 4 Ma date is considered to reflect the age of a single magmatic event.

Although the data are statistically simple, the interpretation of the geological significance of this date is not straightforward. One possible interpretation

is that the date represents the age of crystallization of the mafic protolith. However, the 1571 ± 4 Ma date is similar to, or slightly younger than, a 1577 ± 2 Ma date obtained for monzogranite about 8.5 km to the north (GA 2005670186), which is thought to intrude amphibolite. Whole-rock geochemical data for the sampled amphibolite indicate a very low Zr content (34 ppm), suggesting that there might have been little or no magmatic zircon in this rock. It is thus speculated that the thin, irregular domains containing quartz might represent deformed and attenuated leucogranite veinlets intruded before deformation and recrystallization. If this is the case, then the zircons separated from this sample might represent the magmatic age of the leucogranite rather than the amphibolite. The whole-rock geochemistry of the sampled amphibolite is similar to that of other amphibolites within the Tabletop Terrane, with a low SiO_2 content of 51.7 wt%, indicating that if granitic material was incorporated into the amphibolite, it was insufficient to significantly change the bulk composition, consistent with the volumetrically very small amount of quartz-bearing material observed in thin section.

GA 2006670119 – leucogranite, Tabletop Terrane

A 9 x 5 km body of leucogranite crops out about 11 km east-northeast of Curara Soaks (No. 24 Well) on the Canning Stock Route (Fig. 13). It consists of coarse-grained pink K-feldspar phenocrysts up to 1 cm long in a medium-grained matrix of quartz, feldspar and biotite. The leucogranite is overprinted by a variably developed, but pervasive northwesterly to west-northwesterly trending foliation defined by biotite folia and a preferred orientation of elongate K-feldspar phenocrysts. This foliation appears to be related to a splay from the Camel–Tabletop Fault Zone that passes along the southern margin of the leucogranite body, with the main fault zone itself some 9 km farther to the southwest. The leucogranite is intruded by unfoliated north-northeasterly trending and west-northwesterly trending dolerite dyke sets of unknown age and an elongate thicker body of dolerite subparallel to the west-northwesterly dykes. The leucogranite was sampled near its southern margin (Fig. 49e; MGA 544495E 7448640N). In thin section, the granite consists of coarse-grained K-feldspar phenocrysts wrapped by a foliation defined by biotite and fine- to medium-grained recrystallized quartz, K-feldspar and plagioclase (Fig. 49f). Biotite is commonly altered to epidote and chlorite, and accessory apatite, zircon and titanite are present.

Zircons from the leucogranite consist of pinkish euhedral, equant to elongate grains up to 200 μm long, which in CL images consist of generally moderate intensity oscillatory zoned zircon (Fig. 54a,b). Some grains have a rim of moderate intensity oscillatory zoned zircon that mantles a core of broadly similar character but with a discordant relationship between the patterns of zoning.

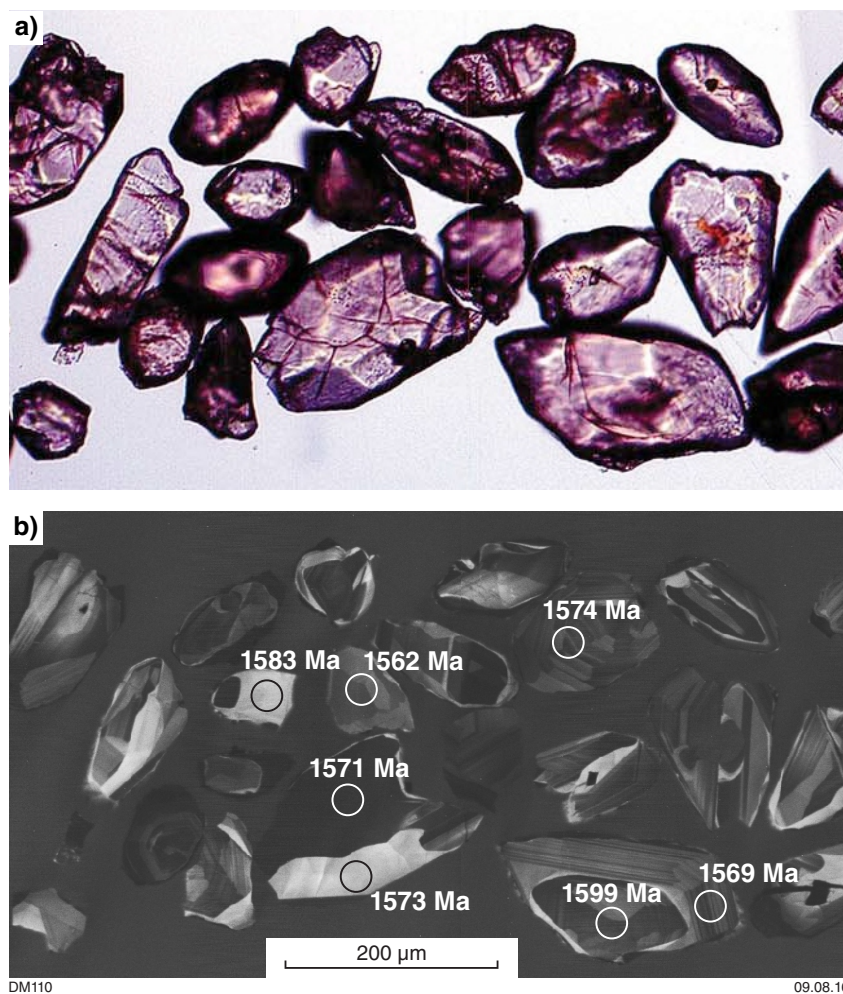


Figure 52. Images of zircons from amphibolite, Tabletop Terrane (GA 2006670110): a) transmitted light; b) CL image, showing differing growth zones yielding indistinguishable dates within analytical uncertainty

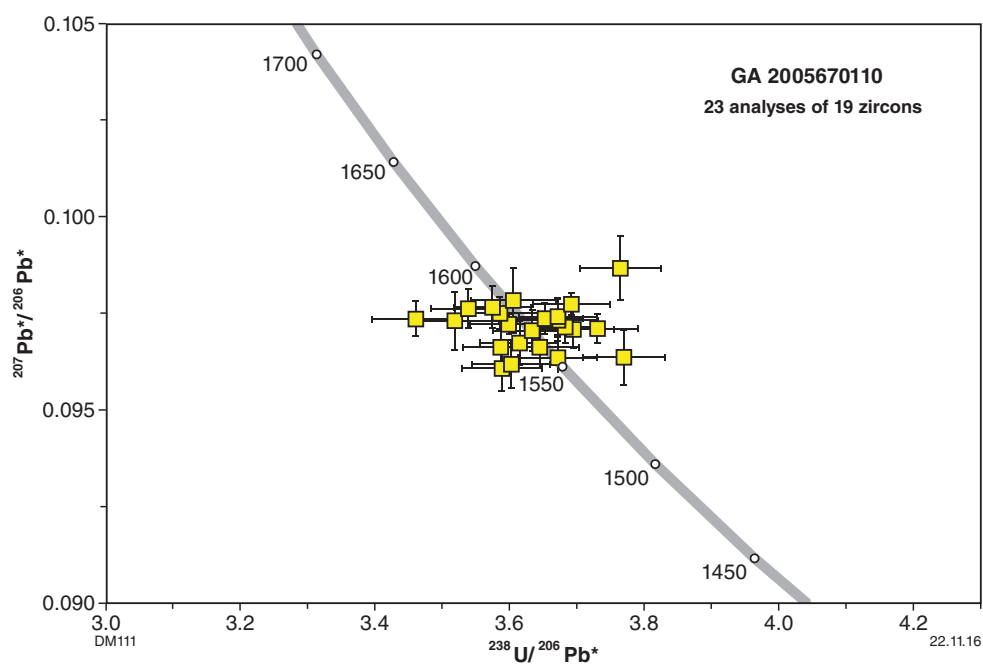


Figure 53. U-Pb analytical data for zircons from amphibolite, Tabletop Terrane (GA 2006670110)

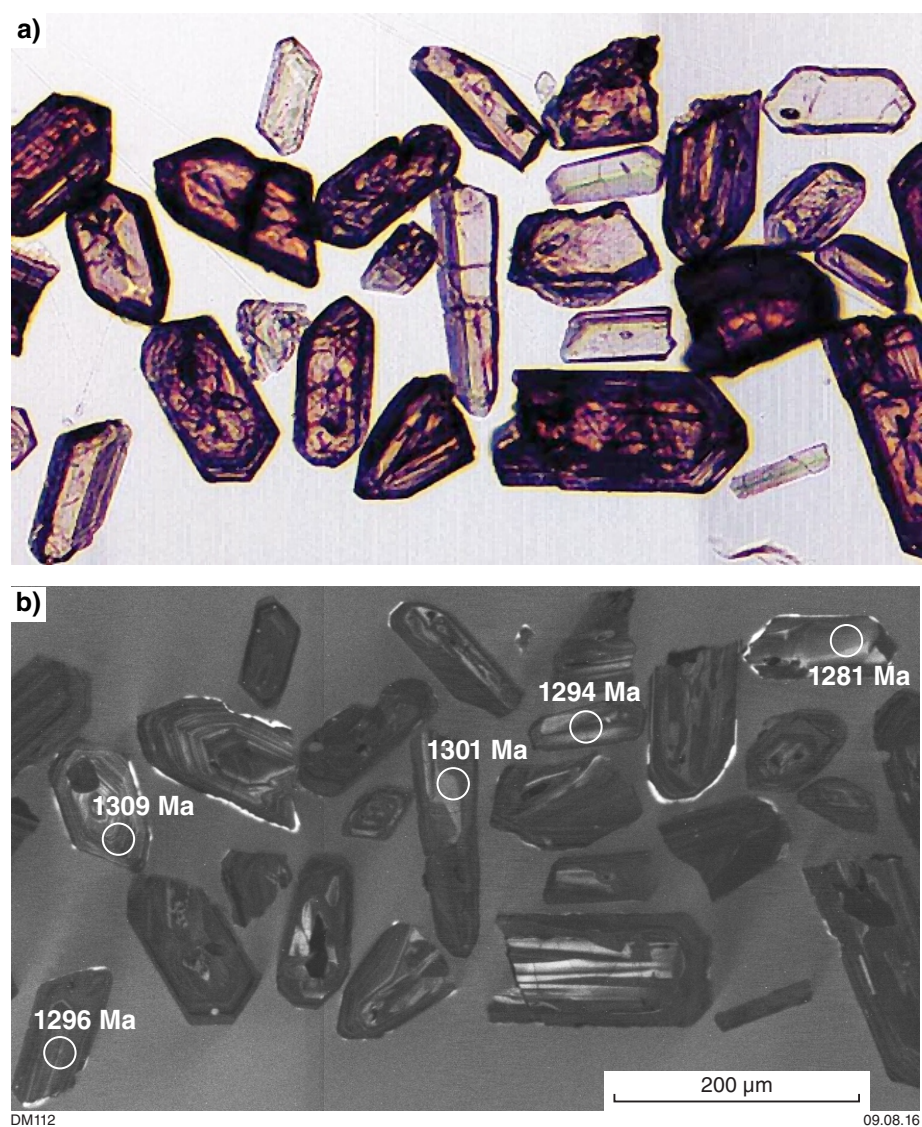


Figure 54. Images of zircons from leucogranite, southeastern Tabletop Terrane (GA 2006670119): a) transmitted light; b) CL image

Twenty analyses were obtained (Fig. 55; Table A2-15), with one (20.1) >10% reversely discordant, and another with a high U content of 1638 ppm (19.1) having high common Pb ($f_{204} > 1\%$). These two analyses are not considered further. The remaining 18 analyses form a concordant to near-concordant group with generally moderate to high U contents (68–1313 ppm), Th/U of 0.25 – 1.53 and $^{207}\text{Pb}^*/^{206}\text{Pb}^*$ dates of 1332–1220 Ma. Seventeen of these analyses form a group with a weighted mean $^{207}\text{Pb}^*/^{206}\text{Pb}^*$ date of 1296 ± 4 Ma (MSWD = 0.78), interpreted as the magmatic age of the leucogranite. One analysis (17.1) with a high U content of 1313 ppm yields a date of c. 1220 Ma, which is significantly younger than the main group, and is considered to have undergone a small degree of ancient radiogenic Pb loss.

Whole-rock geochemistry

Whole-rock geochemical data were collected for igneous rocks in the Rudall Province to characterize the compositions of the various magmatic suites and to potentially constrain their geodynamic settings. Most of the samples analysed were collected from the Tabletop Terrane (Fig. 56), where granitic rocks with compositional similarities to modern arc-related granites have previously been identified (Smithies and Bagas, 1998). Sampling in this terrane is constrained by the limited outcrop but a reasonably representative range of the mapped granitic rocks were sampled and three samples of amphibolite were also collected. A few samples of the Kalkan Supersuite were collected from the Talbot and

Connaughton Terranes. In total, 26 samples collected as part of this study were analysed, while a further 21 pre-existing powders of GSWA geochemical samples collected during field mapping in the 1990s were reanalysed to provide a more complete range of trace element data for these samples.

Geoscience Australia rock samples were prepared for chemical analysis by jaw crushing (2–5 kg) and then grinding a subsample (50–70 g) in a tungsten carbide ring mill. Abundances of major and trace elements were determined at Geoscience Australia, Canberra (XRF and ICP-MS). Major and minor elements (Si, Ti, Al, Fe, Mn, Mg, Ca, Na, K, P and S) were determined by wavelength-dispersive XRF on fused disks using methods similar to those of Norrish & Hutton (1969). Precision for these elements is better than ~1% of the reported values. As, Ba, Cr, Cu, Ni, Sc, V, Zn and Zr were determined by pressed pellet on a wavelength-dispersive XRF using methods similar to those described by Norrish & Chappell (1977). Selected trace elements (Cs, Ga, Nb, Pb, Rb, Sb, Sn, Sr, Ta, Th, U, Y) and the rare earth elements (REE) were analysed at Geoscience Australia by ICP-MS (Perkin Elmer ELAN 6000 and Agilent 7500) using methods similar to those of Eggins et al. (1997), but on solutions obtained by dissolution of fused glass disks (Pyke, 2000). FeO abundances were determined at Geoscience Australia by digestion and electrochemical titration using a modified methodology based on Shapiro and Brannock (1962).

Reanalysis of GSWA samples was carried out on archived powders for which no sample preparation information is now available. Abundances of major and trace elements were determined at the Intertek Australia laboratory in Maddington, Perth, using XRF and LAICP-MS techniques (LITH/204X package), with the precision and accuracy of major and trace elements better than 5% relative standard deviation (RSD), based on analyses of duplicate and reference materials.

Rudall Province granite geochemistry

The geochemical data for granitic rocks of the Rudall Province have been placed into three main groups. The 1804–1762 Ma Kalkan Supersuite in the Talbot and Connaughton Terranes comprises one group, while granitic rocks in the Tabletop Terrane have been subdivided into two groups based on limited geochronological data and the lithological mapping of Bagas and Smithies (1996, 1998a). The main group, with dates of 1589–1549 Ma, is here defined as the Krackatinny Supersuite, which appears to represent the most voluminous magmatism exposed in the Tabletop Terrane. The Krackatinny Supersuite was previously defined to incorporate all the later stage felsic intrusive rocks exposed in the Tabletop Terrane (Bagas, 1999, 2004), for which the only available dates were 1476–1286 Ma.

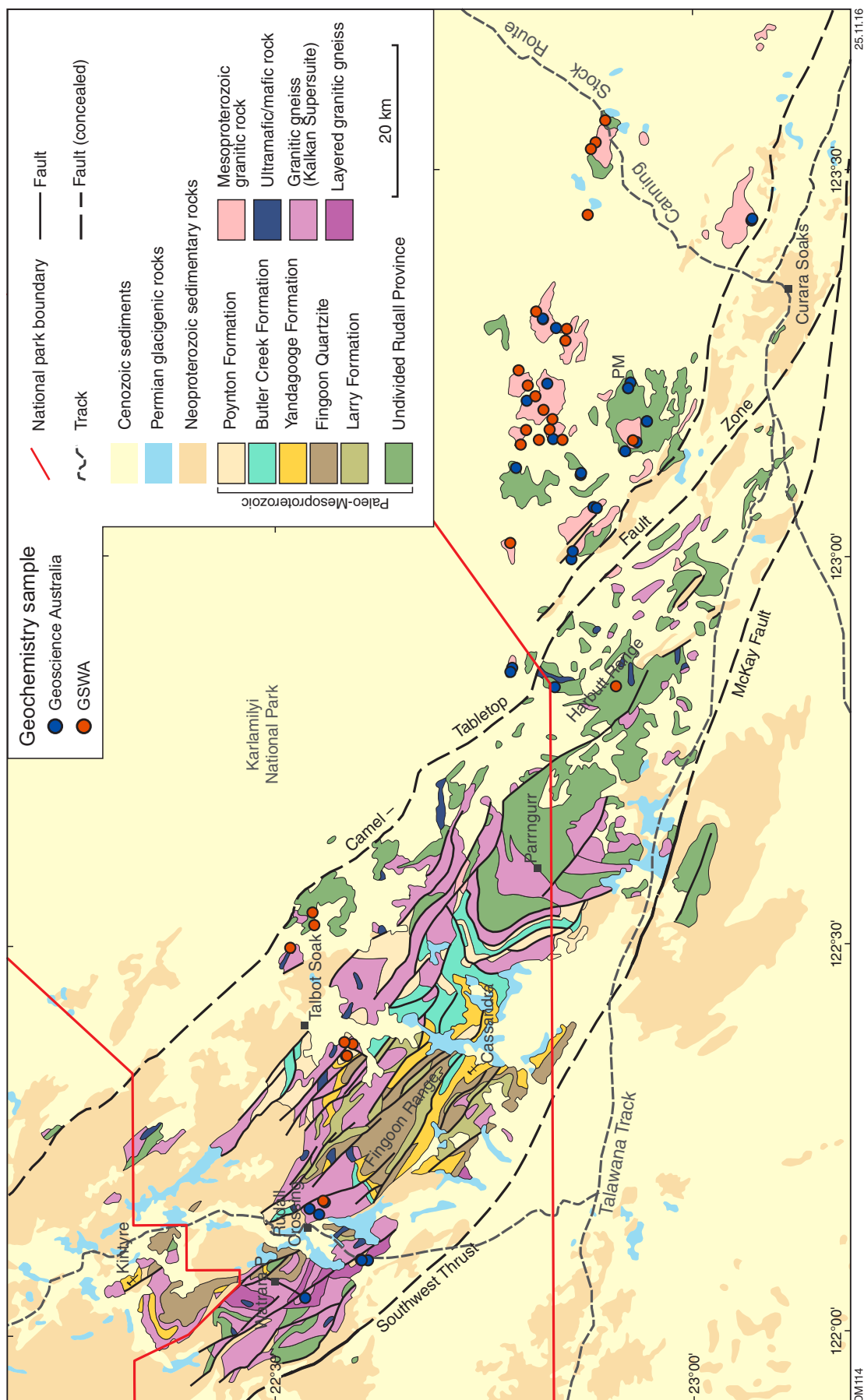


Figure 56. Locations of samples analysed for whole-rock geochemistry in this study (GA samples, this study in blue; reanalysed GSWA samples in red)

The dating in this study, however, indicates that the 1589–1549 Ma granitic rocks are distinct from those emplaced between c. 1476 and 1286 Ma, which may be more spatially restricted. Only one example of a c. 1476 Ma granitic rock is known, a biotite- and muscovite-bearing granodiorite obtained from drillcore in a regolith-covered area in the far southeastern part of the Tabletop Terrane (Thevissen, 1991). The 1310–1286 Ma suite has been dated at three localities proximal to either the Camel–Tabletop Fault Zone or a major splay from this structure, and is here defined as the Camel Suite. Where dated, the Camel Suite consists of weakly deformed leucogranite and pegmatite, and has yielded $^{206}\text{Pb}^*/^{207}\text{Pb}^*$ dates of 1310 ± 4 Ma (Nelson, 1996e), 1296 ± 4 Ma (this study), 1291 ± 10 Ma (Nelson, 1995b) and 1286 ± 6 Ma (Bagas, 2004). Other small, late-stage pegmatite bodies have been identified in the Talbot and Connaughton Terranes and might be part of this suite but the ages of these are not known. One pegmatite that crosscuts a high-grade foliation in the Talbot Terrane, 9 km southwest of the Camel–Tabletop Fault, yielded a Rb–Sr date of 1132 ± 21 Ma (Chin and de Laeter, 1981), which represents a minimum age.

It can be difficult to distinguish between granitic rocks of the Krackatinny Supersuite and Camel Suite in the field, particularly the more potassic varieties, as both may have similar assemblages comprising K-feldspar, plagioclase, quartz and biotite. This is exemplified by the 1589 ± 6 Ma date obtained from a leucogranite intrusion 7 km west-southwest of the PM Prospect, which in regional mapping (Bagas, 1999) was assigned to the same map unit as leucogranite dated at 1296 ± 4 Ma from the southeastern part of the Tabletop Terrane. Despite the similarities, there are differences between the suites, with a tendency for the Camel Suite to have consistently high K-feldspar content compared with the Krackatinny Supersuite, which contains more plagioclase-rich variants mapped as tonalite (Bagas, 1999). Most samples could be assigned to one of the known supersuites but a few were of uncertain affinity and only tentatively classified to be part of the Krackatinny Supersuite.

The Krackatinny Supersuite is the best represented by the geochemical data, comprising 35 of the 47 total analyses (Appendix 3). Eight samples have been assigned to the Kalkan Supersuite and five to the Camel Suite, which are insufficient to characterize these magmatic suites but do provide some indications of their composition. Geochemical variations suggest that rocks grouped into the Krackatinny Supersuite include at least three compositional series (Figs 57, 58):

1. A high Sr/Y sodic series ranging from 68.03 to 78.49 wt% SiO_2 , with K_2O concentrations <2 wt% (i.e. low to medium K), Na_2O between 2.9 and 4.6 wt% and $\text{K}_2\text{O}/\text{Na}_2\text{O}$ ratios <0.5 (Fig. 57). These rocks are magnesian and calcic (terminology of Frost et al., 2001) and mainly metaluminous. They are strongly enriched in Ba (up to 926 ppm) and Sr (up to 943 ppm — decreasing to 280 ppm with increasing silica) and depleted in Rb (<40 ppm) and have very high Sr/Y ratios from 80 to 387. Mantle-normalized incompatible trace element patterns (Fig. 58) show well-developed negative Nb anomalies, positive anomalies for Sr and Eu and strong REE fractionation with LREE enrichments (La up to 36 ppm) and HREE depletions ($\text{Yb} < 0.5$ ppm). These granitic rocks have the compositional characteristics of adakite, formed through melting of mafic crust at pressures sufficiently high (>10 kbar) to destabilise plagioclase and to leave peritectic garnet (e.g. Martin et al., 2005; Richards and Kerrich, 2007; Castillo, 2012). The samples in this series were obtained from a relatively restricted area near the Camel–Tabletop Fault Zone and might represent components of a partially exposed intrusive complex about 5–10 km in diameter, from which a 1589 ± 6 Ma date was obtained in this study.
2. A second sodic series has a more extended silica range (62.80 – 77.51 wt%) and ranges to slightly higher K_2O (up to 3.15 wt%) and Na_2O (5.73 wt%) concentrations, with $\text{K}_2\text{O}/\text{Na}_2\text{O}$ ratios up to 0.8 (Fig. 57). These rocks are dominantly magnesian but weakly ferroan at high SiO_2 , and calcic to calc-alkalic. Compared to the high Sr/Y series, these granites are depleted in Sr and enriched in Rb and are generally enriched in all incompatible trace elements (including Ba) but have lower La/Nb and Sr/Y ratios. Their mantle-normalized incompatible trace element patterns show no Sr or Eu anomalies and REE fractionation is significantly less (Fig. 58). Plots for many incompatible trace elements (e.g. Zr) against silica possibly distinguish two subgroups: one with 62.80 – 68.50 wt% SiO_2 , the other with 72.57 – 77.51 wt% SiO_2 , and both with decreasing trace element concentrations with increasing silica. As with the high Sr/Y sodic series, the compositions of the low Sr/Y sodic rocks are consistent with derivation from a sodic mafic to intermediate source. However, low Sr/Y, La/Yb and Dy/Yb ratios suggest melting did not occur in the presence of garnet, and was at lower pressures (<10 kbar) than was the case for the high Sr/Y sodic series.
3. High-K series granites range in SiO_2 from 70.60 to 76.96 wt%, are typically ferroan, alkali–calcic and range from metaluminous to peraluminous, with K_2O of 3.98 – 6.88 wt%. Their TiO_2 and P_2O_5 and Zr concentrations decrease with increasing silica but at SiO_2 70 wt% are strongly enriched (TiO_2 ~0.6 wt%; P_2O_5 ~0.14 wt%; Zr ~340 ppm). These features, along with strong enrichments in REE, Th, Nb and Ba, are characteristic of many Proterozoic A-type granites formed through very high temperature (up to 1000 °C) melting of thin and anhydrous lower crust from a source that had previously homogenized mantle inputs with melts of lower crust. Mantle-normalized incompatible trace element patterns essentially parallel those of the low Sr/Y sodic rocks but at higher trace element abundances, and show prominent negative anomalies for Sr and less so for Eu — reflecting either feldspar fractionation or source retention (Fig. 58). Three samples of the high-K series were dated in this study, yielding magmatic crystallization ages of c. 1577, 1554 and 1549 Ma.

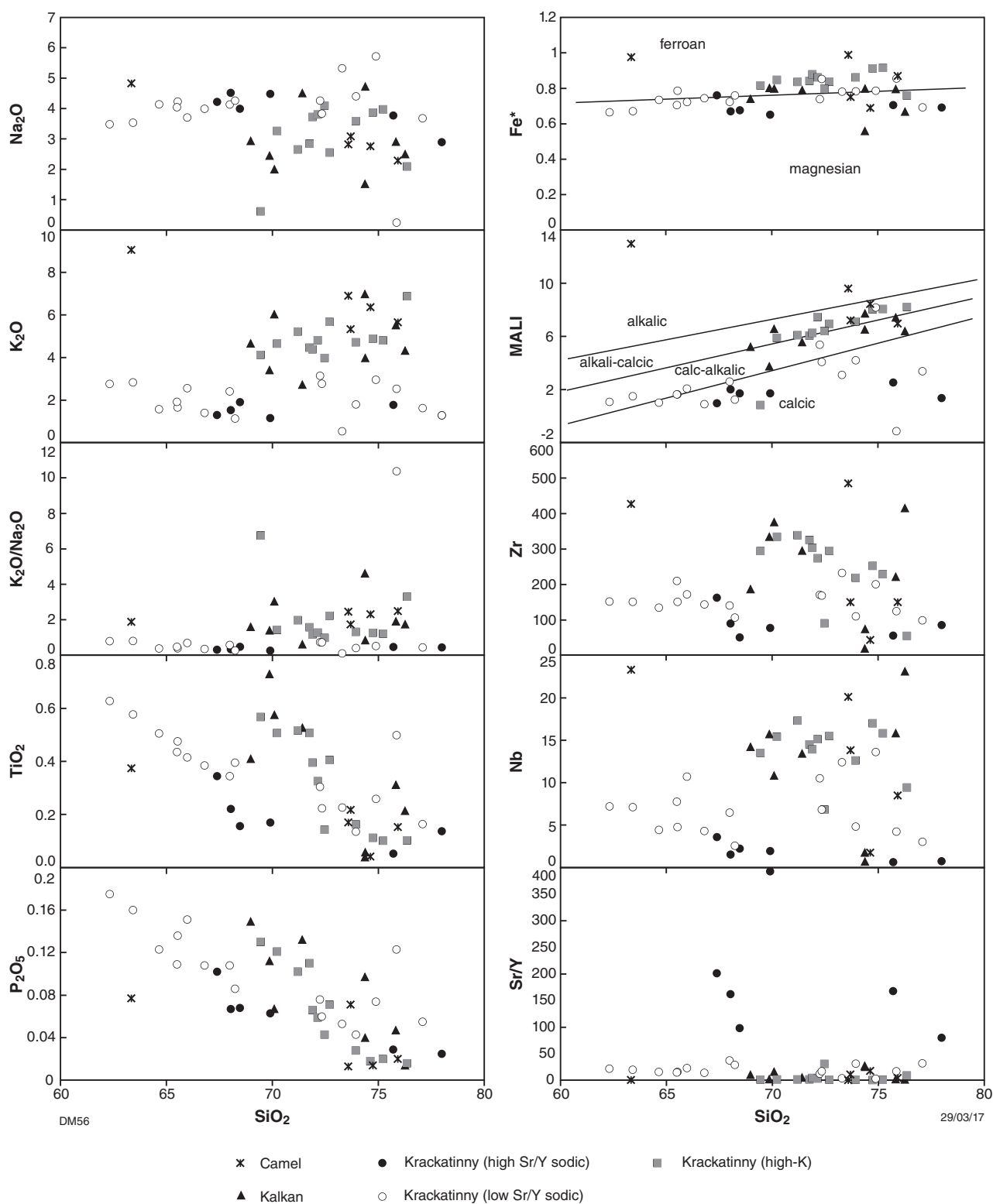


Figure 57. Plot of major elements vs SiO_2 for granitic rocks of the Rudall Province; fields for alkalic, alkali-calcic and calcic rocks, and ferroan and magnesian rocks, are from Frost et al. (2001); MLI (modified alkali-lime index) = $\text{Na}_2\text{O} + \text{K}_2\text{O} - \text{CaO}$

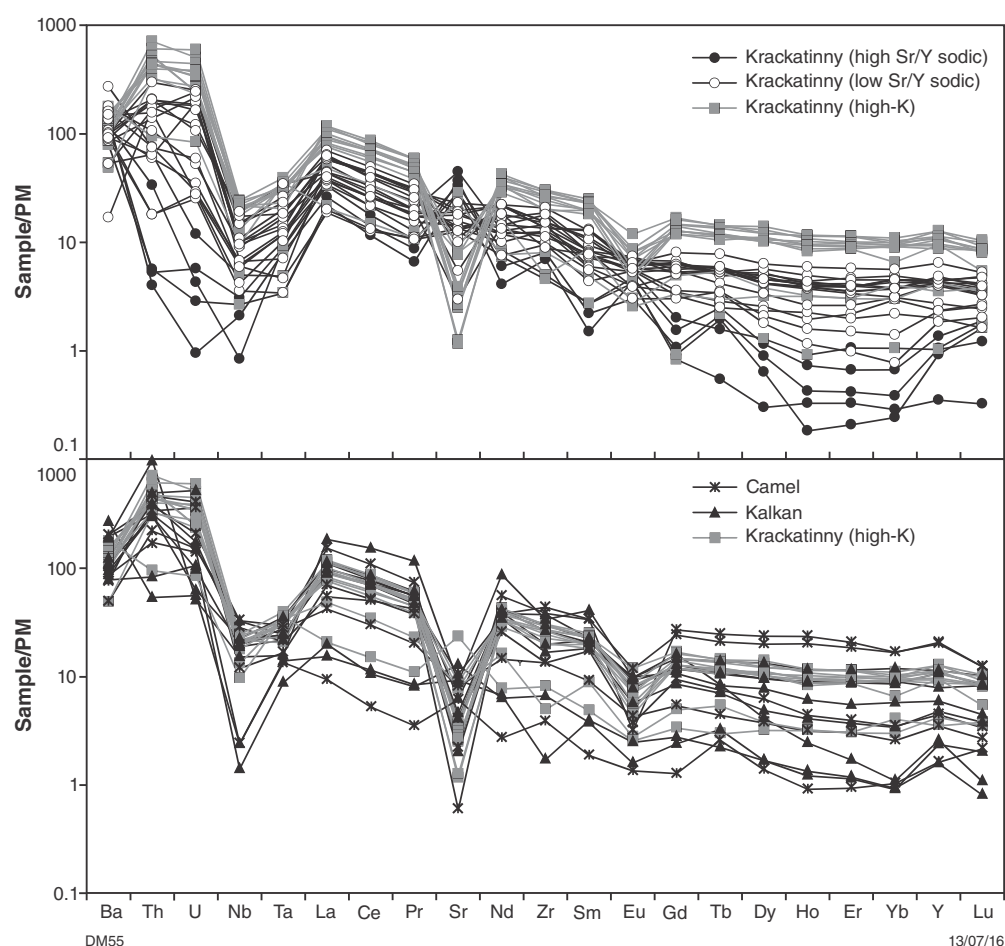


Figure 58. Mantle-normalized multi-element diagrams for granitic rocks of: a) the Krackatinny Supersuite; b) the Kalkan and Krackatinny Supersuites, and the Camel Suite; normalization factors from Sun and McDonough (1989)

The various compositional groups of the Krackatinny Supersuite show an apparent spatial variation, with the high-K series occupying a northwesterly trending zone to the northeast of the high Sr/Y sodic series rocks (Fig. 59). Rocks of the low Sr/Y sodic series spatially overlap the high-K rocks and also occur to the southwest, close to outcrop of the high Sr/Y sodic rocks. The available dating suggests that, in addition to these spatial patterns, there might also be a temporal variation between the three series, with one sample of the high Sr/Y sodic series dated at c. 1589 Ma and three samples of the high-K series having dates of c. 1577, 1554 and 1549 Ma. The low Sr/Y sodic series has not yet been dated.

The remainder of the granite analyses are from the Kalkan Supersuite and Camel Suite. Although of different ages, these extensively overlap the compositional range for the Krackatinny high-K series for most major and trace elements (Figs 57 and 58). The Kalkan Supersuite high-K granites, however, range between calc-alkalic and alkali-calcic. They also range to mainly lower concentrations of Ga, Y and HREE and have generally higher Sr and La/Nb ratios. Of the four Camel Suite analyses, one with low silica (63.3 wt% SiO₂) shows anomalously high Fe*,

mainly due to low MgO and is also very K-rich. The high K value could reflect alteration, given the very high Fe/Mg, although alternatively the rock might be a syenite. The other three samples are virtually indistinguishable from the high-K series Krackatinny Supersuite samples. The extensive overlap in compositions for the various high-K suites in the Rudall Province indicates that different events generated melts of similar compositions, and highlights the uncertainty in assigning undated high-K samples to a particular supersuite based on geochemistry alone.

Tabletop Terrane amphibolite geochemistry

Only three samples of the poorly exposed, upper greenschist to lower amphibolite facies mafic rocks in the Tabletop Terrane were analysed for whole-rock geochemistry but the data show distinctive characteristics that suggest a possible arc setting for this mafic magmatism. The analysed rocks comprise the sample that was dated in this study (GA 2006670110) as well as two samples from an area in the south-central part of the Tabletop Terrane, marginal to the leucogranite dated

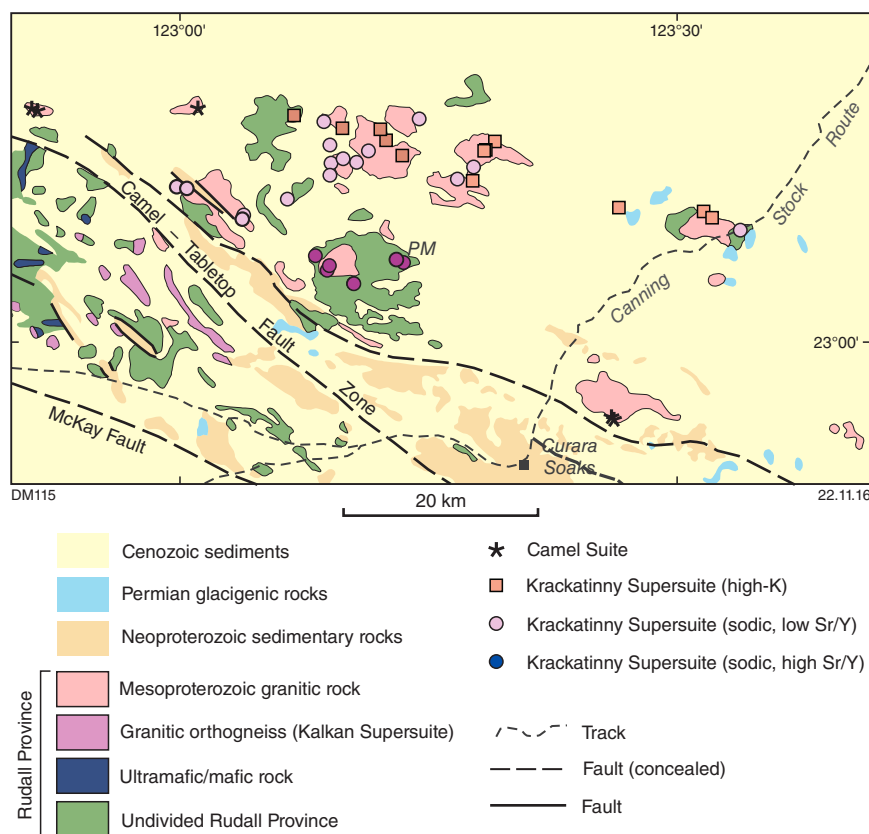


Figure 59. Distribution of the three geochemical groups of the 1589–1549 Ma Krackatinny Supersuite and the 1310–1286 Ma Camel Suite in the Tabletop Terrane; PM indicates the location of the PM prospect

in this study at 1589 ± 6 Ma. These two samples consist of medium-grained, weakly foliated, hornblende- and actinolite-bearing amphibolite (GA 2006670093; MGA 517932E 7462450N) and a fine-grained, moderately foliated, actinolite-bearing amphibolite (GA 200667099B; MGA 522323E 7464940N). In all three samples, plagioclase is strongly saussuritized, which is typical of the mafic rocks in the Tabletop Terrane.

The amphibolites have $\text{SiO}_2 = 50.30, 51.74$ and 55.74 wt%; $\text{MgO} = 9.50, 8.26$ and 6.91 wt%; $\text{Mg\#} = 63, 57$ and 62 ; $\text{TiO}_2 = 0.79, 0.59$ and 0.41 wt%; $\text{K}_2\text{O} = 2.31, 1.70$ and 2.64 wt%; $\text{Ni} = 185, 73$ and 87 ppm; and $\text{Cr} = 445, 153$ and 130 ppm (Appendix 3). A plot of trace element data normalized to N-MORB (Fig. 60) shows significant enrichment in LILE and LREE, HFSE values similar to, or lower than, those of N-MORB, and a slight depletion of HREE — similar characteristics to those of magmas emplaced in subduction zone settings (Murphy, 2007). The strong enrichments in LREE and LILE, coupled with Nb concentrations lower than those of N-MORB, favour subduction over crustal contamination as the cause of this signature. The current lack of precise timing constraints for these rocks and the overall paucity of data make it difficult to apply these results to constrain the geodynamic evolution of the Rudall Province but the apparent arc-like signatures of these rocks make them important targets for future study.

Sm–Nd isotopes

Thirteen samples of igneous and metasedimentary rocks from the Rudall Province were selected for Sm–Nd isotope analysis to provide constraints on the nature of their sources. These comprise granitic rocks of the Kalkan and Krackatinny Supersuites and the Camel Supersuite, amphibolites from the Tabletop Terrane and quartzites from the Connaughton and Tabletop Terranes. For the most part, the ages of the igneous samples are relatively well constrained by geochronology but, as noted above, the age(s) of the mafic rocks in the Tabletop Terrane are uncertain.

Analytical methods

Sm–Nd solution mode isotope analyses were carried out at the University of Melbourne. Sample solutions were equilibrated with a ^{149}Sm – ^{150}Nd spike, followed by extraction of Sm and Nd using EICHRON TRU- and LN-resin columns. Isotope analyses were carried out on a Nu Plasma multi-collector ICP-MS. Instrumental mass bias in Nd runs was corrected by internal normalization to $^{146}\text{Nd}/^{145}\text{Nd} = 2.0719425$ (equivalent to $^{146}\text{Nd}/^{144}\text{Nd} = 0.7219$), as part of an online iterative spike subtraction routine using the exponential law. All $^{143}\text{Nd}/^{144}\text{Nd}$ values were adjusted to a value of 0.511860 for the La Jolla

reference standard. In-run errors (2se) were ± 0.000010 or lower, external precision (2sd) was ± 0.000020 . Values for modern CHUR were taken as $^{147}\text{Sm}/^{144}\text{Nd} = 0.1967$, $^{143}\text{Nd}/^{144}\text{Nd} = 0.512638$, and for modern depleted mantle (DM) as $^{147}\text{Sm}/^{144}\text{Nd} = 0.2136$, $^{143}\text{Nd}/^{144}\text{Nd} = 0.513151$. The BCR2 standard has a nominal $^{147}\text{Sm}/^{144}\text{Nd}$ of 0.1382 and $^{143}\text{Nd}/^{144}\text{Nd}$ of 0.512640 ± 000020 . The ^{147}Sm decay constant was taken as $6.54 \times 10^{-12}\text{y}^{-1}$.

Results

Samarium–neodymium isotope data were collected for three samples of the Kalkan Supersuite, covering a range of emplacement ages (Table 2; Fig. 61). These include the sample of layered granitic gneiss dated in this study at 1804 ± 3 Ma (GA 2005670080) and a sample of K-feldspar augen-bearing biotite monzogranite gneiss from the Split Rock area (MGA 407035E 7499300N; GA2005670094), which was originally dated by Nelson (1995k) and recalculated to 1762 ± 13 Ma by Kirkland et al. (2013a). The sample of K-feldspar megacrystic biotite monzogranite from the Connaughton Terrane (GA2005670162) dated at 1781 ± 4 Ma was also analysed. These samples yielded relatively evolved isotope signatures, with $\epsilon\text{Nd}_{(t)}$ values of -6.4 and -7.4 for the samples from the Talbot Terrane, and a slightly less evolved value of -3.3 for the sample from the Connaughton Terrane, with $T_{2\text{DM}}$ model ages of 2.74 and 2.79 and 2.49 Ga respectively (Table 2). These values indicate a significant component of older crustal material in these granitic rocks that is consistent with Hf isotope data for zircons from the Kalkan Supersuite, which contain a range of grains with $T_{2\text{DM}}$ model ages of 3.4 – 2.6 Ga for the Talbot Terrane and 3.4 – 2.4 Ga for the Connaughton Terrane (Kirkland et al., 2013a).

Isotope data were also collected for four samples of the Krackatinny Supersuite (Table 2; Fig. 60). Three of these (GA 2005670186, GA 2005670187 and GA 2005670188) were splits of the high-K series samples dated at c. 1577, 1549 and 1554 Ma respectively, while another (GA 2006670092) was taken from a monzogranite dyke adjacent to the main high Sr/Y sodic series monzogranite intrusion dated at c. 1589 Ma (MGA 517909E 7462480N). The lithological character and geochemistry of the dyke is similar to that of the dated sample, and its age is also taken to be c. 1589 Ma. The high-K series samples yield relatively evolved $\epsilon\text{Nd}_{(t)}$ values of -5.4 , -4.0 and -6.4 with $T_{2\text{DM}}$ model ages of 2.48, 2.35 and 2.54 Ga (Table 2). The high Sr/Y sodic series sample yielded an even more evolved $\epsilon\text{Nd}_{(t)}$ of -10.2 , with a $T_{2\text{DM}}$ model age of 2.85 Ga. These isotope signatures suggest a significant component of Archean crust was present in the source region of the granitic rocks.

One sample of the Camel Suite was analysed (Table 2; Fig. 61), which is the leucogranite dated in this study at 1296 ± 4 Ma (GA 2006670119). This sample has a slightly more juvenile signature than the samples of the Krackatinny Supersuite, though still indicating a significant crustal component, with $\epsilon\text{Nd}_{(t)}$ of -1.6 and a $T_{2\text{DM}}$ model age of 1.96 Ga. The Sm–Nd isotope signature of this sample is somewhat more juvenile than zircon Hf isotope data collected from another granite of the Camel Suite, which yielded an average $T_{2\text{DM}}$ model age of 2.6 Ga (Kirkland et al., 2013a).

Three samples of amphibolite and a sample of quartzite from the Tabletop Terrane were analysed to provide information about the nature of the host rocks to the Krackatinny Supersuite. Although the interpretation of data from the amphibolite samples is limited by the imprecise constraints on the age of these rocks, the data

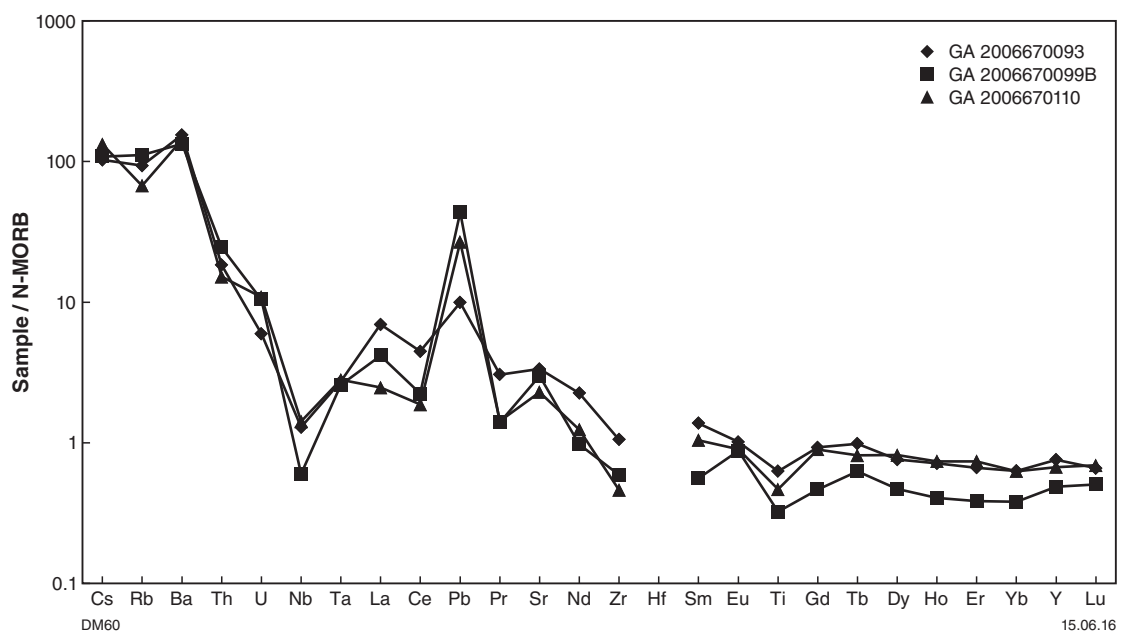


Figure 60. N-MORB-normalized trace element plot of amphibolite from the Tabletop Terrane; normalization factors from Sun and McDonough (1989)

Table 2. Sm–Nd isotopic data for igneous rocks from the Rudall Province

Sample no.	Zone	Age (T)	Lithology	Supersuite	Sm (ppm)	Nd (ppm)	¹⁴³ Nd/ ¹⁴⁴ Nd	¹⁴⁷ Sm/ ¹⁴⁴ Nd	εNd at T	T _{DM} (Ga)	T _{2DM} (Ga)
2005670080	Talbot	1804 Ma	Layered orthogneiss	Kalkan	1.89	8.83	0.511530	0.1297	–6.37	2.95	2.74
2005670094	Talbot	1765 Ma	Monzogranite	Kalkan	8.20	47.04	0.511211	0.1054	–7.43	2.73	2.79
2005670162	Connaughton	1781 Ma	Megacrystic gneiss	Kalkan	19.39	136.39	0.511223	0.0892	–3.28	2.37	2.49
2006670092	Tabletop	1589 Ma	Monzogranite	Krackatinny	1.05	8.49	0.510859	0.0750	–10.18	2.52	2.85
2005670186	Tabletop	1577 Ma	Monzogranite	Krackatinny	9.69	53.69	0.511467	0.1091	–5.38	2.46	2.48
2005670188	Tabletop	1554 Ma	Monzogranite	Krackatinny	8.90	42.37	0.511611	0.1270	–6.40	2.72	2.54
2005670187	Tabletop	1549 Ma	Quartzofeldspathic schist	Krackatinny	8.84	50.13	0.511529	0.1066	–3.99	2.32	2.35
2006670119	Tabletop	1296 Ma	Biotite monzogranite	Camel	3.87	20.18	0.511883	0.1159	–1.55	1.99	1.96
2006670087	Tabletop	<2833 Ma	Quartzite		0.12	0.52	0.511429	0.1405		3.58	3.19
2005670110	Talbot	<1794 Ma	Quartzite		1.82	9.99	0.511320	0.1099		2.69	2.71
2006670110	Tabletop		Metabasite		2.75	9.23	0.512242	0.1802		4.16	2.51
2005670093	Tabletop		Metabasite		3.73	18.33	0.511677	0.1232		2.49	2.40
2005670099B	Tabletop		Metabasite		1.52	6.94	0.511935	0.1322		2.29	2.17

provide some context for interpretation of the younger rocks in the Tabletop Terrane. The amphibolite samples analysed are the same that were analysed for whole-rock geochemistry, described above, and yield T_{2DM} model ages of 2.51, 2.40 and 2.17 Ga (Table 2). It is possible that the mafic protoliths were emplaced in the latest Archean to early Paleoproterozoic if there was little crustal contamination, but a significantly younger age is also possible if the magmas incorporated evolved crustal material, such as the subduction-related component suggested by the geochemical characteristics of these rocks. Analysis of quartzite sample GA 2006670087 yielded a T_{2DM} model age of 3.19 Ga, consistent with the broad range of Archean to early Paleoproterozoic detrital zircons dated in this sample.

Discussion

Age and provenance of the metasedimentary successions

Talbot Terrane

The zircon dates obtained for metasedimentary rocks of the Rudall Province provide constraints on the timing and provenance of sedimentation (Table 3; Fig. 62), although there are still too few dated samples to constrain the succession well. In the Talbot Terrane, the dominant age component of 1794 ± 4 Ma obtained from the Fingoon Quartzite in this study is indistinguishable from a similar age component of 1790 ± 10 Ma previously obtained from the unit at a different location (Nelson, 1995e). The single dominant age component in these samples suggests the source area for the sandstone protoliths was relatively restricted and likely proximal. The nearest potential source rocks are the granitic rocks of the 1804–1762 Ma Kalkan Supersuite in the Rudall Province itself, since there are few sources of this age currently exposed elsewhere in the region. Granitic rocks of the 1803–1793 Ma Bridget Suite in the eastern Pilbara Craton have a similar age but their host rocks are Archean, and the lack of Archean zircons in the quartzite suggests that the Bridget Suite is unlikely to have been a significant source. The zircons from the quartzite are generally slightly elongate, subhedral, oscillatory zoned grains, and do not include acicular zircons that would be suggestive of a synsedimentary volcanic source (Corfu et al., 2003). Thus, the simplest explanation is that the Fingoon Quartzite was sourced from exhumed granitic rocks of the Kalkan Supersuite. This interpretation is consistent with Lu–Hf isotope data for zircons from the Fingoon Quartzite, which show they have similar Hf isotope characteristics to zircons from the Kalkan Supersuite (Kirkland et al., 2013b).

Samples from other interpreted metasedimentary units of the Talbot Terrane — an unassigned quartz–feldspar–muscovite schist (GA 2005670100) and quartz–feldspar–mica gneiss of the Larry Formation (GA 2005670129) — yielded essentially unimodal zircon age components of c. 1780 and 1760 Ma respectively, also similar to the

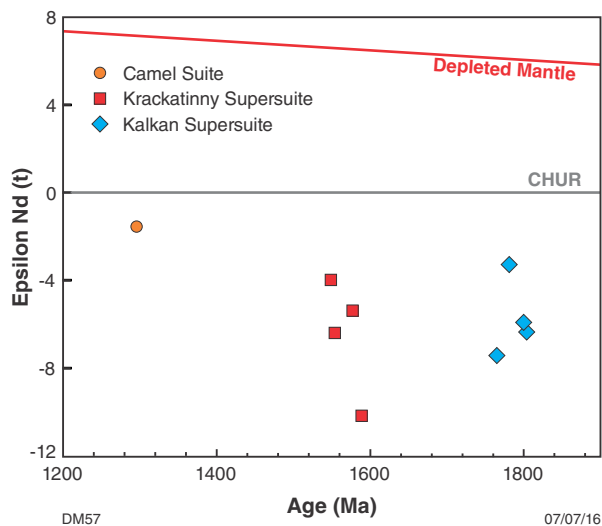


Figure 61. ϵ Nd evolution diagram for granitic rocks of the Rudall Province. DM = depleted mantle; CHUR = bulk silicate earth (chondritic uniform reservoir)

age of Kalkan Supersuite granitic rocks. As discussed previously, it is uncertain whether these samples are paragneisses or orthogneisses but, if these units were feldspar-rich metasedimentary rocks, their zircon age spectra would suggest similar proximal sources to those of the Fingoon Quartzite.

Currently, all the defined stratigraphic units in the Talbot Terrane are considered to be part of a single package, with the Larry Formation, Fingoon Quartzite, Yandagooge Formation and Butler Creek Formation considered to represent an essentially intact succession (Hickman and Bagas, 1999). The relationship of the Poynton Formation with other units is uncertain but has been suggested to possibly represent the youngest unit in the Talbot Terrane. This interpreted stratigraphy is based on gradational contacts between units in some areas and a consistent order of superposition (Hickman and Bagas, 1999). Granitic gneisses of the Kalkan Supersuite situated within parts of the metasedimentary succession are thought to intrude the sequence, though typically the high strain of these rocks makes it difficult to distinguish whether contacts were intrusive or reflect structural interleaving (Hickman and Bagas, 1999). If the granites intruded the entire succession, the c. 1794 and 1790 Ma maximum depositional ages for the Fingoon Quartzite would indicate that sedimentation took place at broadly the same time as magmatism, given the 1804–1762 Ma dates obtained for the granitic gneisses (Hickman and Bagas, 1999). If, however, the c. 1760 Ma date obtained from the Larry Formation represents a maximum depositional age, this would indicate that at least part of the succession post-dated intrusion of the Kalkan Supersuite, raising the possibility that a cover sequence might be present in the Talbot Terrane.

Support for the possibility of complexity within the stratigraphic succession might be provided by the observation that no granitic rocks are known to intrude the Fingoon Quartzite, which could be interpreted as evidence

of a tectonic or disconformable break between the Fingoon Quartzite and older units intruded by the granitic rocks (Hickman and Bagas, 1999). Hickman and Bagas (1999) did not favour such a break, based on field evidence for transitional contacts between the Fingoon Quartzite and Larry Formation at some localities, coupled with the fact that the Fingoon Quartzite structurally underlies units intruded by granite, but they noted that a lack of way-up criteria prevents firm conclusions from being drawn. In this context, it is interesting to note that pre- and post-granite successions within the Talbot Terrane were suggested by Chin et al. (1980) and Clarke (1991), based on earlier mapping of the region. These authors considered that metasedimentary units broadly corresponding to the Larry Formation, Fingoon Quartzite, Yandagooge Formation and unassigned metasedimentary schist might represent a younger succession overlying units corresponding to the Butler Creek and Poynton Formations, which were intruded by the Kalkan Supersuite. This interpretation is compatible with the existing geochronological data if the c. 1780 and 1760 Ma dates obtained for the Larry Formation and muscovite schist in this study are interpreted as maximum deposition ages rather than magmatic crystallization ages. Difficulties in this interpretation arise if granitic gneisses with dates of c. 1801, 1793 and 1782 Ma (Nelson, 1995c, 1995h, 1996a; Kirkland et al., 2013a) adjacent to areas mapped as Larry Formation were intruded into the unit rather than tectonically juxtaposed. In most instances, the contacts between these granitic gneisses and the Larry Formation are either not exposed or sheared but more detailed examination of these contacts would be worthwhile to determine whether intrusive contacts might be present.

The ages of rocks that would have hosted the oldest Kalkan Supersuite intrusion dated at 1804 ± 3 Ma are not well constrained. Quartz–feldspar–muscovite schist adjacent to layered orthogneiss in the northwestern Talbot Terrane was previously suggested to potentially comprise part of an older stratigraphic succession, assuming this unit was intruded by the orthogneiss protoliths (Hickman and Bagas, 1998). However, the c. 1780 Ma unimodal age component obtained in this study for one sample of the quartzofeldspathic schist (GA 2005670100) does not provide a constraint on the age of pre-1804 Ma units and might indicate a structural break between the schist and orthogneiss. A sample of quartz–feldspar–biotite–muscovite–garnet gneiss from an area of layered orthogneiss dated by Nelson (1995a) yielded a slightly dispersed group at 2015 ± 26 Ma, interpreted as the timing of crystallization of a granitic precursor, and a range of older dates between c. 2715 and 2577 Ma. The muscovite- and garnet-rich nature of this rock suggests the presence of a significant sedimentary component, as noted by Nelson (1995a), but it is not certain if this indicates that the rock is a paragneiss, in which case the c. 2015 Ma date could represent a maximum depositional age, or a contaminated granitic rock, in which case the c. 2015 Ma age component could represent xenocrysts or magmatic zircons. The irregularly shaped and pitted forms of the zircons from this sample are more consistent with a metasedimentary protolith, and this rock is here tentatively interpreted to comprise part of a supracrustal succession deposited at or after 2015 ± 26 Ma.

Table 3. Summary of SHRIMP U–Pb zircon dating for the Rudall Province

<i>Sample no.</i>	<i>Unit</i>	<i>Terrane</i>	<i>Date (Ma)</i>	<i>Interpretation (this study)</i>	<i>Source</i>
112160	Garnet-bearing microgneiss	Connaughton	c. 1200	Metamorphism	Nelson (1996c)*
CG3518	Partly recrystallized monzogranite	Tabletop	1286 ± 6	Magmatic	Bagas (2004)
104938	Pegmatite	Connaughton	1291 ± 10	Magmatic	Nelson (1995b)
GA 2006670119	Leucogranite	Tabletop	1296 ± 4	Magmatic	This study
118914	Foliated granite	Tabletop	1310 ± 5	Magmatic	Nelson (1996e)*
GA 2005670162	Megacrystic granitoid	Connaughton	1315 ± 21	Metamorphism	This study
GA 2005670165	Unnamed quartzite	Connaughton	1334 ± 4	Metamorphism	This study
112012	Seriate biotite monzogranite	Talbot	1453 ± 10	Glacigenic clast	Nelson (1996b)*
KA2036	Partly recrystallized granodiorite	Tabletop	1476 ± 10	Magmatic	Thevissen (1991)
GA 2005670187	Quartzofeldspathic schist	Tabletop	1549 ± 3	Magmatic	This study
GA 2005670188	Unnamed granite	Tabletop	1554 ± 2	Magmatic	This study
GA 2006670110	Metabasite	Tabletop	1571 ± 4	Age of felsic veins	This study
GA 2005670186	Unnamed granite	Tabletop	1577 ± 2	Magmatic	This study
GA 2006670087	Unnamed quartzite	Tabletop	1580 ± 34	Contact metamorphism	This study
GA 2005670178	Unnamed leucogranite	Tabletop	1589 ± 5	Magmatic	This study
GA 2005670080	Layered orthogneiss	Talbot	1679 ± 25	Metamorphism	This study
GA 2005670162	Megacrystic granitoid	Connaughton	1688 ± 8	Metamorphism?	This study
GA 2005670129_02	Larry Formation	Talbot	1760 ± 5	Maximum deposition (magmatic?)	This study
112379	Biotite monzogranite (augen) gneiss	Talbot	1762 ± 13	Magmatic	Nelson (1995k)*
104981	Biotite–muscovite monzogranite gneiss	Talbot	1764 ± 13	Magmatic	Nelson (1995d)
113002	Granodiorite gneiss	Connaughton	1768 ± 7	Magmatic	Nelson (1995m)*
112341	Micromonzogranite (meta-aplite) dyke	Talbot	1773 ± 15	Inheritance?	Nelson (1995j)*
113035	Granitic gneiss	Connaughton	1777 ± 6	Magmatic	Nelson (1996d)*
GA 2005670100	Quartz–feldspar–muscovite schist	Talbot	1780 ± 2	Maximum deposition (magmatic?)	This study
GA 2005670162	Megacrystic granitoid	Connaughton	1781 ± 4	Magmatic	This study
111854	Biotite–muscovite granodiorite gneiss	Talbot	1782 ± 12	Magmatic	Nelson (1995h)*
112397	Biotite monzogranite (augen) gneiss	Talbot	1783 ± 6	Magmatic	Nelson (1995l)*
111843	Biotite–muscovite monzogranite gneiss	Talbot	1789 ± 16	Magmatic	Nelson (1995g)*
GA 2006670087	Unnamed quartzite	Tabletop	1790 ± 7	Metamorphism	This study
104989	Fingoon Quartzite	Talbot	1791 ± 10	Maximum deposition	Nelson (1995e)*
112101	Biotite–epidote monzogranite gneiss	Talbot	1793 ± 8	Magmatic	Nelson (1996a)*
GA 2005670110	Fingoon Quartzite	Talbot	1794 ± 4	Maximum deposition	This study
110056	Biotite–hornblende granodiorite gneiss	Talbot	1795 ± 12	Magmatic	Nelson (1995f)*
104980	Monzogranite gneiss	Talbot	1800 ± 3	Magmatic	Nelson (1995c)*
112310	Granodiorite gneiss	Talbot	1801 ± 12	Magmatic	Nelson (1995i)*
GA 2005670080	Layered orthogneiss	Talbot	1804 ± 3	Magmatic	This study
112310	Granodiorite gneiss	Talbot	1972 ± 4	Inheritance?	Nelson (1995i)
104932	Syenogranite gneiss	Talbot	2015 ± 26	Inheritance?	Nelson (1995a)
GA 2005670165	Unnamed quartzite	Connaughton	2284 ± 10	Maximum deposition	This study
GA 2006670087	Unnamed quartzite	Tabletop	2833 ± 5	Maximum deposition	This study

NOTE: * Date recalculated by Kirkland et al. (2013a).

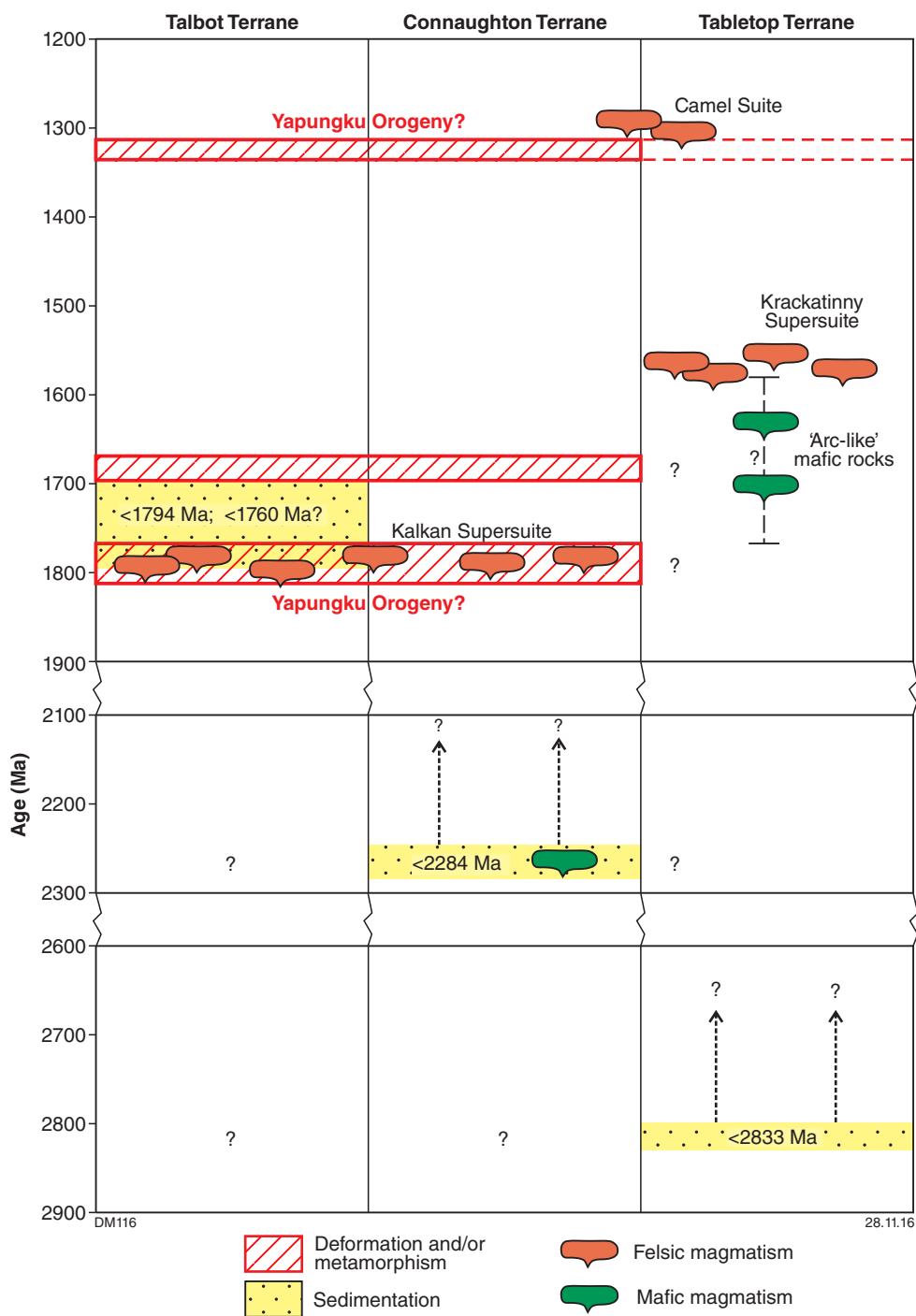


Figure 62. Time-space diagram for the terranes of the Rudall Province based on available geochronological data; considerable uncertainty surrounds the depositional ages of metasedimentary protoliths and the age of arc-like mafic magmatism in the Tabletop Terrane

Ages of zircon xenocrysts in granitic gneisses from the Talbot Terrane also provide some information about the nature of pre-Kalkan Supersuite crust, most of which are dated at 2.7 – 1.8 Ga (Nelson, 1995e, 1995f, 1995g, 1995i; Kirkland et al., 2013a; this study). Kirkland et al. (2013a,b) noted that the xenocryst ages and their Lu–Hf isotope characteristics are consistent with assimilation of sedimentary material from a basin of similar age and source to basins developed to the south of the Pilbara Craton during the 1817–1772 Ma Capricorn Orogeny. Given the possibility that Neoproterozoic to early Paleoproterozoic metasedimentary units occur elsewhere in the Rudall Province, however (see discussion below), the xenocrysts could have contributions from a range of potential sources. The paucity of >2.7 Ga xenocrysts suggests that there was little or no crust of similar character to the 3800–2830 Ma Pilbara Craton in the granite source regions but further data collection is needed to determine if this apparent pattern is representative.

Although the depositional ages of the metasedimentary units in the Talbot Terrane can be interpreted in different ways, two distinct scenarios can be considered based on the currently limited data: (1) deposition of all the named stratigraphic units in a synorogenic setting, coeval with granite intrusion (Hickman and Bagas, 1999), overlying a pre-Kalkan Supersuite succession; or (2) deposition of a ≤1760 Ma cover succession on a basement comprising exhumed granitic rocks of the Kalkan Supersuite and their older Paleoproterozoic host rocks.

Connaughton Terrane

The quartzite sampled in this study (GA 2005670165) is the only clearly metasedimentary unit from the Connaughton Terrane to have been dated.

The only other unit with a possible metasedimentary origin is a garnet-bearing quartzofeldspathic gneiss north of the Harbutt Range dated by Nelson (1996c), which yielded imprecise age components at c. 1800, 1672 and 1222 Ma. This was interpreted as a paragneiss deposited after c. 1672 Ma by Nelson (1996c) but other interpretations are possible, including a multiply metamorphosed ≤1800 Ma metasedimentary rock or a c. 1800 Ma granitic orthogneiss.

The quartzite contains zircons that are much older than those from the dated metasedimentary rocks in the Talbot Terrane, and has a maximum depositional age of c. 2284 Ma, with a range of older dates from 3142–2308 Ma (Fig. 35). Minimum depositional age constraints for this unit include 1334 ± 4 Ma metamorphic zircon rims from the quartzite itself and a c. 1781 Ma age for granitic gneiss within the succession (GA 2005670162), which provide only broad constraints on the depositional age of this unit (i.e. 2280–1780 Ma).

The detrital zircon age spectrum for the dated quartzite includes two dominant groups at 2721–2610 Ma and 2593–2472 Ma, as well as minor maxima at c. 2870, 2315 and 2284 Ma (Fig. 35). The ages of the two dominant groups coincide with deposition of the 2775–2629 Ma Fortescue Group (Fortescue Basin) and the 2629–2445 Ma

Hamersley Group (Hamersley Basin), which overlie the Pilbara Craton and contain felsic volcanic rocks that could have provided suitably aged zircons (Arndt et al., 1991; Trendall et al., 2004; Blake et al., 2004). Minor age components at 2425–2282 Ma have no known sources exposed in the region, but have also been recognized as detrital components in Paleoproterozoic metasedimentary rocks from the Capricorn Orogen sourced from the southern Pilbara Craton and Glenburgh Terrane (Johnson et al., 2010). The dominance of zircons with ages similar to volcanic rocks in the Fortescue and Hamersley Basins, and the paucity of zircons older than c. 2850 Ma, suggest that the protolith to the quartzite was largely sourced from the volcanic and sedimentary units overlying the Pilbara Craton, possibly with a relatively small contribution from the underlying basement rocks. The high degree of compositional maturity of the dated quartzite is also consistent with reworking of a sedimentary source.

If this unit was deposited close to its c. 2283 Ma maximum age, potential time correlatives include sedimentary rocks of the Turee Creek Basin along the southern margin of the Pilbara Craton, which include units formerly assigned to the lower Wyloo Group (Johnson et al., 2013). These siliciclastic, carbonate and mafic volcanic rocks are interpreted to have been deposited within a foreland basin related to the collision of the Pilbara and Yilgarn Cratons during the 2215–2145 Ma Ophthalmia Orogeny (Martin and Morris, 2010). If this was the case, the quartzite in the Connaughton Terrane might reflect the effects of an eastern extension of this collisional zone beneath areas now covered by younger sedimentary basins.

Tabletop Terrane

The quartzite unit dated in this study (GA 2006670087) is the only metasedimentary rock dated from the Tabletop Terrane. The detrital zircon ages from this unit are markedly different from the dates obtained from metasedimentary units in the Connaughton and Talbot Terranes and comprise a range of Archean dates between c. 3579 and 2830 Ma, with a maximum depositional age of 2833 ± 5 Ma (2σ). A minimum age for the quartzite is provided by 1790 ± 7 Ma zircon rims, which are interpreted to reflect in situ metamorphism. The detrital zircon age spectrum has no dominant peak but instead contains multiple discrete maxima (Fig. 41). Most of these coincide with the 11 major magmatic events (supersuites) in the Pilbara Craton defined between c. 3500 and 2830 Ma (McNaughton et al., 1988; Buick et al., 1995; Van Kranendonk et al., 2006, 2007; Hickman and Van Kranendonk, 2008; Hickman, 2012; Kemp et al., 2015). Although the age component at 3400–3360 Ma does not correlate with a known magmatic event in the Pilbara Craton, it is similar to a significant peak in the detrital zircon age spectra obtained from the 2972–2905 Ma Mosquito Creek Formation in the eastern part of the craton (Bagas et al., 2008). The quartzite from the Tabletop Terrane thus appears to have been sourced from the Pilbara Craton, which supports the interpretation of Kirkland et al. (2013b) based on Lu–Hf isotope evidence that all the terranes of the Rudall Province have affinities with the West Australian Craton, and are not exotic blocks.

The lack of zircons dated younger than c. 2830 Ma in the quartzite raises the possibility that the quartzite is an Archean unit deposited relatively close to its maximum depositional age. As noted above, the Fortescue and Hamersley Basins overlying the Pilbara Craton contain numerous felsic volcanic units emplaced between c. 2775 and 2445 Ma, which could have provided a source for <2830 Ma zircons if the protolith to the quartzite had been deposited after their deposition. Although it is possible that sediment was sourced from an exposed area of the Pilbara Craton without a significant contribution from the Fortescue or Hamersley Basins, the widespread distribution of these basins across the Pilbara Craton suggests that it is unlikely that sediment could be sourced from the craton without reworking a significant component of <2775 Ma zircon. The conspicuous absence of dates <2830 Ma, despite the relatively large number of grains analysed ($n = 81$), thus suggests that the quartzite might be a correlative of a siliciclastic unit in the lower part of the Fortescue Group, possibly the Bellary Formation, which was deposited at or before c. 2775 Ma, or the Hardey Formation, deposited at 2766–2749 Ma (Thorne and Trendall, 2001; Trendall et al., 2004).

There is very little dating of detrital zircons from sedimentary units of the Fortescue Group that would allow for robust comparisons of provenance. A sample of volcanoclastic sandstone from the Kylene Formation in the eastern part of the basin yielded a 2735 ± 6 Ma date, interpreted as the age of a tuffaceous component, and a range of detrital ages between c. 3391 and 2781 Ma (Bodorkos et al., 2006). A sample of volcanoclastic sandstone from the Tumbiana Formation in the southern part of the basin yielded a 2719 ± 6 Ma date interpreted as a volcanogenic component, and a range of detrital ages between c. 3327 and 2797 Ma (Nelson, 2001). The depositional age of the dated quartzite in the Tabletop Terrane thus remains somewhat speculative, but an age towards the older limit of the broad 2833–1790 Ma constraints is considered most likely.

An indirect constraint on the potential ages of the rocks hosting the Krackatinny Supersuite is provided by the c. 1310 Ma leucogranite dated in this study (GA 2005670178), which contains inherited zircons dated between c. 2465 and 1694 Ma, including four grains at 1837–1817 Ma. This suggests that the Tabletop Terrane might contain Paleoproterozoic units of similar age to those present in the Talbot and Connaughton Terranes.

The sample of amphibolite dated in this study (GA 2006670110) did not yield a definitive age for the mafic precursor and the timing of ‘arc-like’ mafic magmatism in the Tabletop Terrane remains poorly constrained. The generally low-grade metamorphism of the amphibolite and the granitic rocks of the Krackatinny Supersuite have been used to characterize the regional metamorphic grade of the Tabletop Terrane as greenschist to lower amphibolite facies, distinct from the upper amphibolite to granulite facies conditions preserved in the Talbot and Connaughton Terranes (Bagas, 1999). Given that the age of the amphibolite is unknown, however, it remains a possibility that largely unexposed units within the Tabletop Terrane pre-dating the amphibolite experienced

higher grade tectonism that was not experienced by the mafic rocks. Some evidence that this might be the case is provided by 1790 ± 7 Ma zircon overgrowths from the dated quartzite (GA 2006670087), since the relatively low-grade metamorphism of amphibolite would appear to be insufficient to generate significant metamorphic zircon growth, which typically requires upper amphibolite to granulite facies conditions (Hoskin and Schaltegger, 2003). Although recrystallization of existing zircon and associated isotopic resetting can occur under lower metamorphic grades, the prismatic forms of the zircon rims in the quartzite appear to be caused in part by metamorphic zircon growth at c. 1790 Ma. This might indicate that amphibolite protoliths were emplaced after this metamorphism and before emplacement of granitic rocks at c. 1590 Ma, but more work is required to provide better constraints on the age of this magmatism.

Timing of the Yapungku Orogeny

Constraints from overprinting relationships

In the absence of direct dating of metamorphic minerals, previous interpretations of the timing of the Yapungku Orogeny (and inferred continental collision) have hinged on the interpretations that:

1. A felsic dyke in the Talbot Terrane, with a date of 1778 ± 16 Ma (Nelson, 1995j), was emplaced after the last stages of deformation associated with the orogeny.
2. The 1804–1762 Ma Kalkan Supersuite was generated by the event that caused moderate- to high-P, high-T metamorphism (Hickman and Bagas, 1999; Bagas, 2004).

The inferred structural setting of the dated felsic dyke of Nelson (1995j) was based on the interpretation that the dyke does not contain the high-grade (S_2) foliation present in its ultramafic host rock. Other late-stage felsic units considered to be part of the same suite were also interpreted to crosscut S_2 or be intruded into D_2 shear zones (Hickman and Bagas, 1998). However, as noted above, the felsic dykes in the area of the previously dated sample do contain a high-grade metamorphic foliation, although in places this is not immediately evident due to the low mica content of these rocks. Other dykes in the area were thus examined to better understand their structural setting.

The felsic dykes in the area surrounding the sampled dykes are hosted by strongly foliated K-feldspar augen granitic gneiss and many appear to have been affected by deformation consistent with that assigned to D_2 by previous authors. The D_2 deformation of Hickman and Bagas (1998) is characterized by isoclinal folding with an associated pervasive S_2 foliation defined by aligned mica and quartz, developed under amphibolite facies metamorphic conditions. S_2 was considered to be the oldest foliation developed in the augen granitic gneiss unit

hosting the felsic dykes (Hickman and Bagas, 1998) and is folded by northwesterly trending, upright folds assigned to D_4 (Miles Orogeny). The F_4 folds have an axial plane cleavage but were not associated with the development of a high-grade foliation, having formed under greenschist facies conditions (Hickman and Bagas, 1998, 1999). In the scheme of Hickman and Bagas (1999), D_3 produced faulting and quartz veining along the unconformity between the Rudall Province and the Yeneena Basin but is not thought to have been associated with the development of a high-grade foliation, the event also having taken place under relatively low metamorphic grade. Given the structural framework outlined above, the pervasive high-grade foliation in the granitic gneiss hosting the felsic dykes is consistent with S_2 , which forms a reference point for placing the felsic dykes within a relative structural framework. Dating of metamorphic zircon indicates that more than one high-grade event affected the Rudall Province, which could mean that there are unrecognized generations of foliations within the Rudall Province. Although this complicates the interpretation of the structural setting of the felsic dykes, local field observations are sufficient to determine whether the dykes locally crosscut the foliation in their immediate host rocks.

Some felsic dykes contain a well-developed foliation defined by quartz and feldspar aggregates and minor biotite that is subparallel to the high-grade foliation in the host rocks and typically best developed within thinner dykes (Fig. 63a–f). Many of the dykes observed are subparallel to the high-grade foliation in their host rocks (Fig. 63b), possibly in part due to rotation into parallelism within this fabric during deformation. One thin felsic dyke strikes obliquely to the high-grade foliation in its host rock (Fig. 63e,f) but is folded about a tight recumbent fold ($F_2?$), which has an axial plane foliation subparallel to the high-grade foliation in its host rock (S_2). Another complexly deformed felsic dyke appears to have been partially transposed within the high-grade foliation during similar isoclinal folding (Fig. 63c). The foliations in the felsic dykes and their granitic host rocks are folded and crenulated by upright, northwesterly trending tight folds, which lack a high-grade axial plane foliation and are interpreted as D_4 structures (Fig. 11d,e; Fig. 63d). The limbs of thicker folded dykes are boudinaged in places by this deformation, with quartz infilling spaces generated during fracturing (Fig. 11e).

Although it cannot be conclusively demonstrated that all the felsic dykes and veins in this area are part of the same suite, their close spatial association, similar structural settings, mineralogies, textures and low Zr contents (where analysed) suggest they are related. Thus, the field relationships are interpreted to indicate that the felsic dyke dated by Nelson (1995j) was part of a suite that was affected by the high-grade event assigned to the Yapungku Orogeny by Hickman and Bagas (1999).

In addition to the different interpretation of the structural setting of these dykes, there is uncertainty in the interpretation of the 1778 ± 16 Ma date obtained by Nelson (1995j), which was recalculated to 1773 ± 15 Ma by Kirkland et al. (2013a). Attempts to date the same dyke and another from this suite recovered very few zircons,

which is consistent with the very low Zr contents of these samples (41–56 ppm) and suggests that there was little, if any, magmatic zircon in these rocks. A similarly low, though slightly higher, Zr content of 71 ppm was obtained in this study from analysis of a split of the sample dated by Nelson (1995j). This sample (112341) has similar abundances of most other elements to the sample dated in this study (GA 2005670072; Appendix 3), although with slightly elevated Cr (27 ppm), consistent with minor contamination from its ultramafic host rock. This raises the possibility that the grains dated by Nelson (1995j) might be xenocrysts inherited from the voluminous granitic rock which surrounds the ultramafic body hosting the dyke. This would be consistent with a 1765 ± 15 Ma date obtained from one location within the broad area of granitic gneiss (Nelson, 1995k), recalculated to 1762 ± 13 Ma by Kirkland et al. (2013a). Although the 1778 ± 16 Ma date of Nelson (1995j) for the felsic dyke (recalculated to 1773 ± 15 Ma by Kirkland et al., 2013a) is in fact slightly older than the date from the granitic gneiss hosting these dykes, the dates are indistinguishable within the limits of their relatively large analytical uncertainties. Additional complexity in the interpretation of the date obtained from the dyke is the presence of a concordant $^{207}\text{Pb}^*/^{206}\text{Pb}^*$ date of 1612 ± 44 Ma (1σ) for one grain, which was interpreted to reflect isotopic disturbance during metamorphism (Nelson, 1995j).

The interpretation that the felsic dykes contain the same foliations as their host rocks, coupled with the uncertainty surrounding the interpretation of the dated dyke, suggests that the date of Nelson (1995j) does not provide a robust constraint on the minimum age of the Yapungku Orogeny. Without this constraint, the dates obtained from the Kalkan Supersuite may thus only represent maximum ages for the Yapungku Orogeny, if this event is defined by its association with moderate- to high-P metamorphism. It remains a possibility that the Kalkan Supersuite was emplaced during the earlier stages of a prolonged Yapungku Orogeny but this is not required by the available constraints, and the high-P metamorphism could represent a separate phase of tectonism.

A maximum age constraint for the Yapungku Orogeny is also provided by the metasedimentary rocks in the Talbot Terrane, which are also considered to have been affected by this deformation (Smithies and Bagas, 1997; Hickman and Bagas, 1999). As noted previously, the c. 1794 Ma dominant age peak in the Fingoon Quartzite could be a result of erosion of granites of the Kalkan Supersuite, which implies uplift and exhumation of these rocks from depths of at least several kilometres before deposition. If the samples of the Larry Formation and muscovite schist dated in this study are paragneisses, the dominant c. 1780 and 1760 Ma zircon age components obtained from these rocks could indicate that uplift and erosion of the Kalkan Supersuite took place before, or during, basin development. This is consistent with synorogenic sedimentation, as suggested by Hickman and Bagas (1999), but could alternatively reflect a phase of basin development post-dating exhumation of the Kalkan Supersuite and pre-dating deformation and burial of the metasedimentary succession during the Yapungku Orogeny. In this case, the Yapungku Orogeny might not

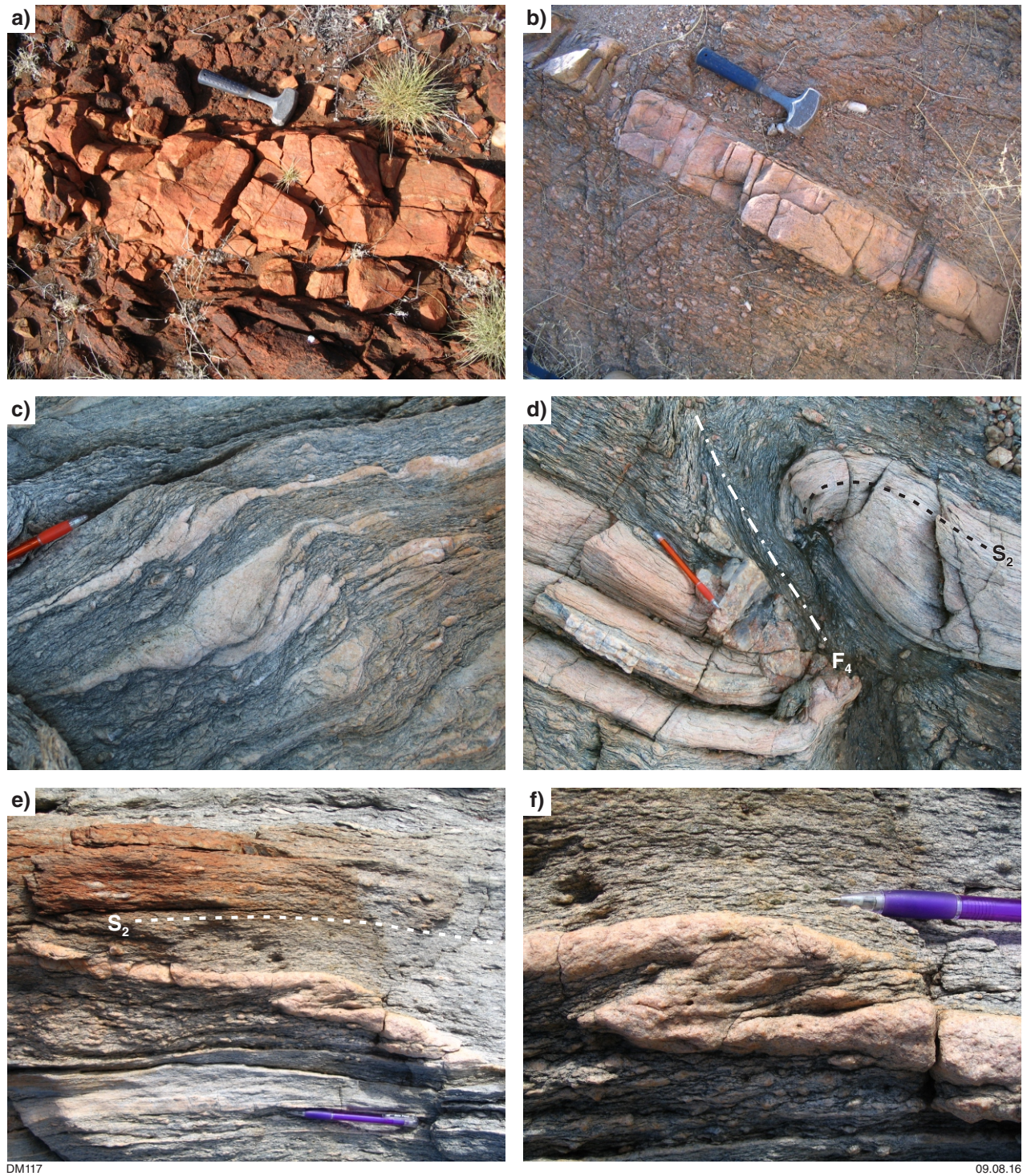


Figure 63. Outcrop photos showing the structural setting of felsic dykes southeast of Rudall Crossing, Talbot Terrane: a) felsic dyke near sampled dyke GA 2005670072, containing interpreted S_2 foliation subparallel to dyke margin; b) felsic dyke subparallel to and containing interpreted S_2 foliation (MGA 414085E 7507060N); c) felsic layers in granitic gneiss of the Kalkan Supersuite, possibly representing deformed and transposed dykes within the S_2 foliation (MGA 414085E 7507060N); d) felsic layer interpreted as a deformed dyke within granitic gneiss, containing the S_2 foliation, with both host rock and dyke deformed by F_4 folding (MGA 414093E 7507160N). Felsic dyke is attenuated and disconnected during D_4 deformation, with massive quartz infill of boudin neck; e) folded felsic dyke within granitic gneiss (MGA 414075E 7507150N); f) close-up of fold, showing axial plane high-grade foliation interpreted as S_2

have been related to the Kalkan Supersuite magmatism. If the 1760 ± 5 Ma date from the Larry Formation instead represents an intrusive age, this still appears to represent a maximum age for the Yapungku Orogeny, since this unit is deformed by tight to isoclinal folding and contains a high-grade, layer-parallel foliation, consistent with S_1 or S_2 foliation of Hickman and Bagas (1999).

Apart from the felsic dykes referred to above, minimum ages for the Yapungku Orogeny have also previously been inferred from dates of other felsic intrusive rocks considered to post-date D_2 . These include a 1453 ± 10 Ma granodiorite in the Talbot Terrane (Nelson, 1996b) and a 1291 ± 10 Ma pegmatite in the Connaughton Terrane (Nelson, 1995b). The 1453 ± 10 Ma date was obtained from a sample of weakly foliated granite in the southern part of the Talbot Terrane that was considered by Bagas (2004) to be a post- D_2 dyke. The sample site is within a broad area mapped as Permian glaciogene sedimentary rocks of the Paterson Formation, which in places contains granite boulders exceeding 5 m in size (Hickman and Bagas, 1998). Examination of the sample area showed no evidence of outcropping Proterozoic basement rocks, although numerous rounded boulders up to several metres in size with a wide range of igneous and metasedimentary compositions and textures are present (Fig. 64a). An irregular boulder 18 m to the northeast of the sample site coordinates provided by Nelson (1996b) — assumed to be obtained using the AGD84 datum — was the only boulder observed in the area that showed evidence of previous sampling (Fig. 64b; MGA 409775E 7498324N, GDA94, Zone 51). This boulder is a weakly foliated, pinkish biotite monzogranite that is indistinguishable in hand specimen and thin section from remnant pieces of the dated sample, and it appears likely that this boulder was the one that was sampled for dating. The area immediately surrounding this boulder contains a range of other boulders and cobbles of granitic and metasedimentary rock (Fig. 64b), including a large boulder of granite gneiss containing an intense high-grade foliation. The lack of definitive basement exposure in this area mapped as Permian glaciogene rock, and the wide range of lithologies present in the surficial boulders mean that the 1453 ± 10 Ma date from this area cannot be considered a reliable constraint on the minimum age of the Yapungku Orogeny. Although it is possible that the dated boulder was derived from the Rudall Province, given a similar date of 1476 ± 10 Ma obtained for a granodiorite in the Tabletop Terrane (Thevissen, 1991), this is not certain, as the glacial flow directions of the Paterson Formation in the region are towards the northwest (Hickman and Bagas, 1998; Whitaker et al., 2010), and detritus might have been derived from outside the Rudall Province. This also has implications for the interpretation of isotope data for zircons from the dated sample, which have the least evolved Hf isotope signature of any analysed from the Rudall Province and show evidence of a 1.9 Ga crustal forming event (Kirkland et al., 2013b).

Direct dating of metamorphism

There are currently few dates for metamorphic minerals in the Rudall Province and none that can be directly related to particular metamorphic assemblages or structures.

Most rims on zircon grains examined in this study were difficult to analyse as they are typically thin and in some cases also have low U contents. This might be due to a general lack of partial melting in the exposed Rudall Province, although it experienced metamorphism under amphibolite to granulite facies conditions. Despite this, rim analyses that could be carried out indicate multiple Paleoproterozoic to Mesoproterozoic events (Table 3). This tectono-thermal history contains more complexity than is represented in the current structural framework (Table 1), which does not incorporate significant deformational events between c. 1760 Ma and c. 800 Ma (i.e. the period between D_1/D_2 and D_3/D_4 of Hickman and Bagas, 1999), though Mesoproterozoic magmatism is noted. Given the current lack of dating able to be assigned to specific structural fabrics or metamorphic mineral assemblages, it is still not yet possible to assign deformational events to the dates obtained in this study, but the available dates suggest significant tectonism took place at c. 1680, 1589–1549 and 1330–1285 Ma.

There is some evidence of metamorphism between 1800 and 1760 Ma in the dated samples. The layered orthogneiss from the Talbot Terrane dated at c. 1804 Ma (GA 2005670080) contains four dispersed, near-concordant analyses between c. 1785 and 1757 Ma but it is unclear whether they represent a discrete event or variable Pb loss during younger metamorphism, which appears to have occurred at 1679 ± 25 Ma, based on dates from low U zircon rims. Quartzite from the Tabletop Terrane (GA 2006670087) yielded analyses of several zircon rims with dates between c. 1820 and 1705 Ma, with five of these having a weighted mean date of 1790 ± 7 Ma. A younger metamorphic event in this quartzite occurred at 1580 ± 34 Ma, which is interpreted to reflect the thermal effects of leucogranite intrusion immediately adjacent to the quartzite, and no evidence of c. 1580 Ma metamorphism has been recognized elsewhere in the Rudall Province. Granitic gneiss from the Connaughton Terrane dated at c. 1781 Ma (GA 2005670162) contains a group of low U, high Th/U zircon core analyses with a weighted mean date of 1739 ± 20 Ma and a relatively tight cluster of three near-concordant analyses at 1688 ± 8 Ma. It is unclear whether these dates reflect discrete events or coincidental clustering of analyses that underwent partial isotopic resetting during younger metamorphism at c. 1334 Ma. Evidence consistent with a metamorphic event at c. 1680 Ma was obtained from a sample of quartzofeldspathic gneiss from the Connaughton Terrane, which yielded an imprecise date of 1672 ± 65 Ma for zircon rims (Nelson, 1996c). A single concordant analysis of 1612 ± 44 Ma (1σ) from a felsic dyke in the Talbot Terrane (Nelson, 1995j) could also be related to an event at c. 1680 Ma.

Evidence of a high-grade Mesoproterozoic metamorphic event is provided by dating of well-developed high U, low Th/U zircon rims from quartzite in the Connaughton Terrane (GA 2005670165), which yielded a date of 1334 ± 4 Ma. No older metamorphic dates were obtained from this sample, which has a maximum depositional age of c. 2284 Ma. A 1315 ± 11 Ma (1σ) date for a zircon overgrowth in granitic gneiss from the Connaughton Terrane (GA 2005670162) also indicates

high-grade metamorphism at this time. Chin and de Laeter (1981) obtained a well-fitted Rb–Sr isochron date of 1333 ± 44 Ma for samples of a granitic gneiss in the northwestern Connaughton Terrane that they considered contained the S_2 foliation and lacked structures associated with younger deformation. A younger, but imprecise, date of 1222 ± 63 Ma was obtained from a small number of analyses of zircon rims from a quartzofeldspathic gneiss in the Connaughton Terrane (Nelson, 1996c). Although limited, the dates for metamorphism are generally similar to, or slightly older than, felsic intrusive rocks of the 1310–1286 Ma Camel Suite (Nelson, 1995b; Nelson, 1996e; this study), suggesting that the metamorphism and magmatism are related.

Although there is limited dating of metamorphism in the Rudall Province, it appears that there was a significant high-grade event at c. 1330 Ma, with less certain evidence of metamorphism, isotopic disturbance, or both, at c. 1680 Ma and 1790–1740 Ma. A more focused study of metamorphic zircon and monazite from the Talbot and Connaughton Terranes (J. Anderson [Adelaide University], 2015, written comm., 29 August) has also yielded metamorphic dates at c. 1300 and 1670 Ma, indicating that the limited metamorphic dates obtained in this study are indeed indicative of the timing of significant events in the province.

Geodynamic setting of the Krackatinny Supersuite

Granitic rocks of the 1589–1549 Ma Krackatinny Supersuite form an important component of the Tabletop Terrane and include rocks with compositions similar to those found in magmatic arcs. In terms of petrogenesis and tectonic setting, the available data do not provide an unequivocal model for the geodynamic setting of the Krackatinny Supersuite, but two possible petrogenetic/tectonic scenarios — subduction and intraplate rifting — are consistent with the geochemical characteristics of these rocks.

In a subduction scenario, the high Sr/Y sodic series might be true adakites (i.e. melts of subducted oceanic lithosphere), the low Sr/Y sodic series might be arc granites formed through assimilation and fractional crystallization (AFC)-type processes involving metasomatized mantle-wedge melts and sodic lower arc crust, and the younger high-K granites might reflect post-accretionary collapse. The high Sr/Y sodic rocks differ from some adakitic rocks, however, in that they show no enrichments in Cr and Ni, or the unusually high Mg#, expected of slab melts that have interacted with mantle-wedge peridotite. This might indicate that these rocks were not formed in an arc setting or reflect conditions that did not favour mantle interaction. The single Nd isotope analysis of these rocks indicates a source that is considerably less radiogenic than pure oceanic lithosphere of Mesoproterozoic age and requires significant involvement of an evolved crustal component, although the geochemical data indicate that crust could not have been typical continental (high-K) crust.

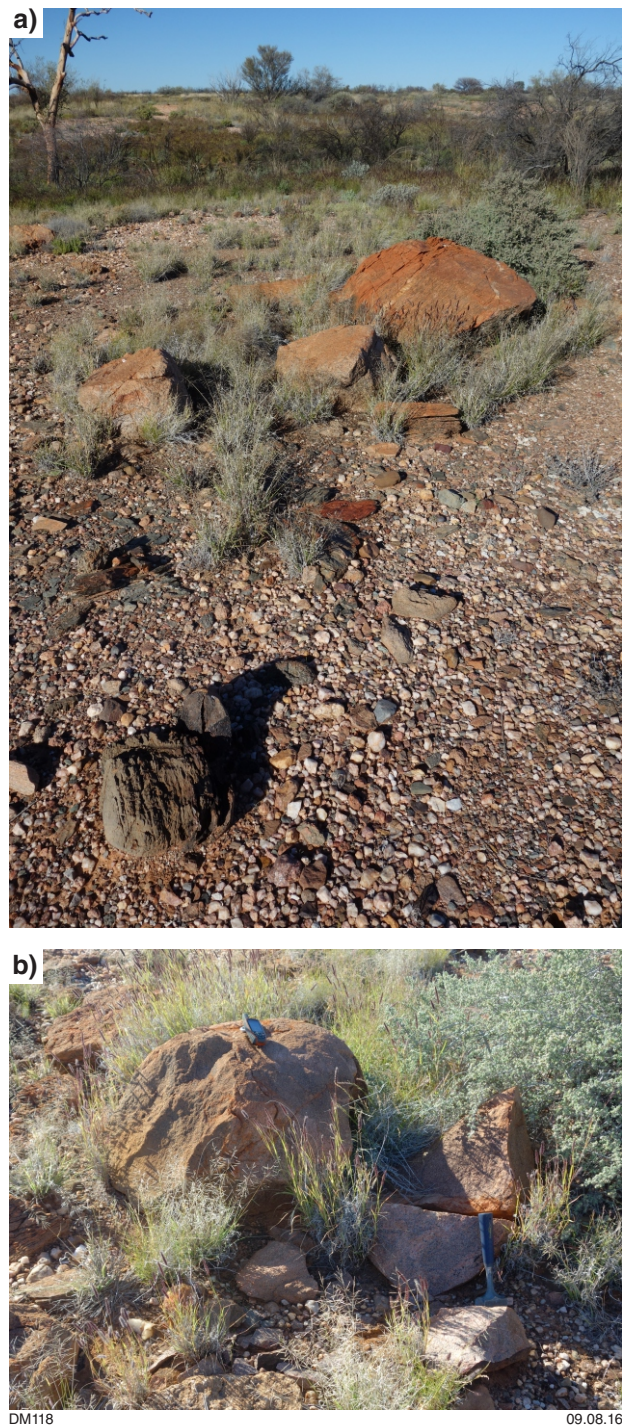


Figure 64. Outcrop photos of monzogranite sample site of Nelson (1996b): a) boulders of various lithologies and textures in the area of the sample site, which are possible glacially derived clasts from the Permian Paterson Formation; b) boulder of K-feldspar rich monzogranite, possibly that which was sampled by Nelson (1996) yielding a date of 1453 ± 10 Ma (MGA 409775E 7498324N)

In an intraplate rifting model, the high Sr/Y sodic series could reflect melting at the base of thickened mafic crust, the low Sr/Y sodic rocks melting at higher crustal levels and the high-K granites later melting at the base of thinned and dehydrated crust. The requirement for this model is that melting of mafic crust began at depths greater than about 35–40 km and, based on the sodic compositions and evolved Nd isotope compositions, was of old (>2.85 Ga) mafic crust. Production of the low Sr/Y sodic granites occurred at depths of <35 km. Both the high and low Sr/Y sodic series have a similar range of ratios for incompatible trace elements (e.g. Nb/Zr) not affected by peritectic garnet, and hence may have resulted through melting of the same mafic crust but at different pressures. Evidence from other central and southern Australian Proterozoic terrains (Musgrave and Madura Provinces) indicates that further high-temperature remelting of mafic crust under low-pressure, dry, conditions can lead to geochemically enriched K-rich compositions like those of the Krackatinny high-K series (e.g. Howard et al., 2015).

There is little or no evidence of regional metamorphism at 1589–1549 Ma in the Rudall Province, with the only metamorphic date of this age apparently related to contact metamorphism, suggesting this event was largely magmatic in character. In this context, the age of amphibolite in the Tabletop Terrane with an apparent subduction-related signature becomes an important unresolved question, as the current highly imprecise constraints allow for these rocks to have been emplaced as late as an early phase of the Krackatinny Supersuite. In the following discussions, both magmatic arc and rift settings are entertained as plausible alternatives, as each model has different implications for the assembly of Proterozoic Australia.

Geodynamic setting of the Kalkan Supersuite and Camel Suite

The geochemical characteristics of the Kalkan Supersuite and Camel Suite are comparable to that of the high-K components of the Krackatinny Supersuite, and might reflect similar processes and sources, but the paucity of data does not allow for any firm conclusions to be drawn. The high-TiO₂ and high P₂O₅ trends of the Kalkan Supersuite are reminiscent of charnockite-series A-type magmas and are consistent with dry high-T, low-P partial melts formed near the crust/mantle interface beneath extended and thinned crust. Similar extensional processes might be responsible for all the high-K, low Sr/Y suites in the Rudall Province but considerably more work on these units is required to test this suggestion.

Reassessing the geodynamic evolution of the Rudall Province

The geological and geochronological data for the Rudall Province allow for the possibility that the Yapungku Orogeny might have occurred later than previously thought, warranting a reevaluation of current geodynamic models in the context of the amalgamation of the West

and North Australian Cratons. Currently, almost all interpretations of the Proterozoic geodynamic evolution of Australia incorporate the 1800–1765 Ma inferred timing of the Yapungku Orogeny as a pinning point, requiring late Paleoproterozoic to mid-Mesoproterozoic reconstructions to accommodate a linked West Australian Craton – North Australian Craton configuration (e.g. NAWAC of Aitken et al., 2016; see also Betts and Giles, 2006; Betts et al., 2008; Cawood and Korsch, 2008). However, if the Yapungku Orogeny occurred after 1760 Ma, it is possible that amalgamation of the West and North Australian Cratons also occurred later than previously thought. Previous interpretations regarding the timing of collision are not only based on the inferred timing of the Yapungku Orogeny, but also upon the interpretation that the high-P metamorphism in the Rudall Province reflects continental collision (Smithies and Bagas, 1997). Although significant crustal thickening and high-P metamorphism are consistent with a collisional setting, metamorphism and exhumation of lower crustal rocks can also take place within intraplate orogens, for example the 580–530 Ma Petermann Orogeny in the Musgrave Province of central Australia (Camacho et al., 1997; Scrimgeour and Close, 1999; Raimondo et al., 2010; Walsh et al., 2013). It is thus worth noting that the amalgamation of the West and North Australian Cratons might not necessarily have been associated with the Yapungku Orogeny.

The most widely accepted geodynamic interpretation of the Yapungku Orogeny is that it occurred near the northeastern margin of the West Australian Craton during a continental collisional event, most likely with the North Australian Craton (Smithies and Bagas, 1997; Bagas, 2004). Southwesterly directed folding, thrusting and crustal thickening has been interpreted to have been coeval with the emplacement of voluminous granitic rocks of the 1804–1762 Ma Kalkan Supersuite. Little deformation is considered to have taken place after this event until the Neoproterozoic Miles Orogeny, apart from Mesoproterozoic felsic magmatism, largely within the Tabletop Terrane. Most of the metasedimentary units in the Talbot Terrane are considered to have been deposited in a continental margin setting, either in a foreland basin (Smithies and Bagas, 1997) or a marginal basin (Hickman and Bagas, 1999) above older passive margin sedimentary rocks deposited on the margin of the Pilbara Craton, now represented by the unassigned metasedimentary rocks of the Talbot and Connaughton Terranes (Smithies and Bagas, 1997).

For this model to fit the existing geochronological and geological constraints, the younger metasedimentary units in the Talbot Terrane would need to have been deposited during the earliest stages of collision — possibly within a pro-foreland basin with sediment sourced from exhumed granites of the Kalkan Supersuite in the core of the orogen (Smithies and Bagas, 1997) — to be eventually underthrust to middle to lower crustal depths during the final stage of collision. This would require that the dates obtained in this study for the Larry Formation and unassigned schist represent ages of highly deformed intrusive rocks rather than maximum depositional ages. If the 1804–1762 Ma Kalkan Supersuite is considered to be associated with collision, it is implied that collision

commenced before c. 1804 Ma and that the development of the high-grade S_2 foliation and F_2 folding continued after the emplacement of the youngest granites. In this scenario, all younger events at c. 1680, 1590–1550, 1330–1285, c. 810 and 670–600 Ma would reflect episodes of intraplate reworking.

An alternative possibility suggested here, that the Yapungku Orogeny took place after 1760 Ma, is also consistent with the available constraints. In this scenario, the oldest rocks in the province formed an Archean to mid-Paleoproterozoic supracrustal succession deposited near the northeastern margin of the West Australian Craton, which was intruded by the Kalkan Supersuite from 1804–1762 Ma (D_1). Field relationships suggest that low-pressure, high-T metamorphism (M_1) was broadly coeval with the emplacement of the Kalkan Supersuite, and was associated with the development of a layer-parallel foliation and minor folding (Clarke, 1991; Hickman and Bagas, 1999). The nature of this tectonism is not well understood but these features can be placed in a locally extensional setting, as opposed to the compressional setting currently envisaged for D_1 . The Kalkan Supersuite is characterized by relatively potassic, low Sr/Y granitic rocks, typical of many Australian Proterozoic granitic rocks, indicative of partial melting at depths of less than about 35 km under relatively high geothermal gradients (Budd et al., 2001), which is also possible during extension.

If the younger stratigraphic units in the Talbot Terrane, such as the Fingoon Quartzite, were deposited at a similar time to magmatism (one possible interpretation), their deposition might thus represent development of an extensional basin, perhaps associated with extensional exhumation of early-formed granites. If this is the case, the moderate- to high-P tectonism of the overprinting Yapungku Orogeny (D_2/M_2) might have been unrelated to the low-P, high-T D_1/M_1 event and Kalkan Supersuite magmatism. If the younger stratigraphic units in the Talbot Terrane were instead deposited after c. 1760 Ma, a phase of basin development is constrained to have occurred at some point between D_1 and D_2 , suggesting a more significant time break between these events, as noted above.

In either case, assuming a largely intact succession, the lithological changes between the Larry Formation, Fingoon Quartzite and Yandagoo Formation in the Talbot Terrane are consistent with a trend of increased compositional maturity and deeper water conditions up-sequence. The Larry Formation is dominated by subarkosic to arkosic compositions that grade upwards into quartz-rich lithologies of the Fingoon Quartzite. Both of these units contain essentially unimodal detrital zircon populations indicating proximal sources. The overlying Yandagoo Formation contains graphitic and iron-rich metapelitic rocks associated with chert, indicative of deeper water deposition and lower rates of sedimentation. This succession would appear to be more consistent with an extensional or passive margin setting rather than a

foreland basin within a continental collision zone, since foreland basins tend to be characterized by upwards-coarsening successions and high rates of sedimentation (DeCelles and Giles, 1996; DeCelles, 2011).

Geodynamic context from other parts of Proterozoic Australia

If the Yapungku Orogeny occurred after c. 1760 Ma, it is difficult to determine which of the dated metamorphic events might reflect this orogeny, since the samples with dated metamorphic zircon do not have diagnostic metamorphic assemblages. Some constraints on the potential timing of the Yapungku Orogeny and the amalgamation of the West and North Australian Cratons can be obtained by considering other regions of Proterozoic Australia at the times of the main tectonic events. As has been discussed by previous authors, the dates of magmatic and metamorphic events in Rudall Province are similar to events within other areas of the West and North Australian Cratons, such as the Arunta Province of the North Australian Craton and the Capricorn Orogen of the West Australian Craton (Bagas, 2004; Kirkland et al., 2013b). The similarities of event timing become even more apparent with the dates obtained in this study, which reveal events at c. 1680 and 1590–1550 Ma, which also have time-equivalents in other terranes. Although time-equivalence does not necessarily indicate direct linkages between different regions, the patterns and nature of tectonism provide one way of assessing the broader geodynamic setting.

Summaries of tectonism in different parts of western and central Australia are presented and discussed below for the main periods of Paleoproterozoic and Mesoproterozoic tectonism identified in the Rudall Province, and a simplified time–space plot for the period 1800–1200 Ma is shown in Figure 65. The easternmost parts of Proterozoic Australia are not considered in detail as part of this comparison, as they are less likely to reflect tectonism that can be directly related to events in the Rudall Province.

1800–1760 Ma regional geodynamic setting

It is striking that many parts of Paleoproterozoic Australia were affected by tectonism between c. 1810 and 1760 Ma (Figs 65, 66; Table 4). Some of these areas are considered to have been proximal to plate margins at this time, including the Rudall Province, the southern margin of the Arunta Orogen and the Albany–Fraser Orogen (Bagas, 2004; Ahmad and Scrimgeour, 2013; Spaggiari et al., 2015). Other events appear to have taken place in an intraplate setting (e.g. basin development and magmatism in the MacArthur and Kimberley Basins and tectonism and basin development in the Capricorn Orogen), although possibly driven by plate margin processes.

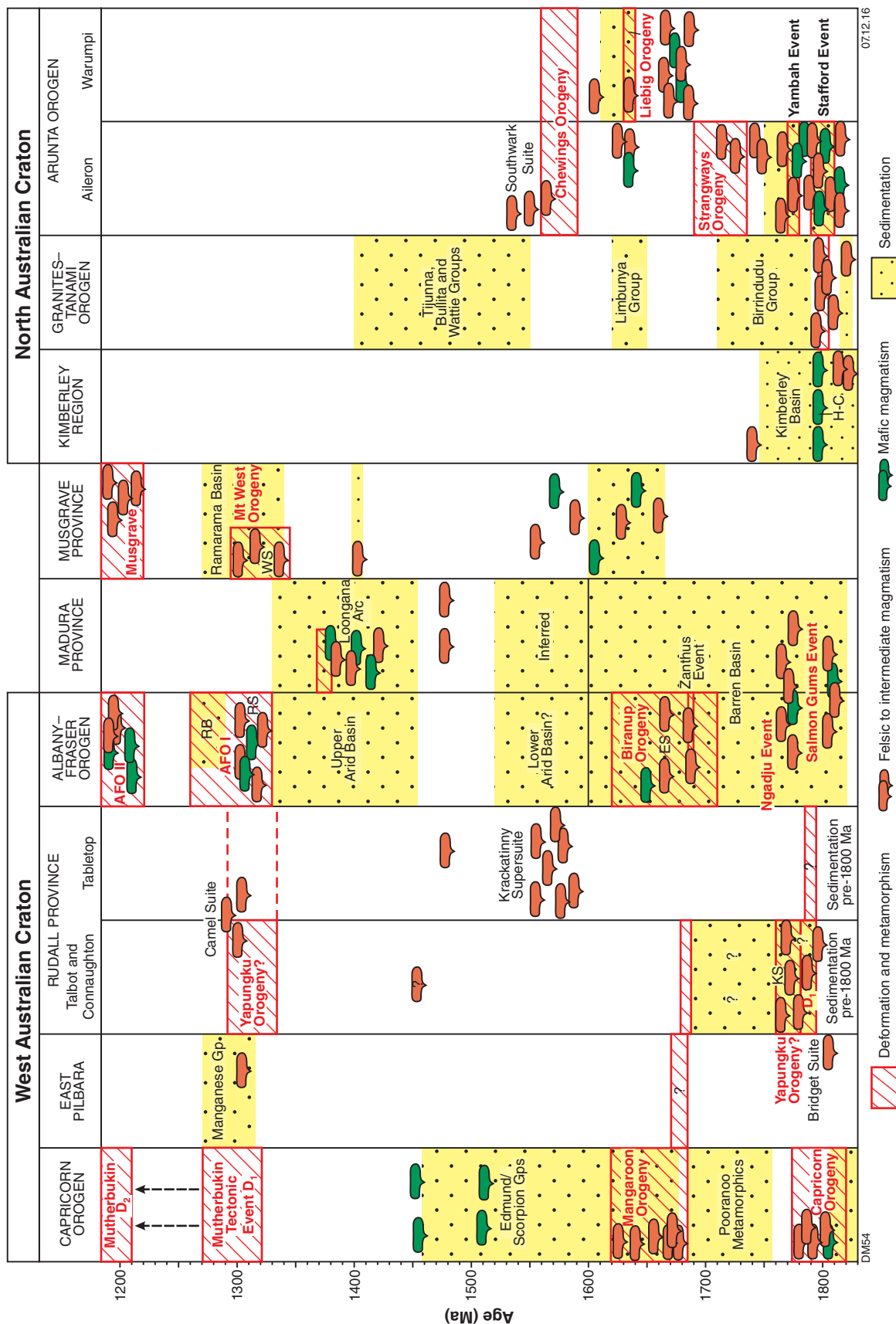


Figure 65. Time-space diagram of 1800–1200 Ma tectonic events in western and central Australia

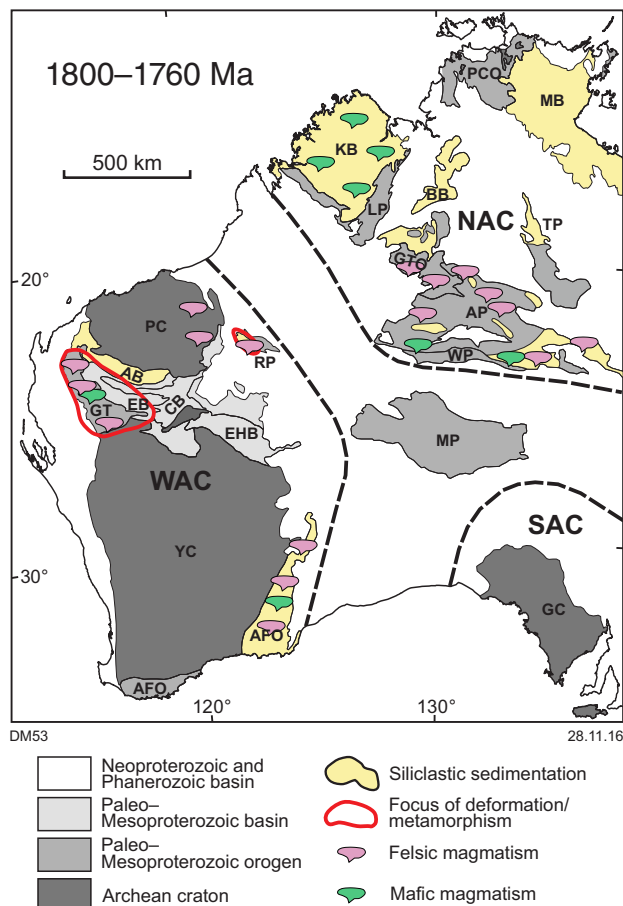


Figure 66. Tectonism from 1800–1760 Ma in western and central Australia using current geographic positions, with no attempt made to reconstruct true relationships at this time; dashed lines group terranes considered to be part of the West (WAC), North (NAC) and South Australian Cratons (SAC). AB – Ashburton Basin; AFO – Albany–Fraser Orogen; AP – Aileron Province; BB – Birrindudu Basin; CB – Collier Basin; EB – Edmund Basin; EHB – Earaheedy Basin; GC – Gawler Craton; GT – Glenburgh Terrane; GTO – Granites–Tanami Orogen; KB – Kimberley Basin; LP – Lamboo Province; MB – McArthur Basin; MP – Musgrave Province; PC – Pilbara Craton; PCO – Pine Creek Orogen; RP – Rudall Province; TP – Tomkinson Province; YC – Yilgarn Craton; WP – Warumpi Province

In the Aileron Province of the Arunta Orogen, the 1810–1790 Ma Stafford and 1780–1770 Yambah Events are considered by many authors to have developed in a plate margin setting involving north-directed subduction (e.g. Betts and Giles, 2006; Scrimgeour, 2006; Howlett et al., 2015), although this is not universally accepted (e.g. Gibson et al., 2008). Magmatism, sedimentation and high-T, low-P metamorphism have been suggested to have taken place within a predominantly extensional back-arc setting (Scrimgeour, 2006; Howlett et al., 2015) and 1770–1750 Ma granitic rocks with arc-like geochemical signatures are consistent with an open margin at this time (Foden et al., 1988; Zhao and Bennett, 1995; Zhao and McCulloch, 1995).

Two episodes of felsic to intermediate magmatism and sedimentation with similar ages to those in the Arunta Orogen also took place in the Albany–Fraser Orogen along the southeastern margin of the West Australian Craton (Spaggiari et al., 2014a). The 1815–1800 Ma Salmon Gums Event resulted in the emplacement of felsic and lesser mafic rocks that were associated with the initiation of the long-lived Barren Basin along the margin of the Yilgarn Craton. The 1780–1760 Ma Ngadju Event coincided with development of sub-basins within the Barren Basin and granitic magmatism. The magmatism, sedimentation and associated metamorphism have been interpreted in terms of a continental rift, extension due to a retreating subduction zone or a back-arc setting (Spaggiari et al., 2014a, 2015a; Smithies et al., 2015a).

Volumetrically minor intraplate magmatism of the c. 1803 Ma Bridget Suite occurs in the eastern Pilbara Craton, which comprises a series of relatively small, calc-alkaline, felsic intrusive rocks forming a narrow north-northwesterly trending zone up to 250 km long (Hickman, 1978; Budd et al., 2001; Nelson, 2002c; Bagas, 2005; Van Kranendonk, 2010). These felsic intrusive rocks were comagmatic with trachyandesites, trachyte and lamprophyre dykes and have high Sr/Y, contrasting with the low Sr/Y Kalkan Supersuite in the Rudall Province. Kirkland et al. (2013a) obtained a range of evolved zircon Lu–Hf isotope signatures for these samples, consistent with a significant component of Pilbara Craton crust. The geodynamic setting of this magmatism is not clear but the north-northwesterly trend of these intrusions suggests that magmatism was related to processes along the margin of the Pilbara Craton, with Bagas (2005) suggesting a relationship with collision, assuming an 1800–1765 Ma age for the Yapungku Orogeny. The geochemical characteristics of the Bridget Suite, however, are not necessarily diagnostic of a collisional setting. Collins et al. (1988) proposed a two-stage evolution for these rocks, with an older stage of potassic mafic to intermediate magmatism forming an underplate that was subsequently partially melted in a younger event to form the Bridget Suite. This does not necessarily require a collisional setting, and both compressional and extensional settings are possible.

Intraplate tectonism is recorded in the Granites–Tanami Orogen, which contains voluminous 1820–1780 Ma granitic rocks associated with folding, low- to moderate-grade metamorphism and orogenic gold mineralization (Dean, 2001; Bagas et al., 2010; Ahmad et al., 2013). Many of these granitic rocks have low Sr/Y, but some high Sr/Y granites have been recognized (Dean, 2001; Bagas et al., 2010). This tectonism is considered to be related to convergence along the southern or northwestern margins of the North Australian Craton (Crispe et al., 2007; Huston et al., 2007; Ahmad and Scrimgeour, 2013), although Bagas et al. (2010) postulated a collision between the Granites–Tanami and Arunta Orogens.

Intraplate tectonism is also recorded in the 1817–1772 Ma Capricorn Orogeny within the West Australian Craton (Johnson et al., 2010; Sheppard et al., 2010a,b). This was associated with the emplacement of voluminous granitic rocks, high-T, low-P metamorphism, local development of a layer-parallel foliation and folding and shear zone

Table 4. Summary of 1800–1760 Ma tectono-thermal events in western and central Australia

Geological domain	Event	Metamorphism	Structure	Magmatism	Sedimentation	Interpreted setting(s)	References
East Pilbara Craton (WAC)	Bridget Suite (c. 1803 Ma)	–	–	Calc-alkaline felsic intrusive; high Sr/Y trachyandesite, trachyte, lamprophyre	–	Near plate margin; syn-convergence/collision?	Collins (1998); Budd et al. (1991); Nelson (2002c); Bodorkos (2006b); Bagas (2005); Van Kranendonk (2010)
Capricorn Orogen (WAC)	Capricorn Orogeny (1817–1772 Ma)	High-T, low-P	Layer-parallel schistosity, shearing, upright folding	1817–1773 Ma Moorarie Supersuite (voluminous granite, minor mafic)	Siliclastic in Ashburton Basin	Dominantly extensional, with short-lived compressional episodes; intraplate orogen	Johnson et al. (2010); Sheppard et al. (2010a, b); Johnson (2013)
Aileron Province, Arunta Orogen (NAC)	Stafford Event (1810–1790 Ma)	High-T, low-P	Upright folding and steep foliations	Bimodal intrusive and extrusive	Volcaniclastic, siliclastic, carbonate	Back-arc; retreating convergent margin	Zhao and McCulloch, 1995; Betts and Giles (2006); Scrimgeour (2006); Scrimgeour et al. (2013a); Howlett et al. (2015)
Aileron Province, Arunta Orogen (NAC)	Yambah Event (1780–1770 Ma)	Variable, moderate- to high-T, low- to moderate-P	Uncertain	Felsic and mafic intrusive, including 'arc-like' calc-alkaline	–	Continental arc with compressional events; intraplate	Foden et al. (1988); Zhao and Bennett (1995); Gibson et al. (2008); Scrimgeour et al. (2013a); Anderson et al. (in press)
Granites–Tanami Orogen (NAC)	Stafford Event (1810–1790 Ma)	Low- to moderate-T, low-P	Folding, faulting	Voluminous felsic intrusive, calcic to calc-alkaline, including some high Sr/Y	–	Intraplate, related to convergence along southern and/or northwestern margins of NAC	Dean (2001); Crispe et al. (2007); Huston et al. (2007); Bagas et al. (2010); Ahmad et al. (2013); Ahmad and Scrimgeour (2013)
Albany–Fraser Orogen (WAC)	Salmon Gums Event (1815–1800 Ma)	–	–	Felsic and lesser mafic magmatism	Siliclastic; associated with initiation of >1800–1600 Ma Barren Basin	Continental rift; extension due to retreating subduction zone; back-arc	Spaggiari et al. (2014a)
Albany–Fraser Orogen (WAC)	Ngadiju Event (1780–1760 Ma)	–	–	Felsic intrusive	Siliclastic in Barren Basin	Continental rift; extension due to retreating subduction zone; back-arc	Spaggiari et al. (2014a); Smithies et al. (2015); Spaggiari et al. (2015a)
Pine Creek Orogen (NAC)	Shoobridge Event (c. 1780 Ma)	Widespread retrogression	NW- to N-trending shear zones	–	–	?	Ahmad and Hollis (2013)

movement. The deformation overlapped sedimentation and subsidiary bimodal magmatism in the 1806–1799 Ma Ashburton Basin, which has been suggested to have developed in a pro-foreland setting, but extensional processes may also have played a significant role (Johnson, 2013; Johnson et al., 2013).

Extensive intraplate basins with coeval felsic and mafic magmatism developed within the North Australian Craton at this time, including the MacArthur, Kimberley and Birrindudu Basins (Betts and Giles, 2006; Ahmad and Scrimgeour, 2013). These basins are characterized by fluvial to shallow-marine sedimentation, with subsidiary mafic and minor felsic magmatism, with the most voluminous mafic magmatism associated with the c. 1795 Ma Hart–Carson Large Igneous Province in the Kimberley region (Sheppard et al., 2012). Scott et al. (2000) and Giles et al. (2002) suggested that the development of the northern Australian basins during this period was a result of far-field extension related to subduction along the southern margin of the craton. Retrograde reactivation of shear zones is recorded in the Pine Creek Orogen during the c. 1780 Ma Shoobridge Event, which might be related to the development of the McArthur Basin (Ahmad and Hollis, 2013).

The magmatism, sedimentation and metamorphism in the Arunta and Albany–Fraser Orogens along the margins of the North and West Australian Cratons can be placed within a setting of prolonged extension, punctuated by short-lived episodes of compression and deformation. These have many of the characteristics of extensional (retreating) accretionary orogens, in which dominantly extensional conditions are established in the back-arc region during continued convergence (Collins, 2002a,b; Cawood et al., 2009; Spaggiari et al., 2015a). Intraplate subsidence and sedimentation, bimodal magmatism and locally developed high-T, low-P metamorphism in the North and West Australian Cratons can also be placed in distal ‘back-arc’ settings, with periods of compressional deformation related to arrival of more buoyant crust at the subduction zone, or changes in the rate of convergence.

The voluminous felsic magmatism in the Rudall Province at 1805–1760 Ma is broadly coeval with low-P, high-T metamorphism and the development of a layer-parallel foliation during M_1/D_1 (Hickman and Bagas, 1999). As discussed above, it is possible that sedimentation also took place during or after this magmatism, largely derived from exhumed local granitic rocks. These features might also have developed within a dominantly extensional setting associated with a retreating accretionary orogen developed along the northeastern margin of the West Australian Craton.

The prolonged tectonism along the margins and within the North and West Australian Cratons, which might have been dominantly extensional, is difficult to reconcile with a collision of the North and West Australian Cratons at this time. Although the timing of tectonism in these widely separated areas is broadly synchronous, a collisional

driver is not required, and the similarities might instead reflect similar processes operating near the margins of separated cratons. If the intraplate basins developed in the North Australian Craton during this period were indeed generated by subduction along the southern margin of the craton, the presence of the Kimberley Basin in the northwestern part of the craton might also be evidence that subduction took place during this period along the now covered southwestern part of the North Australian Craton. It is thus possible that the 1805–1760 Ma tectonism in the Rudall Province was not a consequence of collision but extension related to prolonged convergence along an open craton margin.

1680 Ma regional geodynamic setting

Tectonism of this age is less widespread than events at 1805–1760 Ma, but includes events in the Arunta and Albany–Fraser Orogens along the interpreted margins of the North and West Australian Cratons, as well as intraplate tectonism in the West Australian Craton (Figs 65, 67; Table 5).

There is limited evidence of tectonism during this period in the Pilbara Craton. A complex hornblende $^{40}\text{Ar}/^{39}\text{Ar}$ plateau was obtained from a granitic rock of the Bridget Suite in the eastern part of the craton, which yielded a weighted mean date of 1674 ± 4 Ma and oldest steps at 1703 ± 6 Ma (Nelson, 2004). A K–Ar date of 1674 ± 33 Ma was also obtained from this unit (Nelson, 2002b).

In the Capricorn Orogen, intraplate tectonism of the Mangaroon Orogeny affected the Gascoyne Province between c. 1680 and 1620 Ma (Sheppard et al., 2005). The Mangaroon Orogeny was associated with 1680–1620 Ma granitic intrusions, which were most abundant at 1680–1675 Ma. This magmatism was broadly coeval with high-T, low-pressure metamorphism, partial melting and the development of a layer-parallel foliation, which was partitioned into a relatively narrow zone in the northern Gascoyne Province. The tectonism was possibly also associated with the deposition of sedimentary rocks (Sheppard et al., 2005) and is interpreted to reflect intraplate extension (Johnson et al., 2011b, 2013). Dating of xenotime from the Paulsens orogenic gold deposit in the northern part of the orogen has yielded a date of 1.68 Ga, interpreted to reflect an episode of hydrothermal fluid flow during this period (Fielding et al., 2016). A similarly aged hydrothermal event has been inferred from a U–Pb xenotime age of 1673 ± 15 Ma obtained from the Tom Price iron ore deposit, also in the northern part of the orogen (Rasmussen et al., 2007). $^{40}\text{Ar}/^{39}\text{Ar}$ muscovite dates of c. 1650 Ma obtained from quartz–muscovite schist in the northern Earraheedy Basin (Pirajno et al., 2009) and c. 1653 Ma from a shear zone in the Sylvania Inlier associated with southeast–northwest directed extension (Sheppard et al., 2006), also appear to be related to this tectonism.

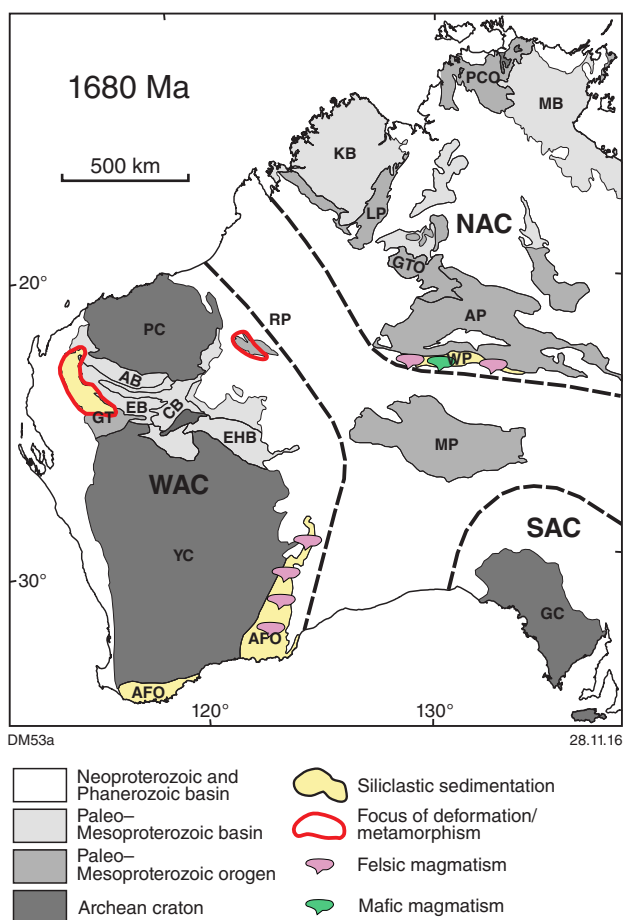


Figure 67. Tectonism at c. 1680 Ma in western and central Australia using current geographic positions. AB – Ashburton Basin; AFO – Albany–Fraser Orogen; AP – Aileron Province; BB – Birrindudu Basin; CB – Collier Basin; EB – Edmund Basin; EHB – Eeraheedy Basin; GC – Gawler Craton; GT – Glenburgh Terrane; GTO – Granites–Tanami Orogen; KB – Kimberley Basin; LP – Lamboo Province; MB – McArthur Basin; MP – Musgrave Province; PC – Pilbara Craton; PCO – Pine Creek Orogen; RP – Rudall Province; TP – Tomkinson Province; YC – Yilgarn Craton; WP – Warumpi Province

In the Arunta Orogen, voluminous felsic and subordinate mafic intrusive rocks of the 1690–1660 Ma Argilke Igneous Event and associated metasedimentary rocks form the oldest units within the 1690–1600 Ma Warumpi Province, an east–west trending belt along the southern margin of the North Australian Craton (Scrimgeour et al., 2005; Scrimgeour, 2013b). Rocks of the Warumpi Province are significantly younger than those of the Aileron Province to the north, and the belt has been interpreted as a magmatic arc that was accreted to the North Australian Craton during the Liebig Orogeny at 1640–1635 Ma (Close et al., 2005; Scrimgeour et al., 2005). Hollis et al. (2013) proposed a different geodynamic setting based on Lu–Hf and U–Pb isotope data, which indicate involvement of crust of a similar age to the Aileron Province in the generation of the

Argilke magmas. These authors suggest that a ribbon of continental crust represented by the Warumpi Province might have been rifted from the southern margin of the Aileron Province during extension at, or before, 1690 Ma. Younger convergence resulted in southerly directed subduction beneath the continental fragment, generation of arc magmatism and eventual collision of the Warumpi Province with the North Australian Craton. Both models imply a convergent margin along the southern margin of the North Australian Craton at c. 1680 Ma.

In the Albany–Fraser Orogen, the 1710–1650 Ma Biranup Orogeny was associated with episodic emplacement of felsic and mafic intrusive rocks, with most magmatism at 1690–1660 Ma (Spaggiari et al., 2011; Spaggiari et al., 2014a), coeval with deposition of siliciclastic sedimentary rocks in the Barren Basin. The discrete c. 1680 Ma Zanthus Event produced folding under high-grade metamorphic conditions and is interpreted as a compressional episode within the Biranup Orogeny (Spaggiari et al., 2014a). Current models for this event favour a locally extensional regime near an active plate margin, possibly a rift (Hall et al., 2008), distal back-arc (Kirkland et al., 2011a) or both (Korsch et al., 2014). The Zanthus Event might represent a short-lived episode of compression within an otherwise extensional setting, possibly driven by a change in plate dynamics or the effects of a seamount entering a subduction zone (Johnson, 2013).

The character of tectonism at c. 1680 Ma in the West and North Australian Cratons does not suggest a collisional event at this time. Events along the margins of the cratons have been inferred to occur in back-arc or arc settings during ongoing subduction, although the nature of the covered southwestern margin of the North Australian Craton is not known. The driver of extension in the Capricorn Orogen is not clear but might reflect the partitioning of plate margin stresses into an intraplate suture zone.

Currently, there is little evidence from the Rudall Province to constrain the nature of tectonism at c. 1680 Ma. There is no known magmatism of this age and the sporadic evidence for isotopic resetting might indicate that this tectonism was not a major event, but this is difficult to assess given the overall paucity of data. A c. 1680 Ma timing for the Yapungku Orogeny would be consistent with the structural overprinting of units as young as c. 1760 Ma and might also explain the lack of pervasive high-grade metamorphism and deformation in 1589–1549 Ma granitic rocks of the Tabletop Terrane. However, the absence of clear evidence of a major event at this time, coupled with the regional constraints outlined above, make it difficult to place this event in a collisional setting.

1590–1550 Ma regional geodynamic setting

There is little evidence for significant tectonism in the West Australian Craton during this period, apart from the emplacement of the Krackatiny Supersuite and localized 1610–1590 Ma hydrothermal activity at the Abra polymetallic deposit in the Capricorn Orogen

Table 5. Summary of c. 1680 Ma tectono-thermal events in western and central Australia

Geological domain	Event	Metamorphism	Structure	Magmatism	Sedimentation	Interpreted setting(s)	References
Capricorn Orogen (WAC)	Mangaroo Orogeny (1680–1620 Ma)	High-T, low-P	Layer-parallel foliation	Durlacher Supersuite granites, most abundant at 1680–1675 Ma	Possible siliciclastic	Intraplate extension	Sheppard et al. (2005); Johnson et al. (2011b); Johnson et al. (2013)
Warumpi Province, Arunta Orogen (NAC)	Argilke Event (1690–1660 Ma)			Felsic and minor mafic intrusive and extrusive rocks. Calc-alkaline components	Minor siliciclastic and calc-silicate	Continental arc on rifted or exotic crustal block	Close et al. (2005); Scrimgeour et al. (2005, 2013b); Hollis et al. (2013)
Albany–Fraser Orogen (WAC)	Biranup Orogeny (1710–1650 Ma)			Episodic felsic intrusive, mostly at 1690–1660 Ma	Siliciclastic in Barren Basin	Locally extensional regime near active plate margin; rift, distal back-arc	Hall et al. (2008); Kirkland et al. (2011a); Spaggiari et al. (2011, 2014a); Korsch et al. (2014)
Albany–Fraser Orogen (WAC)	Zanthus Event (1680–1675 Ma)	High-T	Folding	–	–	Short-lived compressional event within broader extensional period	Johnson (2013); Spaggiari et al. (2014a)
Granites–Tanami Orogen (NAC)	Stafford Event (1810–1790 Ma)	Low- to moderate-T, low-P	Folding, faulting	Voluminous felsic intrusive, calcic to calc-alkaline, including some high Sr/Y	–	Intraplate, related to convergence along southern and/or northwestern margins of NAC	Dean (2001); Crispe et al. (2007); Huston et al. (2007); Bagas et al. (2010); Ahmad (2013); Ahmad and Scrimgeour (2013)
Albany–Fraser Orogen (WAC)	Salmon Gums Event (1815–1800 Ma)	–	–	Felsic and lesser mafic magmatism	Siliciclastic: associated with initiation of > 1800–1600 Ma Barren Basin	Continental rift: extension due to retreating subduction zone; back-arc	Spaggiari et al. (2014a)
Albany–Fraser Orogen (WAC)	Ngadiju Event (1780–1760 Ma)	–	–	Felsic intrusive	Siliciclastic in Barren Basin	Continental rift: extension due to retreating subduction zone; back-arc	Spaggiari et al. (2014a); Smithies et al. (2015a); Spaggiari et al. (2015a)
Pine Creek Orogen (NAC)	Shoobridge Event (c. 1780 Ma)	Widespread retrogression	NW- to N-trending shear zones	–	–	?	Ahmad and Hollis (2013)

(Johnson et al., 2015; Figs 65, 68; Table 6). Depositional Packages 3 and 4 of the Edmund Basin were deposited between c. 1590 and 1455 Ma in an overall extensional intracratonic setting (Martin and Thorne, 2004; Johnson et al., 2013; Cutten et al., 2016). In the Albany–Fraser Orogen, this period is interpreted to record the development of a long-lived passive margin associated with extension following the end of the Biranup Orogeny at c. 1600 Ma (Spaggiari et al., 2015b). Aside from one sample adjacent to a Krackatinnu Supersuite intrusion, there are no 1590–1550 Ma metamorphic zircon dates from the Rudall Province, suggesting that this event does not date the Yapungku Orogeny.

In the Arunta Orogen, the Chewings Orogeny resulted in high-T, low- to medium-P metamorphism associated with south-southwesterly directed thrusting and isoclinal folding (Vry et al., 1996; Hand and Buick, 2001; Rubatto et al., 2001; Scrimgeour, 2013a). The main phase of tectonism occurred at 1590–1560 Ma (Scrimgeour, 2013a) but granitic rocks have been dated at 1570–1530 Ma (Scrimgeour, 2013a) and late-stage partial melts at 1523–1513 Ma (Morrissey et al., 2014). Outcropping amphibolite to granulite facies metamorphism is restricted to the central and southern part of the orogen but lower temperature thermal effects have been noted from the northwestern and eastern parts of the Aileron Province (Scrimgeour and Raith, 2001; Fraser et al., 2006). The driver for this intraplate deformation and metamorphism is unclear but might be related to plate margin interactions in the southern Musgrave Province (Wade et al., 2006, 2008; Payne et al., 2009).

In the Musgrave Province, the oldest exposed basement rocks comprise isotopically juvenile 1600–1550 Ma calc-alkaline orthogneiss and metamorphosed supracrustal rocks, which are generally considered to have formed within an oceanic arc setting between the North and South Australian Cratons (Camacho and Fanning, 1995; Edgoose et al., 2004; Wade et al., 2006; Howard et al., 2015; Kirkland et al., 2015a; Quentin De Gromard et al., 2016). The polarity of any subduction taking place during this period is not well constrained, and both northerly directed (Payne et al., 2009) and southerly directed (Wade et al., 2008) subduction have been proposed. In the covered Coompana Province, south of the Musgrave Province, dating of metamorphosed calc-alkaline granitic gneiss from drillcore yielded dates of 1613–1604 Ma (Wingate et al., 2015). These rocks comprise the Toolgana Supersuite, which has arc-like geochemical characteristics (Smithies et al., 2015b). Similarly aged, arc-like granitic rocks of the c. 1620 Ma St Peter Suite have also been recognized at the southwestern margin of the Gawler Craton (Swain et al., 2008). This was followed by the emplacement of voluminous felsic intrusive and extrusive igneous rocks in the central Gawler Craton during the 1595–1575 Ma Hiltaba Event, and deformation and high-grade metamorphism associated with the 1580–1540 Ma Kararan Orogeny in the northern Gawler Craton (Hand et al., 2007). There are a variety of models attempting to explain the complex evolution of the Gawler Craton through the 1620–1550 Ma period. While most of these incorporate the presence of an arc at 1620–1600 Ma, there are differing interpretations of the number and polarity of subduction zones in the region, the effects of

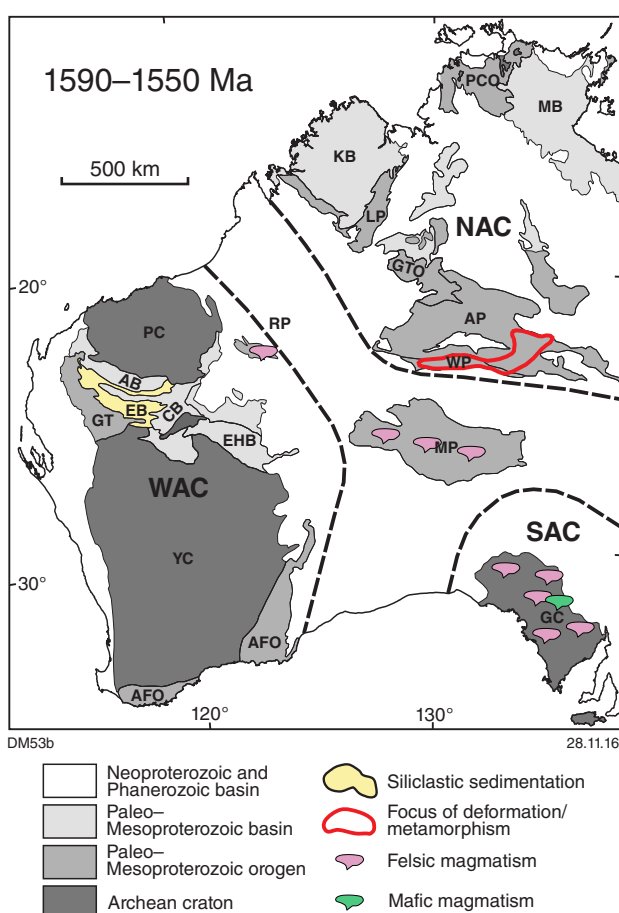


Figure 68. Tectonism from 1590–1550 Ma in western and central Australia using current geographic positions. AB – Ashburton Basin; AFO – Albany–Fraser Orogen; AP – Aileron Province; BB – Birindudu Basin; CB – Collier Basin; EB – Edmund Basin; EHB – Earaheedy Basin; GC – Gawler Craton; GT – Glenburgh Terrane; GTO – Granites–Tanami Orogen; KB – Kimberley Basin; LP – Lamboo Province; MB – McArthur Basin; MP – Musgrave Province; PC – Pilbara Craton; PCO – Pine Creek Orogen; RP – Rudall Province; TP – Tomkinson Province; YC – Yilgarn Craton; WP – Warumpi Province

an interpreted mantle plume, potential later rotation of the Gawler Craton and the degree to which tectonism might have been driven by events along the eastern margin of Proterozoic Australia (Giles et al., 2004; Swain et al., 2008; Betts et al., 2009).

On an even broader scale, the age of the Krackatinnu Supersuite is notably similar to events in eastern Proterozoic Australia, including the Olarian Orogeny in the Curnamona Province, the Isan Orogeny in the Mount Isa Inlier and the Ewamin–Janan Orogenies in the Georgetown and Yambo Inliers (Giles et al., 2004; Fraser et al., 2007; Betts et al., 2007; Payne et al., 2009; Betts et al., 2009), although most of these events appear to reflect interactions along the eastern margin of Proterozoic Australia or the effects of a mantle plume, or both (Betts et al., 2007, 2009).

Table 6. Summary of 1590–1550 Ma tectono-thermal events in western and central Australia

Geological domain	Event	Metamorphism	Structure	Magmatism	Sedimentation	Interpreted setting(s)	References
Arunta Orogen, Aileron and Warumpi Provinces (NAC)	Chewings Orogeny (1590–1560 Ma)	High-T, low- to medium-P in south-central Arunta Orogen; low-grade in other areas	SW-directed thrusts and folds	High-heat producing granites of the Southwork Suite (1570–1530 Ma) in west Aileron Province	–	Intraplate NE–SW shortening, possibly driven by convergence on southern NAC margin; possible heat contribution from radiogenic basement	Vry et al. (1996); Hand and Buick (2001); Rubatto et al. (2001); Scrimgeour and Raith (2001); Fraser et al. (2006); Cawood and Korsch (2011); Scrimgeour (2013a); Morrissey et al. (2014)
Gawler Craton (SAC)	Kararan Orogeny (1570–1540 Ma)	Ranges to high T/ultra-high T	E–W to ENE-trending folds and shears in north	–	–	N–S to NW–SE	Hand et al. (2007); Payne et al. (2008); Cutts et al. (2011); Reid and Hand (2012); Cawood and Korsch (2011)
Gawler Craton (SAC)	Hilltaba Event (1595–1575 Ma)	Ranges to high T/ultra-high T	NE to ENE-trending folds and thrusts	Felsic large igneous province (A-type Gawler Range Volcanics and Hiltaba Suite granites); lesser mafic rocks	Minor siliciclastic associated with volcanics	Regional NW–SE shortening; possible continental back-arc; compression driven by plate margin collision or accretion; possible hot-spot involvement	Betts et al. (2007); Hand et al. (2007)
Musgrave Province	Magmatic event(s)	–	–	Rare calc-alkaline granite gneiss and granulite, includes 1607–1583 Ma Warlawurru Supersuite	–	Oceanic arc developed in regionally extensive juvenile terrane; north- and/or south-directed subduction proposed	Camacho and Fanning (1995); Edgoose et al. (2004); Wade et al. (2006); Howard et al. (2015); Kirkland et al. (2015a); Quentin de Gromard et al. (2016)

Excluding events along the eastern margin of Australia, the widely separated evidence of magmatism, deformation and metamorphism during this period forms a northwesterly trending zone extending from the Gawler Craton in the southeast to the Rudall Province in the northwest. The close similarity between the range of ages obtained from Krackatinny Supersuite and those of events to the southeast suggest a related tectonic driver for these events, although local settings might have differed. One possibility is that these events reflect convergence between elements of northern and southern Australia. This would be consistent with interpreted arc magmatism at 1620–1610 Ma in the Coompana Province and Gawler Craton and at 1590–1550 Ma in the Musgrave Province. In this scenario, Krackatinny Supersuite magmatism might be related to a subduction zone that extended between the West and North Australian Cratons, which would indicate that final amalgamation had not yet occurred. Interpreted collision of the Warumpi Province with the Aileron Province of the Arunta Orogen during the 1640–1630 Ma Liebig Orogeny (Scrimgeour et al., 2005; Scrimgeour, 2013b) could also be compatible with such a setting.

Alternatively, if the Krackatinny Supersuite reflects rifting of previously thickened continental crust in the previously amalgamated West and North Australian Cratons, the relationships between areas active at 1590–1550 Ma would be more complex. Most previous interpretations of the 1590–1550 Ma period infer a high angle between the east–west trending southern margin of the North Australian Craton and the north-northeasterly trending eastern margin of the West Australian Craton (Betts et al., 2002; Giles et al., 2004; Betts and Giles, 2006; Betts et al., 2008; Swain et al., 2008; Wade et al., 2008; Payne et al., 2009; Huston et al., 2012; Johnson, 2013). This configuration is constrained by the assumption that the West and North Australian Cratons had collided by c. 1760 Ma and would appear to require an active (dominantly strike-slip?) boundary to the east of the Albany–Fraser Orogen at 1590–1550 Ma, if subduction in central and southeastern Proterozoic Australia continued through this period.

Given the uncertainties, it is difficult to confidently determine the tectonic setting of the Rudall Province during this period but intraplate rifting of thickened crust and subduction-related magmatism both remain plausible alternatives. Both options are thus considered when evaluating the geological history of the region, and as discussed later, the two different possibilities each have significantly different implications for the Proterozoic assembly of Australia and the mineral prospectivity of the region.

1330–1285 Ma regional geodynamic setting

It is notable that during the 1330–1285 Ma period various parts of the West Australian Craton experienced significant deformation and magmatism whereas little tectonism is known from the North and South Australian Cratons (Figs 65, 69; Table 7). Tectonism occurred along the margins of the West Australian Craton in the Albany–Fraser Orogen and the Rudall Province, as well as along

major intraplate structures in the Capricorn Orogen. The only known deformation at this time outside the West Australian Craton is magmatism in the western Musgrave Province and intraplate alkaline mafic magmatism in the North Australian Craton.

In the eastern Pilbara Craton, a felsic tuff dated at 1317 ± 11 Ma constrains the deposition of sedimentary rocks assigned to the lower part of the Manganese Group (Blake et al., 2011; Jones, 2011). Similarly aged tuffs from the base of a siliciclastic metasedimentary succession overlying the northeastern Pilbara Craton have been dated at 1318 ± 7 and 1310 ± 8 Ma by Sheppard et al. (2016). This defines a belt of intraplate felsic magmatism and siliciclastic sedimentation parallel to the margin of the Pilbara Craton, termed the Wongawobbin Basin by Sheppard et al. (2016), which they considered to have been generated by far-field effects of convergent tectonism in the Albany–Fraser Orogen.

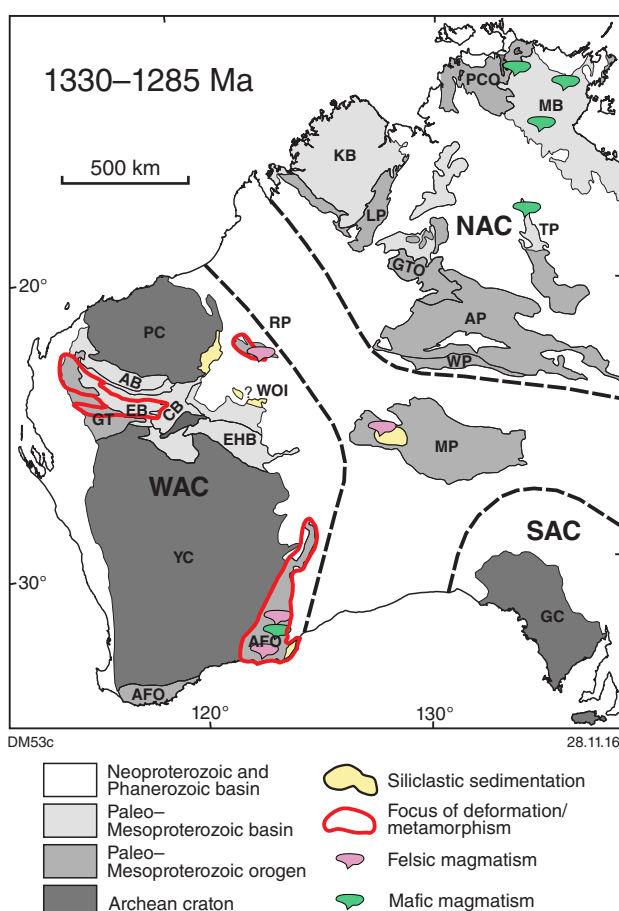


Figure 69. Tectonism at 1330–1285 Ma in the western and central parts of Australia (current geographic positions). AB – Ashburton Basin; AFO – Albany–Fraser Orogen; AP – Aileron Province; BB – Birrindudu Basin; CB – Collier Basin; EB – Edmund Basin; EHB – Earaheedy Basin; GC – Gawler Craton; GT – Glenburgh Terrane; GTO – Granites–Tanami Orogen; KB – Kimberley Basin; LP – Lamboo Province; MB – McArthur Basin; MP – Musgrave Province; PC – Pilbara Craton; PCO – Pine Creek Orogen; RP – Rudall Province; TP – Tomkinson Province; YC – Yilgarn Craton; WP – Warumpi Province

Table 7. Summary of 1330–1285 Ma tectono-thermal events in western and central Australia

Geological domain	Event	Metamorphism	Structure	Magmatism	Sedimentation	Interpreted setting(s)	References
South-east Pilbara Craton	Manganese Group sedimentation	–	–	Minor felsic extrusive (c. 1317 Ma)	Shallow marine to marine siliciclastic (Manganese Group). Possible siliciclastic in Ward and Oldham Inliers (if not part of 1170–1070 Ma Collier Basin)	Manganese Group thickens towards Rudall Province. NE–SW extension. NW-propagating transgressive events. Intraplate extension; foreland basin?	
Ward and Oldham Inliers	Sedimentation	–	–	–	Possible deposition of Coonabie Formation and Cornelia and Oldham Sandstones at this time (maximum ages 1410–1279 Ma)	Deltaic to shallow marine setting; paleocurrents from east and north. Possible 1.3 Ga synorogenic deposition. Alternatively units are correlatives of younger 1170–1070 Ma Collier Basin	Williams (1995); Nelson (2002a, 2005a, 2005b); Bodorkos et al. (2006a); Wingate and Bodorkos (2007)
Capricorn Orogen (Gascoyne Province and Edmund Basin)	Mutherbukin Tectonic Event (1321–1171 Ma)	Moderate-P; moderate-T	Dextral transposition on ESE-trending structures	–	–	Prolonged intraplate orogen; possible heat contribution from high heat-producing basement	Johnson et al. (2011b); Korhonen et al. (2015)
Albany–Fraser Orogen	Abany–Fraser Orogeny Stage I (1330–1260 Ma)	Moderate- to high-P; high-T	Folding and thrusting	Voluminous felsic intrusive (1330–1280 Ma Recherche Supersuite); mafic intrusive (1305–1290 Ma Fraser Suite)	Termination of Arid Basin sedimentation at start of orogeny; Ragged Basin sedimentation syn- to post-orogeny	Convergent plate margin; early accretion of arc; magmatism during later extension (relaxation/delamination?)	Clark et al. (2000); Bodorkos and Clark (2004); Oorschot (2011); Adams (2012); Spaggiari et al. (2014a, 2014b, 2015a); Waddell et al. (2015)
Western Musgrave Province	Mount West Orogeny (1345–1293 Ma)	?	?	Arc-like felsic intrusive (1345–1295 Ma Wankanki Supersuite) and extrusive (1340–1270 Ma Wirku Metamorphics)	Felsic volcanoclastic	Continental arc favoured, but inherited arc signature also possible	Howard et al. (2011b, 2015); Smithies et al. (2010, 2011); Evins et al. (2012)
North Australia (McArthur Basin, Pine Creek Orogen and Tomkinson Province)	Alkaline mafic magmatism	–	–	Alkaline mafic intrusive (1324 ± 4 Ma Derim Derim Dolerite, 1325 ± 36 Ma Galiwinku Dolerite, 1316 ± 40 Ma phonolite, 1295 ± 14 Ma alkali gabbro sill)	–	Intraplate; possible 1325–1295 Ma large igneous province following last phase of McArthur Basin	Page et al. (1980); Abbott et al. (2001); Melville (2010); Whelan et al. (2016)

In the Ward and Oldham Inliers, about 200 km to the south of the Rudall Province, siliciclastic sedimentary rocks have yielded imprecise maximum depositional ages of 1410–1279 Ma (Nelson, 2002a, 2005a, 2005b; Bodorkos et al., 2006a; Wingate and Bodorkos, 2007). These units consist of quartz-rich and micaceous sandstone, with some pebbly lenses, as well as minor shale and siltstone deposited in a deltaic to shallow-marine setting, with paleocurrent directions indicating sources to the east and north (Williams, 1995; Nelson, 2005a). The younger detrital zircon ages are similar to igneous and metamorphic events in the Rudall Province, and suggest that the belt of late Mesoproterozoic tectonism extended further southeast than the currently exposed area. These units are intruded by dolerite sills thought to be correlatives of c. 1070 Ma Warakurna Supersuite intrusions in the Edmund and Collier Basins farther to the west (Wingate, 2002) and have been deformed by northwesterly trending open folds that pre-date deposition of the Neoproterozoic Savory Group (Williams, 1995). The relatively broad constraints allow for deposition of these units as either syn- to post-orogenic sediments during the 1330–1290 Ma event or correlatives of the younger (1170–1070 Ma) Collier Basin and thus unrelated to this deformation.

In the Capricorn Orogen, this period coincides with the 1321–1271 Ma Mutherbukin Tectonic Event, which affected the Gascoyne Province and Edmund Basin (Johnson et al., 2011a; Korhonen et al., 2015; Cutten et al., 2016). Dextral transpression on east-southeasterly trending structures resulted in crustal thickening and metamorphism at moderate temperatures and pressures (Korhonen et al., 2015). Deformation was not accompanied by significant magmatism but the thermal effects of this tectonism were long-lived, extending to c. 1210 Ma (Korhonen et al., 2015).

In the Albany–Fraser Orogen, the 1330–1260 Ma Stage 1 of the Albany–Fraser Orogeny was associated with felsic and mafic magmatism, deformation and metamorphism (Clark et al., 2000; Bodorkos and Clark, 2004; Spaggiari et al., 2014a,b, 2015a). The onset of tectonism broadly coincides with the termination of sedimentation in the Arid Basin, which is interpreted to have been initiated as a marginal basin on the passive margin of the West Australian Craton after c. 1600 Ma, and which later evolved into a foreland basin related to the encroachment of the c. 1410 Ma Loongana oceanic arc (Spaggiari et al., 2015a). The earliest stages of tectonism are interpreted to reflect initial accretion of the Loongana arc, with subsequent magmatism occurring within an extensional setting, possibly as a result of relaxation and delamination (Spaggiari et al., 2015a, 2015b). Sedimentation in the <1310 Ma Ragged Basin commenced during or after the later stages of Stage 1 tectonism and appears to reflect an extensional intraplate basin developed over the orogen (Waddell et al., 2015).

Away from the West Australian Craton, the 1345–1293 Ma Mount West Orogeny affected the western part of the Musgrave Province, resulting in the emplacement of granitic rocks, mostly at 1326–1312 Ma, in an interpreted continental arc setting (Smithies et al., 2010, 2011; Howard et al., 2011b, 2015). The granitic rocks were essentially coeval with the deposition of volcanoclastic

and volcanic rocks at 1340–1270 Ma (Evins et al., 2012). In the northern part of the North Australian Craton, 1324 ± 4 Ma alkaline mafic rocks were emplaced into the basal parts of the McArthur Basin (Abbott et al., 2001) and as a radiating dyke swarm at 1325 ± 36 Ma (Whelan et al., 2016). These dates are similar to a 1316 ± 40 Ma Rb–Sr date for peralkaline phonolitic rocks in the Pine Creek Orogen (Page et al., 1980) and a 1295 ± 14 Ma alkali gabbro sill in the Tomkinson Province in central Australia (Melville, 2010), suggesting these rocks might form part of a 1325–1295 Ma large igneous province following the last phase of sedimentation in the McArthur Basin (Whelan et al., 2016).

The similar ages of tectonism in disparate parts of the West Australian Craton suggest that all these events could have had a common driver. The focusing of tectonism along the northeastern and southeastern margins of the craton, as well as reactivation of a suture in the central part of the craton, may indicate relative motion of the West Australian Craton with respect to the other elements of Mesoproterozoic Australia. If final docking of the West and North Australian Cratons had occurred before c. 1330 Ma, the tectonism in the Rudall Province would represent intraplate reworking near the suture between the two cratons, similar to that of the Mutherbukin Event in the Capricorn Orogen. If, however, the northeastern margin of the craton had remained open to this point, as might have been the case if the Krackatinny Supersuite was emplaced in plate margin setting, deformation could reflect collision of the West and North Australian Cratons. The origin of the 1325–1295 Ma alkaline mafic magmatism in the North Australian Craton is not known but the timing suggests a possible connection with orogenic events in the West Australian Craton and a significant change in geodynamics following the cessation of sedimentation in the greater McArthur Basin.

If the Yapungku Orogeny occurred at 1330–1285 Ma, shortening at this time was south-southwesterly directed, based on the orientation of D_2 folds and thrusts in the Rudall Province. This stress field would be broadly consistent with that in the Capricorn Orogen during the Mutherbukin Event, where west-northwesterly trending faults were reactivated in a dextral transpressional setting. A collisional setting for this event would be consistent with the nature of deformation and metamorphism (possibly high-P), the emplacement of leucogranites and the deposition of synorogenic sedimentary rocks along a belt parallel to the orogen, although it is also consistent with compressional intraplate reworking. The tectonism at 1330–1285 Ma is the last high-grade metamorphic event known to affect the northeastern margin of the West Australian Craton before deposition of c. 850 Ma sedimentary rocks of the Yeneena Basin as part of the Centralian Superbasin, which was deposited across all the cratonic elements of Australia (Walter et al., 1995). The 1330–1285 Ma event would thus appear to represent the latest possible timing for amalgamation of the West and North Australian Cratons. It is interesting to note that a Mesoproterozoic age for collision is the same as that proposed by Myers et al. (1996), an interpretation that was not favoured after the interpretation of a Paleoproterozoic amalgamation became widely accepted.

One possible difficulty with a collision at 1330–1285 Ma is the apparently near-synchronous initiation of tectonism across the West Australian Craton at c. 1330 Ma. A collisional event along the eastern margin of the craton might be expected to be somewhat diachronous as a result of oblique convergence or irregularities in the shape of the opposing plate margin. Intraplate reworking, in contrast, might be expected to respond relatively quickly to plate margin events, with stresses propagated rapidly across the craton. Currently, there are insufficient geochronological data, particularly in the Rudall Province, to more precisely constrain any potential diachroneity, and a more detailed assessment of this aspect requires further work. Another potential difficulty with a collision at c. 1330 Ma is that the 1589–1549 Ma granitic rocks exposed in the Tabletop Terrane did not experience the same pervasive deformation and high-grade metamorphism as rocks of the Talbot and Connaughton Terranes. Although zones of high strain are not uncommon in the Tabletop Terrane, the exposed felsic and mafic rocks have not been pervasively deformed and metamorphosed to the degree observed to the southwest of the Camel–Tabletop Fault Zone, and no geochronological evidence for a c. 1330 Ma metamorphic event has yet been found in the Tabletop Terrane. If the margin of the West Australian Craton was to the northeast of the Rudall Province, as indicated by geochronological and isotope data, then it might be expected that the most intense deformation would occur along the margin of the craton. One possible explanation for the differences in metamorphic grade and deformation across the Camel–Tabletop Fault Zone is significant Neoproterozoic movement along this structure, juxtaposing blocks that were at different crustal levels during the Yapungku Orogeny.

Paleomagnetic constraints on craton assembly

Several studies have sought to constrain the timing of amalgamation of Proterozoic Australia by comparing the paleopoles of different cratons for similar times, or by identifying periods when the apparent polar wander paths for different cratons show similarities, implying coherent movement and prior amalgamation (Li, 2000; Wingate and Evans, 2003; Schmidt et al., 2006). Although paleomagnetic data have the potential to be a key constraint on the timing of craton assembly, the dataset for the Australian Precambrian is relatively sparse, despite segments of the apparent polar wander path being relatively well constrained for a few crustal elements (Schmidt, 2014). Interpretations based on this technique are hampered by difficulties in assigning ages to paleopoles, particularly where poles are based on secondary overprints or where the primary age of a rock is not known with confidence. Notwithstanding these limitations, it is worthwhile evaluating the constraints provided by paleomagnetic data, particularly as some workers have proposed a Paleoproterozoic minimum age for collision of the West and North Australian Cratons using these data (Li, 2000).

Li (2000) suggested that amalgamation of the West and North Australian Cratons was complete by 1.7 Ga, based on the similarity of paleopoles obtained from the Kimberley, McArthur and Hamersley Basins. However, ages of some of these paleopoles are not well constrained. The assumed 1.7 Ga age for magnetization of the Elgee Siltstone in the Kimberley Basin was based on xenotime dates from other units within the basin but Schmidt and Williams (2008) suggested that the actual age of magnetization is more likely to be close to the c. 1790 Ma depositional age of these rocks (Schmidt and Williams, 2008; Hollis et al., 2014). More significantly, an inferred 1.7 Ga age for overprint magnetizations in the Hamersley Basin was based on the interpretation that this event occurred after the last major folding event, which was assigned to the 1817–1772 Ma Capricorn Orogeny by Li (2000), with the paleopole considered to be developed in the last stages of this deformation, interpreted as 1.7 Ga. Recent work, including a better understanding of the timing of tectonism in the Capricorn Orogen, suggests other interpretations are possible. Schmidt (2014) assigned a 2.2 Ga (i.e. Ophthalmia Orogeny) age to paleopoles from the Hamersley Province, noting that pre- to synfolding paleopoles are similar to post-folding paleopoles, and suggested that both formed during the 2.2 Ga event. The currently available evidence thus suggests that the paleopoles used to constrain an interpreted pre-1.7 Ga collision might not be coeval, and might thus not constrain the age of craton assembly.

Li and Evans (2011) noted that apparently coeval paleopoles in northern and southern Australia showed systematic differences at 1.8, 1.07 and 0.75 Ga that can be brought into approximate alignment with a major (40°) clockwise rotation of southern Australia relative to northern Australia after 0.75 Ga. An arcuate northwesterly to easterly trending corridor of 650–550 Ma deformation linking the Paterson Orogen and the Musgrave Province was suggested as the major zone of dislocation along which this rotation took place. If correct, the paleopoles discussed by Li and Evans (2011) might then be consistent with amalgamation of the West and North Australian Cratons at 1.8 Ga. Although this model resolves angular differences between paleopole groups, there are complications associated with the assumed timings of paleopoles comprising the 1.8 Ga group. The relevance of the Frere Formation pole for the West Australian Craton is reduced by recent dating which indicates that this unit was deposited at c. 1.88 Ga (Rasmussen et al., 2012), 80–90 Ma earlier than the inferred age of the Kimberley paleopoles for the North Australian Craton. Also, as noted above, the age of the Hamersley Basin paleopoles is not certain to be 1.8 Ga, and might instead be 2.2 Ga. Another complication with the rotational model is a lack of offset of pre-650 Ma units across the proposed zone of dislocation. In the Musgrave Province, igneous rocks of the 1220–1120 Ma Pitjantjatjara and 1085–1040 Ma Warakurna Supersuites as well as sedimentary and volcanic rocks of the 1080–1040 Ma Bentley Supergroup occur on both sides of, and within, the interpreted zone of dislocation (Howard et al., 2011a; Close, 2013). Mafic dykes of the c. 825 Ma Gairdner Dolerite form a relatively

coherent northwesterly trending swarm extending from southern South Australia, through the Musgrave Province, and probably farther to the northwest (Pirajno and Hoatson, 2012), and do not appear to be offset by a continental-scale strike-slip structure. These observations indicate that it is difficult to interpret that the North and West Australian Cratons had similar paleopoles at 1.8 Ga based on the available paleomagnetic data and geological constraints.

Wingate and Evans (2003) discussed paleomagnetic data that suggest the West and North Australian Cratons were assembled by 1360–1320 Ma, based on paleopoles from the Morawa Lavas in the western Yilgarn Craton, which were assigned a preliminary date of c. 1360 Ma (Idnurm and Giddings, 1988), and a paleopole for the Roper Group of the McArthur Basin, interpreted to be due to intrusion of c. 1320 Ma dolerite. This is consistent with most models, which consider that final assembly occurred before this time, although there are uncertainties associated with the interpreted ages of these paleopoles as well, with no reliable ages of eruption or magnetization for the Morawa Lavas.

It is thus apparent that the paucity of reliably dated paleopoles for the 1.8 – 1.3 Ga period makes it difficult to determine the time of amalgamation of the West and North Australian Cratons using paleomagnetic techniques. Previous studies that interpreted collision by 1.8 – 1.7 Ga were limited by a lack of robustly time-constrained data points, and the timing of collision remains an open question.

Nature of the Anketell Regional Gravity Ridge

The affinity between the Rudall Province terranes and the West Australian Craton, as indicated by detrital zircon ages and the Lu–Hf isotope characteristics of zircon (Kirkland et al., 2013b), suggests that the Camel–Tabletop Fault Zone was not a suture zone, implying that any suture present would be farther to the northeast. Nevertheless, as noted above, there are significant differences between aspects of the geology of the Tabletop Terrane and the rest of the Rudall Province that suggest the Camel–Tabletop Fault is a major structure that has undergone significant movement. The differences across the fault are also reflected in gravity images that show the Tabletop Terrane has a higher average value than the Talbot and Connaughton Terranes (Fig. 70), although local variations in the proportions of mafic and felsic rocks complicate the pattern. The gravity high coinciding with the Tabletop Terrane forms a linear zone extending northwest to the coast and offshore along the axis of the Paterson Orogen, and southeast to the Musgrave Province, where it coincides with the exhumed core of the Petermann Orogen (Fig. 70). This gravity feature has been termed the Anketell Regional Gravity Ridge (Fraser, 1976), and extends for ~2000 km, if the gravity ridge in central Australia is included as part of this feature.

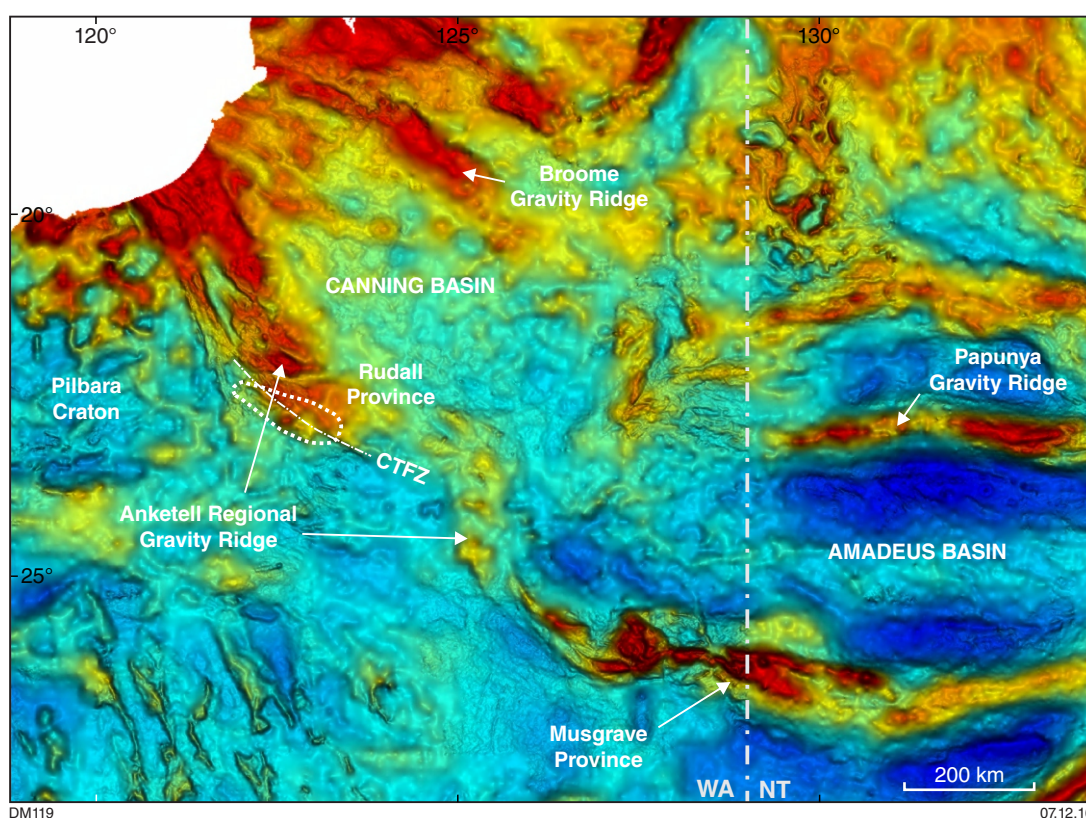


Figure 70. Bouguer gravity image of the Paterson and Petermann Orogens, showing the location of the Anketell Gravity Ridge, which appears to trace the locus of Neoproterozoic deformation. Data extracted from Geoscience Australia national gravity database (Wynne and Bacchin, 2009)

In the northwestern Paterson Orogen, the margins of the Anketell Regional Gravity Ridge are in part delineated by the effects of differential subsidence associated with graben formation during development of the Phanerozoic Canning Basin. In this area, the gravity ridge coincides with an elongate zone of outcropping to shallowly covered Paleoproterozoic to Neoproterozoic ‘basement’ rocks that are bound to the northeast by thicker sedimentary rocks of the Canning Basin and to the west by granite-dominated crust of the Pilbara Craton. Basement uplift and associated crustal thickening appears to be related to Neoproterozoic tectonism, which affects basement rocks where exposed along the gravity ridge. In the Rudall Province, the gravity ridge coincides, in a broad sense, with the zone of Paleoproterozoic to Neoproterozoic rocks affected by the Miles and Paterson Orogenies to the east of the Pilbara Craton, which was not significantly affected by these events. The generally lower gravity signature of the Talbot and Connaughton Terranes suggests that at least part of the gravity signature might also be due to lithological or structural variations across the Camel–Tabletop Fault Zone and it is possible that the widespread outcrops of amphibolite in the Tabletop Terrane are indicative of a significant mafic component to the northeast of the fault. In the Musgrave Province, the gravity ridge coincides with the exhumed core of the 580–530 Ma Petermann Orogen, with a significant offset of the mantle modelled in the core of a transpressional flower structure (Aitken et al., 2009). The highest gravity values within the core of the orogen occur in areas of mafic and ultramafic intrusive rocks of the 1080–1050 Ma Giles Complex, which broadly coincide with the zone of Neoproterozoic deformation. Recent dates of 630–625 Ma obtained for metamorphic zircon and muscovite as well as pegmatite from the western part of the Musgrave Province (Kirkland et al., 2011b, 2013c, 2014a,b) indicate that this belt was also active at a similar time to the Miles Orogeny in the Paterson Province.

The Anketell Regional Gravity Ridge thus appears to correspond to a Neoproterozoic continental-scale zone of transpressional to compressional deformation (Bagas, 2004), with similar deformation likely to have affected unexposed segments of the gravity ridge covered by younger sedimentary basins. Given the scale of this feature, it is possible that deformation and magmatism was partitioned into pre-existing boundaries between major crustal elements. One possibility is that this gravity ridge approximately defines the northeastern margin of the West Australian Craton. The area to the northeast of the gravity ridge beneath the Canning Basin has a relatively uniform character in gravity imagery and this domain is bound in turn by the northwesterly trending Broome Gravity Ridge, 300–350 km to the northeast. The nature of the basement in the crustal element beneath the southwestern Canning Basin is largely unknown, but could represent part of the North Australian Craton or an intervening crustal block between the West and North Australian Cratons (Bagas, 2004), perhaps similar to that of the Warumpi Province of the Arunta Orogen, which is thought to underlie much of the Amadeus Basin. If the margin of the West Australian Craton broadly coincides with the Anketell Regional Gravity Ridge, the magmatism of the Krackatinny Supersuite might reflect arc magmatism near this margin or extensional reactivation of an earlier major structure.

Geodynamic evolution of the Rudall Province — plausible alternatives

In the above discussions regarding the possible geological evolution of the Rudall Province, two distinctly different models for the geodynamic evolution of the Rudall Province emerge. The first involves early amalgamation of the West and North Australian Cratons at 1800–1760 Ma in line with previous interpretations (Hickman and Bagas, 1999; Bagas, 2004). The second involves later amalgamation, possibly as late as c. 1300 Ma. These scenarios are not the only interpretations possible but they form ‘end-members’ of possible timings for the amalgamation of the West and North Australian Cratons, and underscore the point that the widely accepted 1800–1760 Ma collisional event is not the only possible way to interpret the available data. In both scenarios, the moderate- to high-pressure metamorphism of the Yapungku Orogeny is taken to reflect the collision of the West and North Australian Cratons for the sake of simplicity although as noted previously this need not necessarily be the case.

Scenario 1: ‘early’ amalgamation

This scenario involves amalgamation of the West and North Australian Cratons from 1800–1760 Ma. This requires that high-P metamorphism and deformation occurred during or shortly after emplacement of the Kalkan Supersuite, and that the Fingoon Quartzite was deposited as part of a syntectonic sedimentary succession. In this scenario, all younger events would represent episodes of intraplate reworking, either extensional or compressional in nature. Aspects of the geology that might be inconsistent with this interpretation or that could be interpreted in different ways include: the consistent overprint of 1800–1765 Ma igneous rocks by fabrics assigned to the Yapungku Orogeny; the possibility that sedimentary rocks considered to be affected by the Yapungku Orogeny were deposited after 1760 Ma; an apparent paucity of metamorphic zircon of this age; and the possibility that mafic and felsic magmatism in the Tabletop Terrane was emplaced in a continental margin setting at 1589–1549 Ma.

Scenario 2: ‘late’ amalgamation

This scenario assumes a 1330–1290 Ma age for the Yapungku Orogeny and amalgamation with the North Australian Craton or an intervening crustal element. This interpretation suggests that 1800–1760 Ma magmatism, low-P metamorphism, and possibly basin development might be a consequence of dominantly extensional conditions established near the margin of the West Australian Craton, although conceivably within an overall convergent setting. In this scenario, magmatism of the Krackatinny Supersuite might reflect the development of a continental arc or back-arc at 1590–1550 Ma, representing the northwestern part of a zone of

convergence between northern and southern Australia that extended through central Australia to the Gawler Craton. Final amalgamation in this scenario took place at 1330–1290 Ma as the West Australian Craton docked with a combined North and South Australian Craton. This scenario is consistent with widespread evidence of tectonism along the northeastern and southeastern margins of the West Australian Craton at 1330–1290 Ma, as well as along major intraplate structures. Broadly coeval sedimentation in the eastern Pilbara Craton, and possibly also to the south of the Rudall Province, appears to reflect synorogenic sedimentation inboard of the orogen. Interpreted accretion of an oceanic arc in the Albany–Fraser Orogen at this time suggests that amalgamation could not have been a result of continent–continent collision along the entire eastern margin of the West Australian Craton, as oceanic crust is interpreted to have been preserved between the West and South Australian Cratons within the Madura Province.

Aspects of the geology that might be difficult to resolve in this scenario include: the apparently near-synchronous timing of the onset of deformation at c. 1330 Ma along the craton margin; the lack of a high-grade 1330–1290 Ma event in the Tabletop Terrane or voluminous magmatism of this age; and the possibility that the Krackatinny Supersuite was not related to subduction but intraplate rifting of previously thickened crust, possibly as a result of a prior collision.

In this study, a post-1760 Ma amalgamation of the West and North Australian Cratons is tentatively favoured. Although this was conceivably as late as c. 1330 Ma, a late Paleoproterozoic age is also possible, given the lack of pervasive high-grade reworking of the 1589–1549 Ma Krackatinny Supersuite.

It is apparent that none of the scenarios as proposed account for all the currently available evidence, which highlights the need for further data collection and model testing. In particular, further dating of metamorphism using zircon and monazite would be important to more precisely establish the timing of the main tectonic events. Detailed work to link these events with specific metamorphic mineral assemblages and structures is also important to constrain the nature of these events. Additionally, a better understanding of the spatial distribution of tectonism of different ages may help discriminate between pervasive events and those related to more partitioned movement along major structures. Further dating of detrital zircon from metasedimentary units in the province is also needed to better constrain the depositional ages of the protoliths, which will also provide information about the nature and timing of tectonism. Additional work is required to more fully characterize the geochemical and isotope characteristics of the various granitic suites of the Rudall Province. Similarly, further study of the geochemistry and age of the widespread mafic rocks in the Tabletop Terrane is warranted, since the limited geochemical data for these rocks suggest emplacement in an arc setting. Direct dating of these rocks might prove difficult due to their generally low Zr content but targeting of more fractionated units might prove worthwhile.

Implications for mineral systems

There are numerous mineral occurrences within the Rudall Province, with the most significant of these to date being the Kintyre unconformity-related U deposit in the northwestern part of the province (Fig. 3; Ferguson et al., 2005; Huston et al., 2010). Many occurrences of hydrothermal veining in reducing units of the Talbot and Connaughton Terranes have been identified, containing U in association with a variety of metals, including Au, Ag, Pb, Zn, Cu, Ni, Co, Bi, W and PGE, and may be variants of the unconformity-related U style (Ferguson et al., 2005). In the Tabletop Terrane there are fewer known mineral occurrences, to some degree due to the extensive sediment cover, with shear-hosted Cu–Ag–Au–Pt–Pd mineralization at the Copper Hills prospects having experienced the most exploration activity.

If the West and North Australian Cratons amalgamated after c. 1760 Ma, then the Rudall Province potentially remained close to a plate margin for longer than previously thought and might thus have unrecognized potential for Paleoproterozoic to Mesoproterozoic plate margin mineral systems. In particular, the Tabletop Terrane might have potential for porphyry-style mineralization if the Krackatinny Supersuite and older mafic rocks were indeed emplaced in a magmatic arc setting. Conversely, if the Krackatinny Supersuite was relatively anhydrous and emplaced within an intraplate rift setting distant from a plate margin, there would be a low potential for porphyry-style mineralization of this age. The Tabletop Terrane is generally poorly exposed but regional aeromagnetic and airborne electromagnetic data (Roach et al., 2010) indicate that the unconsolidated sediment cover is relatively thin across much of the Tabletop Terrane, meaning that much of the area is accessible for mineral exploration.

In assessing the potential for porphyry Cu–Au and related styles of mineralization in the case of a continental arc scenario, the source(s) of the Krackatinny Supersuite magmas are an important control on fertility, as is the water content of the magmas as a means to transport metals and focus their deposition. The geochemical compositions of the sodic components of the Krackatinny Supersuite are consistent with derivation from dominantly mafic sources, with the more potassic components involving a higher contribution of more felsic crust. This suggests the more sodic variants might have a higher Cu–Au prospectivity than the potassic variants. In the samples analysed, there is a general absence of elevated Ni and Cr values that would indicate the magmas were sourced from, or interacted with, a mantle wedge and a dominantly lower crustal mafic source is inferred, consistent with the relatively evolved Sm–Nd isotope signature of the Krackatinny Supersuite. A sample of the high Sr/Y sodic component of the Krackatinny Supersuite yielded a particularly evolved isotope signature and, if derived from a dominantly mafic source at >35 km depth as implied by its geochemical signature, might reflect partial melting of an older (Archean?) mafic underplate rather than subducted juvenile oceanic crust. The water contents of magmas derived from such a postulated mafic

underplate are likely to have an important control on Cu–Au fertility. An old, anhydrous mafic underplate that experienced dehydration melting in an intraplate setting is not sufficiently hydrous (<7 wt% H₂O) to generate significant porphyry-style mineralization (Lu et al., 2015). Fluid-fluxed melting of lower crustal mafic rocks in an arc- or post-collisional extensional setting could, however, produce relatively hydrous magmas that might be more prospective (>10 wt% H₂O; Lu et al., 2015). Further work aimed at understanding the hydration state and geodynamic setting of the Krackatinny Supersuite is thus an important requirement to better understand the prospectivity of the Tabletop Terrane.

Geochemical criteria have been proposed as a means to assess the potential fertility of arc magmas for porphyry-style Cu–Au mineralization (Loucks, 2014). This is based on the observation that certain trace elements show enrichments or depletions in Phanerozoic arc magmas associated with Cu–Au deposits compared with arc magmas not associated with porphyry Cu–Au mineralization. In particular, magmatic rocks with Sr/Y >35 and V/Sc >(32.5 – 0.385 × wt% SiO₂) show an association with mineralization. This has been attributed to hornblende fractionation and the suppression of plagioclase and magnetite crystallization by high H₂O contents (Loucks, 2014). Some samples of the high Sr/Y sodic series of the Krackatinny Supersuite satisfy these criteria, with two analyses (GSWA 124737 and 124894) having V/Sc of 14.1 and 10.2, higher than the threshold value of 10 noted for unambiguously prospective Phanerozoic arc rocks (Loucks, 2014). The application of such fertility indicators to a poorly understood Mesoproterozoic magmatic suite does require caution, however, particularly as it is not certain whether the Krackatinny Supersuite is arc-related. High Sr/Y and V/Sc values by themselves are not sufficient to determine Cu–Au fertility, and other processes can result in similar values, e.g. high Sr/Y values caused by partial melting at depths >35 km (Lu et al., 2015). Nevertheless, it is worth noting that some of the components of the Krackatinny Supersuite satisfy some of the criteria used to assess fertility.

The water content of fractionating magmas can also be assessed by evaluating normalized REE patterns. Arc magmas with a high water content will crystallize amphibole ± garnet in lower crustal MASH zones, and thus develop listric or concave-shaped REE patterns, compared with the more linear REE patterns formed when garnet is the main fractionating or residual phase, since hornblende tends to incorporate a higher proportion of MREE than garnet (Richards and Kerrich, 2007; Alonzo-Perez et al., 2009; Richards, 2011). In the high Sr/Y sodic components of the Krackatinny Supersuite, the mantle-normalized REE patterns are not particularly diagnostic, with patterns that range between steep linear and concave in form (Fig. 58). Normalized Dy/Yb ratios (a measure of the steepness of the MREE to HREE segment) are >1 for all but two samples, but Dy/Yb shows no correlation with SiO₂, as might be expected with progressive hornblende removal during fractionation.

Instead, Dy/Yb increases with decreasing Mg#, P₂O₅, and with increasing Rb, suggesting that MREE–HREE patterns become steeper with compositional evolution, more consistent with increased garnet-control on lower fraction partial melts and opposite to the trends expected for hornblende fractionation. However, it should be noted that the geochemical dataset for the Krackatinny Supersuite is relatively limited and that the high Sr/Y sodic series analyses effectively relate to a single intrusion or intrusive complex. Further data are required to better constrain the nature of the Krackatinny Supersuite and its potential fertility, particularly for granitic rocks beneath the extensive shallow cover for which there are currently no analyses.

The limited whole-rock geochemistry obtained in this study for the greenschist to lower amphibolite facies mafic rocks of the Tabletop Terrane suggests that at least some of these might have formed in a subduction setting. Although a more comprehensive geochemical and isotope dataset is required to confirm this, this could also indicate some potential for plate margin-related mineral systems associated with this event, the age of which is currently very poorly constrained.

In the context of potential porphyry-style mineral systems, the present level of erosion in the Tabletop Terrane is also an important consideration. There is an apparent lack of 1.59 – 1.55 Ga supracrustal rocks in the Tabletop Terrane, such as volcanic or volcanoclastic units, and no evidence of shallow-level emplacement textures have been observed in exposed granitic rocks, suggesting that the highest crustal levels might have been removed by later uplift and erosion. This has the potential to have removed any epithermal or shallow-level porphyry mineralization. However, it should be noted that the ‘adakitic’ body dated in this study might have had only the uppermost part of the intrusion removed by erosion, with the remainder of the body possibly present below the margins of the exposed body, where granitic dykes are abundant. This suggests that some granitic rocks might not be too deeply eroded to preserve their potentially more prospective apical parts. It is also worth noting that the lack of outcrop in the Tabletop Terrane means that there is potential for substantial variations in compositions and exposure level across the area, and zones of higher magnetization might also indicate areas of differing granite or basement compositions.

Conclusions

Geochronological and geochemical data collected in this study, coupled with a re-assessment of previous geochronological data and field relationships, provide a number of constraints on the geological evolution of the Rudall Province, although many important aspects remain poorly understood. Quartzites that might represent parts of the oldest successions in the province yield maximum depositional ages of c. 2833 Ma in the Tabletop Terrane and c. 2284 Ma in the Connaughton Terrane, and have age spectra consistent with sources in the

Pilbara Craton or overlying Archean basins, supporting previous interpretations that the Rudall Province is not an exotic terrane. The apparent absence of Neoproterozoic zircons in quartzite from the Tabletop Terrane suggests it could be Archean in age and a possible correlative of the Fortescue Group, which could represent the first recognition of Archean rocks in the Rudall Province. An essentially unimodal age spectra at c. 1794 Ma obtained from the Fingoon Quartzite in the Talbot Terrane is similar to a previously obtained spectra obtained from this unit and is interpreted to have been derived from a local granitic source during or after emplacement of the 1804–1762 Ma Kalkan Supersuite. Unimodal zircon dates at c. 1780 and 1760 Ma obtained from quartz–feldspar–muscovite schist and gneiss in the Talbot Terrane might also represent part of a metasedimentary cover succession, although these dates can alternatively be interpreted as the magmatic ages of deformed igneous rocks.

Dating of granitic rocks from the Tabletop Terrane has revealed the presence of voluminous 1589–1549 Ma magmatism, distinct from previous dates of c. 1476 and 1310 Ma obtained for other granitic rocks in the area. The 1589–1549 Ma granitic rocks have been assigned to the Krackatinny Supersuite, and can be further subdivided into three series based on their geochemistry: a high Sr/Y sodic (adakitic) series; a low Sr/Y sodic series; and a high-K series. The geochemical characteristics of the Krackatinny Supersuite are able to be interpreted within a continental arc setting, involving early adakitic magmatism at c. 1589 Ma, progressing to younger shallower melting and greater crustal involvement towards the end of magmatism at c. 1549 Ma. Alternatively, the geochemistry of the Krackatinny Supersuite can also be placed in a continental rift setting, with early partial melting of previously thickened mafic crust, followed by progressively shallower partial melting. The relatively evolved Sm–Nd isotope character of these rocks is indicative of a significant crustal component, which could reflect the presence of an Archean mafic underplate in the source region.

A c. 1296 Ma date for a high-K leucogranite in the Tabletop Terrane is similar to a c. 1310 Ma date obtained from a similar high-K granite and confirms the presence of a Mesoproterozoic magmatic suite, here termed the Camel Suite. The geochemical characteristics of the Camel Suite are similar to both the high-K Krackatinny Supersuite rocks and the 1804–1762 Ma Kalkan Supersuite in the Talbot and Connaughton Terranes, for which dates of c. 1804 and 1781 Ma were obtained in this study. The geochemical characteristics of all three high-K suites are consistent with emplacement in extensional settings, although their broader geodynamic settings are not well constrained by the geochemical data alone.

Deformation and moderate- to high-P metamorphism of the Yapungku Orogeny has long been considered to have

occurred at the same time as emplacement of the Kalkan Supersuite between c. 1804 and 1762 Ma. The younger age limit of a 1778 ± 16 Ma date for an interpreted post-tectonic felsic dyke in the Talbot Terrane has been used as a minimum constraint for this tectonism (Hickman and Bagas, 1999; Bagas, 2004). Reevaluation of the field context of these dykes suggests that the dykes do in fact contain foliations that are similar to those in their host rocks, which have previously been assigned to the Yapungku Orogeny, and do not appear to define a robust minimum age constraint. Attempts to re-date these low Zr dykes did not return appreciable amounts of zircon, raising the possibility that these dykes do not contain significant magmatic zircon and that the previous date reflects the age of xenocrysts. Removal of this constraint means that the Kalkan Supersuite provides only a maximum age for the Yapungku Orogeny, and conceivably might not have been associated with the high-P metamorphism previously interpreted to reflect continental collision. In this scenario, deformation could coincide with one of two episodes of metamorphic zircon formation dated at c. 1680 and 1330 Ma.

Assuming the Yapungku Orogeny reflects a collisional event associated with the amalgamation of the West and North Australian Cratons, the possibility that this event occurred later than previously thought opens up new ways of interpreting the amalgamation of Proterozoic Australia. Two conceptual ‘end-member’ scenarios for the amalgamation of the West and North Australian Cratons are possible. The first scenario involves a collision at 1800–1760 Ma, with deformation continuing after emplacement of the Kalkan Supersuite. This is in line with previous interpretations, and remains a possibility given the relatively permissive geological constraints. The second scenario considers a significantly younger amalgamation with the North Australian Craton or an intervening crustal block. This might have occurred as late as c. 1330 Ma if the Yapungku Orogeny occurred at this time (and was a consequence of collision), and if the Krackatinny Supersuite formed in a continental arc rather than an intraplate rift. One implication of the Rudall Province remaining near an open plate margin for longer than currently thought would be an increased potential for mineral systems such as porphyry Cu–Au in the Tabletop Terrane.

Acknowledgements

Simon Bodorkos (GA) is thanked for his thorough review of the processing of the geochronological data in this report and their interpretation. David Huston (GA) kindly provided a review that substantially improved the manuscript. Fieldwork and geochronology were carried out while the author was an employee of GA.

References

- Abbott, ST, Sweet, IP, Plumb, KA, Young, DN, Cutovinos, A, Ferenczi, PA, Brakel, A and Pietsch, BA 2001, Roper Region: Urupunga and Roper River Special, Northern Territory (2nd edition): Northern Territory Geological Survey and Geoscience Australia (National Geoscience Mapping Accord), 1:250 000 geological map series explanatory notes SD53-10, SD53-11, 100p.
- Adams, M 2012, Structural and geochronological evolution of the Malcolm Gneiss, Nornalup Zone, Albany–Fraser Orogen, Western Australia: Geological Survey of Western Australia, Record 2012/4, 132p.
- Ahmad, M and Hollis, JA 2013, Pine Creek Orogen, *in* Geology and mineral resources of the Northern Territory *compiled by* M Ahmad and TJ Munson: Northern Territory Geological Survey, Darwin, Special Publications 5, p. 5:1–5:133.
- Ahmad, M and Scrimgeour, IR 2013, Geological Framework, *in* Geology and mineral resources of the Northern Territory *compiled by* M Ahmad and TJ Munson: Northern Territory Geological Survey, Darwin, Northern Territory, Special Publication 5, p. 2:1–2:16.
- Ahmad, M, Vandenberg, LC and Wygralak, AS 2013, Tanami Region, *in* Geology and mineral resources of the Northern Territory *compiled by* M Ahmad and TJ Munson: Northern Territory Geological Survey, Darwin, Northern Territory Geological Survey, Special Publication 5, p. 11:1–11:41.
- Aitken, ARA, Betts, PG, Weinberg, RF and Gray, DJ 2009, Constrained potential field modeling of the crustal architecture of the Musgrave Province in central Australia: Evidence for lithospheric strengthening due to crust–mantle boundary uplift: *Journal of Geophysical Research*, v. 114, no. B12, doi:10.1029/2008JB006194.
- Aitken, ARA, Betts, PG, Young, DA, Blankenship, DD, Roberts, JL and Siegert, MJ 2016, The Australo-Antarctic Columbia to Gondwana transition: *Gondwana Research*, v. 29, no. 1, p. 136–152.
- Alonzo-Perez, R, Müntener, O and Ulmer, P 2009, Igneous garnet and amphibole fractionation in the roots of island arcs: experimental constraints on andesitic liquids: *Contributions to Mineralogy and Petrology*, v. 157, p. 541–558.
- Arndt, NT, Nelson, DR, Compston, W, Trendall, AF and Thorne, AM 1991, The age of the Fortescue Group, Hamersley Basin, Western Australia, from ion microprobe zircon U–Pb results: *Australian Journal of Earth Sciences*, v. 38, p. 261–281.
- Bagas, L 1999, Geology of the Blanche-Cronin 1:100 000 sheet: Geological Survey of Western Australia, 1:100 000 Geological Series Explanatory Notes, 16p.
- Bagas, L 2000, Geology of the Paterson 1:100 000 sheet: Geological Survey of Western Australia, 1:100 000 Geological Series Explanatory Notes, 20p.
- Bagas, L 2004, Proterozoic evolution and tectonic setting of the northwest Paterson Orogen, Western Australia: *Precambrian Research*, v. 128, p. 475–496.
- Bagas, L 2005, Geology of the Nullagine 1:100 000 sheet: Geological Survey of Western Australia, 1:100 000 Geological Series Explanatory Notes, 33p.
- Bagas, L, Bierlein, FP, Anderson, JAC and Maas, R 2010, Collision-related granitic magmatism in the Granites–Tanami Orogen: *Precambrian Research*, v. 177, p. 212–226.
- Bagas, L, Bierlein, FP, Bodorkos, S and Nelson, DR 2008, Tectonic setting, evolution, and orogenic gold potential of the late Mesoproterozoic Mosquito Creek Basin, North Pilbara Craton, Western Australia: *Precambrian Research*, v. 160, p. 237–44.
- Bagas, L and Lubieniecki, Z 2001, Copper and associated polymetallic mineralization along the Camel-Tabletop Fault Zone in the Paterson Orogen, Western Australia, *in* Geological Survey of Western Australia Annual Review 1999–2000: Geological Survey of Western Australia, Perth, Western Australia, p. 36–41.
- Bagas, L and Nelson, DR 2005, Provenance of Neoproterozoic sedimentary rocks in the northwest Paterson Orogen, Western Australia, *in* Symposium handbook *edited by* TJ Munson and GJ Ambrose: Northern Territory Geological Survey, Special Publication 2; Central Australian Basins Symposium, Alice Springs, Northern Territory, August 2005, 10p.
- Bagas, L and Smithies, RH 1996, Connaughton, WA Sheet 3452: Geological Survey of Western Australia, 1:100 000 Geological Series.
- Bagas, L and Smithies, RH 1998a, Blanche-Cronin, WA Part Sheets 3551 and 3552: Geological Survey of Western Australia, 1:100 000 Geological Series.
- Bagas, L and Smithies, RH 1998b, Geology of the Connaughton 1:100 000 sheet: Geological Survey of Western Australia, 1:100 000 Geological Series Explanatory Notes, 38p.
- Bagas, L, Williams, IR and Hickman, AH 2000, Rudall, Western Australia (2nd edition): Geological Survey of Western Australia, 1:250 000 Geological Series Explanatory Notes, 50p.
- Betts, PG, Armit, RJ, Stewart, J, Aitken, ARA, Ailleres, L, Donchak, P, Hutton, L, Withnall, I and Giles, D 2016, Australia and Nuna, *in* Supercontinent cycles through Earth history *edited by* ZX Li, DAD Evans and JB Murphy: Geological Society of London, Special Publication 424, p. 47–81.
- Betts, PG and Giles, D 2006, The 1800–1100 Ma tectonic evolution of Australia: *Precambrian Research*, v. 144, p. 92–125.
- Betts, PG, Giles, D, Foden, J, Schaefer, BF, Mark, G, Pankhurst, MJ, Forbes, CJ, Williams, HA, Chalmers, NC and Hills, Q 2009, Mesoproterozoic plume-modified orogenesis in eastern Precambrian Australia: *Tectonics*, v. 28, TC3006.
- Betts, PG, Giles, D, Lister, GS and Frick, LR 2002, Evolution of the Australian Lithosphere: *Australian Journal of Earth Sciences*, v. 49, p. 661–695.
- Betts, PG, Giles, D and Schaefer, BF 2008, Comparing 1800–1600 Ma accretionary and basin processes in Australia and Laurentia: possible geographic connections in Columbia: *Precambrian Research*, v. 166, p. 81–92.
- Betts, PG, Giles, D, Schaefer, BF and Mark, G 2007, 1600–1500 Ma hotspot track in eastern Australia: implications for Mesoproterozoic continental reconstructions: *Terra Nova*, v. 19, p. 496–501.
- Black, LP, Kamo, SL, Williams, IS, Mundil, R, Davis, DW, Korsch, RJ and Foudoulis, CF 2003, The application of SHRIMP to Phanerozoic geochronology: a critical appraisal of for zircon standards: *Chemical Geology*, v. 200, p. 171–188.
- Blake, TS, Buick, R, Brown, SJA and Barley, ME 2004, Geochronology of a Late Archaean flood basalt province in the Pilbara Craton, Australia: constraints on basin evolution, volcanic and sedimentary accumulation, and continental drift rates: *Precambrian Research*, v. 133, no. 3–4, p. 143–173.
- Blake, TS, Rothery, E, Muhling, JR, Drake-Brockman, JAP, Sprigg, LC, Ho, SE, Rasmussen, B and Fletcher, IR 2011, Two episodes of regional-scale Precambrian hydrothermal alteration in the eastern Pilbara, Western Australia: *Precambrian Research*, v. 188, p. 73–103.
- Bodorkos, S and Clark, DJ 2004, Evolution of a crustal-scale transpressive shear zone in the Albany–Fraser Orogen, SW Australia: 2. Tectonic history of the Coramup Gneiss and a kinematic framework for Mesoproterozoic collision of the West Australian and Mawson cratons: *Journal of Metamorphic Geology*, v. 22, no. 8, p. 713–731, DOI: 10.1111/j.1525-1314.2004.00544.x.
- Bodorkos, S, Love, GJ, Nelson, DR and Wingate, MTD 2006a, 149698: quartz sandstone, Cornelia Range; Geochronology Record 617: Geological Survey of Western Australia, 5p.
- Bodorkos, S, Love, GJ, Nelson, DR and Wingate, MTD 2006b, 178232: trondhjemitic pegmatite vein, Whatsamatta Well; Geochronology Record 654: Geological Survey of Western Australia, 4p.

- Bodorkos, S, Nelson, DR, Love, GJ and Wingate, MTD 2006, 178090: tuffaceous volcanoclastic sandstone, Dingo Well; Geochronology Record 633: Geological Survey of Western Australia, 4p.
- Budd, AR, Wyborn, LAI and Bastrakova, IV 2001, The metallogenic potential of Australian Proterozoic granites: Geoscience Australia, Canberra, Record 2001/12, 152p.
- Buick, R, Thorne, J, McNaughton, N, Smith, JB, Barley, ME and Savage, MD 1995, Record of emergent continental crust ~3.5 billion years ago in the Pilbara Craton of Australia: *Nature*, v. 375, p. 574–577.
- Camacho, A, Compston, W, McCulloch, MT and McDougall, I 1997, Timing and exhumation of eclogite facies shear zones, Musgrave Block, central Australia: *Journal of Metamorphic Geology*, v. 15, p. 735–751.
- Camacho, A and Fanning, CM 1995, Some isotopic constraints on the evolution of the granulite and upper amphibolite facies terranes in the eastern Musgrave Block, central Australia: *Precambrian Research*, v. 71, p. 155–172.
- Carr, HW 1989, The geochemistry and platinum group element distribution of the Rudall River ultramafic bodies, Paterson Province, Western Australia: The University of Western Australia, Perth, Western Australia, BSc (Hons) thesis (unpublished), 144p.
- Castillo, PR 2012, Adakite petrogenesis: *Lithos*, v. 134–135, p. 304–316.
- Cawood, PA and Korsch, RJ 2008, Assembling Australia: Proterozoic building of a continent: *Precambrian Research*, v. 166, no. 1–4, p. 1–38.
- Chin, RJ and de Laeter, JR 1981, The relationship of new Rb-Sr isotopic dates from the Rudall Metamorphic Complex to the geology of the Paterson Province, in Annual report for the year 1980: Geological Survey of Western Australia, Perth, Western Australia, p. 80–87.
- Chin, RJ, Williams, IR, Williams, SJ and Crowe, RWA (compilers) 1980, Rudall, Western Australia: Geological Survey of Western Australia, 1:250 000 Geological Series Explanatory Notes, 22p.
- Claoué-Long, JC, Compston, W, Roberts, J and Fanning, CM 1995, Two Carboniferous ages: a comparison of SHRIMP zircon dating with conventional zircon ages and $^{40}\text{Ar}/^{39}\text{Ar}$ analysis, in *Geochronology, time scales and global stratigraphic correlation edited by WA Berggren, DV Kent, M-P Aubry and J Hardenbol*: Society for Sedimentary Geology, Special Publication 54, p. 3–21.
- Clark, DJ, Hensen, BJ and Kinny, PD 2000, Geochronological constraints for a two-stage history of the Albany–Fraser Orogen, Western Australia: *Precambrian Research*, v. 102, no. 3, p. 155–183.
- Clarke, GL 1991, Proterozoic tectonic reworking in the Rudall Complex, Western Australia: *Australian Journal of Earth Sciences*, v. 38, p. 31–44.
- Close, DF 2013, Chapter 21: Musgrave Province, in *Geology and mineral resources of the Northern Territory compiled by M Ahmad and TJ Munson*: Northern Territory Geological Survey, Darwin, Northern Territory, Special Publication 5, p. 21.1–21.24.
- Close, DF, Scrimgeour, IR, Edgoose, CJ, Wingate, MTD and Selway, K 2005, Late Paleoproterozoic accretion of a 1690–1660 Ma magmatic arc onto the North Australian Craton: Geological Society of Australia, Abstracts 81, p. 36.
- Collins, WJ 2002a, Hot orogens, tectonic switching, and creation of continental crust: *Geology*, v. 30, p. 535–538.
- Collins, WJ 2002b, Nature of extensional accretionary orogens: *Tectonics*, v. 21, no. 4, p. 6–1–6–12, 10.1029/2000TC001272.
- Collins, WJ, Gray, CM and Goode, ADT 1988, The Parnell Quartz Monzonite: a Proterozoic zoned pluton in the Archaean Pilbara Block, Western Australia: *Australian Journal of Earth Sciences*, v. 35, p. 535–547.
- Compston, W, Williams, IS and Meyer, C 1984, U–Pb geochronology of zircons from lunar breccia 73217 using a sensitive high mass-resolution ion microprobe: *Journal of Geophysical Research*, v. 89, no. S02, p. B525–B534.
- Corfu, F, Hanchar, JM, Hoskin, PWO and Kinny, PD 2003, Atlas of zircon textures, in *Zircon edited by JM Hanchar and PWO Hoskin*: Mineralogical Society of America, Reviews in Mineralogy and Geochemistry 53, p. 469–500.
- Crispe, AJ, Vandenberg, LC and Scrimgeour, IR 2007, Geological framework of the Archean and Paleoproterozoic Tanami Region, Northern Territory: *Mineralium Deposita*, v. 42, p. 3–26.
- Cross, A, Jaireth, S, Rapp, R and Armstrong, R 2011, Reconnaissance-style EPMA chemical U–Th–Pb dating of uraninite: *Australian Journal of Earth Sciences*, v. 58, no. 6, p. 675–683.
- Cutten, HN, Johnson, SP, Thorne, AM, Wingate, MTD, Kirkland, CL, Belousova, EA, Blay, OA and Zwingmann, H 2016, Deposition, provenance, inversion history and mineralization of the Proterozoic Edmund and Collier Basins, Capricorn Orogen: Geological Survey of Western Australia, Report 127, 74p.
- Cutts, K, Hand, M and Kelsey, DE 2011, Evidence for early Mesoproterozoic (ca. 1590 Ma) ultrahigh-temperature metamorphism in southern Australia: *Lithos*, v. 124, p. 1–16.
- Dean, AA 2001, Igneous rocks of the Tanami Region (Electronic pre-release edition): Northern Territory Geological Survey, NTGS Record GS 2001-003, 78p.
- DeCelles, PG 2011, Foreland basin systems revisited: variations in response to tectonic settings, in *Tectonics of sedimentary basins: recent advances edited by A Busby and A Azor*: John Wiley & Sons, Ltd., Chichester, UK, p. 405–426.
- DeCelles, PG and Giles, KA 1996, Foreland basin systems: *Basin Research*, v. 8, p. 105–123.
- Dunphy, JM and McNaughton, NJ 1998, Geochronology of the Telfer granitoids: zircon and titanite U–Pb SHRIMP data, in *Abstracts: Geological Society of Australia*, Sydney, New South Wales 49, p. 127.
- Durocher, KE, Kyser, TK, Marlatt, J and Hanly, A 2003, New $^{40}\text{Ar}/^{39}\text{Ar}$ ages from the central Paterson Orogen, Western Australia: *Australian Journal of Earth Sciences*, v. 50, p. 601–610.
- Edgoose, CJ 2013, Ngalia Basin, in *Geology and mineral resources of the Northern Territory edited by M Ahmad and TJ Munson*: Northern Territory Geological Survey, Darwin, Special Publication 5, p. 24.1–24.24.
- Edgoose, CJ, Scrimgeour, IR and Close, DF 2004, Geology of the Musgrave Block, Northern Territory: Northern Territory Geological Survey, Report 15, 46p.
- Eggins, SM, Woodhead, JD, Kinsley, LPJ, Mortimer, GE, Sylvester, PJ, McCulloch, MT, Hergt, JM and Handler, MR 1997, A simple method for the precise determination of >40 trace elements in geological samples by ICPMS using enriched isotope internal standardisation: *Chemical Geology*, v. 134, p. 311–326.
- Evins, PM, Kirkland, CL, Wingate, MTD, Smithies, RH, Howard, HM and Bodorkos, S 2012, Provenance of the 1340–1270 Ma Ramarama Basin in the west Musgrave Province, Central Australia: Geological Survey of Western Australia, Report 116, 39p.
- Ferguson, KM, Bagas, L and Ruddock, I 2005, Mineral occurrences and exploration potential of the Paterson area: Geological Survey of Western Australia, Report 97, 43p.
- Fielding, I, Johnson, SJ, Rasmussen, B, Muhling, J, Dunkley, D, Jianwei, Z, Wingate, M and Sheppard, S 2016, Dating orogenic gold mineralization at the Paulsens deposit, Western Australia, in *Geological Society of Australia Abstracts No 118: Australian Earth Sciences Convention 2016*, Adelaide, 26–30 June 2016, p. 220–220.

- Foden, JD, Buick, IS and Mortimer, GE 1988, The petrology and geochemistry of granitic gneisses from the east Arunta Inlier, central Australia — implications for Proterozoic crustal development: *Precambrian Research*, v. 40/41, p. 233–259.
- Fraser, AR 1976, Gravity provinces and their nomenclature: *BMR Journal of Australian Geology and Geophysics*, v. 1, p. 350–352.
- Fraser, G, Huston, D, Bagas, L, Hussey, K, Clauouè-Long, J, Cross, A, Vandenburg, L, Wygralak, A and Crispe, A 2006, $^{40}\text{Ar}/^{39}\text{Ar}$ constraints on the episodic history of mineralisation and tectonism in the southern North Australian Craton, *in* Conference Abstracts: Geoscience Australia; Record 2006/16, p. 13–14.
- Fraser, GL, Huston, DL, Gibson, GM, Neumann, NL, Maidment, D, Kositsin, N, Skirrow, RG, Jaireth, S, Lyons, P, Carson, C, Cutten, H and Lambeck, A 2007, Geodynamic and metallogenic evolution of Proterozoic Australia from 1870–1550 Ma: a discussion: *Geoscience Australia, Geoscience Australia Record 2007/16*, 76p.
- Frost, BR, Barnes, CG, Collins, WJ, Arculus, RJ, Ellis, DJ and Frost, CD 2001, A geochemical classification for granitic rocks: *Journal of Petrology*, v. 42, no. 11, p. 2033–2048.
- Gibson, GM, Rubenach, MJ, Neumann, NL, Southgate, PN and Hutton, LJ 2008, Syn- and post-extensional tectonic activity in the Palaeoproterozoic sequences of Broken Hill and Mount Isa and its bearing on reconstructions of Rodinia: *Precambrian Research*, v. 166, p. 350–369.
- Giles, D, Betts, P and Lister, G 2002, Far-field continental backarc setting for the 1.80 – 1.67 Ga basins of northeastern Australia: *Geology*, v. 30, no. 9, p. 823–826.
- Giles, D, Betts, PG and Lister, GS 2004, 1.8–1.5 Ga links between the North and South Australian Cratons and the Early–Middle Proterozoic configuration of Australia: *Tectonophysics*, v. 380, p. 27–41.
- Grey, K, Hocking, RM, Stevens, MK, Bagas, L, Carlsen, GM, Irimes, F, Pirajno, F, Haines, PW and Apak, SN 2005, Lithostratigraphic nomenclature of the Officer Basin and correlative parts of the Paterson Orogen, Western Australia: *Geological Survey of Western Australia, Report 93*, 89p.
- Hall, CE, Jones, SA and Bodorkos, S 2008, Sedimentology, structure and SHRIMP zircon provenance of the Woodline Formation, Western Australia: implications for the tectonic setting of the West Australian Craton during the Paleoproterozoic: *Precambrian Research*, v. 162, p. 577–598, doi:10.1016/j.precamres.2007.11.001.
- Hand, M and Buick, IS 2001, Tectonic history of the Reynolds – Anmatjira Ranges: a case study of reactivation in central Australia, *in* *Continental Reactivation and Reworking* edited by JA Miller, R Holdsworth, IS Buick and M Hand: Geological Society, London, Special Publication 184, p. 237–260.
- Hand, M, Reid, A and Jagodzinski, L 2007, Tectonic Framework and Evolution of the Gawler Craton, Southern Australia: *Economic Geology*, v. 102, no. 8, p. 1377–1395.
- Hewson, SAJ 1996, A structural examination of the Telfer gold–copper deposit and surrounding region, northwest Western Australia: the role of polyphase orogenic deformation in ore-deposit development and implications for exploration (online PDF): James Cook University, Townsville, Queensland, PhD thesis (unpublished).
- Hickman, AH (compiler) 1978, Nullagine, Western Australia: Geological Survey of Western Australia, 1:250 000 Geological Series Explanatory Notes, 22p.
- Hickman, AH 2012, Review of the Pilbara Craton and Fortescue Basin, Western Australia: crustal evolution providing environments for early life: *Island Arc*, v. 21, p. 1–31.
- Hickman, AH and Bagas, L 1996, Rudall, WA Sheet 3352: Geological Survey of Western Australia, 1:100 000 Geological Series.
- Hickman, AH and Bagas, L 1998, Geology of the Rudall 1:100 000 sheet: Geological Survey of Western Australia, 1:100 000 Geological Series Explanatory Notes, 30p.
- Hickman, AH and Bagas, L 1999, Geological evolution of the Palaeoproterozoic Talbot Terrane and adjacent Meso- and Neoproterozoic successions, Paterson Orogen, Western Australia: Geological Survey of Western Australia, Report 71, 91p.
- Hickman, AH and Clarke, GL 1994, Geology of the Broadhurst 1:100 000 sheet: Geological Survey of Western Australia, 1:100 000 Geological Series Explanatory Notes, 40p.
- Hickman, AH and Van Kranendonk, MJ 2008, Archean crustal evolution and mineralization of the northern Pilbara Craton — a field guide: Geological Survey of Western Australia, Record 2008/13, 79p.
- Hollis, JA, Kemp, AIS, Tyler, IM, Kirkland, CL, Wingate, MTD, Phillips, C, Sheppard, S, Belousova, E and Greau, Y 2014, Basin formation by orogenic collapse: zircon U–Pb and Lu–Hf isotope evidence from the Kimberley and Speewah Groups, northern Australia: Geological Survey of Western Australia, Report 137, 46p.
- Hollis, JA, Kirkland, CL, Spaggiari, CV, Tyler, IM, Haines, PW, Wingate, MTD, Belousova, EA and Murphy, RC 2013, Zircon U–Pb–Hf isotope evidence for links between the Warumpi and Aileron Provinces, west Arunta region: Geological Survey of Western Australia, Record 2013/9, 30p.
- Hoskin, PWO and Schaltegger, U 2003, The composition of zircon and igneous and metamorphic petrogenesis: *Reviews in Mineralogy and Geochemistry*, v. 53, p. 27–62.
- Howard, HM, Smithies, RH, Evins, P, Kirkland, CL, Wingate, MTD and Pirajno, F 2011a, Explanatory Notes for the west Musgrave Province: Geological Survey of Western Australia Perth, Western Australia, 349p.
- Howard, HM, Smithies, RH, Kirkland, CL, Kelsey, DE, Aitken, A, Wingate, MTD, Quentin De Gromard, R, Spaggiari, CV and Maier, WD 2015, The burning heart — The Proterozoic geology and geological evolution of the west Musgrave Region, central Australia: *Gondwana Research*, v. 27, no. 1, p. 64–94.
- Howard, HM, Werner, M, Smithies, RH, Evins, PM, Kirkland, CL, Kelsey, DE, Hand, M, Collins, AS, Pirajno, F, Wingate, MTD, Maier, WD and Raimondo, T 2011b, The geology of the west Musgrave Province and the Bentley Supergroup — a field guide: Geological Survey of Western Australia, Record 2011/4, 116p.
- Howlett, D, Raimondo, T and Hand, M 2015, Evidence for 1808–1770 Ma bimodal magmatism, sedimentation, high-T deformation and metamorphism in the Aileron Province, central Australia: *Australian Journal of Earth Sciences*, v. 62, p. 831–852.
- Huston, DL, Blewett, RS and Champion, DC 2012, Australia through time: a summary of its tectonic and metallogenic evolution: *Episodes*, v. 35, no. 1, p. 23–43.
- Huston, DL, Czarnota, K, Jaireth, S, Williams, N, Maidment, DW, Cassidy, KF, Duerden, P and Miggins, D 2010, Mineral systems of the Paterson region: *Geoscience Australia, Record 2010/12*, p. 155–218.
- Huston, DL, Vandenberg, L, Wygralak, AS, Mernagh, TP, Bagas, L, Crispe, A, Lambeck, A, Cross, A, Fraser, G, Williams, N, Worden, K, Meixner, T, Goleby, B, Jones, L, Lyons, P and Maidment, D 2007, Lode-gold mineralization in the Tanami region, northern Australia: *Mineralium Deposita*, v. 42, p. 175–204.
- Idnurm, M and Giddings, JW 1988, Australian Precambrian polar wander: a review: *Precambrian Research*, v. 40/41, p. 61–88.
- Johnson, SP 2013, The birth of supercontinents and the Proterozoic assembly of Western Australia: Geological Survey of Western Australia, Perth, Western Australia, 78p.

- Johnson, SP, Sheppard, S, Rasmussen, B, Wingate, MTD, Kirkland, CL, Muhling, JR, Fletcher, IR and Belousova, E 2010, The Glenburgh Orogeny as a record of Paleoproterozoic continent–continent collision: Geological Survey of Western Australia, Record 2010/5, 54p.
- Johnson, SP, Sheppard, S, Thorne, AM, Rasmussen, B, Fletcher, IR, Wingate, MTD and Cutten, HN 2011a, The role of the 1280–1250 Ma Mutherbukin Tectonic Event in shaping the crustal architecture and mineralization history of the Capricorn Orogen, *in* GSWA 2011 extended abstracts: promoting the prospectivity of Western Australia: Geological Survey of Western Australia, Record 2011/2, p. 1–3.
- Johnson, SP, Thorne, AM, Cutten, HN, Tyler, IM and Blay, OA 2011b, Geology of the Gascoyne Province, *in* Capricorn Orogen seismic and magnetotelluric (MT) workshop 2011: extended abstracts *edited by* SP Johnson, AM Thorne and IM Tyler: Geological Survey of Western Australia, Record 2011/25, p. 27–41.
- Johnson, SP, Thorne, AM, Tyler, IM, Korsch, RJ, Kennett, BLN, Cutten, HN, Goodwin, J, Blay, OA, Blewett, RS, Joly, A, Dentith, MC, Aitken, ARA, Holzschuh, J, Salmon, M, Reading, A, Heinson, G, Boren, G, Ross, J, Costelloe, RD and Fomin, T 2013, Crustal architecture of the Capricorn Orogen, Western Australia and associated metallogeny: Australian Journal of Earth Sciences, v. 60, no. 6–7, p. 681–705, doi:10.1080/08120099.2013.826735.
- Johnson, SP, Zi, J, Rasmussen, B, Muhling, JR, Fletcher, IR, Dunkley, DJ, Thorne, AM, Cutten, HN and Korhonen, FJ 2015, Abracadabra — dating hydrothermal mineralization and fluid flow in a long-lived crustal structure, *in* GSWA 2015 extended abstracts: promoting the prospectivity of Western Australia: Geological Survey of Western Australia, Perth, Record 2015/2, p. 1–4.
- Jones, S 2011, Proterozoic deformation in the east Pilbara Craton and tectonic setting of fault-hosted manganese at the Woodie Woodie Mine: Australian Journal of Earth Sciences, v. 58, no. 6, p. 639–673.
- Kemp, AIS, Hickman, AH, Kirkland, CL and Vervoort, JD 2015, Hf isotopes in detrital and inherited zircons of the Pilbara Craton provide no evidence for Hadean continents: Precambrian Research, v. 261, p. 112–126.
- Kirkland, CL, Johnson, SP, Smithies, RH, Hollis, JA, Wingate, MTD, Tyler, IM, Hickman, AH, Cliff, JB, Belousova, EA, Murphy, RC and Tessalina, S 2013a, The crustal evolution of the Rudall Province from an isotopic perspective: Geological Survey of Western Australia, Report 122, 30p.
- Kirkland, CL, Johnson, SP, Smithies, RH, Hollis, JA, Wingate, MTD, Tyler, IM, Hickman, AH, Cliff, JB, Tessalina, S, Belousova, EA and Murphy, RC 2013b, Not-so-suspect terrane: constraints on the crustal evolution of the Rudall Province: Precambrian Research, v. 235, p. 131–149.
- Kirkland, CL, Jourdan, F, Wingate, MTD, Quentin De Gromard, R, Howard, HM and Smithies, RH 2013c, 185414: quartzite, Great Central Road; Geochronology Record 1139: Geological Survey of Western Australia, 4p.
- Kirkland, CL, Smithies, RH and Spaggiari, CV 2015a, Foreign contemporaries — unravelling disparate isotopic signatures from Mesoproterozoic Central and Western Australia: Precambrian Research, v. 265, p. 218–231.
- Kirkland, CL, Smithies, RH, Taylor, RJM, Evans, N and McDonald, B 2015b, Zircon Th/U ratios in magmatic environs: Lithos, v. 212–215, p. 397–414.
- Kirkland, CL, Spaggiari, CV, Wingate, MTD, Smithies, RH, Belousova, EA, Murphy, R and Pawley, MJ 2011a, Inferences on crust–mantle interaction from Lu–Hf isotopes: a case study from the Albany–Fraser Orogen: Geological Survey of Western Australia, Record 2011/12, 25p.
- Kirkland, CL, Wingate, MTD, Quentin De Gromard, R, Howard, HM and Smithies, RH 2014a, 205194: psammitic gneiss, Mitika Homestead; Geochronology Record 1203: Geological Survey of Western Australia, 5p.
- Kirkland, CL, Wingate, MTD, Quentin De Gromard, R, Howard, HM and Smithies, RH 2014b, 208414: quartzite, Mitika Homestead; Geochronology Record 1205: Geological Survey of Western Australia, 6p.
- Kirkland, CL, Wingate, MTD and Smithies, RH 2011b, 187175: muscovite–tourmaline pegmatite, Morgan Range; Geochronology Record 936: Geological Survey of Western Australia, 4p.
- Korhonen, FJ, Johnson, SP, Fletcher, IR, Rasmussen, B, Sheppard, S, Muhling, JR, Dunkley, DJ, Wingate, MTD, Roberts, MP and Kirkland, CL 2015, Pressure–temperature–time evolution of the Mutherbukin Tectonic Event, Capricorn Orogen: Geological Survey of Western Australia, Report 146, 64p.
- Korsch, RJ, Blewett, RS, Wyche, S, Zibra, I, Ivanic, TJ, Doublier, MJ, Romano, SS, Pawley, MJ, Johnson, SP, Van Kranendonk, MJ, Jones, LEA, Kositcin, N, Gessner, K, Hall, CE, Chen, SF, Patison, N, Kennett, BLN, Jones, T, Goodwin, JA, Milligan, P and Costelloe, RD 2014, Geodynamic implications of the Youanmi and southern Carnarvon deep seismic reflection surveys: a ~1300 km traverse from the Pinjarra Orogen to the eastern Yilgarn craton, *in* Youanmi and southern Carnarvon seismic and magnetotelluric (MT) workshop 2013 *compiled by* S Wyche, TJ Ivanic and I Zibra: Geological Survey of Western Australia, Perth, Record 2013/6, p. 147–166.
- Li, ZX 2000, Palaeomagnetic evidence for unification of the North and West Australian Cratons by ca. 1.7 Ga: new results from the Kimberley Basin of northwestern Australia: Geophysical Journal International, v. 142, p. 173–180.
- Li, ZX and Evans, DAD 2011, Late Neoproterozoic 40° intraplate rotation within Australia allows for a tighter-fitting and longer-lasting Rodinia: Geology, v. 39, no. 1, p. 39–42.
- Loucks, RR 2014, Distinctive composition of copper-ore-forming arc magmas: Australian Journal of Earth Sciences, v. 61, p. 5–16.
- Lu, YJ, Loucks, R, Fiorentini, ML, Yang, ZM and Hou, ZQ 2015, Fluid flux melting generated postcollisional high Sr/Y copper ore-forming water-rich magmas in Tibet: Geology, v. 43, no. 7, p. 583–586.
- Ludwig, KR 2003, Isoplot 3.00; a geochronological toolkit for Microsoft Excel: Berkeley Geochronology Centre, Special Publication 4, 70p.
- Ludwig, KR 2009, Squid 2.50, a user's manual: Berkeley Geochronology Centre, Berkeley, California, USA, 95p. (unpublished).
- Macdonald, FM, Wingate, MTD and Mitchell, K 2005, Geology and age of the Glikson impact structure, Western Australia: Australian Journal of Earth Sciences, v. 52, p. 641–651.
- Maidment, D 2014, When did the WAC whack the NAC? Docking of the West and North Australian cratons, *in* Geological Society of Australia, Abstracts No 110: Geological Society of Australia; 2014 Australian Earth Sciences Convention (AESC), Newcastle, NSW, 7 July 2014, p. 211–211.
- Maidment, D, Huston, DL, Maas, R, Czarnota, K, Neumann, N, McIntyre, A and Bagas, L 2008, The Nifty–Kintyre–Duke Cu–U–Pb–Zn mineralizing events: links to the evolution of the Yeneena Basin, northwest Paterson Orogen, *in* GSWA 2008 extended abstracts: promoting the prospectivity of Western Australia: Geological Survey of Western Australia, Record 2008/2, p. 27–29.
- Maidment, DW, Huston, DL and Heamann, L 2010, The age of the Telfer Au–Cu deposit and its relationship with granite emplacement, Paterson Province, Western Australia: Geoscience Australia, Professional Opinion 2010/05, 40p.
- Martin, DM and Morris, PA 2010, Tectonic setting and regional implications of ca. 2.2 Ga mafic magmatism in the southern Hamersley Province, Western Australia: Australian Journal of Earth Sciences, v. 57, no. 7, p. 911–931.
- Martin, DM and Thorne, AM 2004, Tectonic setting and basin evolution of the Bangemall Supergroup in the northwestern Capricorn Orogen: Precambrian Research, v. 128, no. 3–4, p. 385–409.

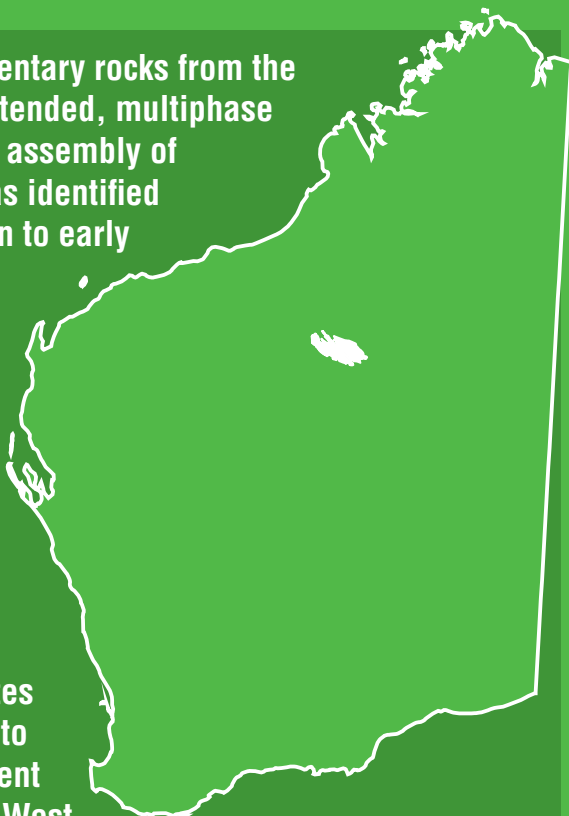
- Martin, H, Smithies, RH, Rapp, R, Moyen, J-F and Champion, DC 2005, An overview of adakite, tonalite–trondhjemite–granodiorite (TTG), and sanukitoid: relationships and some implications for crustal evolution: *Lithos*, v. 79, p. 1–24.
- McNaughton, NJ, Green, MD, Compston, W and Williams, IS 1988, Are anorthositic rocks basement to the Pilbara Craton?, *in* Achievements in Australian geoscience: Geological Society of Australia; 9th Australian Geological Convention, University of Queensland, Brisbane, 1 February 1988; Abstracts 21, p. 272–273.
- Melville, PM 2010, Geophysics and drilling collaboration final report for drilling program, Lake Woods Project, EL23687, EL24520, EL25631, EL27317, EL27318: Northern Territory Geological Survey, Open File Report CR2010-0226, 24p.
- Morrissey, LJ, Hand, M, Raimondo, T and Kelsey, DE 2014, Long-lived high-T, low-P granulite facies metamorphism in the Arunta Region, central Australia: *Journal of Metamorphic Geology*, v. 32, p. 25–47.
- Murphy, JB 2007, Igneous rock associations 8. Arc magmatism II: geochemical and isotopic characteristics: *Geoscience Canada*, v. 34, no. 1, p. 7–35.
- Myers, JS, Shaw, RD and Tyler, IM 1996, Tectonic evolution of Proterozoic Australia: *Tectonics*, v. 15, p. 1431–1446.
- Nelson, DR 1995a, 104932: garnet–biotite–muscovite syenogranite gneiss, Sundowner drillhole; *Geochronology Record* 31: Geological Survey of Western Australia, 4p.
- Nelson, DR 1995b, 104938: pegmatite, Coondegoon; *Geochronology Record* 35: Geological Survey of Western Australia, 4p.
- Nelson, DR 1995c, 104980: monzogranite gneiss, Graphite Valley; *Geochronology Record* 3: Geological Survey of Western Australia, 4p.
- Nelson, DR 1995d, 104981: biotite–muscovite monzogranite gneiss, southern part of Graphite Valley; *Geochronology Record* 4: Geological Survey of Western Australia, 4p.
- Nelson, DR 1995e, 104989: muscovite quartzite, Fingoon Quartzite; *Geochronology Record* 5: Geological Survey of Western Australia, 4p.
- Nelson, DR 1995f, 110056: biotite–hornblende granodiorite gneiss, Rooney Creek; *Geochronology Record* 518: Geological Survey of Western Australia, 4p.
- Nelson, DR 1995g, 111843: biotite–muscovite monzogranite gneiss, Poynton Creek; *Geochronology Record* 520: Geological Survey of Western Australia, 5p.
- Nelson, DR 1995h, 111854: biotite–muscovite granodiorite gneiss, Poonemerlarr Creek west; *Geochronology Record* 521: Geological Survey of Western Australia, 5p.
- Nelson, DR 1995i, 112310: granodiorite gneiss, Dunn Creek west; *Geochronology Record* 471: Geological Survey of Western Australia, 4p.
- Nelson, DR 1995j, 112341: micromonzogranite (meta-aplite) dyke, Rudall airstrip; *Geochronology Record* 472: Geological Survey of Western Australia, 4p.
- Nelson, DR 1995k, 112379: biotite monzogranite (augen) gneiss, Split Rock; *Geochronology Record* 473: Geological Survey of Western Australia, 4p.
- Nelson, DR 1995l, 112397: coarse-grained porphyritic biotite monzogranite (augen) gneiss, Watrara Inlier; *Geochronology Record* 474: Geological Survey of Western Australia, 4p.
- Nelson, DR 1995m, 113002: granodiorite gneiss, Cotton Creek; *Geochronology Record* 475: Geological Survey of Western Australia, 4p.
- Nelson, DR 1996a, 112101: biotite–epidote monzogranite gneiss, Larry Creek; *Geochronology Record* 522: Geological Survey of Western Australia, 4p.
- Nelson, DR 1996b, 112102: seriate biotite metamonzogranite, southern part of the Watrara Inlier; *Geochronology Record* 523: Geological Survey of Western Australia, 3p.
- Nelson, DR 1996c, 112160: garnet microgneiss, Harbutt Range; *Geochronology Record* 489: Geological Survey of Western Australia, 4p.
- Nelson, DR 1996d, 113035: orthogneiss, east of South Rudall Dome; *Geochronology Record* 476: Geological Survey of Western Australia, 5p.
- Nelson, DR 1996e, 118914: foliated granite, north of Harbutt Range; *Geochronology Record* 485: Geological Survey of Western Australia, 4p.
- Nelson, DR 1997, Compilation of SHRIMP U–Pb zircon geochronology data, 1996: Geological Survey of Western Australia, Record 1997/2.
- Nelson, DR 2001, 168935: volcanoclastic sandstone, Sophie Tank; *Geochronology Record* 206: Geological Survey of Western Australia, 4p.
- Nelson, DR 2002a, 168983: metasandstone, Weld Spring; *Geochronology Record* 155: Geological Survey of Western Australia, 4p.
- Nelson, DR 2002b, 169032: hornblende–clinopyroxene–quartz micromonzonite, Mount Edgar; *Geochronology Record* 149: Geological Survey of Western Australia, 2p.
- Nelson, DR 2002c, Compilation of geochronology data, 2001: Geological Survey of Western Australia, Record 2002/2, 282p.
- Nelson, DR 2004, 169032: hornblende–clinopyroxene–quartz micromonzonite, Mount Edgar; *Geochronology Record* 63: Geological Survey of Western Australia, 3p.
- Nelson, DR 2005a, 149665: quartz sandstone, Phenoclast Hill; *Geochronology Record* 540: Geological Survey of Western Australia, 5p.
- Nelson, DR 2005b, 149683: quartz sandstone, CSR Well 14; *Geochronology Record* 541: Geological Survey of Western Australia, 5p.
- Oorschot, CW 2011, P–T–t evolution of the Fraser Zone, Albany–Fraser Orogen, Western Australia: Geological Survey of Western Australia, Record 2011/18, 101p.
- Page, RW, Compston, W and Needham, RS 1980, Geochronology and evolution of the late Archaean basement and Proterozoic rocks in the Alligator Rivers uranium field, Northern Territory, Australia, *in* Uranium in the Pine Creek Geosyncline: Proceedings of the International Uranium Symposium on the Pine Creek Geosyncline *edited by* J Ferguson and AB Goleby: International Atomic Energy Agency, Vienna, p. 39–68.
- Payne, JL, Hand, M, Barovich, KM and Wade, P 2008, Temporal constraints on the timing of high-grade metamorphism in the northern Gawler Craton: implications for assembly of the Australian Proterozoic: *Australian Journal of Earth Sciences*, v. 55, p. 623–640.
- Payne, JL, Hand, MP, Barovich, KM, Reid, AJ and Evans, DAD 2009, Correlations and reconstruction models for the 2500–1500 Ma evolution of the Mawson Continent, *in* Palaeoproterozoic Supercontinents and Global Evolution *edited by* SM Reddy, R Mazumder and DAD Evans: Geological Society, London, UK, Special Publication 323, p. 319–355.
- Pirajno, F, Hocking, RM, Reddy, SM and Jones, JA 2009, A review of the geology and geodynamic evolution of the Palaeoproterozoic Earahedy Basin, Western Australia: *Earth-Science Reviews*, v. 94, p. 39–77.
- Pirajno, F and Hoatson, DM 2012, A review of Australia's Large Igneous Provinces and associated mineral systems: Implications for mantle dynamics through geological time: *Ore Geology Reviews*, v. 48, p. 2–54.

- Pyke, J 2000, Minerals laboratory staff develops ICP-MS preparation method: Australian Geological Survey Organisation Newsletter, v. 33, p. 12–14.
- Quentin De Gromard, R, Wingate, MTD, Kirkland, CL, Howard, HM and Smithies, RH 2016, Geology and U–Pb geochronology of the Warlawurru Supersuite and MacDougall Formation in the Mitika and Wanarn areas, west Musgrave Province: Geological Survey of Western Australia, Record 2016/4, 29p.
- Raimondo, T, Collins, AS, Hand, M, Walker-Hallam, A, Smithies, RH, Evins, PM and Howard, HM 2010, The anatomy of a deep intracontinental orogen: Tectonics, v. 29 (TC4024), doi:10.1029/2009TC002504.
- Rasmussen, B, Fletcher, IR, Muhling, JR, Thorne, WS and Broadbent, GC 2007, Prolonged history of episodic fluid flow in giant hematite ore bodies: evidence from in situ U–Pb geochronology of hydrothermal xenotime: Earth and Planetary Science Letters, v. 258, p. 249–259.
- Rasmussen, B, Fletcher, IR, Bekker, A, Muhling, JR, Gregory, CJ and Thorne, AM 2012, Deposition of 1.88-billion-year-old iron formations as a consequence of rapid crustal growth: Nature, v. 484, p. 498–501.
- Reed, A 1996, The structural, stratigraphic and temporal setting of the Maroochydore copper prospect, Paterson Orogen, Western Australia: The University of Western Australia, Perth, Australia, PhD thesis (unpublished), 289p.
- Reid, AJ and Hand, M 2012, Mesoarchean to Mesoproterozoic evolution of the southern Gawler Craton, South Australia: Episodes, v. 35, no. 1, p. 216–225.
- Richards, JP 2011, High Sr/Y arc magmas and porphyry Cu \pm Mo \pm Au deposits: just add water: Economic Geology, v. 106, p. 1075–1081.
- Richards, JP and Kerrich, R 2007, Special paper: adakite-like rocks: their diverse origins and questionable role in metallogenesis: Economic Geology, v. 102, no. 4, p. 537–575.
- Roach, IC, Costelloe, MT and Hutchinson, DK 2010, Interpretations of AEM data, in Geological and energy implications of the Paterson airborne electromagnetic (AEM) survey, Western Australia edited by IC Roach: Geoscience Australia, Record 2010/12, p. 107–154.
- Rubatto, D, Williams, IS and Buick, IS 2001, Zircon and monazite response to prograde metamorphism in the Reynolds Range, central Australia: Contributions to Mineralogy and Petrology, v. 140, no. 4, p. 458–468.
- Schmidt, PW 2014, A review of Precambrian palaeomagnetism of Australia: Palaeogeography, supercontinents, glaciations and true polar wander: Gondwana Research, v. 25, p. 1164–1185.
- Schmidt, PW and Williams, GE 2008, Palaeomagnetism of red beds from the Kimberley Group, Western Australia: implications for the palaeogeography of the 1.8 Ga King Leopold Glaciation: Precambrian Research, v. 167, p. 267–280.
- Schmidt, PW, Williams, GE, Camacho, A and Lee, JKW 2006, Assembly of Proterozoic Australia: implications of a revised pole for the ~1070 Ma Alcurra Dyke Swarm, central Australia: Geophysical Journal International, v. 167, p. 626–634.
- Scott, DL, Rawlings, DJ, Page, RW, Tarlowski, CZ, Idnurm, M, Jackson, MJ and Southgate, PN 2000, Basement framework and geodynamic evolution of the Palaeoproterozoic superbasins of north-central Australia: an integrated review of geochemical, geochronological and geophysical data: Australian Journal of Earth Sciences, v. 47, p. 341–380.
- Scrimgeour, IR 2006, The Arunta Region: links between tectonics and mineralisation, in Record of abstracts: Northern Territory Geological Survey; Annual Geoscience Exploration Seminar (AGES) 2006, Alice Springs, Northern Territory, 28 March 2006; Record 2006-002, p. 7–10.
- Scrimgeour, IR 2013a, Aileron Province (Chapter 12), in Geology and mineral resources of the Northern Territory compiled by M Ahmad and TJ Munson: Northern Territory Geological Survey, Darwin, Special Publication 5, p. 12.1–12.74.
- Scrimgeour, IR 2013b, Chapter 13: Warumpi Province, in Geology and mineral resources of the Northern Territory compiled by M Ahmad and TJ Munson: Northern Territory Geological Survey, Darwin, Northern Territory, Special Publication 5, p. 13.1–13.21.
- Scrimgeour, IR and Close, DF 1999, Regional high pressure metamorphism during intracratonic deformation: the Petermann Orogeny, central Australia: Journal of Metamorphic Geology, v. 17, p. 557–572.
- Scrimgeour, IR, Kinny, PD, Close, DF and Edgoose, CJ 2005, High-T granulites and polymetamorphism in the southern Arunta Region, central Australia: evidence for a 1.64 Ga accretional event: Precambrian Research, v. 142, p. 1–27.
- Scrimgeour, IR and Raith, JG 2001, Tectonic and thermal events in the northeastern Arunta Province: Northern Territory Geological Survey, Report 12, 45p.
- Shapiro, L and Brannock, WW 1962, Rapid analysis of silicate, carbonate, and phosphate rocks: United States Geological Survey, Bulletin 1144-A, p. A1–A56.
- Sheppard, S, Occhipinti, SA and Nelson, DR 2005, Intracontinental reworking in the Capricorn Orogen, Western Australia: the 1680–1620 Ma Mangaroon Orogeny: Australian Journal of Earth Sciences, v. 52, p. 443–460.
- Sheppard, S, Farrell, TR, Bodorkos, S, Hollingsworth, D, Tyler, IM and Pirajno, F 2006, Late Paleoproterozoic (1680–1620 Ma) sedimentation, magmatism, and tectonism in the Capricorn Orogen, in GSWA 2006 extended abstracts: promoting the prospectivity of Western Australia: Geological Survey of Western Australia, Record 2006/3, p. 11–12.
- Sheppard, S, Bodorkos, S, Johnson, SP, Wingate, MTD and Kirkland, CL 2010a, The Paleoproterozoic Capricorn Orogeny: intracontinental reworking not continent–continent collision: Geological Survey of Western Australia, Report 108, 33p.
- Sheppard, S, Johnson, SP, Wingate, MTD, Kirkland, CL and Pirajno, F 2010b, Explanatory Notes for the Gascoyne Province: Geological Survey of Western Australia, Perth, Western Australia, 336p.
- Sheppard, S, Krapež, B, Zi, J, Rasmussen, B and Fletcher, I 2016, The 1320 Ma intracontinental Wongawobbin Basin, Pilbara, Western Australia: A far-field response to Albany–Fraser–Musgrave tectonics: Precambrian Research, v. 285, p. 58–79.
- Sheppard, S, Page, RW, Griffin, TJ, Rasmussen, B, Fletcher, IR, Tyler, IM, Kirkland, CL, Wingate, MTD, Hollis, J and Thorne, AM 2012, Geochronological and isotopic constraints on the tectonic setting of the c. 1800 Ma Hart Dolerite and the Kimberley and Speewah Basins, northern Western Australia: Geological Survey of Western Australia, Record 2012/7, 28p.
- Smithies, RH and Bagas, L 1997, High pressure amphibolite–granulite facies metamorphism in the Palaeoproterozoic Rudall Complex, central Western Australia: Precambrian Research, v. 83, p. 243–265.
- Smithies, RH and Bagas, L 1998, The Tabletop Terrane of the Proterozoic Rudall Complex: preliminary notes on the geology, granitoid geochemistry and tectonic implications, in Geological Survey of Western Australia Annual Review 1996–97: Geological Survey of Western Australia, Perth, Western Australia, p. 89–94.
- Smithies, RH, Howard, HM, Evins, PM, Kirkland, CL, Kelsey, DE, Hand, M, Wingate, MTD, Collins, AS and Belousova, E 2011, High-T granite magmatism, crust–mantle interaction and the Mesoproterozoic intracontinental evolution of the Musgrave Province, Central Australia: Journal of Petrology, v. 52, no. 5, p. 931–958.

- Smithies, RH, Howard, HM, Evins, PM, Kirkland, CL, Kelsey, DE, Hand, M, Wingate, MTD, Collins, AS, Belousova, E and Allchurch, S 2010, Geochemistry, geochronology, and petrogenesis of Mesoproterozoic felsic rocks in the west Musgrave Province, Central Australia, and implications for the Mesoproterozoic tectonic evolution of the region: Geological Survey of Western Australia, Report 106, 73p.
- Smithies, RH, Spaggiari, CV and Kirkland, CL 2015a, Building the crust of the Albany–Fraser Orogen; constraints from granite geochemistry: Geological Survey of Western Australia, Report 150, 49p.
- Smithies, RH, Spaggiari, CV, Kirkland, CL, Wingate, MTD and England, RN 2015b, Forrest Zone: geochemistry and petrogenesis, in Eucla basement stratigraphic results release workshop: extended abstracts compiled by CV Spaggiari and RH Smithies: Geological Survey of Western Australia, Record 2015/10, p. 41–51.
- Spaggiari, CV, Kirkland, CL, Pawley, MJ, Smithies, RH, Wingate, MTD, Doyle, MG, Blenkinsop, TG, Clark, C, Oorschot, CW, Fox, LJ and Savage, J 2011, The geology of the east Albany–Fraser Orogen — a field guide: Geological Survey of Western Australia, Record 2011/23, 97p.
- Spaggiari, CV, Kirkland, CL, Smithies, RH, Occhipinti, SA and Wingate, MTD 2014a, Geological framework of the Albany–Fraser Orogen, in Albany–Fraser Orogen seismic and magnetotelluric (MT) workshop: extended abstracts 2014 compiled by CV Spaggiari and IM Tyler: Geological Survey of Western Australia, Record 2014/6, p. 12–27.
- Spaggiari, CV, Kirkland, CL, Smithies, RH and Wingate, MTD 2014b, Tectonic links between Proterozoic sedimentary cycles, basin formation and magmatism in the Albany–Fraser Orogen, Western Australia: Geological Survey of Western Australia, Report 133, 63p.
- Spaggiari, CV, Kirkland, CL, Smithies, RH, Wingate, MTD and Belousova, EA 2015a, Transformation of an Archean craton margin during Proterozoic basin formation and magmatism: the Albany–Fraser Orogen, Western Australia: Precambrian Research, v. 266, p. 440–466.
- Spaggiari, CV, Smithies, RH, Kirkland, CL, England, RN, Occhipinti, SA and Wingate, MTD 2015b, Eucla basement results: implications for geodynamics and mineral prospectivity, in Eucla basement stratigraphic drilling results release workshop: extended abstracts compiled by CV Spaggiari and RH Smithies: Geological Survey of Western Australia, Record 2015/10, p. 53–58.
- Stacey, JS and Kramers, JD 1975, Approximation of terrestrial lead isotope evolution by a two-stage model: Earth and Planetary Science Letters, v. 26, p. 207–221.
- Steiger, RH and Jäger, E 1977, Subcommission on geochronology: convention on the use of decay constants in geo- and cosmochronology: Earth and Planetary Science Letters, v. 36, p. 359–362.
- Sun, S-S and McDonough, WF 1989, Chemical and isotopic systematics of oceanic basalts: implications for mantle composition and processes, in Magmatism in the Ocean Basins edited by AD Saunders and MJ Norry: Geological Society, London, Special Publication 42, p. 313–345.
- Swain, G, Barovich, K, Hand, M, Ferris, G and Schwarz, M 2008, Petrogenesis of the St Peter Suite, southern Australia: Arc magmatism and Proterozoic crustal growth of the South Australian Craton: Precambrian Research, v. 166, no. 1–4, p. 283–296.
- Thevissen, J 1991, 1990–91 Annual Report, Karara Well Project, E45/841, Rudall River area, W.A.; PNC Exploration (Australia) Pty Ltd: Geological Survey of Western Australia, Statutory mineral exploration report, A33945.
- Thorne, AM and Trendall, AF 2001, Geology of the Fortescue Group, Pilbara Craton, Western Australia: Geological Survey of Western Australia, Bulletin 144, 249p.
- Trendall, AF, Compston, W, Nelson, DR, de Laeter, JR and Bennett, VC 2004, SHRIMP zircon ages constraining the depositional chronology of the Hamersley Group, Western Australia: Australian Journal of Earth Sciences, v. 51, no. 5, p. 621–644.
- Tyler, IM 2000, Palaeoproterozoic orogeny in Western Australia, in GSWA 2000 extended abstracts: Geological data for WA explorers in the new millennium: Geological Survey of Western Australia, Record 2000/8, p. 7–8.
- Van Kranendonk, MJ 2010, Geology of the Coongan 1:100 000 sheet: Geological Survey of Western Australia, 1:100 000 Geological Series Explanatory Notes, 67p.
- Van Kranendonk, MJ, Hickman, AH and Huston, DL 2007, Geology and mineralization of the east Pilbara — a field guide: Geological Survey of Western Australia, Record 2006/16, 90p.
- Van Kranendonk, MJ, Hickman, AH, Smithies, RH, Williams, IR, Bagas, L and Farrell, TR 2006, Revised lithostratigraphy of Archean supracrustal and intrusive rocks in the northern Pilbara Craton, Western Australia: Geological Survey of Western Australia, Record 2006/15, 57p.
- Vry, JK, Compston, W and Cartwright, I 1996, SHRIMP II dating of zircons and monazites: reassessing the timing of high-grade metamorphism and fluid flow in the Reynolds Range, north Arunta Block, Australia: Journal of Metamorphic Geology, v. 14, no. 3, p. 335–350, doi: 10.1111/j.1525-1314.1996.00335.x.
- Waddell, P-JA, Timms, NE, Spaggiari, CV, Kirkland, CL and Wingate, MTD 2015, Analysis of the Ragged Basin, Western Australia: insights into syn-orogenic basin evolution within the Albany–Fraser Orogen: Precambrian Research, v. 261, p. 166–187.
- Wade, BP, Barovich, KM, Hand, M, Scrimgeour, IR and Close, DF 2006, Evidence for early Mesoproterozoic arc magmatism in the Musgrave Block, Central Australia: implications for Proterozoic crustal growth and tectonic reconstructions of Australia: Journal of Geology, v. 114, p. 43–63.
- Wade, BP, Kelsey, DE, Hand, M and Barovich, KM 2008, The Musgrave Province: stitching north, west and south Australia, in Assembling Australia: Proterozoic building of a continent: Precambrian Research, v. 166, no. 1–4, p. 370–386.
- Walsh, AK, Raimondo, T, Kelsey, DE, Hand, M, Pfitzner, HL and Clark, C 2013, Duration of high-pressure metamorphism and cooling during the intraplate Petermann Orogeny: Gondwana Research, v. 24, no. 3–4, p. 969–983, doi:10.1016/j.gr.2012.09.006.
- Walter, MR, Veevers, JJ, Calver, CR and Grey, K 1995, Neoproterozoic stratigraphy of the Centralian Superbasin, Australia: Precambrian Research, v. 73, no. 1–4, p. 173–195.
- Wells, AT, Forman, DJ, Ranford, LC and Cook, PJ 1970, Geology of the Amadeus Basin, central Australia: Bureau of Mineral Resources, Bulletin 100, 222p.
- Wells, AT and Moss, FJ 1983, The Ngalia Basin, Northern Territory: stratigraphy and structure: Australia Bureau of Mineral Resources, Bulletin 212, 88p.
- Whelan, JA, Beyer, EE, Donnellan, N, Bleeker, W, Chamberlain, KR, Söderlund, U and Ernst, RE 2016, 1.4 billion years of Northern Territory geology: Insights from collaborative U-Pb zircon and baddeleyite dating, in AGES 2016 Proceedings: Northern Territory Geological Survey; Annual Geoscience Exploration Seminar 2016, Alice Springs, Northern Territory, 15–16 March 2016, p. 115–123, 9p.
- Whitaker, AJ, Roach, IC, Liu, SF and Wilford, JR 2010, Geology, in Geological and energy implications of the Paterson airborne electromagnetic (AEM) survey, Western Australia edited by IC Roach: Geoscience Australia, Record 2010/12, p. 49–86.
- Williams, IR 1992, Geology of the Savory Basin, Western Australia: Geological Survey of Western Australia, Bulletin 141, 115p.

- Williams, IR 1994, The Neoproterozoic Savory Basin, Western Australia, *in* The sedimentary basins of Western Australia *edited by* PG Purcell and RR Purcell: Petroleum Exploration Society of Australia, Western Australian Branch, Perth, Western Australia, p. 842–850.
- Williams, IR 1995, Trainor, Western Australia (2nd edition): Geological Survey of Western Australia, 1:250 000 Geological Series Explanatory Notes, 31p.
- Wingate, MTD 2002, Age and palaeomagnetism of dolerite sills of the Bangemall Supergroup on the Edmund 1:250 000 sheet, Western Australia: Geological Survey of Western Australia, Record 2002/4, 48p.
- Wingate, MTD and Bodorkos, S 2007, 149699: quartz sandstone, Cornelia Range; Geochronology Record 680: Geological Survey of Western Australia, 6p.
- Wingate, MTD and Evans, DAD 2003, Palaeomagnetic constraints on the Proterozoic tectonic evolution of Australia, *in* Proterozoic East Gondwana: Supercontinent Assembly and Breakup *edited by* M Yoshida, BF Windley and S Dasgupta: Geological Society, London, Special Publication 206, p. 77–91.
- Wingate, MTD, Kirkland, CL, Spaggiari, CV and Smithies, RH 2015, U–Pb geochronology of the Forrest Zone of the Coompana Province, *in* Eucla basement stratigraphic drilling results release workshop: extended abstracts *compiled by* CV Spaggiari and RH Smithies: Geological Survey of Western Australia, Record 2015/10, p. 37–40.
- Wynne, P and Bacchin, M (compilers) 2009, Index of gravity surveys (2nd edition): Geoscience Australia, Record 2009/07.
- Zhao, J-X and Bennett, VC 1995, SHRIMP U–Pb zircon geochronology of granites in the Arunta Inlier, central Australia: implications for Proterozoic crustal evolution: Precambrian Research, v. 71, p. 17–43.
- Zhao, JX and McCulloch, MT 1995, Geochemical and Nd isotopic systematics of granites from the Arunta Inlier, central Australia: implications for Proterozoic crustal evolution: Precambrian Research, v. 71, p. 265–299.

U–Pb zircon dating of igneous and metasedimentary rocks from the Rudall Province has revealed aspects of an extended, multiphase history that has implications for models of the assembly of Proterozoic Australia. Detrital zircon dating has identified metasedimentary units of possible Neoproterozoic to early Paleoproterozoic age, and a possible cover succession deposited after c. 1794 Ma. The Krackatinny Supersuite in the eastern part of the province yields ages of 1589–1549 Ma and has a range of geochemical compositions consistent with emplacement in a magmatic arc or a rift developed in thickened continental crust. Felsic magmatism and high-grade metamorphism at 1330–1285 Ma reflects a major tectono-thermal event, and possibly dates the Yapungku Orogeny, previously considered to have taken place at c. 1800–1765 Ma. This event has been linked with the amalgamation of the West and North Australian Cratons, and might indicate assembly later than previously thought.



Further details of geological products and maps produced by the Geological Survey of Western Australia are available from:

Information Centre
Department of Mines and Petroleum
100 Plain Street
EAST PERTH WA 6004
Phone: (08) 9222 3459 Fax: (08) 9222 3444
www.dmp.wa.gov.au/GSWApublications